AD-A140 012 IONOSPHERIC RESEARCH USING DIGITAL IONOSONDES(U) LOWELL 1/3
UNIV MA CENTER FOR ATMOSPHERIC RESEARCH
B W REINISCH ET AL. JUL 83 ULRF-425/CAR AFGL-TR-83-0184
UNCLASSIFIED F19628-80-C-0064 F/G 4/1 NL

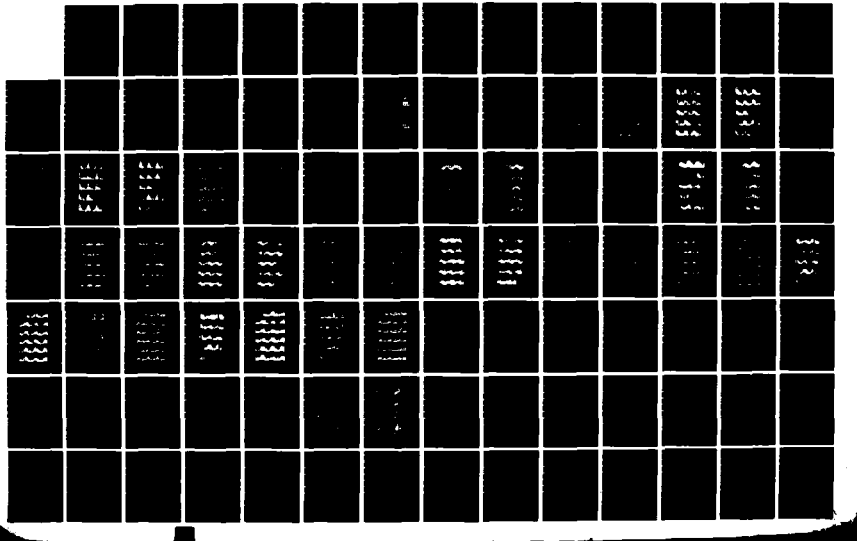

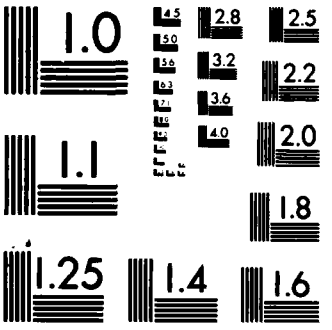

MICROCOPY RESOLUTION TEST CHART
NATIONAL BUREAU OF STANDARDS 1963-A

AFGL-TR-83-0184

IONOSPHERIC RESEARCH USING DIGITAL IONOSONDES

Bodo W. Reinisch
Klaus Bibl

University of Lowell
Center for Atmospheric Research
450 Aiken Street
Lowell, Massachusetts 01854

Final Report
March 1980 - April 1983

July 1983

Approved for public release; distribution unlimited.

AIR FORCE GEOPHYSICS LABORATORY
AIR FORCE SYSTEMS COMMAND
UNITED STATES AIR FORCE
HANSCOM AFB, MASSACHUSETTS 01731

This report has been reviewed by the ESD Public Affairs Office (PA) and is releasable to the National Technical Information Service (NTIS).

This technical report has been reviewed and is approved for publication

JACKIE B. WAARAMAA
Contract Manager

for HERBERT C. CARLSON
Branch Chief

FOR THE COMMANDER

RITA C. SAGALYN
Division Director

Qualified requestors may obtain additional copies from the Defense Technical Information Center. All others should apply to the National Technical Information Service.

If your address has changed, or if you wish to be removed from the mailing list, or if the addressee is no longer employed by your organization, please notify AFGL/DAA, Hanscom AFB, MA 01731. This will assist us in maintaining a current mailing list.

Do not return copies of this report unless contractual obligations or notices on a specific document requires that it be returned.

UNCLASSIFIED

SECURITY CLASSIFICATION OF THIS PAGE *(When Data Entered)*

REPORT DOCUMENTATION PAGE		READ INSTRUCTIONS BEFORE COMPLETING FORM
1. REPORT NUMBER AFGL-TR-83-0184	2. GOVT ACCESSION NO. AD-A140 012	3. RECIPIENT'S CATALOG NUMBER
4. TITLE *(and Subtitle)* IONOSPHERIC RESEARCH USING DIGITAL IONOSONDES		5. TYPE OF REPORT & PERIOD COVERED Final March 1980-April 1983
		6. PERFORMING ORG. REPORT NUMBER ULRF-425/CAR
7. AUTHOR(s) Bodo W. Reinisch Klaus Bibl		8. CONTRACT OR GRANT NUMBER(s) F19628-80-C-0064
9. PERFORMING ORGANIZATION NAME AND ADDRESS University of Lowell, Center for Atmospheric Research, 450 Aiken Street, Lowell, Massachusetts 01854		10. PROGRAM ELEMENT, PROJECT, TASK AREA & WORK UNIT NUMBERS 62101F 464306AJ
11. CONTROLLING OFFICE NAME AND ADDRESS Air Force Geophysics Laboratory Hanscom AFB, Massachusetts 01731 Contract Monitor: J. B. Waaramaa/PHY		12. REPORT DATE July 1983 13. NUMBER OF PAGES 231
14. MONITORING AGENCY NAME & ADDRESS*(if different from Controlling Office)*		15. SECURITY CLASS. *(of this report)* Unclassified 15a. DECLASSIFICATION/DOWNGRADING SCHEDULE

16. DISTRIBUTION STATEMENT *(of this Report)*

Approved for public release; distribution unlimited.

17. DISTRIBUTION STATEMENT *(of the abstract entered in Block 20, if different from Report)*

18. SUPPLEMENTARY NOTES

19. KEY WORDS *(Continue on reverse side if necessary and identify by block number)*

Auroral Ionosphere	Irregularities
HF Sounding	Polar Cap
Digisonde	Digital Ionograms
Doppler Drift	Real Time Processing
Plasma Convection	True Height

20. ABSTRACT *(Continue on reverse side if necessary and identify by block number)*

New digital HF sounding techniques are used for the study of the high latitude and the equatorial ionosphere: Doppler and incidence angle measurements allow to identify irregularities in the ionospheric plasma and to determine their velocities. In the drift mode of observation the Digisonde with a four antenna receiving array measured the plasma bulk motion at Goose Bay. The results show that the HF Doppler technique measures

DD FORM 1 JAN 73 1473 EDITION OF 1 NOV 65 IS OBSOLETE

UNCLASSIFIED

SECURITY CLASSIFICATION OF THIS PAGE *(When Data Entered)*

20. ABSTRACT

the plasma convection also observed by incoherent scatter and satellite techniques.

Automatic scaling of Digisonde ionograms is now routinely carried out at the Goose Bay Ionospheric Observatory. The E and F region echo traces ~~h'(f)~~ are reliably determined also under spread conditions. The Automatic Real Time Ionogram Scaler with True Height ~~(ARTIST)~~ also finds all standard ionospheric parameters and the electron density profile in real time.

TABLE OF CONTENTS

LIST OF FIGURES

LIST OF FIGURES (Continued)

LIST OF FIGURES (Continued)

LIST OF FIGURES (Continued)

LIST OF FIGURES (Continued)

LIST OF FIGURES (Continued)

LIST OF FIGURES (Continued)

LIST OF TABLES

1.0 INTRODUCTION

From March 1980 to March 1983 the University of Lowell Center for Atmospheric Research (ULCAR) conducted ionospheric radio research using Digisonde data in support of AFGL's ongoing research work in the polar cap, the auroral regions and at the magnetic equator. The complicated structures of the ionization in these regions result in different signatures of the HF radio echoes. Interpretation of the observations is therefore not easy, but the multi-parameter Digisonde ionograms helped us in understanding some of the processes that take place. This final report summarizes the results of our observations and activities, and frequent reference is made to scientific reports and papers that have been published in the course of our work.

Section 2 discusses vertical and backscatter ionogram observations and relates them to aircraft measurements and to local magnetic activity. A summary of the scaled hourly ionogram values for Goose Bay for the period January 1979 to September 1982 is given in the appendix. Special observational programs in support of the over-the-horizon radar tests are described in Section 3. Section 4 summarizes the results of the Doppler-Drift measurements with the Digisonde 128PS at Goose Bay. The drift data that were analyzed seem to indicate that the Goose Bay ionosphere is connected, at least part of the time, to the two-cell polar cap convection pattern. The direction of the drift velocity vectors is consistently westward in the evening hours and switches to eastward at local midnight. Although not enough data were analyzed to generalize the results we believe now that HF Doppler-drift measurements are a powerful and low cost method to study motions in the ionosphere. Digisonde and optical measurements in the polar cap at Thule, Greenland, show during quiet conditions the dawn-to-dusk drift of F-region arcs, and F-region

ionization patches moving anti-sunward during disturbed magnetic conditions (Section 5).

One of the annoying facts in ionogram based research is the normally tedious process of reducing the ionograms to the vertical electron density distribution. After years of study we succeeded to develop fully automatic methods of scaling the Digisonde ionograms and calculating the electron profiles (Section 6). The Automatic Real Time Ionogram Scaler with True Height Analysis (ARTIST), now operating at Goose Bay with the Digisonde 128PS is the first and only instrument, as far as we know, that outputs the standard ionospheric parameters and profiles in real time, even under disturbed conditions. This breakthrough will make it possible in the future to instantaneously update the global ionospheric model, thus greatly improving short term HF and VHF predictions.

In 1982, AFGL organized an equatorial spread F (ESF) campaign including chemical releases from rockets launched at Natal, Brazil. The Brazilian Ionospheric Modification Experiments (BIME) were designed to test the understanding of the nighttime ESF phenomenon. ULCAR participated with Digisonde observations at West Catre, near Natal, and airborne measurements. The Digisonde ionograms monitored F-layer height and upward velocity, specifying the right launch time. Incidence angle and Doppler informations in the ionograms allowed to track the chemical releases and natural irregularities (Section 7).

Airborne Digisonde observations were also conducted during another active ionospheric experiment. In September 1981, the HF heating facility near Arecibo was illuminating the F-region at 7 and 5 MHz. The airborne sounder recorded oblique echo returns from the heated volume only at specific aircraft positions. It is believed that echoes were received when ray paths at right angles to the field aligned irregularities existed (Section 8).

Section 9 covers the installation of a modified Digisonde 128 at Kennedy Space Center, Florida.

2.0 IONOGRAM OBSERVATIONS AT GOOSE BAY

The Goose Bay Ionospheric Observatory, operated by personnel of Canadian Marconi for AFGL, uses a Digisonde 128PS system (Bibl and Reinisch, 1978) to record vertical and backscatter ionograms.

2.1 Observational Programs

At the present time four vertical and four backscatter ionograms per hour are recorded on magnetic tape (7 track, 556 cpi). Every other ionogram pair is printed on an electrostatic plotter showing side-by-side the amplitude ionogram with numbers in 4 dB steps and the status ionogram with numbers expressing Doppler and/or directional information. The vertical ionograms use a vertical rhombic antenna for transmission and an array of four crossed-loop antennas for reception. The backscatter ionograms use a log-periodic transmitting antenna and a linear twelve antenna (log-periodic loop) array for reception. Until January 1983 the boresight of the linear array was magnetic north (32° west of geographic north). The auroral oval is not centered at the magnetic pole and as a result the oval aligned ionospheric features such as the trough and the poleward trough wall approach in the evening sector from a direction between 30° east of magnetic north (early evening) to 20° east of magnetic north (later evening). To improve the signal-to-noise ratio for backscatter echoes from the oval aligned features, we turned the boresight of the array by 25° to the east, so that since mid-January 1983 the boresight is 7° west of geographic north. As of now we have not verified whether the intensity and/or frequency of occurrence of the backscatter echoes has increased as we expected. It should be mentioned that the log-periodic transmitter antenna is still pointing due magnetic north. For the

vertical ionograms the receiving array consists of four crossed-loop antennas that allow beam steering and polarization measurements. All vertical ionograms compare the vertical O and X echoes and signals from two slightly oblique directions. It would require too much sounding time to probe many different directions for echoes. The Digisonde allows azimuthal scans in 30° increments for two fixed zenith angles: 18° and 38°. Until mid-January 1983 the hourly ionograms steered the receiving beam toward magnetic north at the two zenith angles of 18° and 38°, while the other vertical ionograms probed the azimuth angles of ±30° around magnetic north at a zenith angle of approximately 18°. No clear indication of ionization moving in the magnetic north-south or east-west direction was obtained. So in January 1983, the beam directions were changed. The hourly ionogram, i.e. the "C program" with Z = 1, steers the beam toward magnetic north and 60° east of north at a zenith angle of 18° (in addition to the vertical direction). The Z-parameter in the Digisonde 128PS selects the desired antenna steering directions (see Table 1). The other vertical ionograms, i.e. the "A program" with Z = 9, looks 30° and 210° east of magnetic north (zenith angle = 18°), essentially sampling the geographic north-south direction. We have not yet analyzed the recent data in terms of north-south propagating disturbances. Echo signals arriving from directions other than the programmed beam direction will be wrongly identified in the ionograms, depending upon which antenna beam is picking up these signals better. This complicates the interpretation of the ionograms. Each amplitude value in the ionograms is accompanied by a status number, as shown in the playback from magnetic tape in Figure 1. The insets in Figure 1 show the optically weighted font (Patenaude et al, 1973) that is used to print the ionograms. The meaning of the status values for different time periods is explained in Table 1.

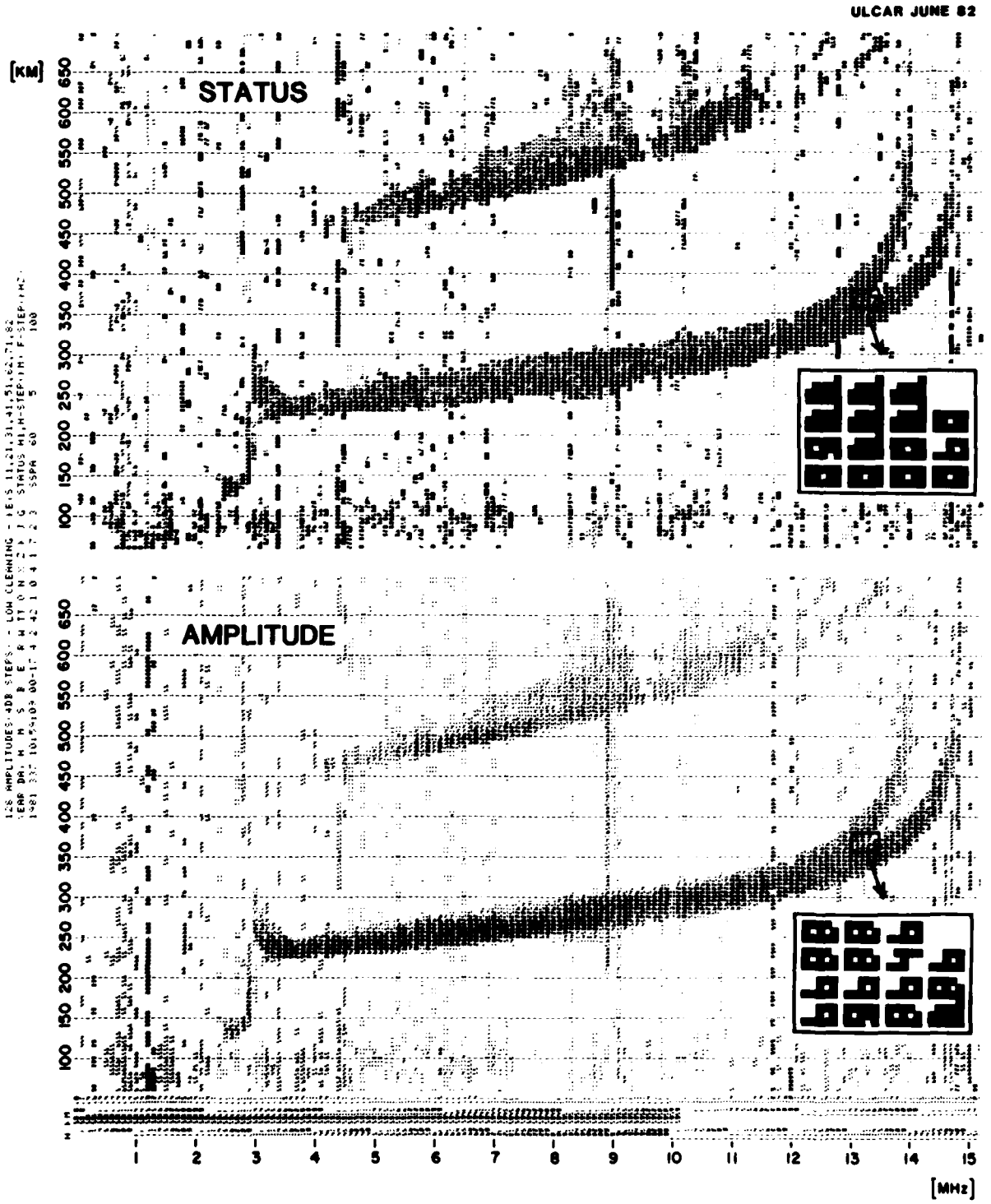

DIGISONDE IONOGRAM

GOOSE BAY 3 DEC 1981 11:00 AST

Figure 1

IONOGRAM	BEGIN		STATUS 0	1	2	3	4	5	6	7	8	9	10	11	12	13	14	15	Tt	Z
Vertical Hourly	July 1979	I	N_2	N_2	V_X	V_X	N_1	N_1	V_O	V_O	N_2	N_2	V_X	V_X	N_1	N_1	V_O	V_O	42	1
		S	-1	-2	-1	-2	-1	-2	-1	-2	+1	+2	+1	+2	+1	+2	+1	+2		
	14 Jun 1980	I	N_2	N_1	V_X	V_O	N_2	N_1	V_X	V_O	N_2	N_1	V_X	V_O	N_2	N_1	V_X	V_O	42	1
		S	-2	-2	-2	-2	-1	-1	-1	-1	+1	+1	+1	+1	+2	+2	+2	+2		
	Jan 1983	I	F_1	N_1	V_X	V_O	F_1	N_1	V_X	V_O	F_1	N_1	V_X	V_O	F_1	N_1	V_X	V_O	42	1
		S	-2	-2	-2	-2	-1	-1	-1	-1	+1	+1	+1	+1	+2	+2	+2	+2		
Other Vertical	July 1979	I	O_2	O_2	V_X	V_X	G_2	G_2	V_O	V_O	O_2	O_2	V_X	V_X	G_2	G_2	V_O	V_O	42	7
		S	-1	-2	-1	-2	-1	-2	-1	-2	+1	+2	+1	+2	+1	+2	+1	+2		
	14 Jun 1980	I	O_2	G_2	V_X	V_O	O_2	G_2	V_X	V_O	O_2	G_2	V_X	V_O	O_2	G_2	V_X	V_O	42	7
		S	-2	-2	-2	-2	-1	-1	-1	-1	+1	+1	+1	+1	+2	+2	+2	+2		
	20 Jan 1983	I	G_1	Y_1	V_X	V_O	G_1	Y_1	V_X	V_O	G_1	Y_1	V_X	V_O	G_1	Y_1	V_X	V_O	42	9
		S	-2	-2	-2	-2	-1	-1	-1	-1	+1	+1	+1	+1	+2	+2	+2	+2		
Backscatter	July 1979	I	*	D_1	V_O	N_2	*	D_1	V_O	N_2	*	D_1	V_O	N_2	*	D_1	V_O	N_2	45	0
		S	*	-1	-1	-1	*	-2	-2	-2	*	+1	+1	+1	*	+2	+2	+2		
	Nov 1979	I	D_1	D_1	D_1	D_1	D_1	D_1	D_1	D_1	D_1	D_1	D_1	D_1	D_1	D_1	D_1	D_1	77	0
		S	-8	-7	-6	-5	-4	-3	-2	-1	+1	+2	+3	+4	+5	+6	+7	+8		
	Jan 1983	I	D_2	D_2	D_2	D_2	D_2	D_2	D_2	D_2	D_2	D_2	D_2	D_2	D_2	D_2	D_2	D_2	77	0
		S	-8	-7	-6	-5	-4	-3	-2	-1	+1	+2	+3	+4	+5	+6	+7	+8		

I = Incidence Angle and Polarization
S = Spectrum, Relative Doppler Frequencies
N_2 = Mag. North, 52° Elevation
V_O = Vertical, Ordinary Component
O_2 = Mag. 30° West, 52° Elevation
V_X = Vertical, Extraordinary Component
G_2 = Mag. 30° East, 52° Elevation
D_1 = Linear DAASM Array, boresight magnetic north
N_1 = Mag. North, 72° Elevation
D_2 = Linear DAASM Array, boresight 25° east of north
F_1 = Mag. 60° East, 72° Elevation

Table 1. Interpretation of Status for Goose Bay Ionograms Rev. 30 Jun 83, Rei

2.2 Ionogram Characteristics and Local Magnetic Activity at Goose Bay

An ionogram is, in essence, a snapshot of the ionosphere, and to study the morphology of the ionosphere requires the analysis of many ionograms. The University of Lowell in cooperation with AFGL has developed computer software to compress each ionogram into a linear array by either integrating the amplitudes along the height or the frequency axis. In the first case the result is the so-called frequency characteristic, in the second the height characteristic (Bibl, 1956; Buchau et al, 1978). For the frequency characteristic the height intervals above and below 160 km are processed independently giving the E (Figures 2 and 3) and F-region (Figures 4 and 5) frequency characteristics. The signal amplitudes as function of frequency for each ionogram are printed as one vertical line. Because of the photographic reduction the individual numbers become too small to be identifiable. As Figure 1 shows, the Optifont (Bibl, 1974) creates a qualitative image, however. The variation of the critical frequencies of the E and F layers as function of time can conveniently be read from these characteristics and, as we will show later, they help in identifying periods of disturbed conditions.

Figures 6 and 7 show height characteristics of the E and F layers. The dark traces (large integrated amplitudes) indicate the approximate minimum virtual heights of the layers. Since the echo signatures in the vertical and backscatter ionograms are quite different, separate characteristics were prepared for the backscatter data (Figures 8 to 11).

In an effort to compare the local magnetic activity with the ionogram data we prepared ionospheric characteristics for the months January, April, July and September 1980 (see Figures 2 to 41) covering four different seasons. Three characteristic magnetic indices DY, DZ and K were derived from the

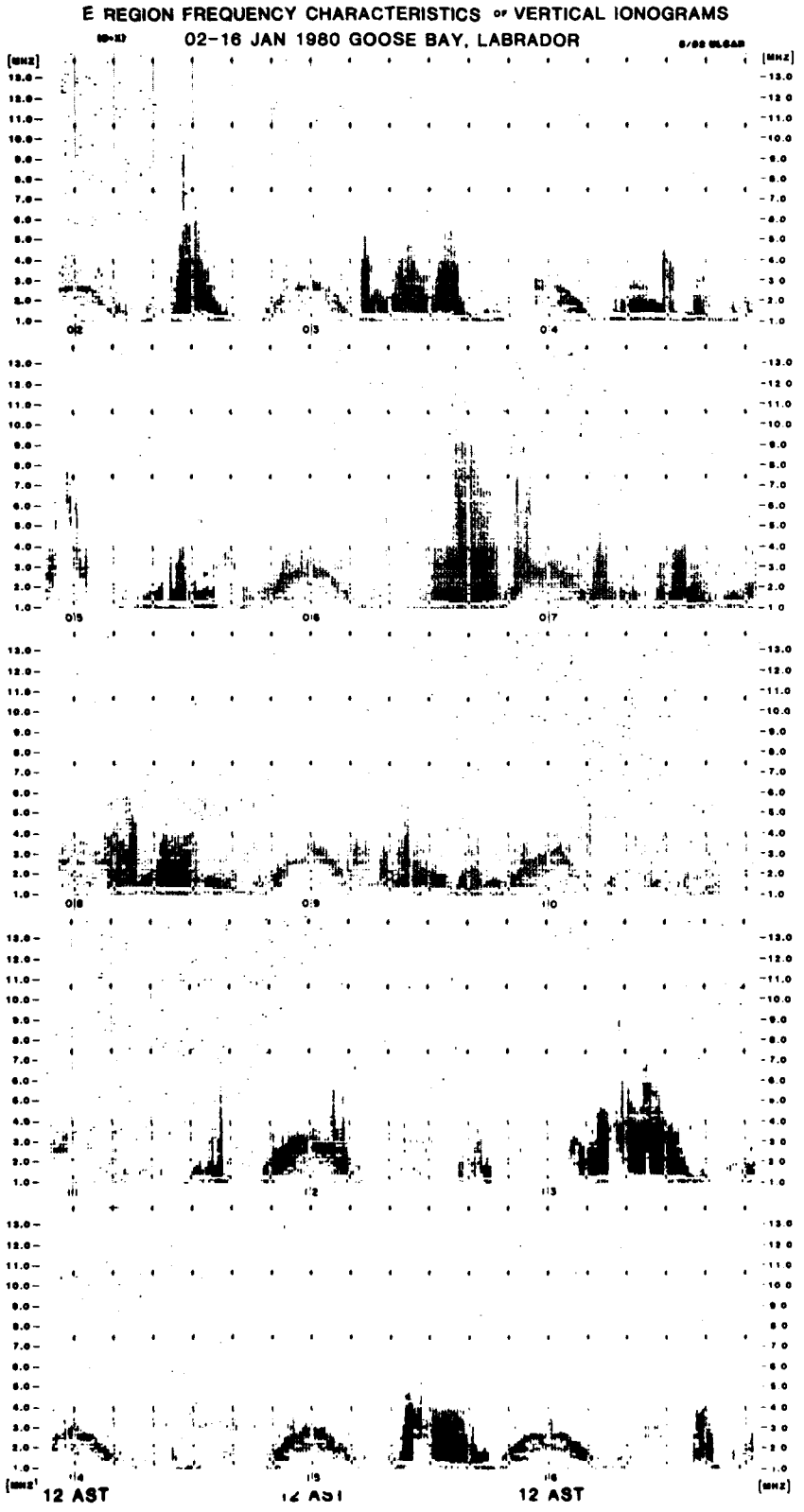
E REGION FREQUENCY CHARACTERISTICS OF VERTICAL IONOGRAMS
02-16 JAN 1980 GOOSE BAY, LABRADOR
[MHZ]
12 AST
12 AST
12 AST
[MHZ]

Figure 2

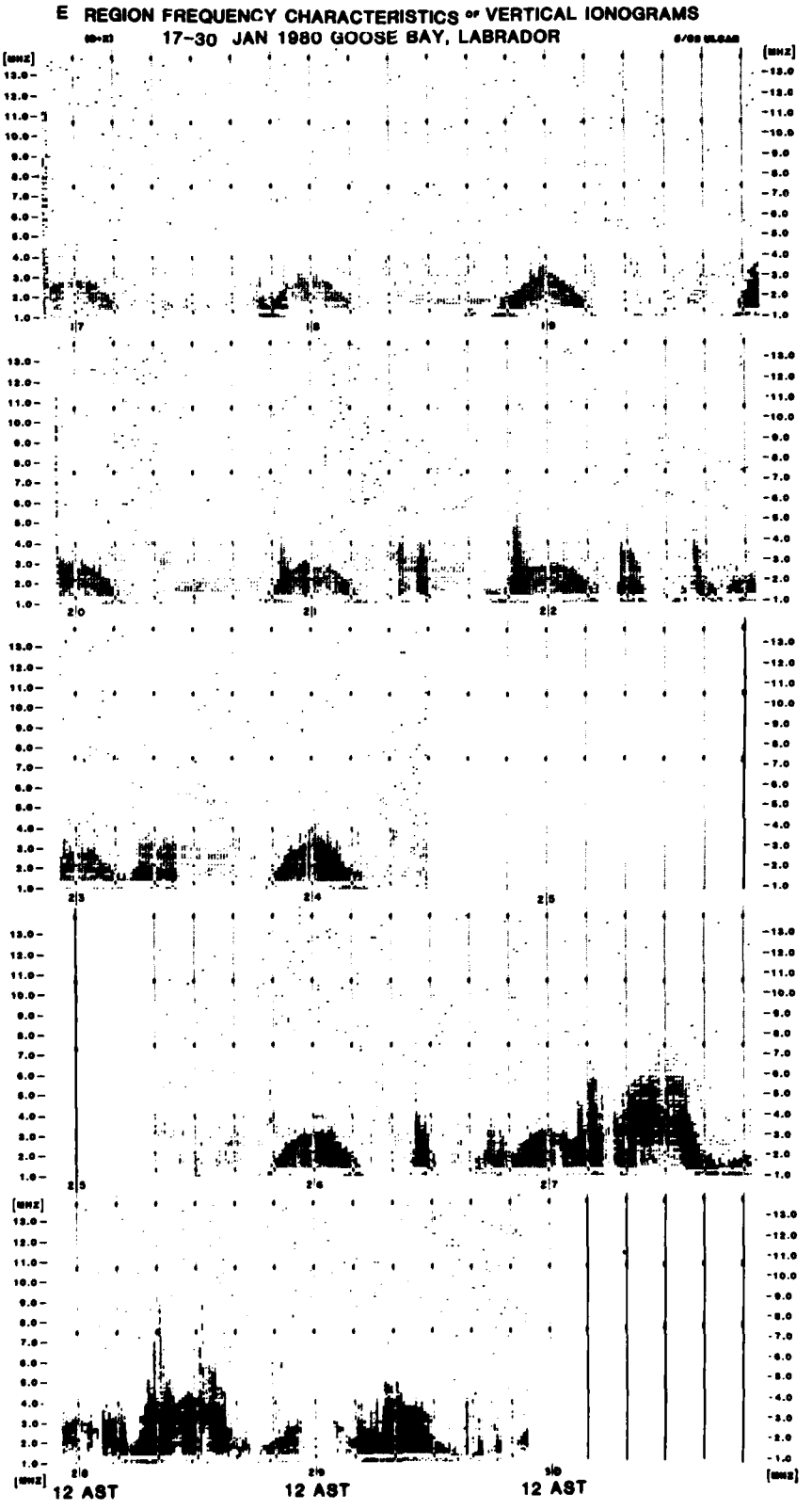
E REGION FREQUENCY CHARACTERISTICS OF VERTICAL IONOGRAMS
17-30 JAN 1980 GOOSE BAY, LABRADOR
12 AST
12 AST
12 AST

Figure 3

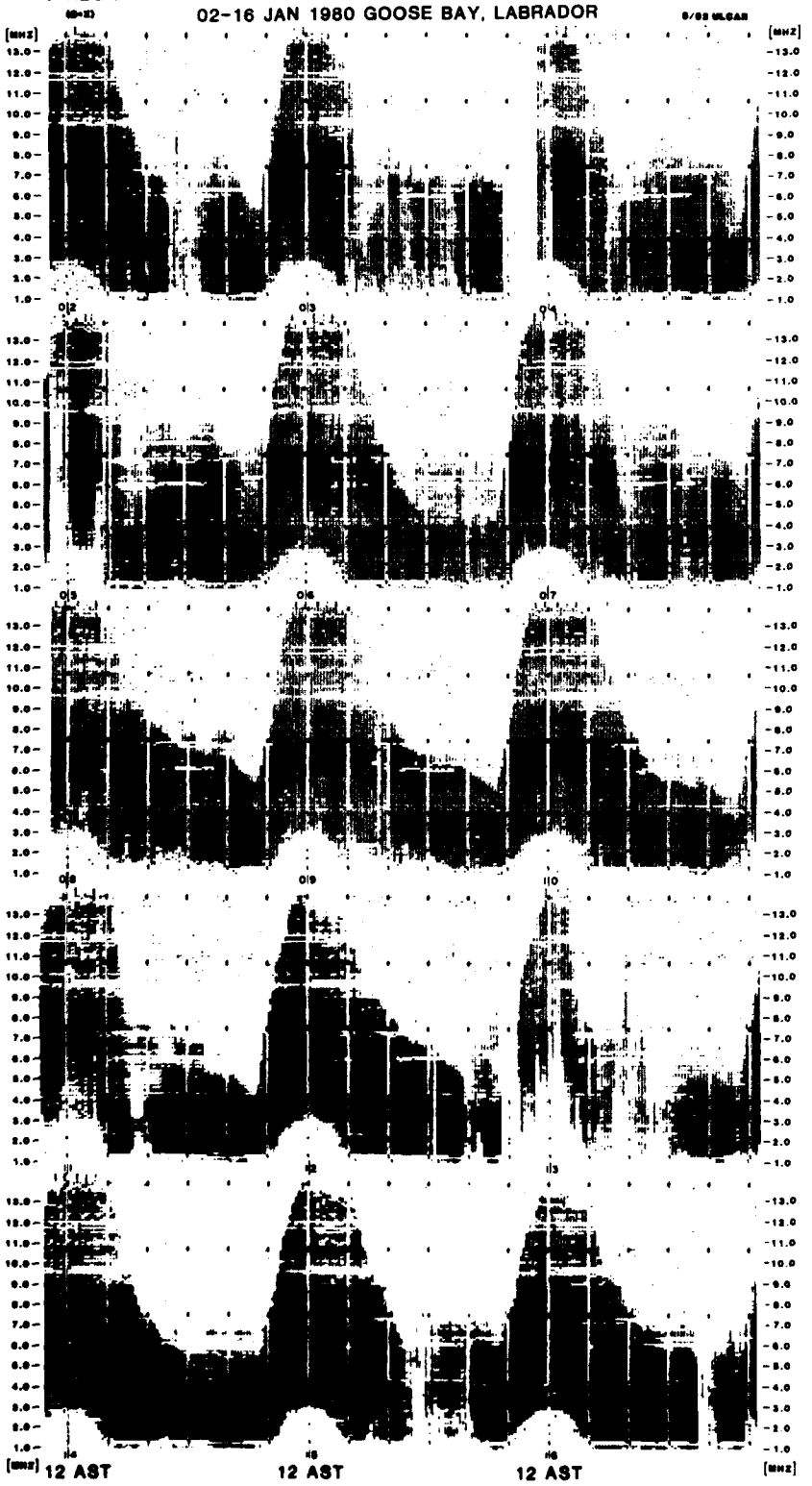
F REGION FREQUENCY CHARACTERISTICS OF VERTICAL IONOGRAMS
02-16 JAN 1980 GOOSE BAY, LABRADOR
[MHZ]
12 AST
12 AST
12 AST
[MHZ]

Figure 4


F REGION FREQUENCY CHARACTERISTICS OF VERTICAL IONOGRAMS
17-30 JAN 1980 GOOSE BAY, LABRADOR
12 AST
12 AST
12 AST

Figure 5

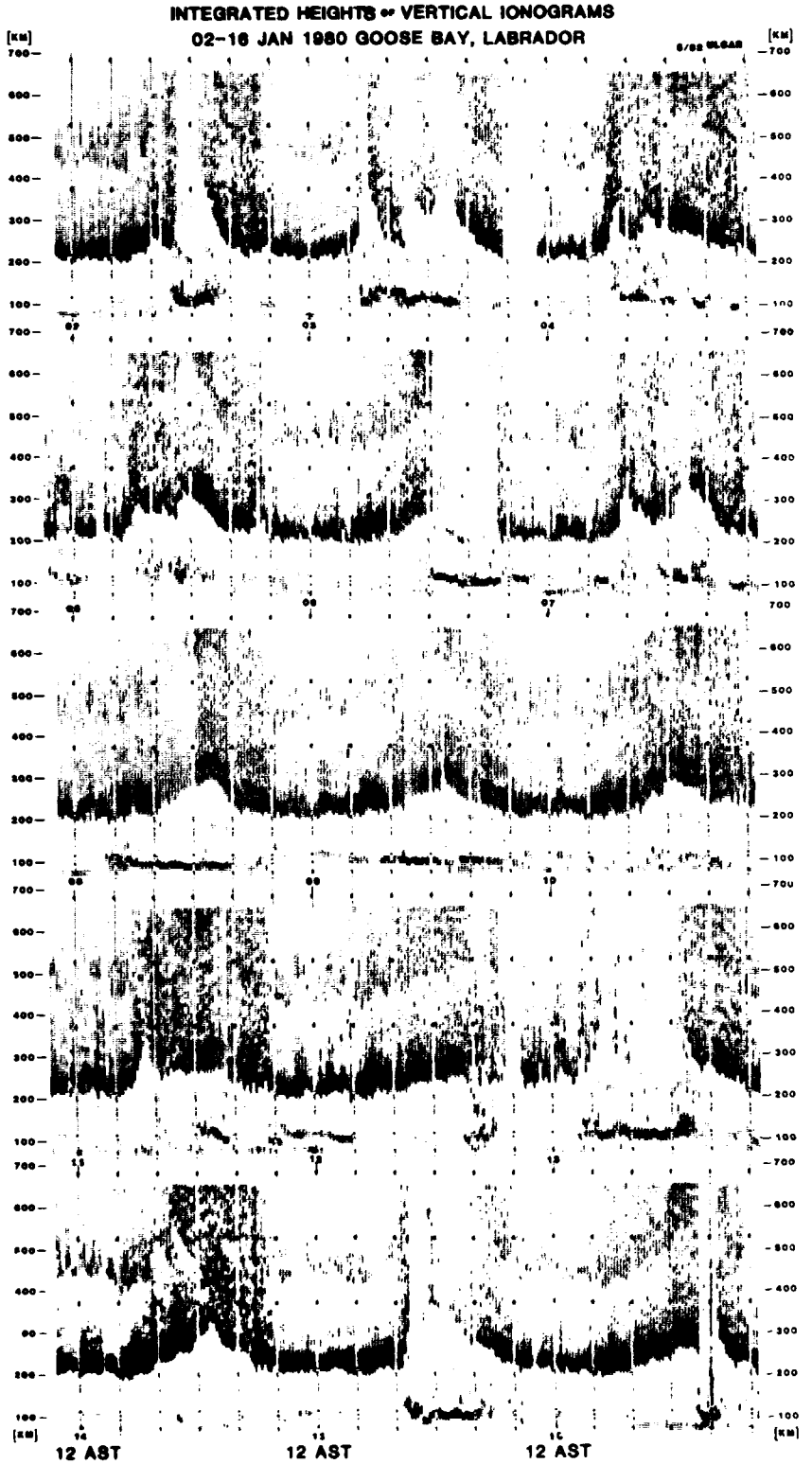
INTEGRATED HEIGHTS of VERTICAL IONOGRAMS
02-16 JAN 1980 GOOSE BAY, LABRADOR
[KM]
12 AST
12 AST
12 AST

Figure 6

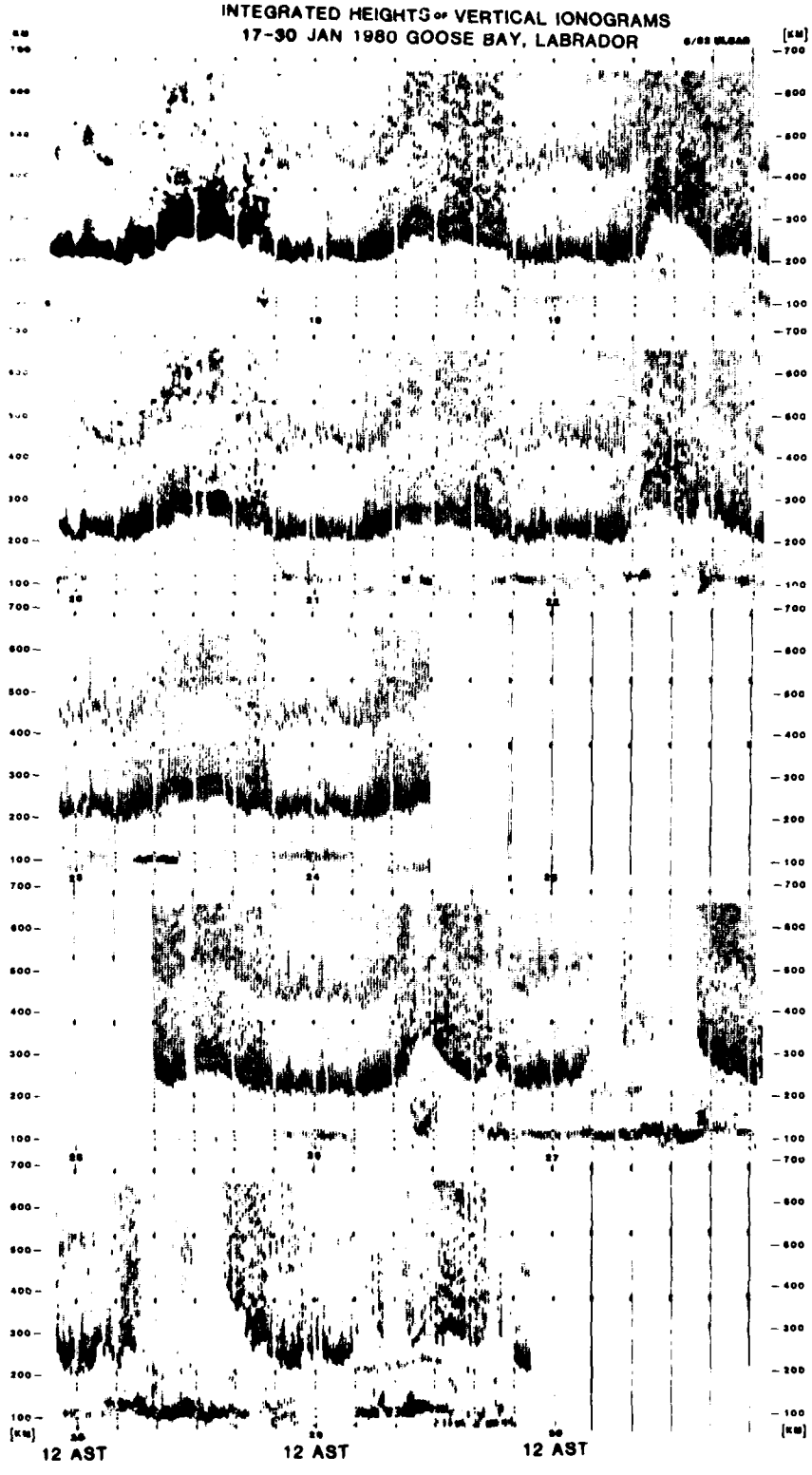
INTEGRATED HEIGHTS OF VERTICAL IONOGRAMS
17-30 JAN 1980 GOOSE BAY, LABRADOR
[KM]
12 AST
12 AST
12 AST

Figure 7

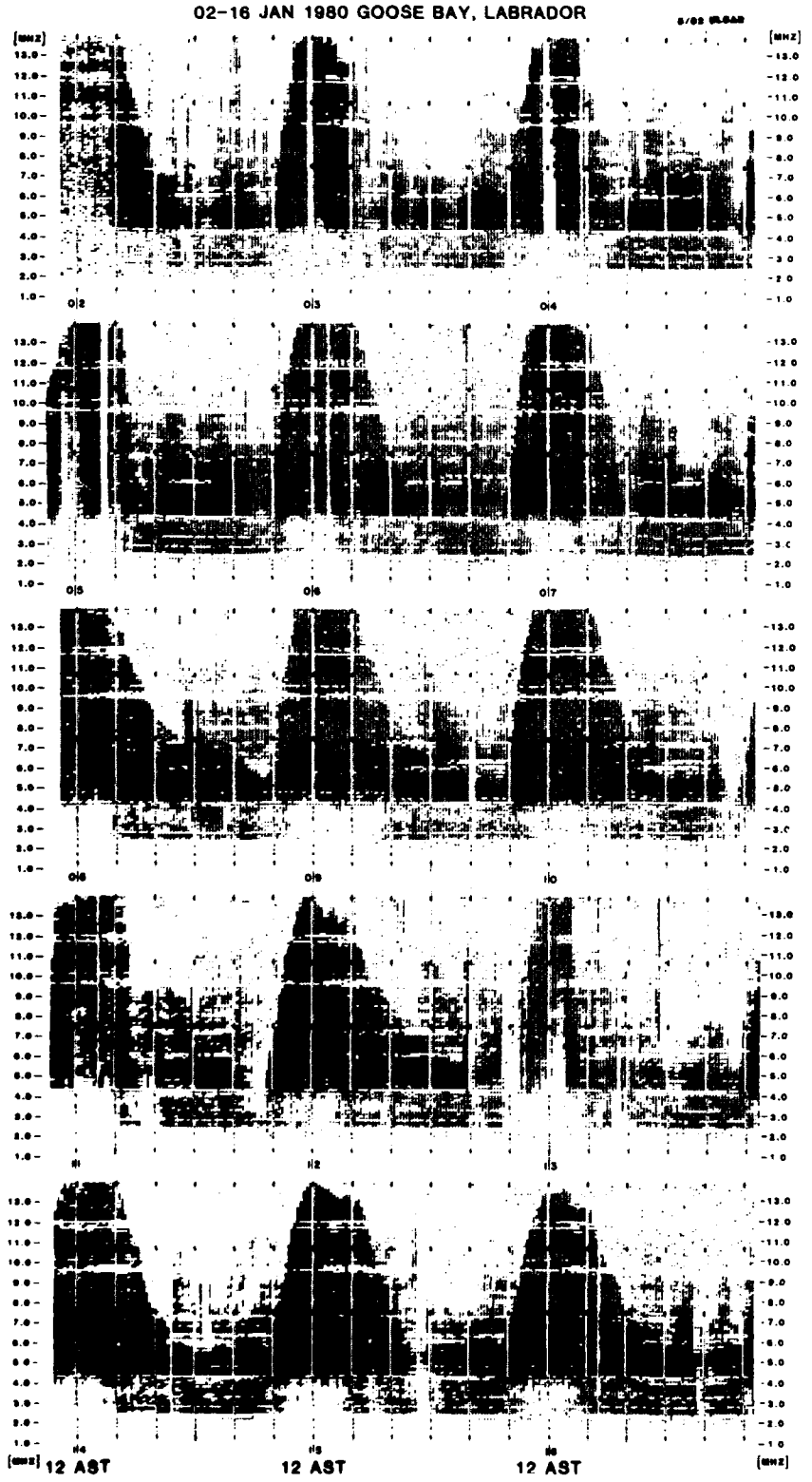
F REGION FREQUENCY CHARACTERISTICS OF BACKSCATTER IONOGRAMS
02-16 JAN 1980 GOOSE BAY, LABRADOR
12 AST
12 AST
12 AST

Figure 8

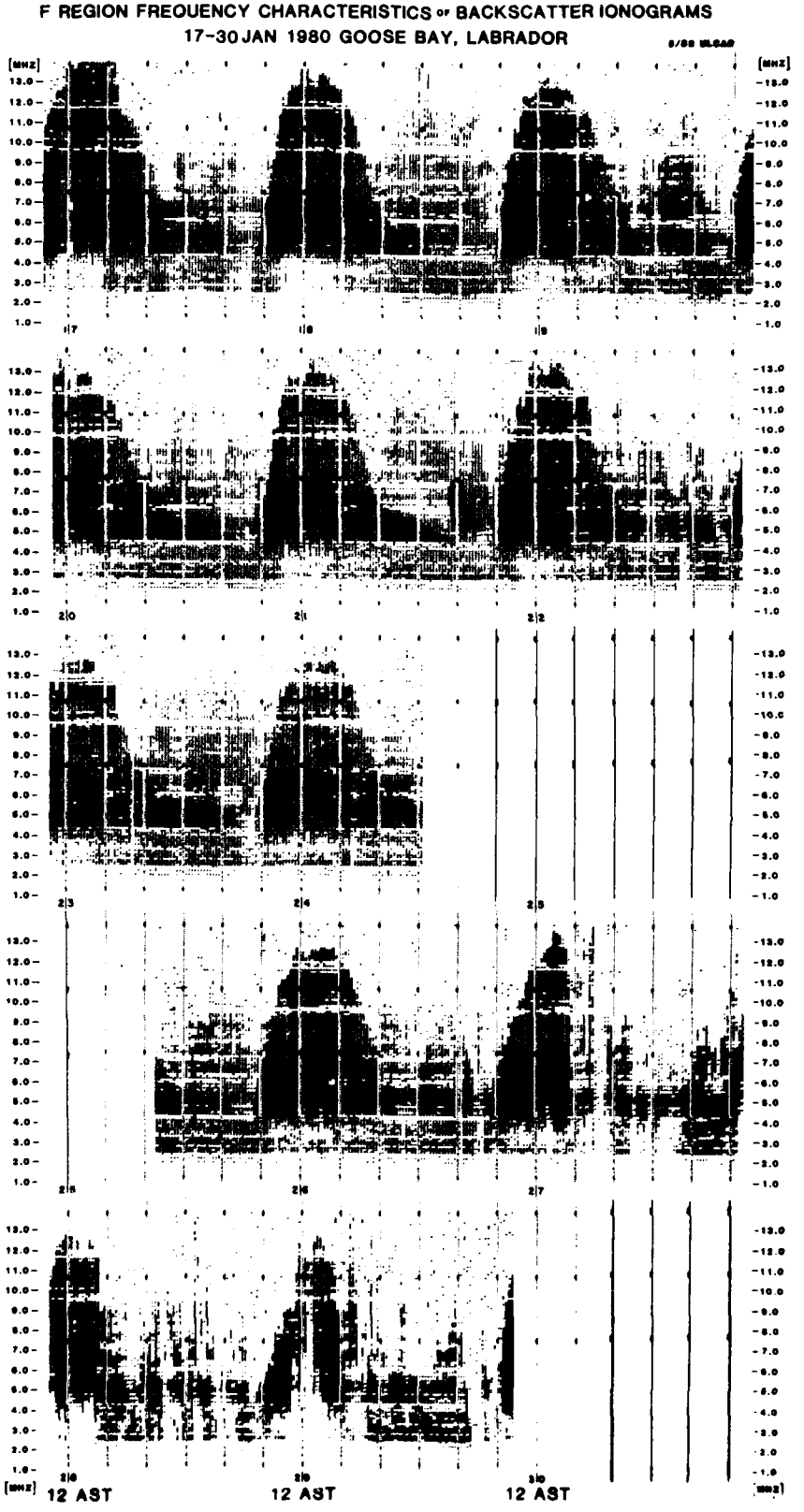
F REGION FREQUENCY CHARACTERISTICS OF BACKSCATTER IONOGRAMS
17-30 JAN 1980 GOOSE BAY, LABRADOR
12 AST
12 AST
12 AST

Figure 9

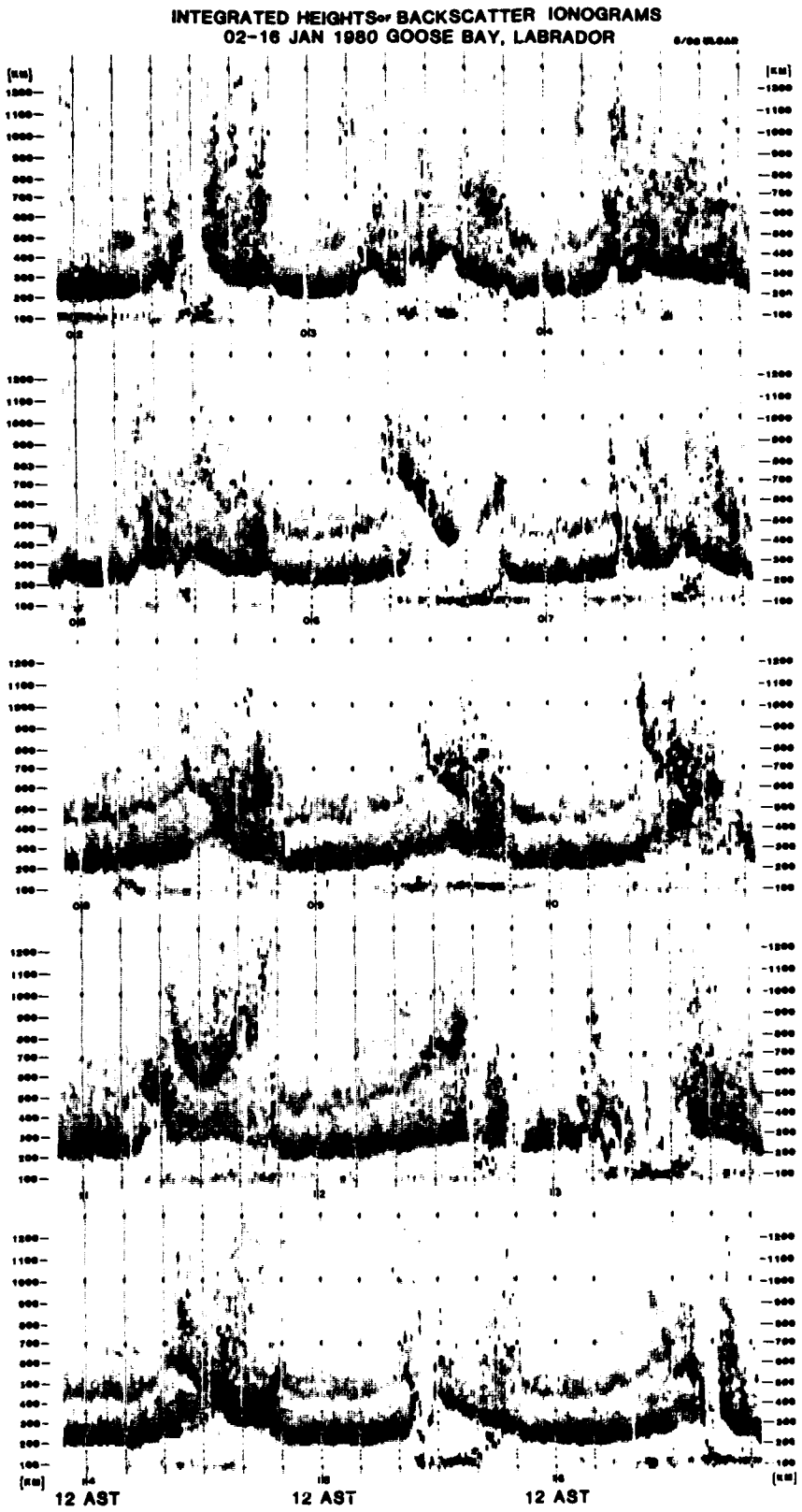
INTEGRATED HEIGHTS OF BACKSCATTER IONOGRAMS
02-16 JAN 1980 GOOSE BAY, LABRADOR
12 AST
12 AST
12 AST

Figure 10

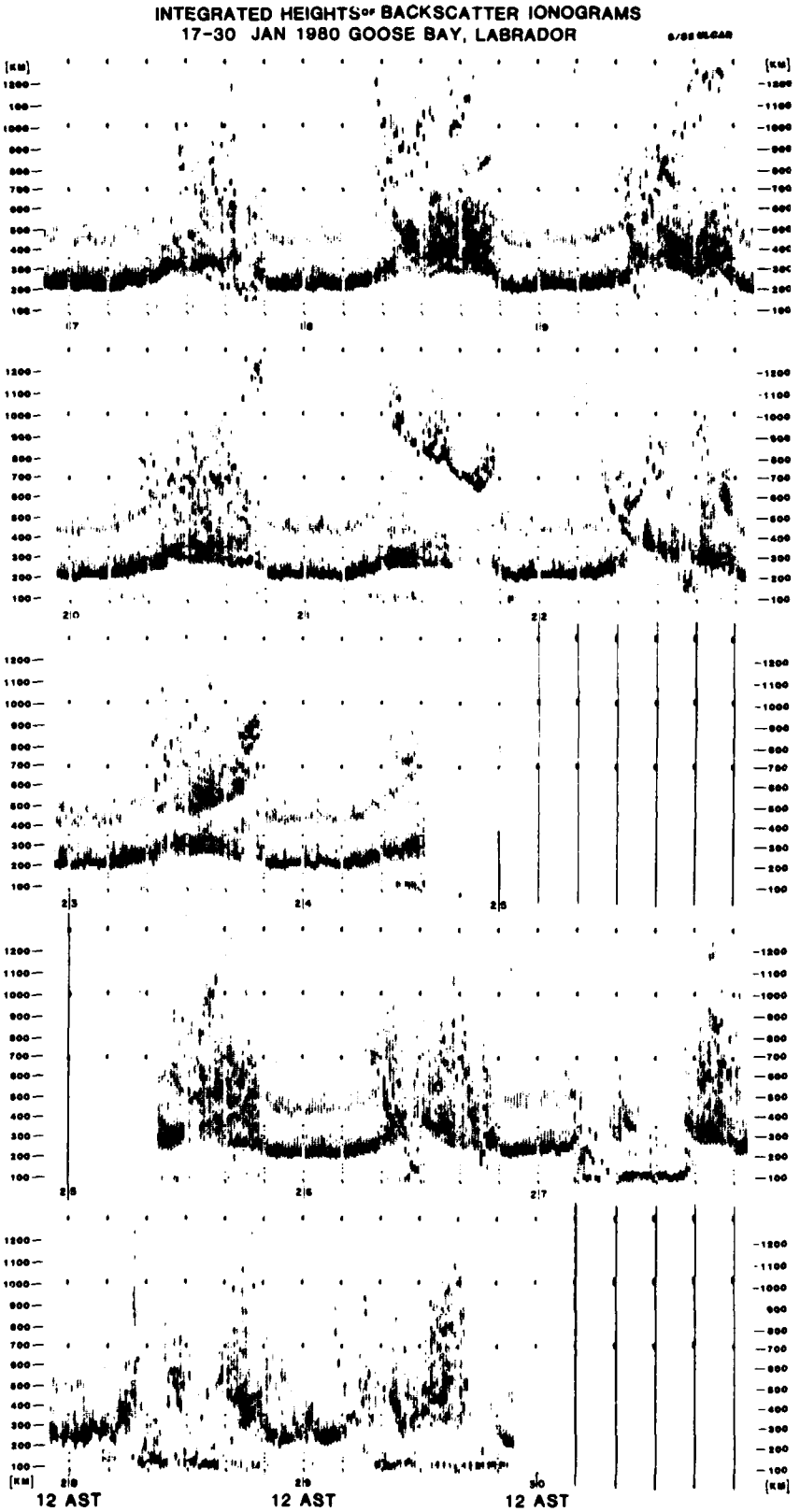
INTEGRATED HEIGHTS OF BACKSCATTER IONOGRAMS
17-30 JAN 1980 GOOSE BAY, LABRADOR
12 AST
12 AST
12 AST

Figure 11

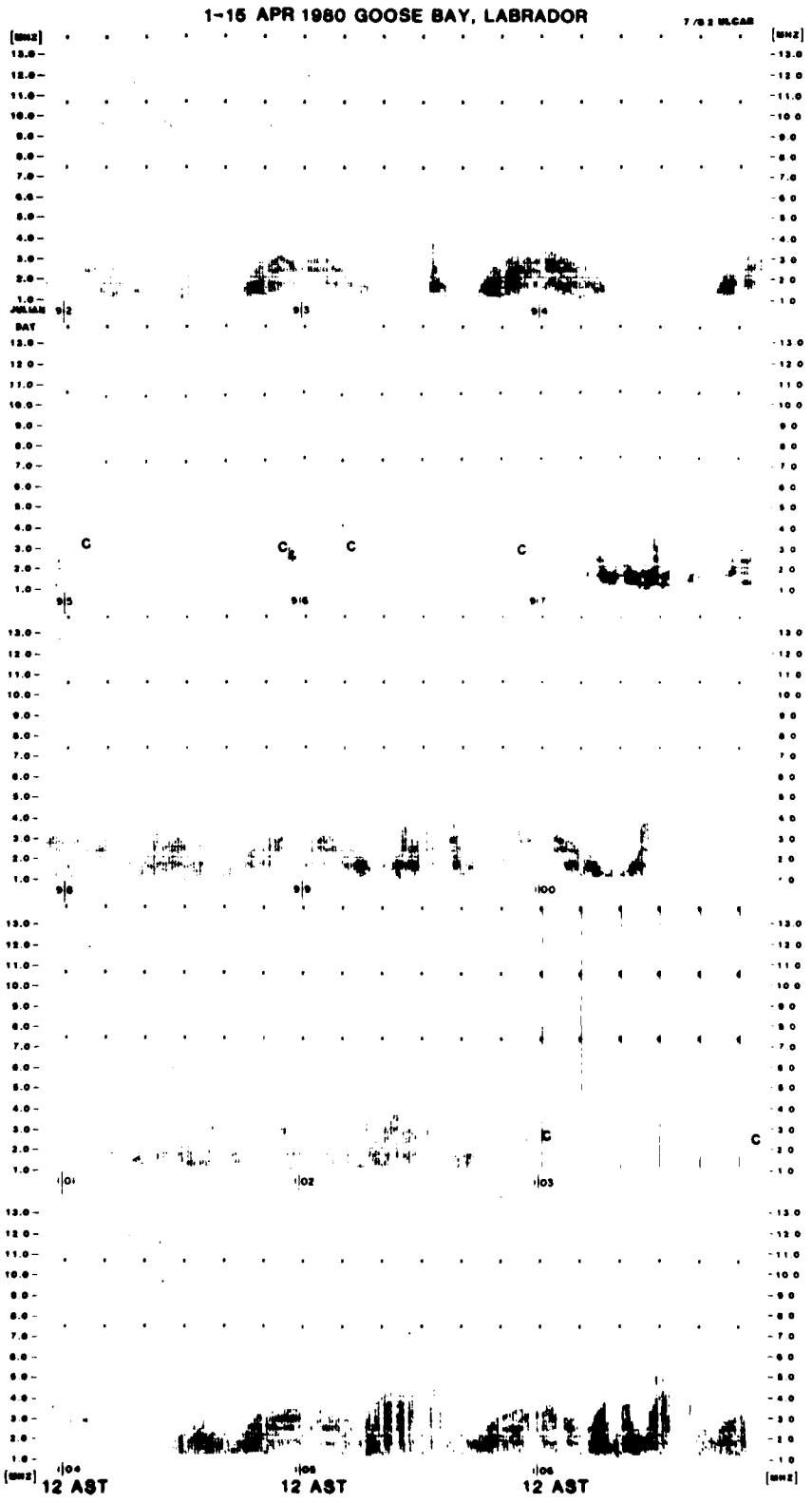
E REGION FREQUENCY CHARACTERISTICS ∞ VERTICAL IONOGRAMS
1-15 APR 1980 GOOSE BAY, LABRADOR
12 AST
12 AST
12 AST

Figure 12

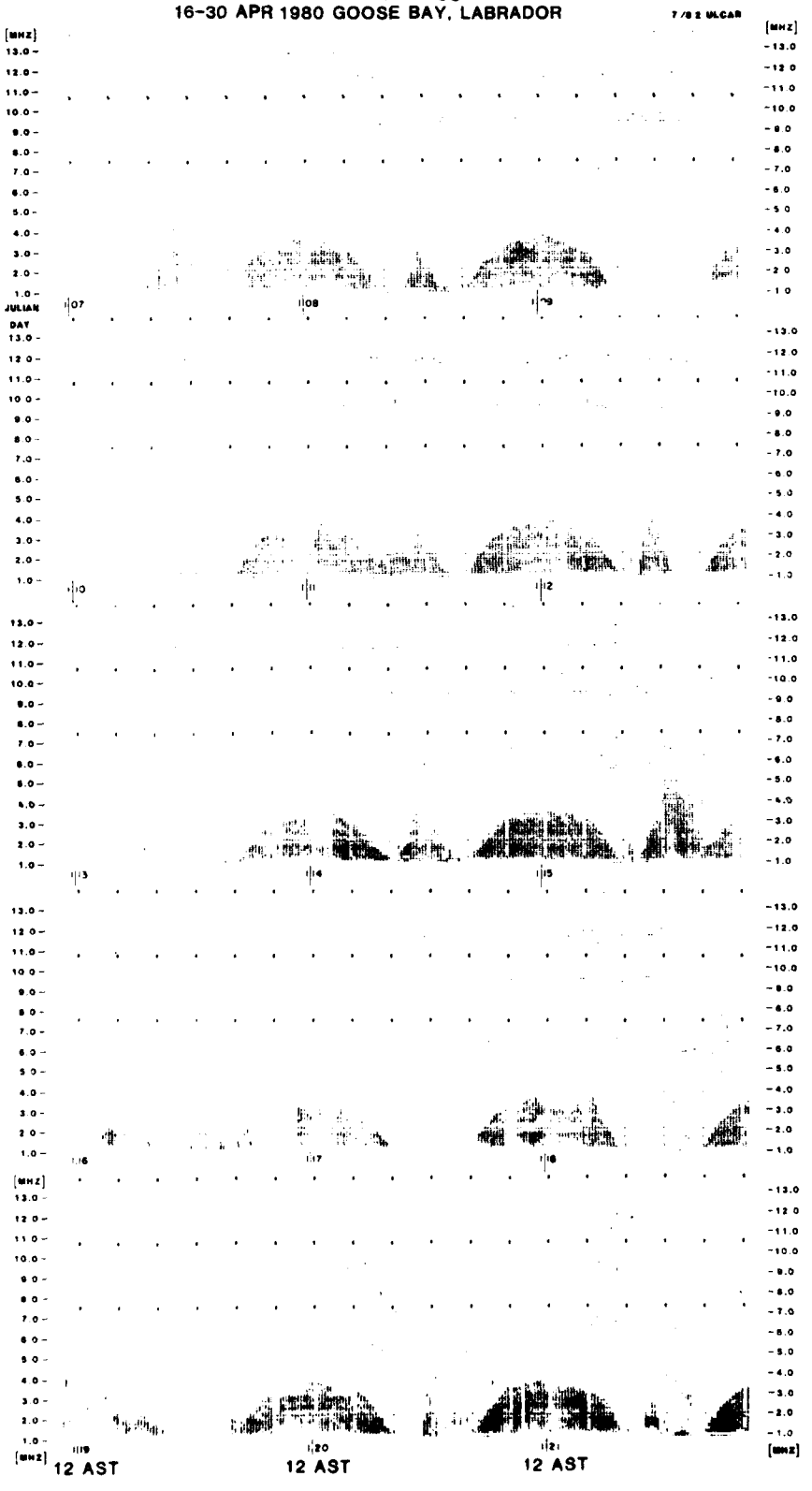
E REGION FREQUENCY CHARACTERISTICS OF VERTICAL IONOGRAMS
16-30 APR 1980 GOOSE BAY, LABRADOR
7/82 ULCAR
[MHZ]
JULIAN DAY
07
08
09
10
11
12
13
14
15
16
17
18
19
20
21
12 AST
12 AST
12 AST

Figure 13

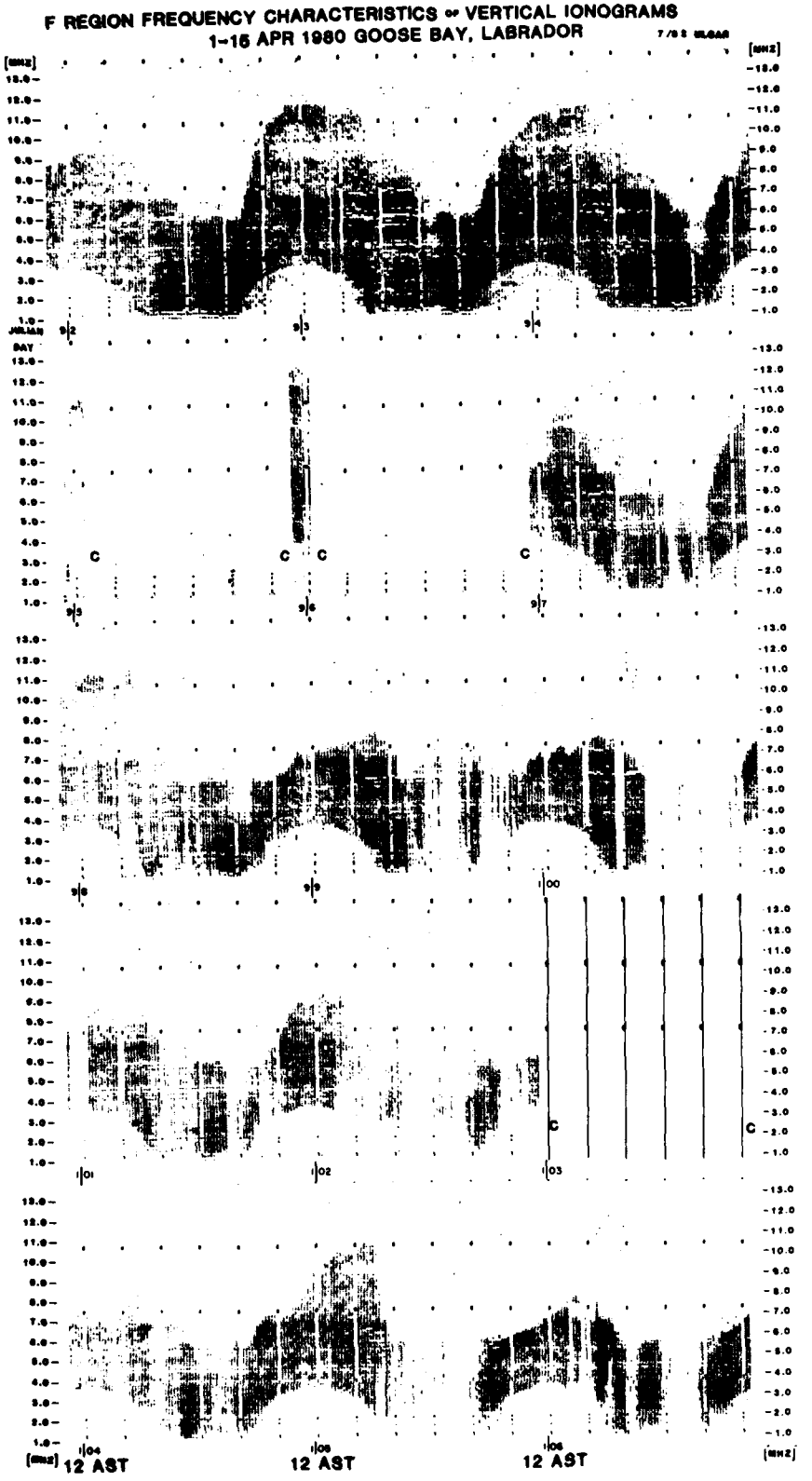
F REGION FREQUENCY CHARACTERISTICS ∞ VERTICAL IONOGRAMS
1-15 APR 1980 GOOSE BAY, LABRADOR
[MHz]
JULIAN DAY
12 AST
12 AST
12 AST
[MHz]

Figure 14

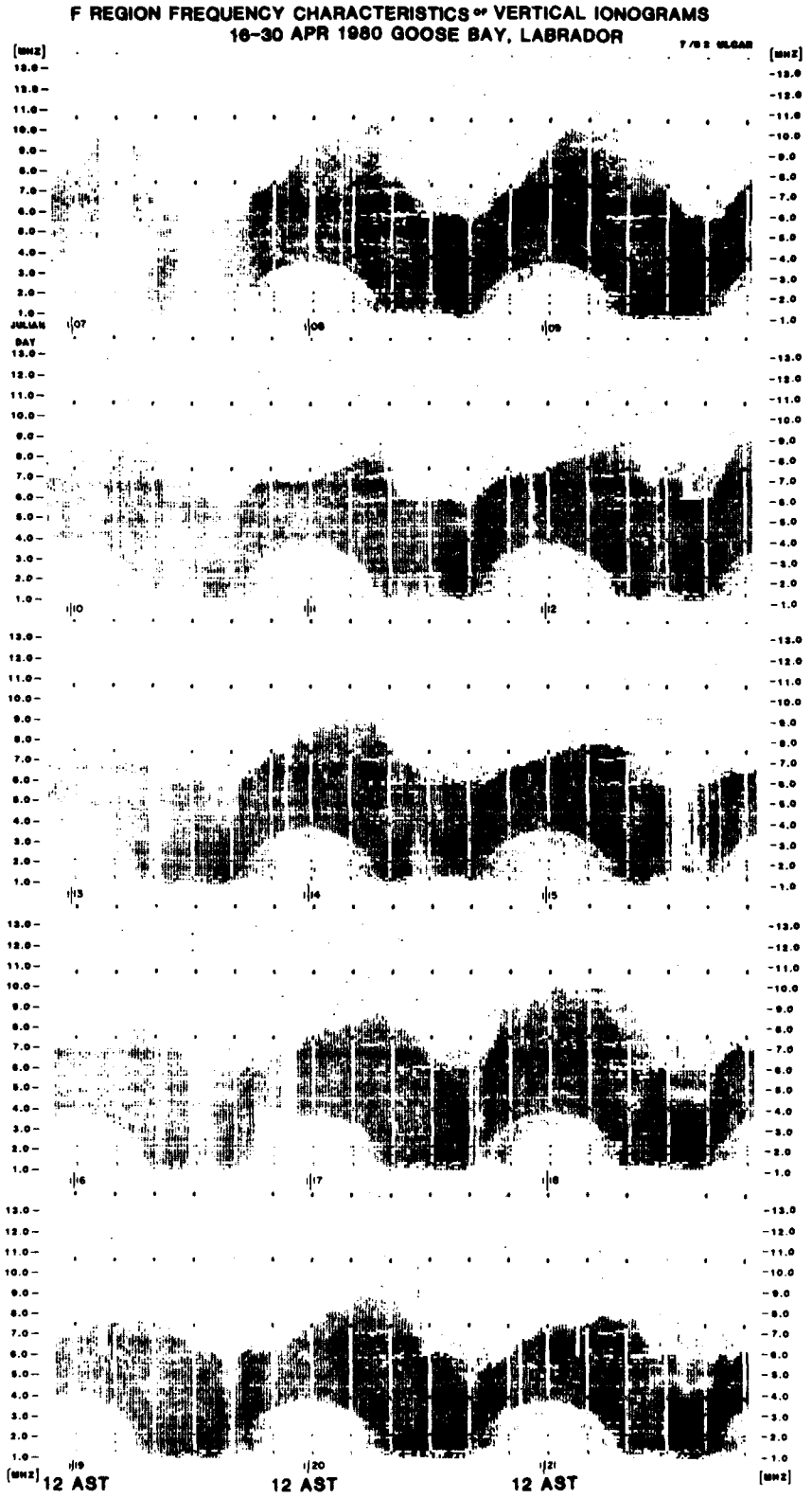
F REGION FREQUENCY CHARACTERISTICS OF VERTICAL IONOGRAMS
16-30 APR 1980 GOOSE BAY, LABRADOR
[MHZ]
JULIAN DAY
07
08
09
10
11
12
13
14
15
16
17
18
19
20
21
12 AST
12 AST
12 AST

Figure 15

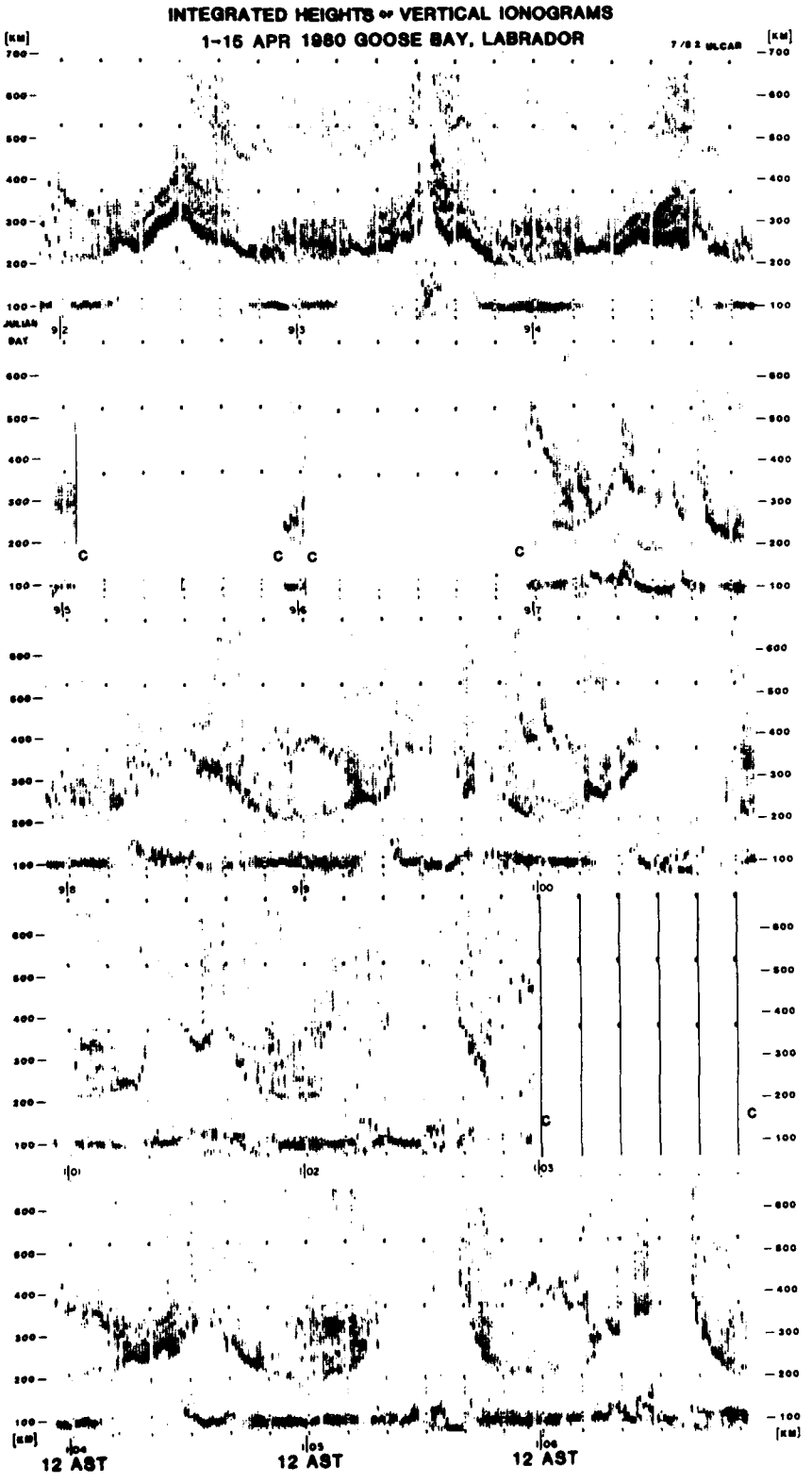
INTEGRATED HEIGHTS OF VERTICAL IONOGRAMS
1-15 APR 1980 GOOSE BAY, LABRADOR
[KM]
JULIAN DAY
9|2
9|3
9|4
9|5
9|6
9|7
9|8
9|9
10|0
10|1
10|2
10|3
10|4
10|5
10|6
C
12 AST
12 AST
12 AST

Figure 16

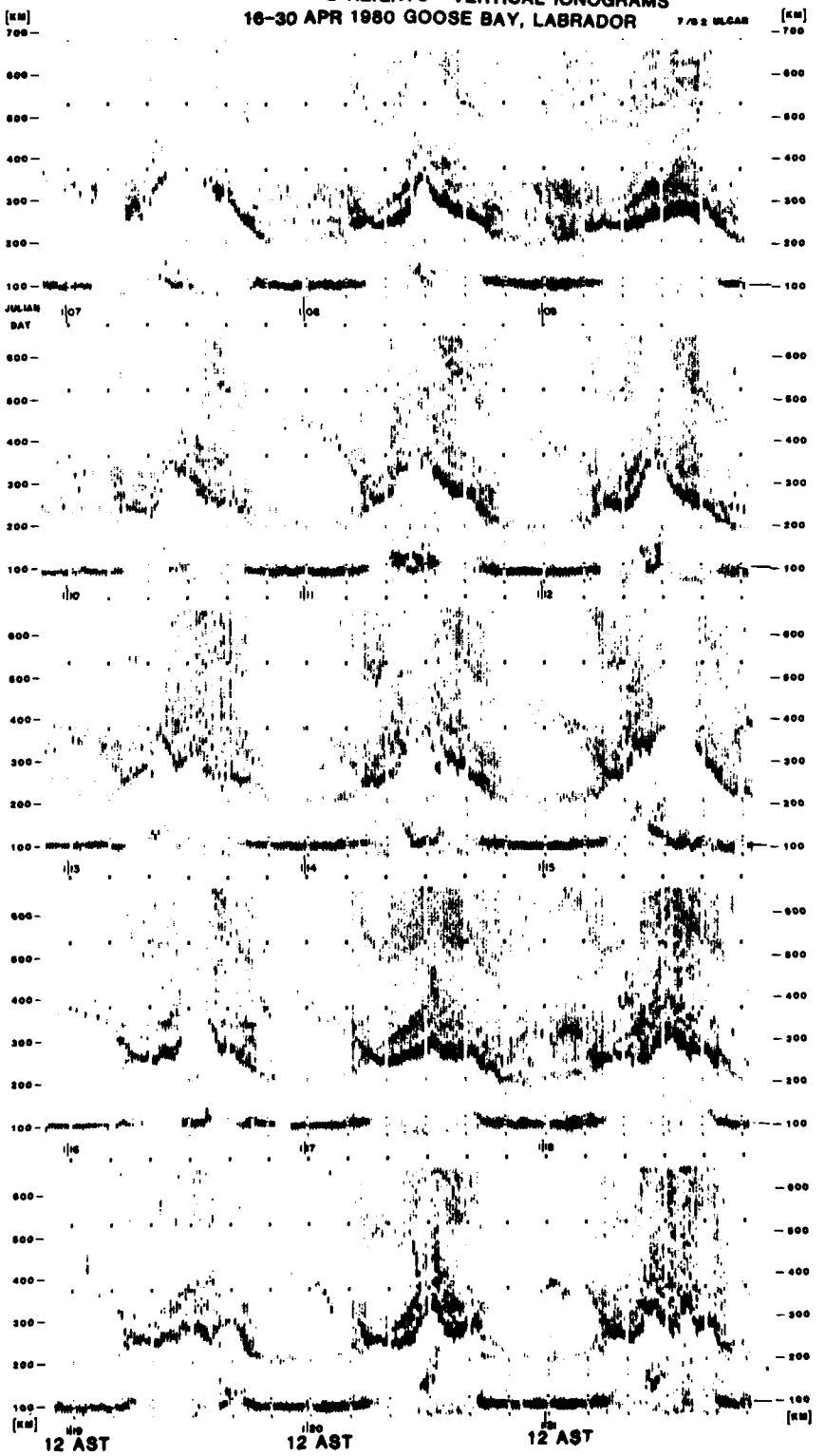
INTEGRATED HEIGHTS OF VERTICAL IONOGRAMS
16-30 APR 1980 GOOSE BAY, LABRADOR
[KM]
JULIAN DAY
12 AST
12 AST
12 AST

Figure 17

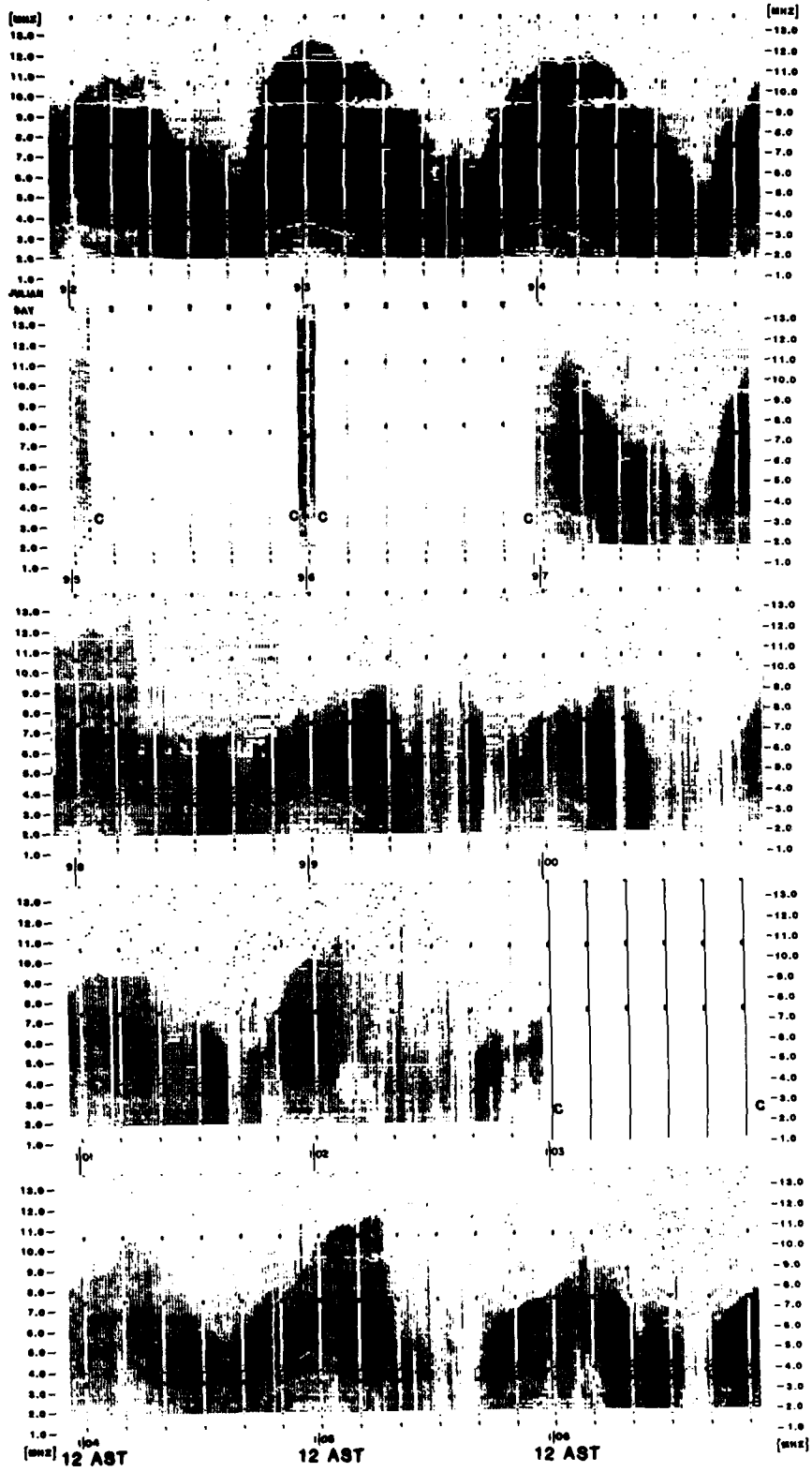
F REGION FREQUENCY CHARACTERISTICS OF BACKSCATTER IONOGRAMS
1-15 APR 1980 GOOSE BAY, LABRADOR
12 AST
12 AST
12 AST

Figure 18

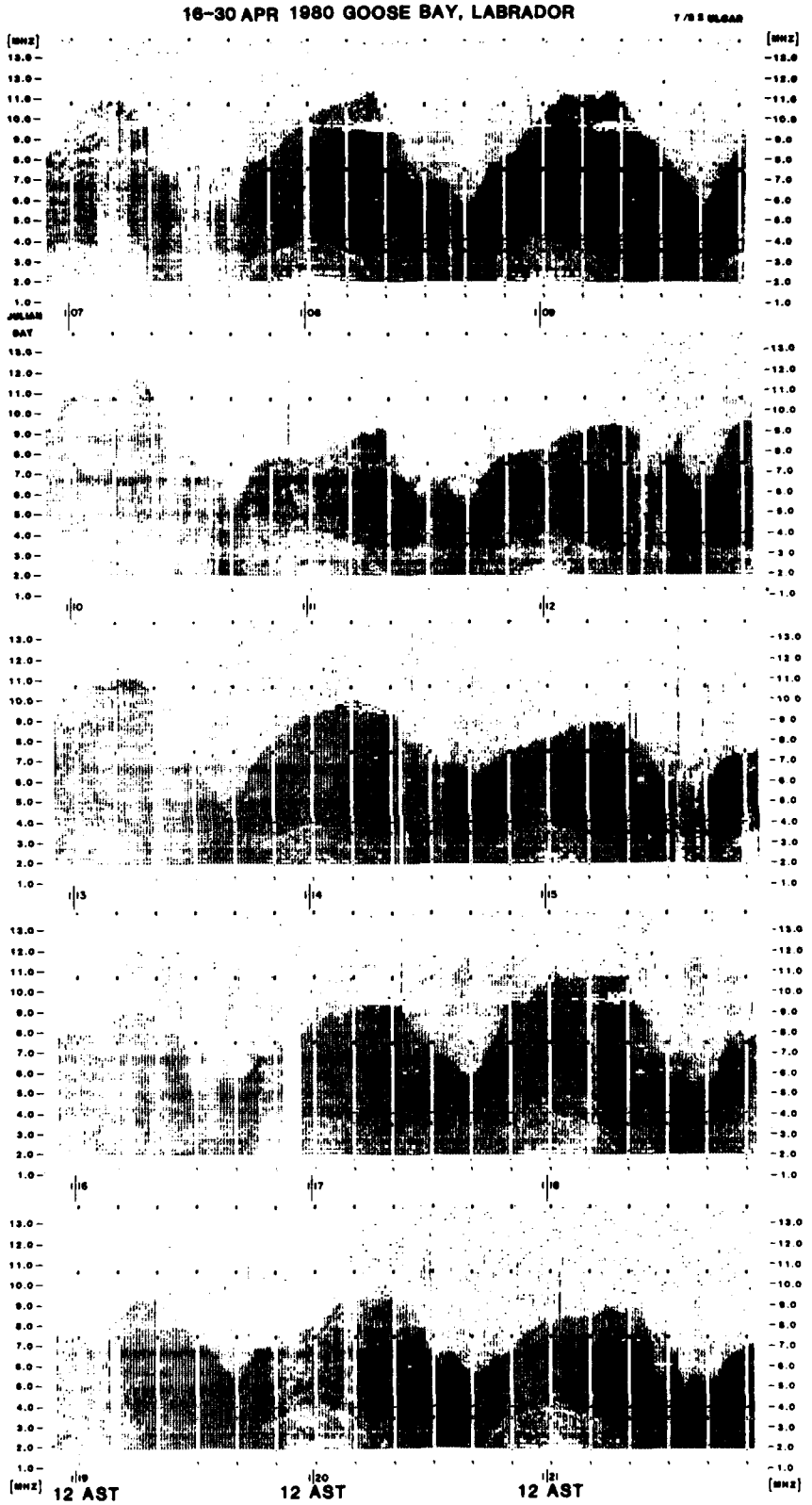
F REGION FREQUENCY CHARACTERISTICS OF BACKSCATTER IONOGRAMS
16-30 APR 1980 GOOSE BAY, LABRADOR
[MHZ]
JULIAN DAY
12 AST
12 AST
12 AST

Figure 19

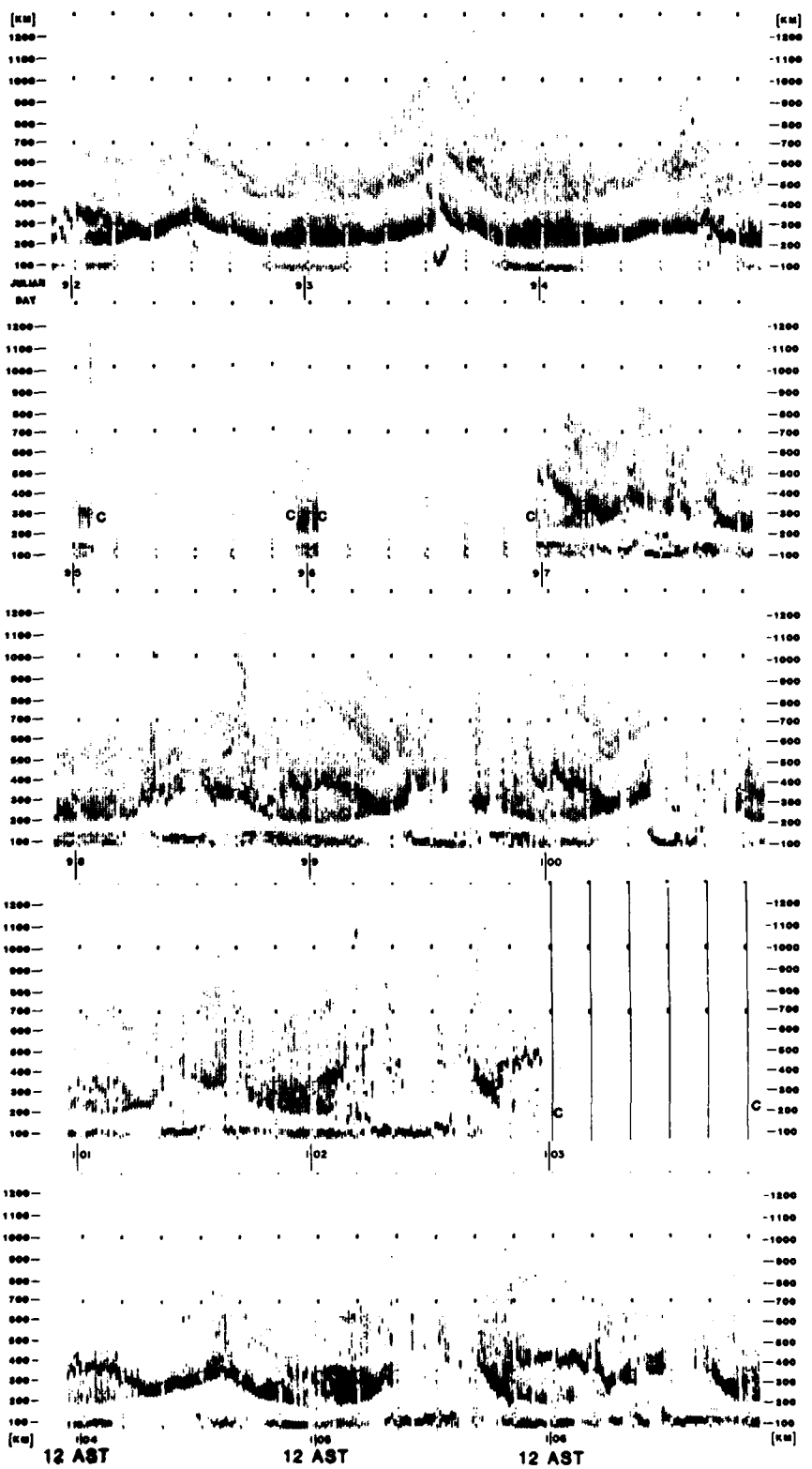
INTEGRATED HEIGHTS OF BACKSCATTER IONOGRAMS
1-15 APR 1980 GOOSE BAY, LABRADOR
12 AST
12 AST
12 AST

Figure 20

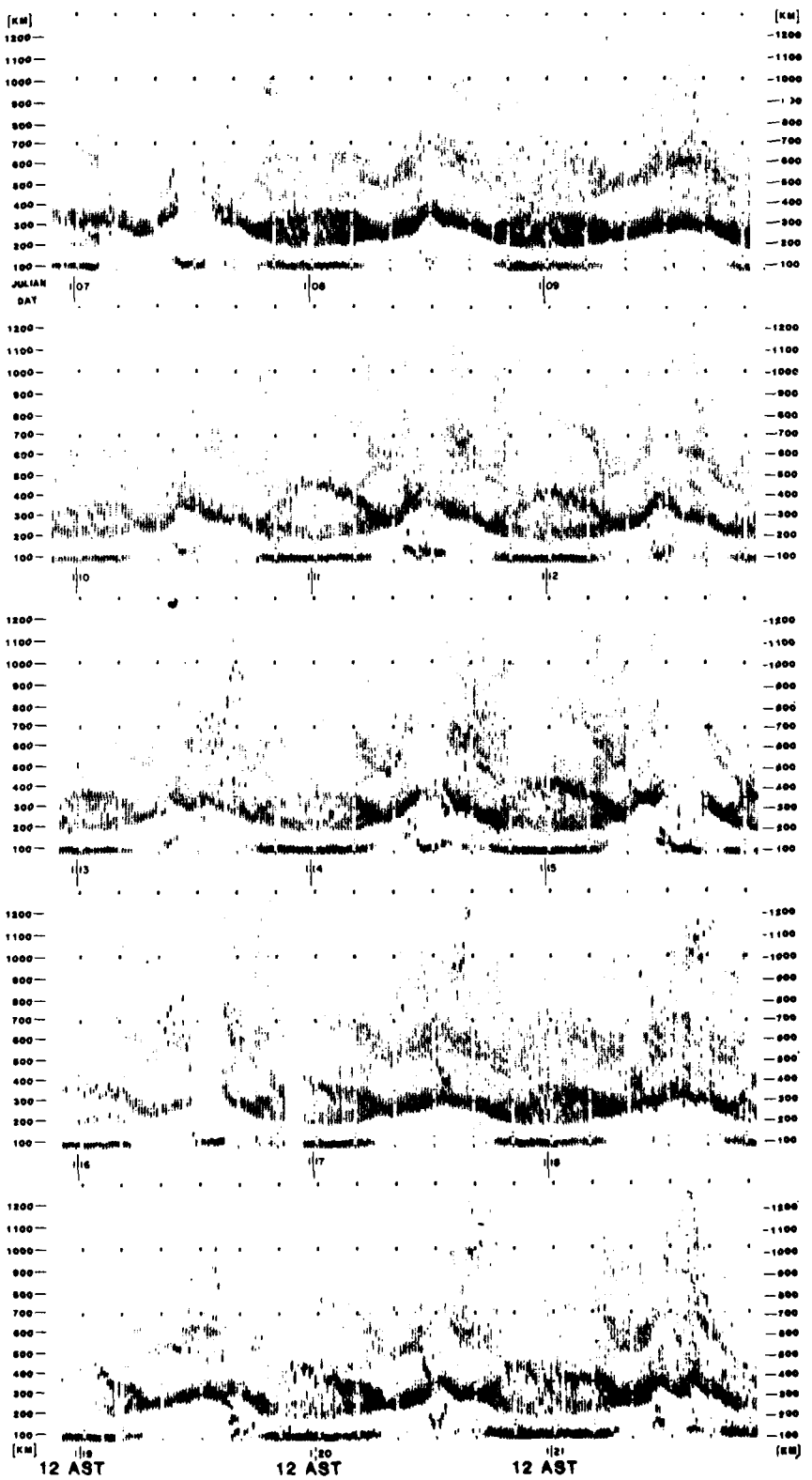
INTEGRATED HEIGHTS OF BACKSCATTER IONOGRAMS
16-30 APR 1980 GOOSE BAY, LABRADOR
7/82 MLCAB
[KM]
JULIAN DAY
07
08
09
10
11
12
13
14
15
16
17
18
19
20
21
12 AST
12 AST
12 AST

Figure 21

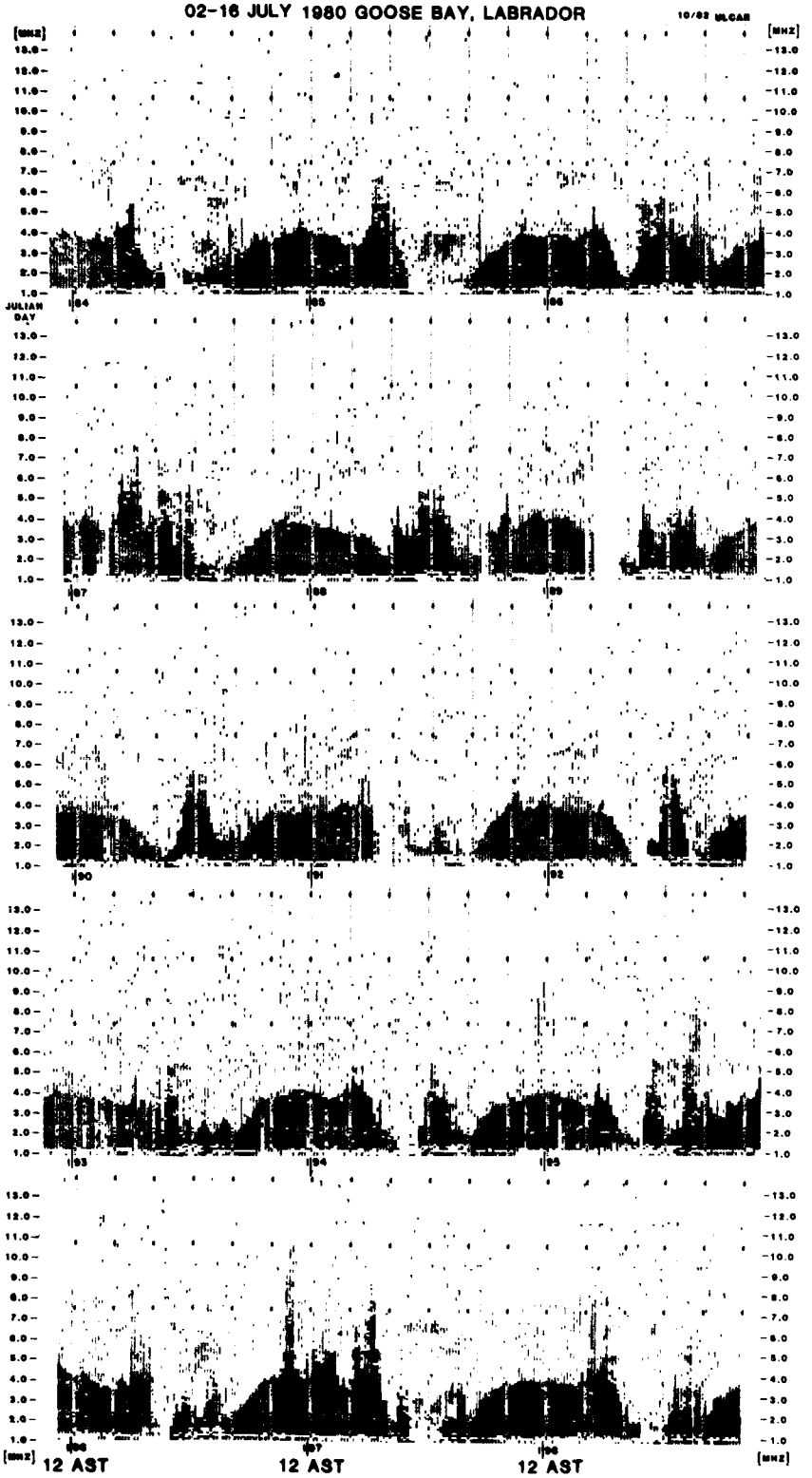
E REGION FREQUENCY CHARACTERISTICS OF VERTICAL IONOGRAMS
02-16 JULY 1980 GOOSE BAY, LABRADOR
10/83 MLCAR
[MHZ]
JULIAN DAY
12 AST
12 AST
12 AST
[MHZ]

Figure 22

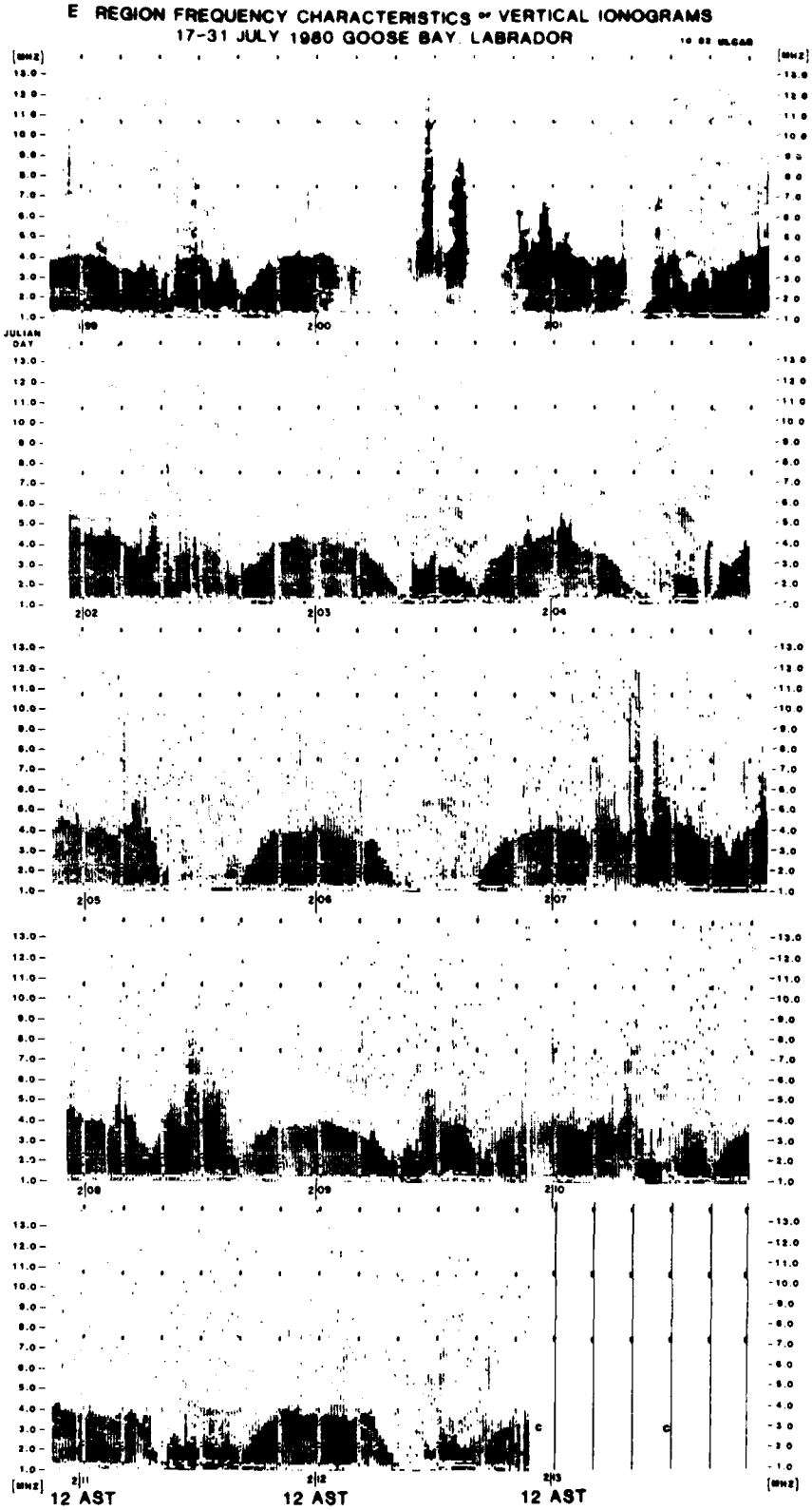
E REGION FREQUENCY CHARACTERISTICS OF VERTICAL IONOGRAMS
17-31 JULY 1980 GOOSE BAY, LABRADOR
JULIAN DAY
12 AST
12 AST
12 AST

Figure 23

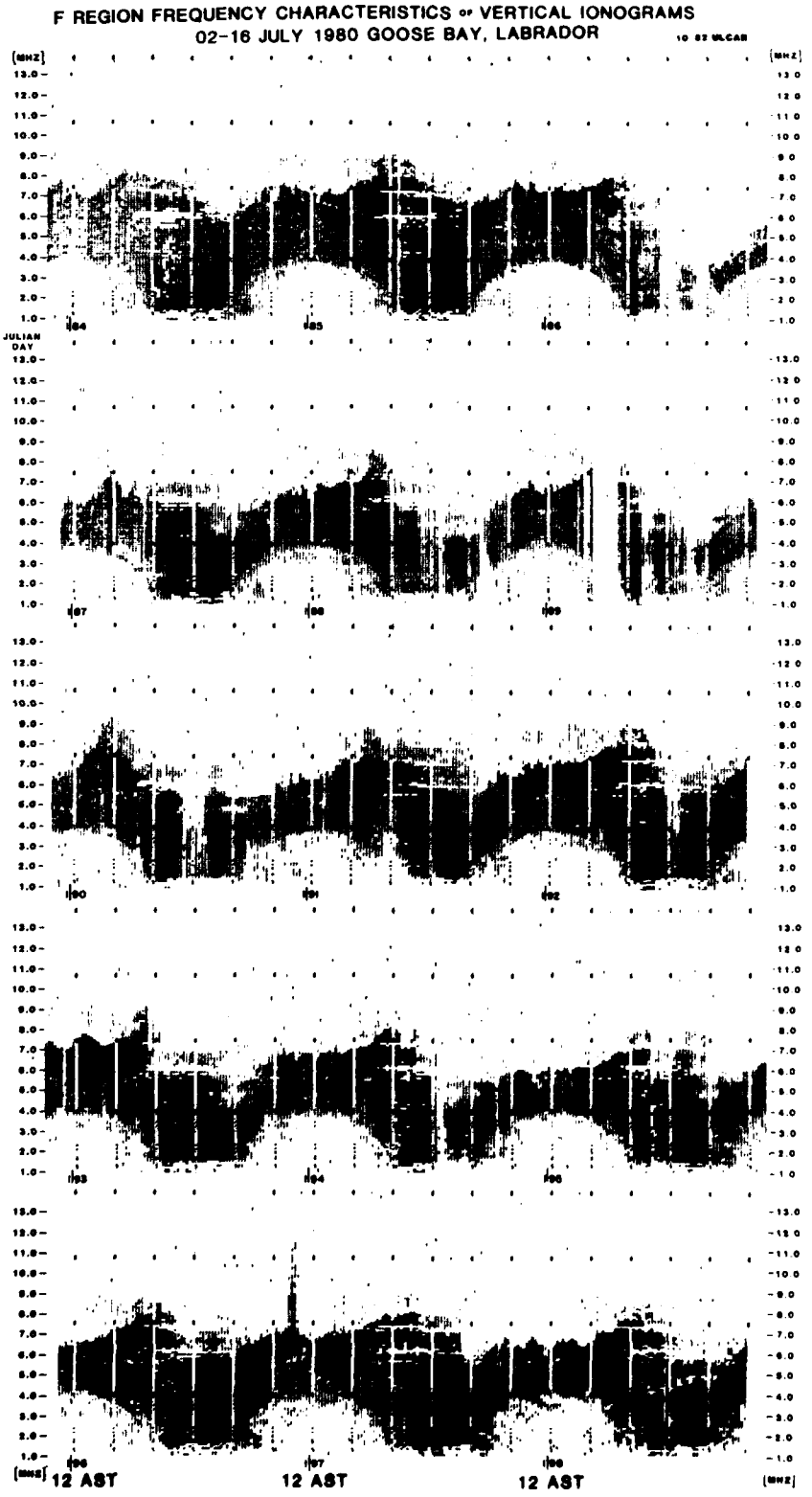
F REGION FREQUENCY CHARACTERISTICS OF VERTICAL IONOGRAMS
02-16 JULY 1980 GOOSE BAY, LABRADOR
JULIAN DAY
12 AST
12 AST
12 AST

Figure 24

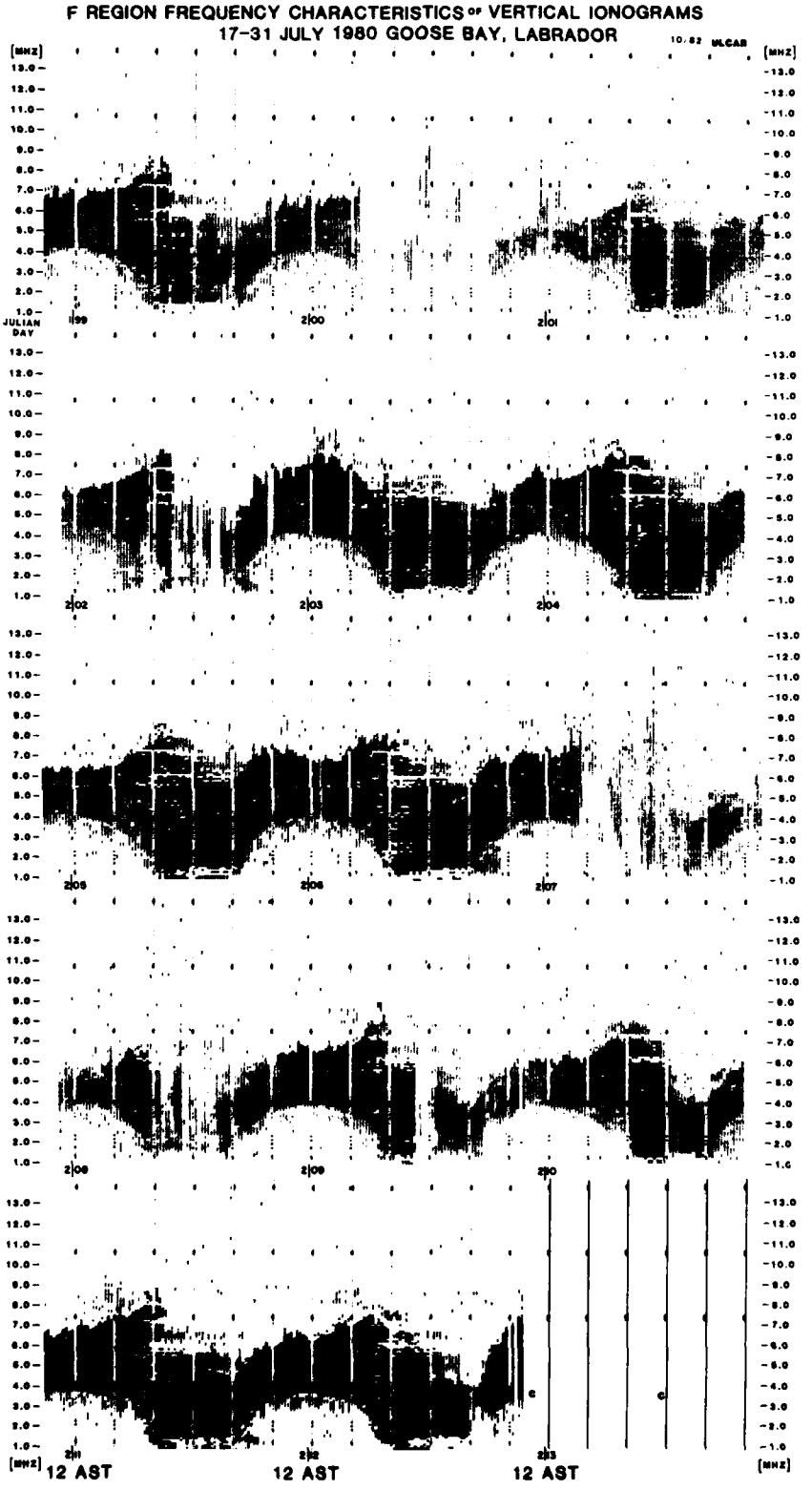
F REGION FREQUENCY CHARACTERISTICS OF VERTICAL IONOGRAMS
17-31 JULY 1980 GOOSE BAY, LABRADOR
10.82 WLCAB
[MHZ]
JULIAN DAY
199
200
201
202
203
204
205
206
207
208
209
210
211
212
213
12 AST
12 AST
12 AST

Figure 25

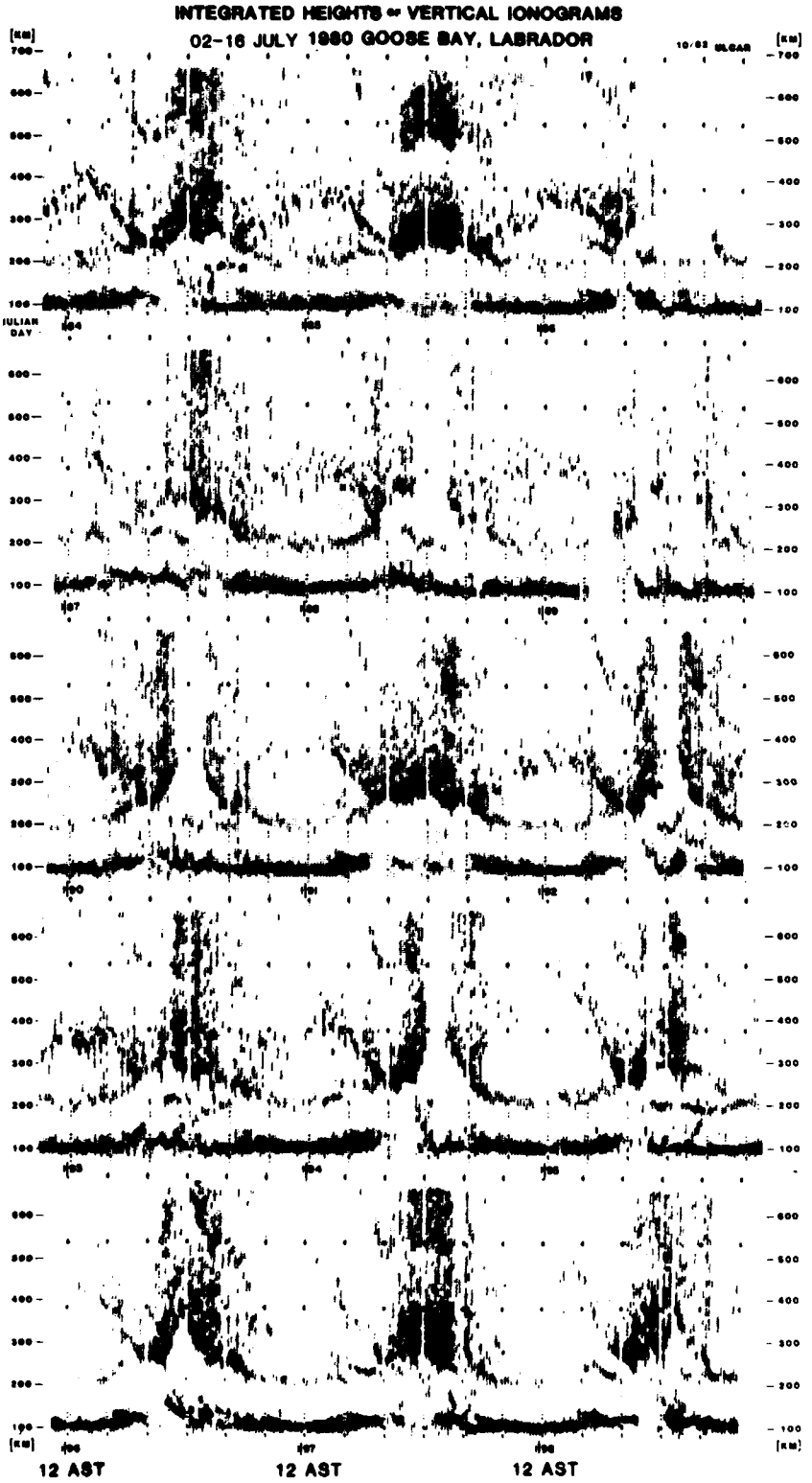
INTEGRATED HEIGHTS of VERTICAL IONOGRAMS
02-16 JULY 1980 GOOSE BAY, LABRADOR
JULIAN DAY
12 AST
12 AST
12 AST

Figure 26

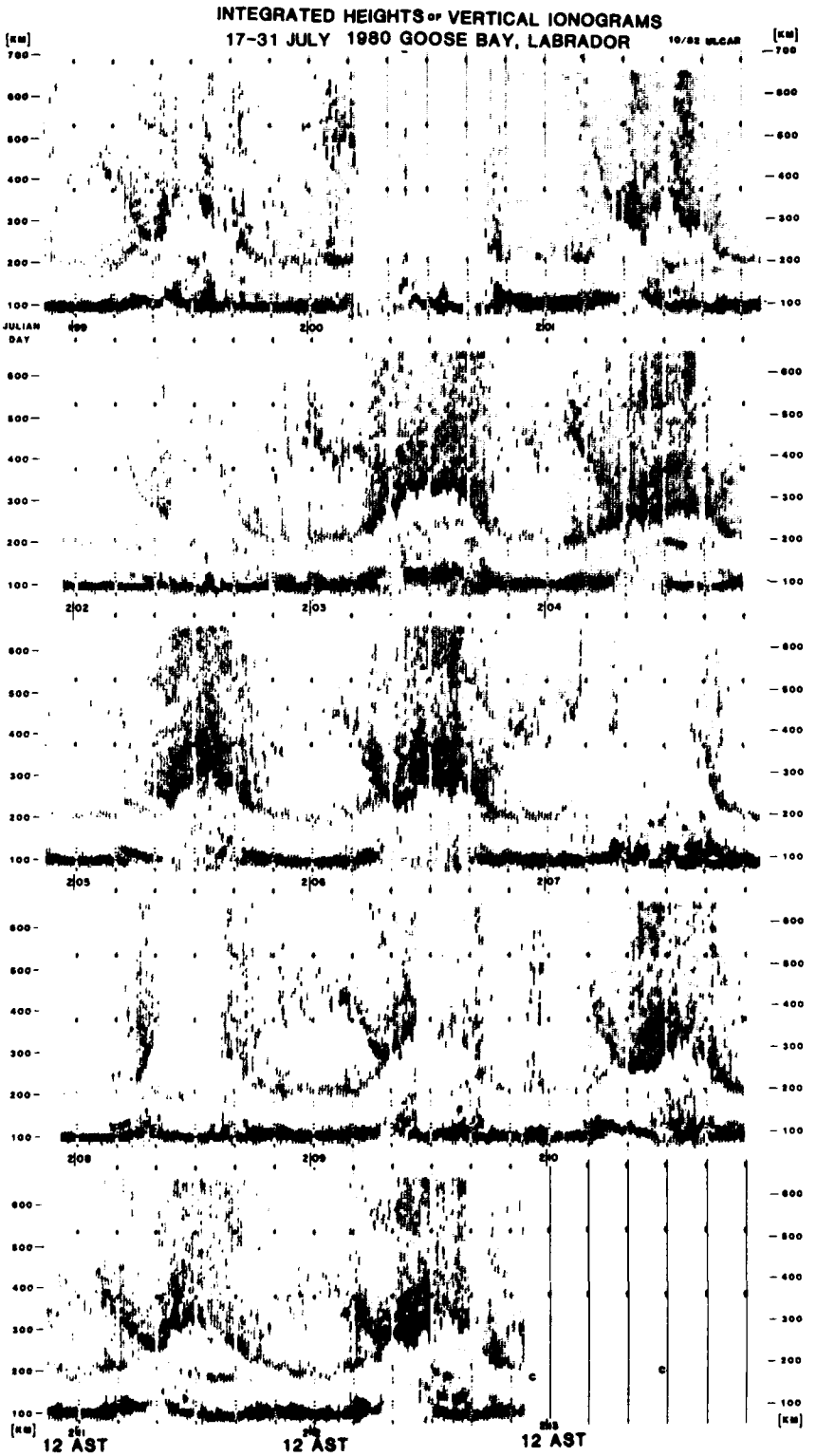
INTEGRATED HEIGHTS OF VERTICAL IONOGRAMS
17-31 JULY 1980 GOOSE BAY, LABRADOR
[KM]
JULIAN DAY
199
200
201
202
203
204
205
206
207
208
209
210
211
212
213
12 AST
12 AST
12 AST

Figure 27

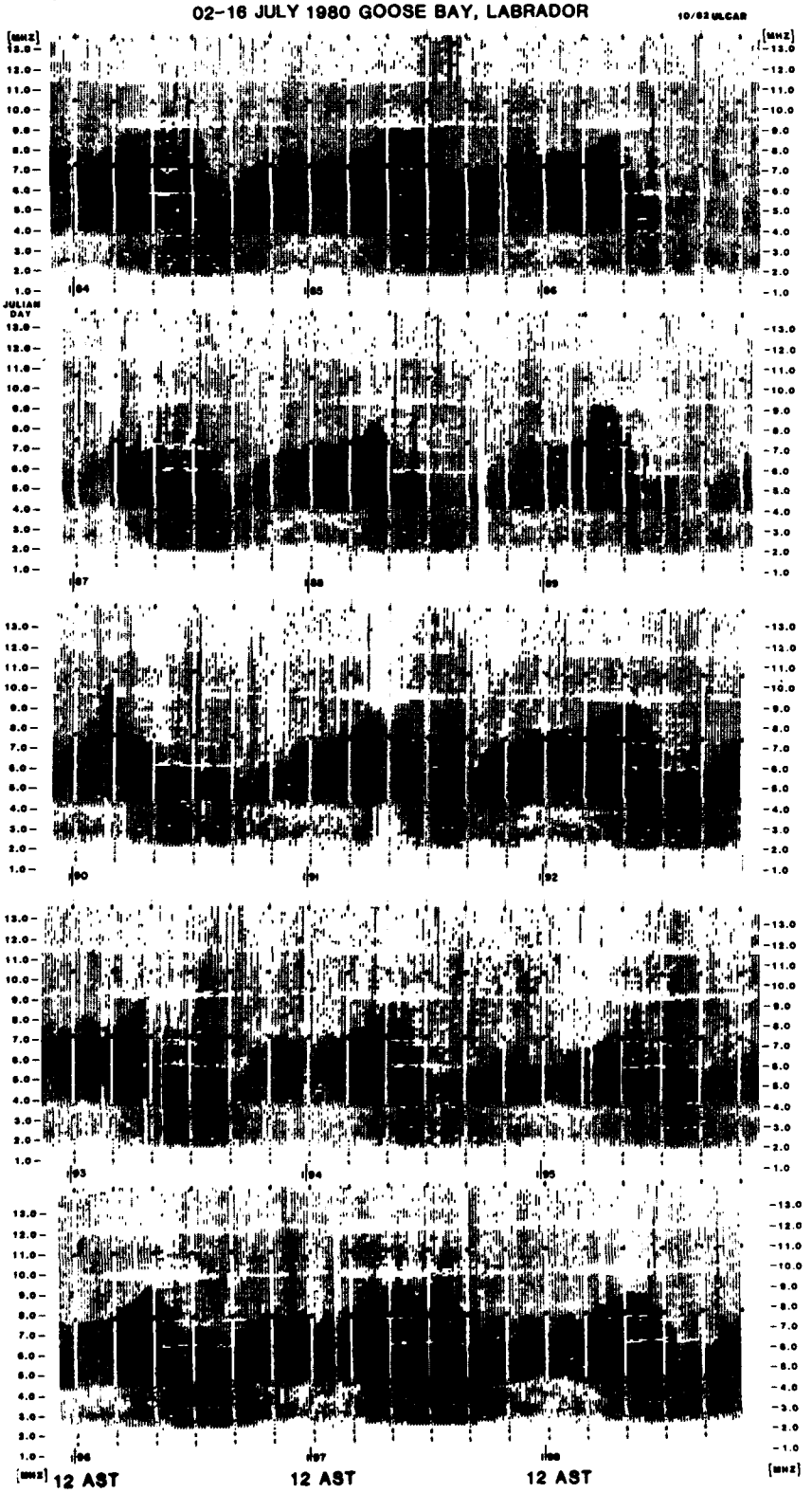
F REGION FREQUENCY CHARACTERISTICS OF BACKSCATTER IONOGRAMS
02-16 JULY 1980 GOOSE BAY, LABRADOR
JULIAN DAY
12 AST
12 AST
12 AST

Figure 28

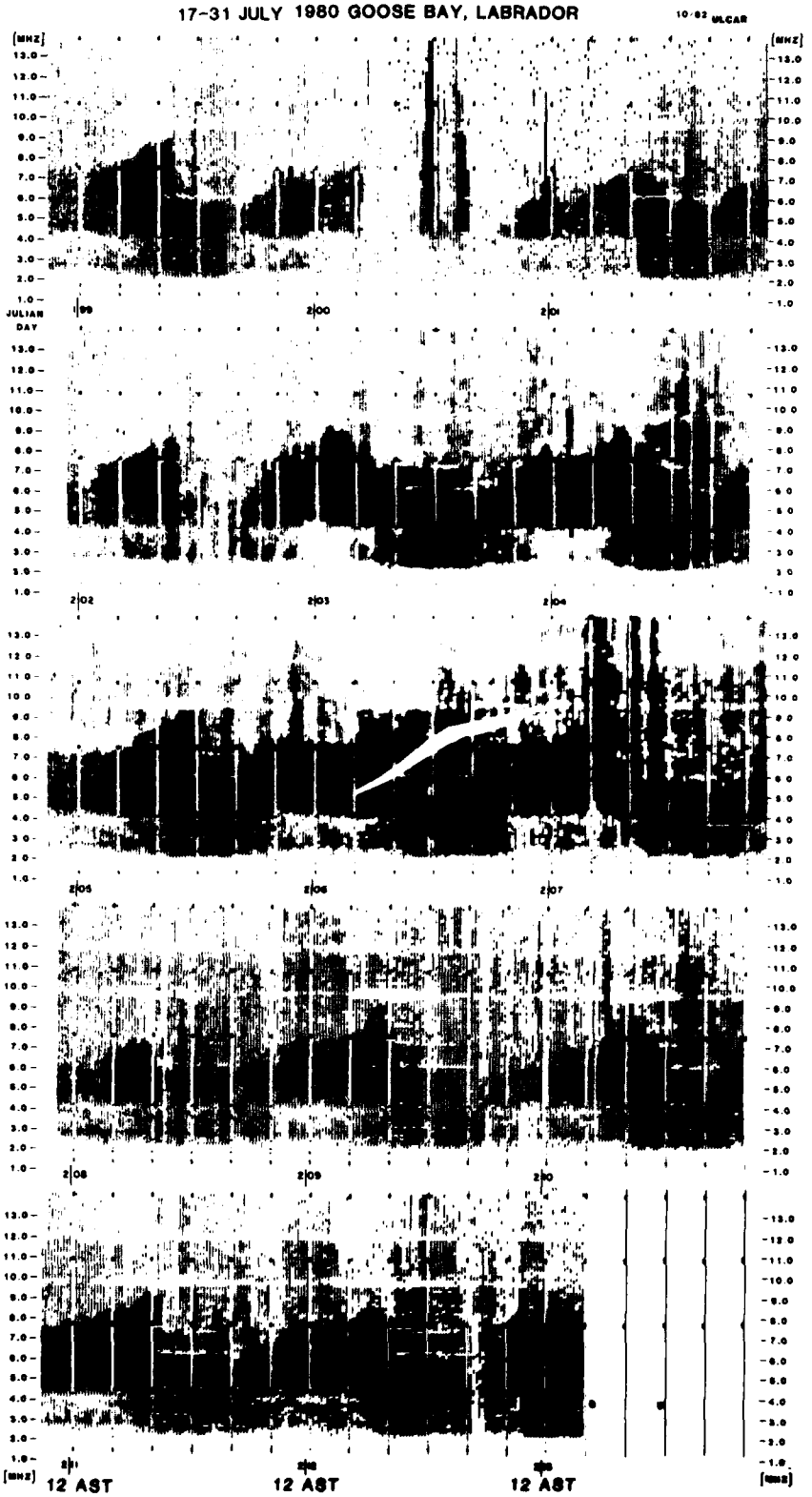
F REGION FREQUENCY CHARACTERISTICS OF BACKSCATTER IONOGRAMS
17-31 JULY 1980 GOOSE BAY, LABRADOR
10/82 ULCAR
[MHZ]
JULIAN DAY
12 AST
12 AST
12 AST
[MHZ]

Figure 29

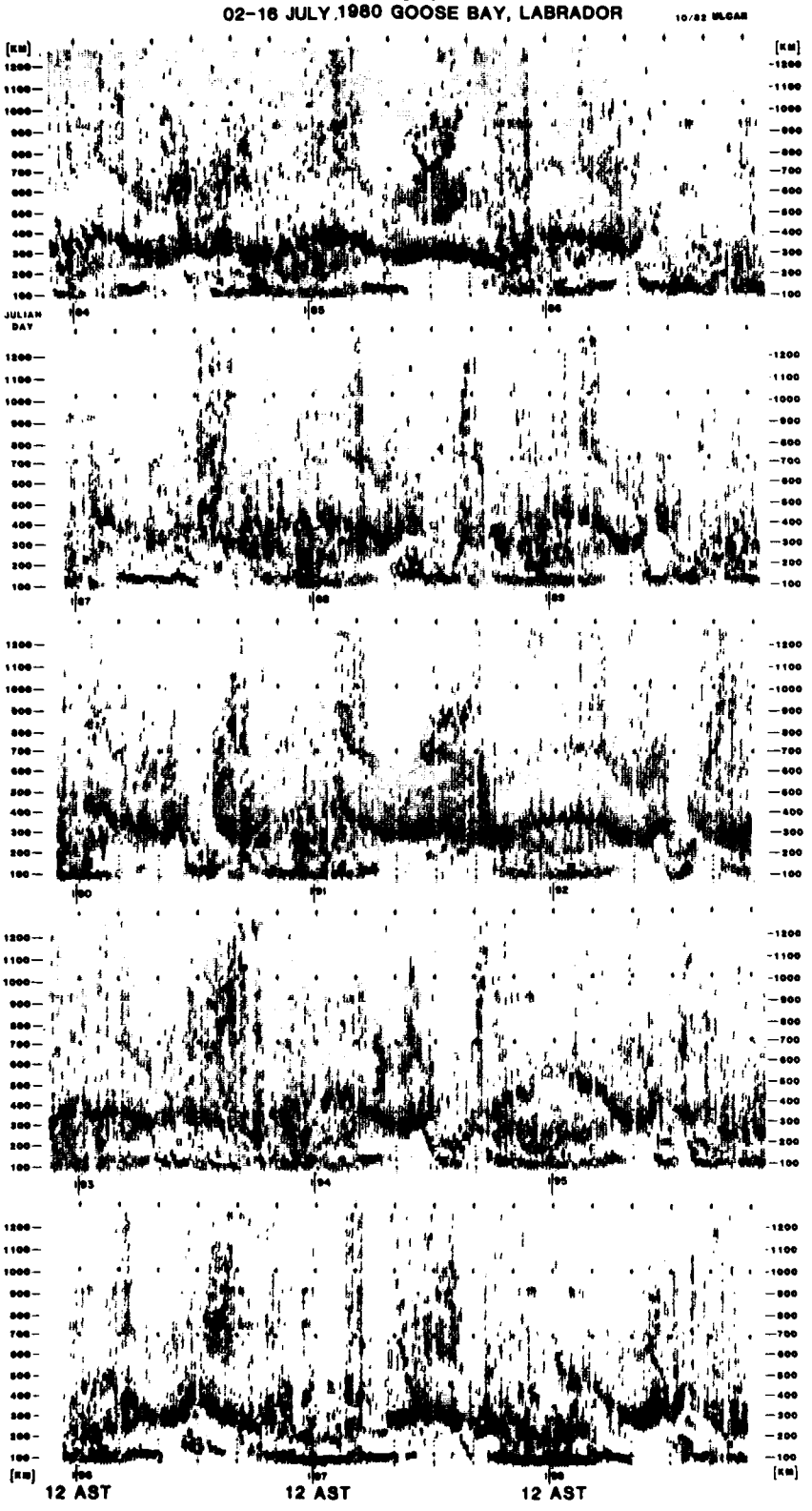
INTEGRATED HEIGHTS OF BACKSCATTER IONOGRAMS
02-16 JULY 1980 GOOSE BAY, LABRADOR
10/82 WLCAR
[KM]
JULIAN DAY
12 AST
12 AST
12 AST

Figure 30

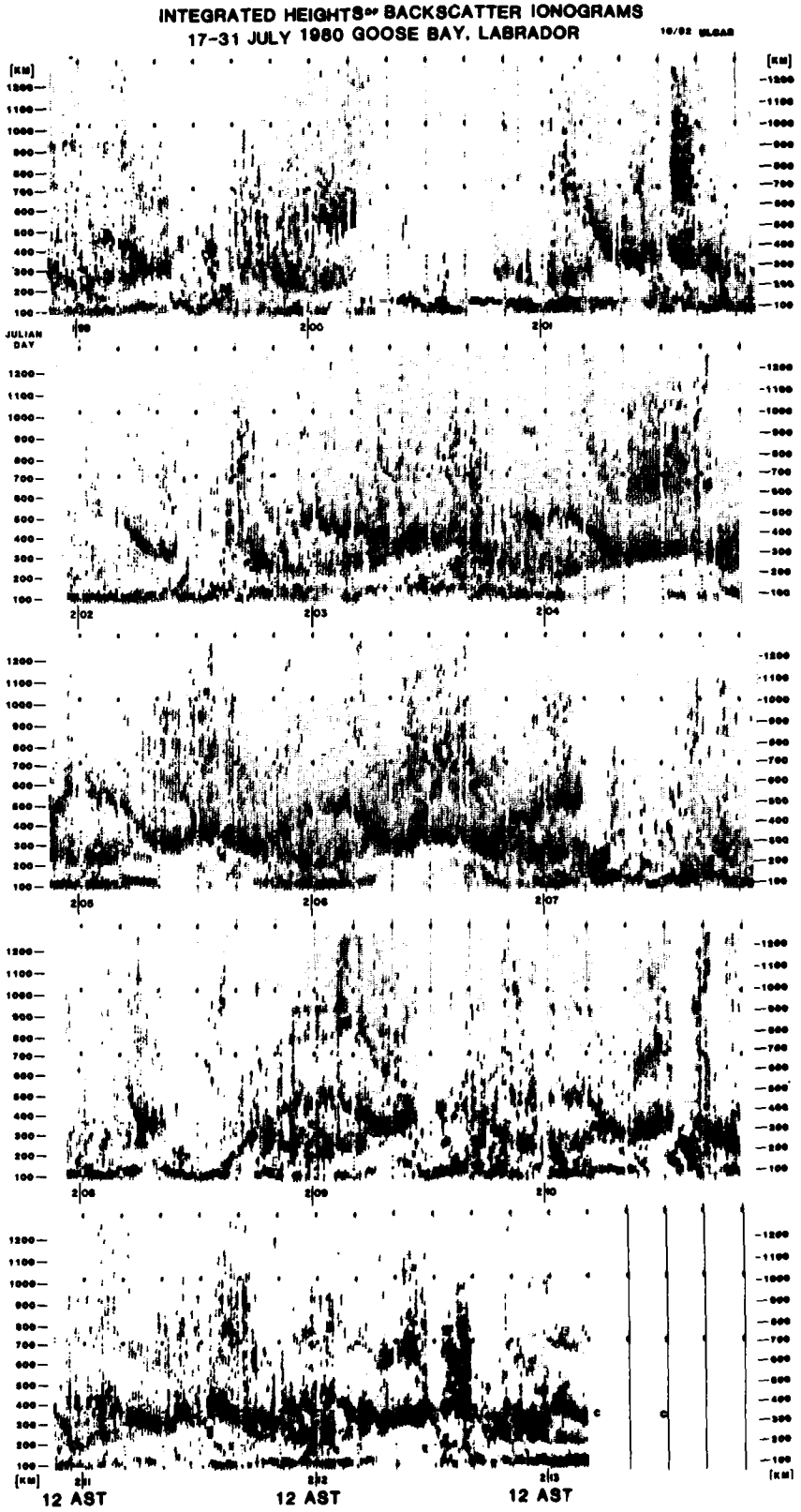
INTEGRATED HEIGHTS OF BACKSCATTER IONOGRAMS
17-31 JULY 1980 GOOSE BAY, LABRADOR
[KM]
JULIAN DAY
12 AST
12 AST
12 AST

Figure 31

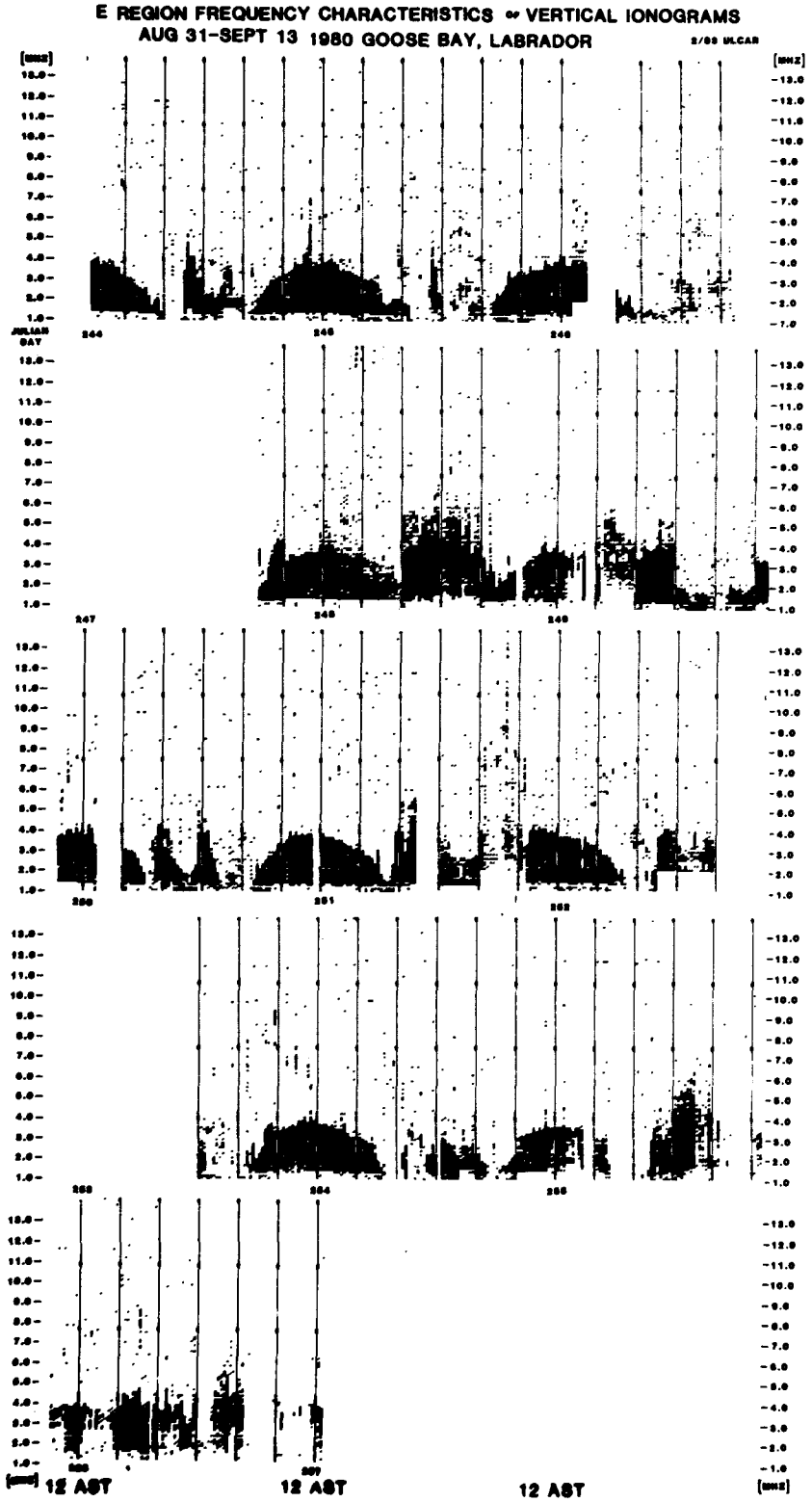
E REGION FREQUENCY CHARACTERISTICS ∞ VERTICAL IONOGRAMS
AUG 31-SEPT 13 1980 GOOSE BAY, LABRADOR
12 AST
12 AST
12 AST

Figure 32

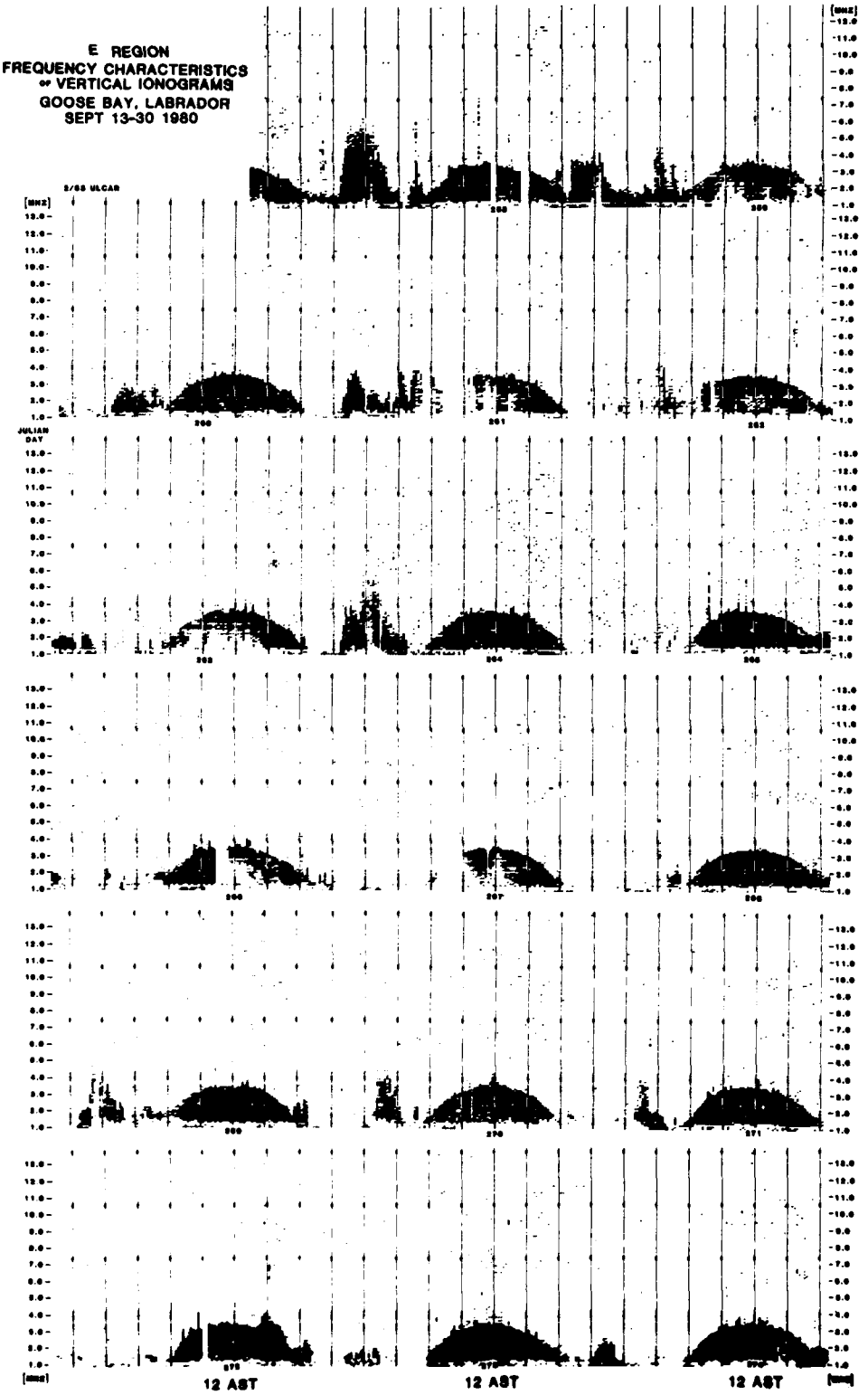
E REGION
FREQUENCY CHARACTERISTICS
OF VERTICAL IONOGRAMS
GOOSE BAY, LABRADOR
SEPT 13-30 1980
12 AST
12 AST
12 AST

Figure 33

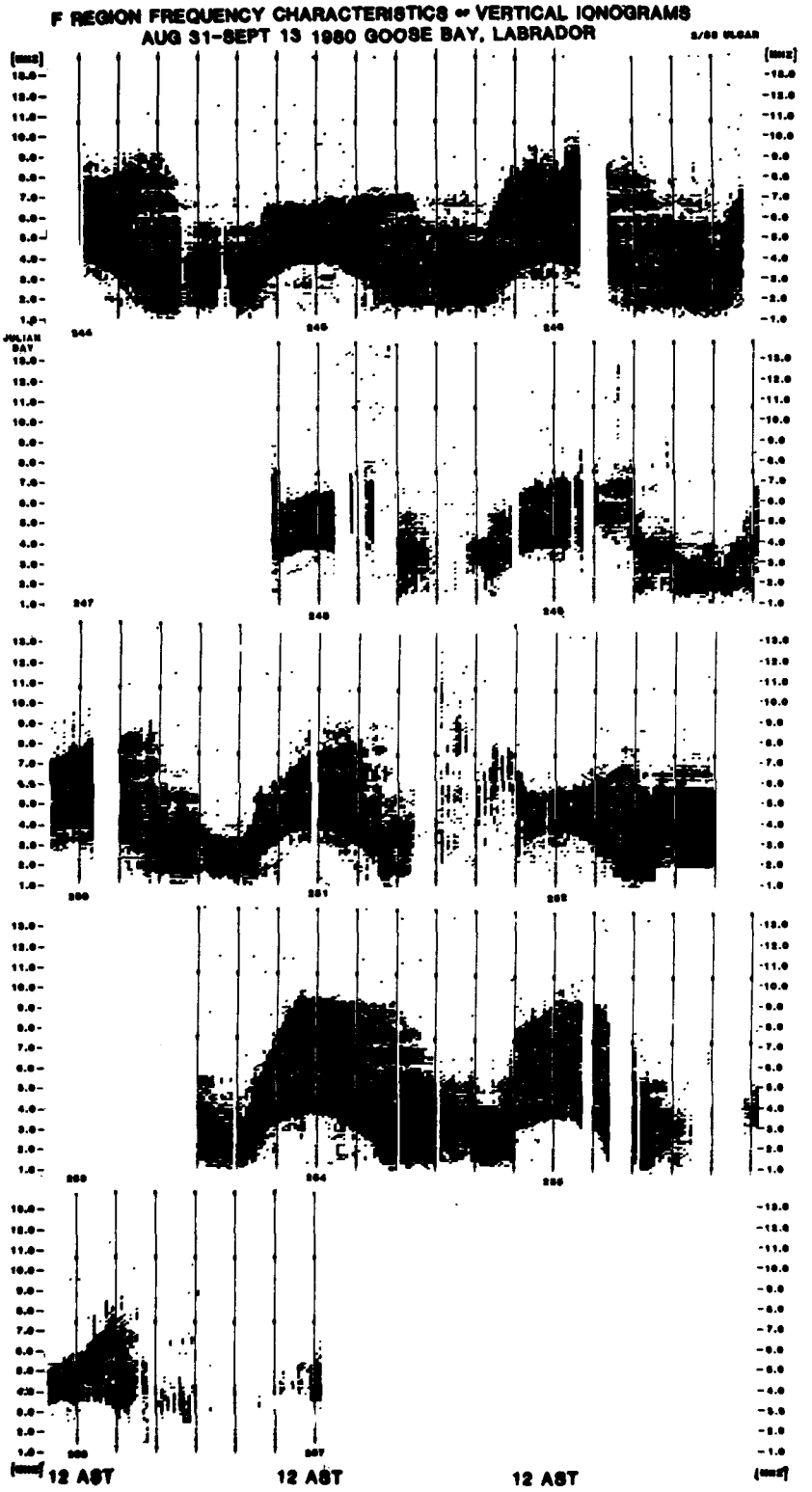
F REGION FREQUENCY CHARACTERISTICS OF VERTICAL IONOGRAMS
AUG 31-SEPT 13 1980 GOOSE BAY, LABRADOR
JULIAN DAY
12 AST
12 AST
12 AST

Figure 34

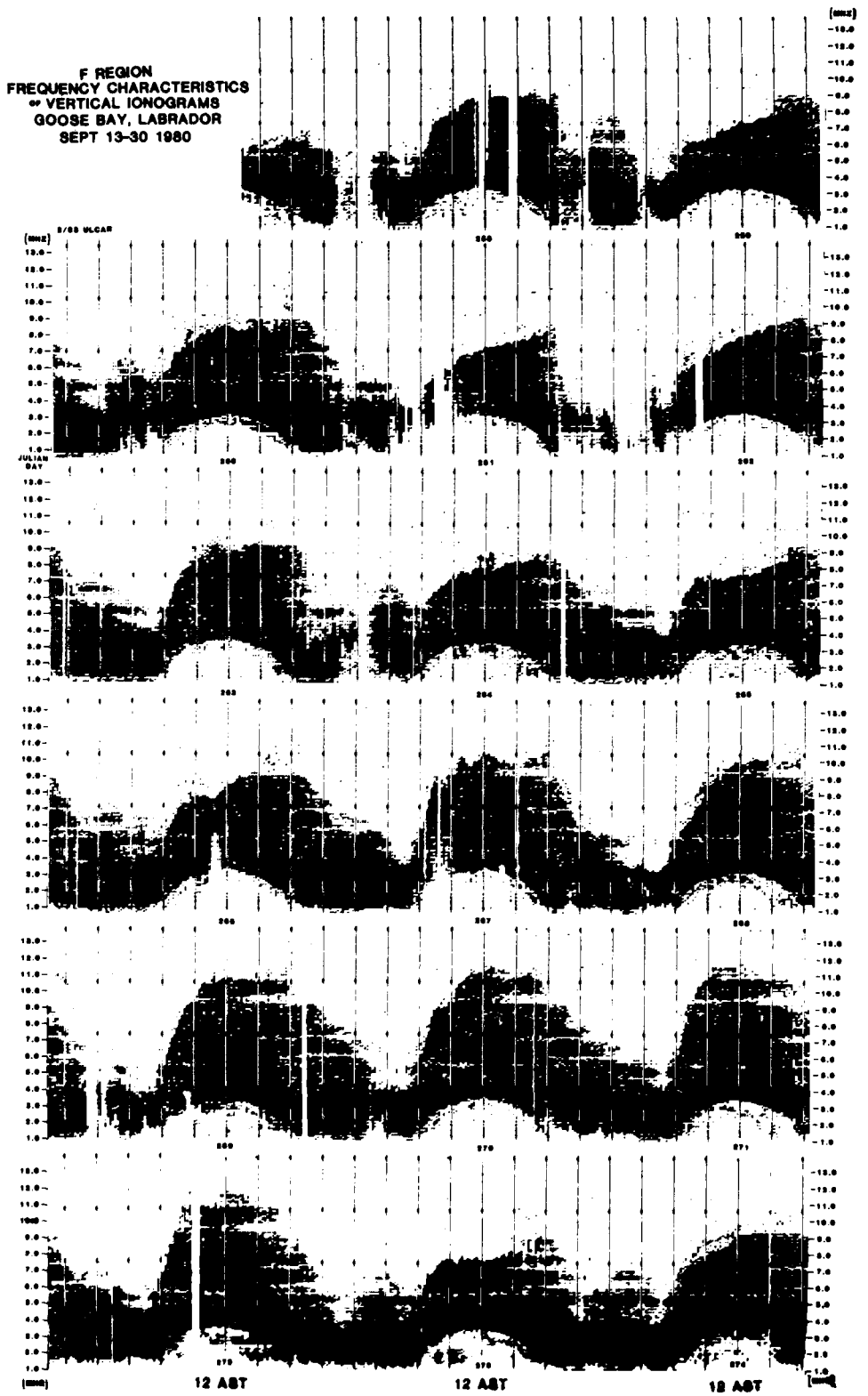
F REGION
FREQUENCY CHARACTERISTICS
OF VERTICAL IONOGRAMS
GOOSE BAY, LABRADOR
SEPT 13-30 1980
12 AST
12 AST
18 AST

Figure 35

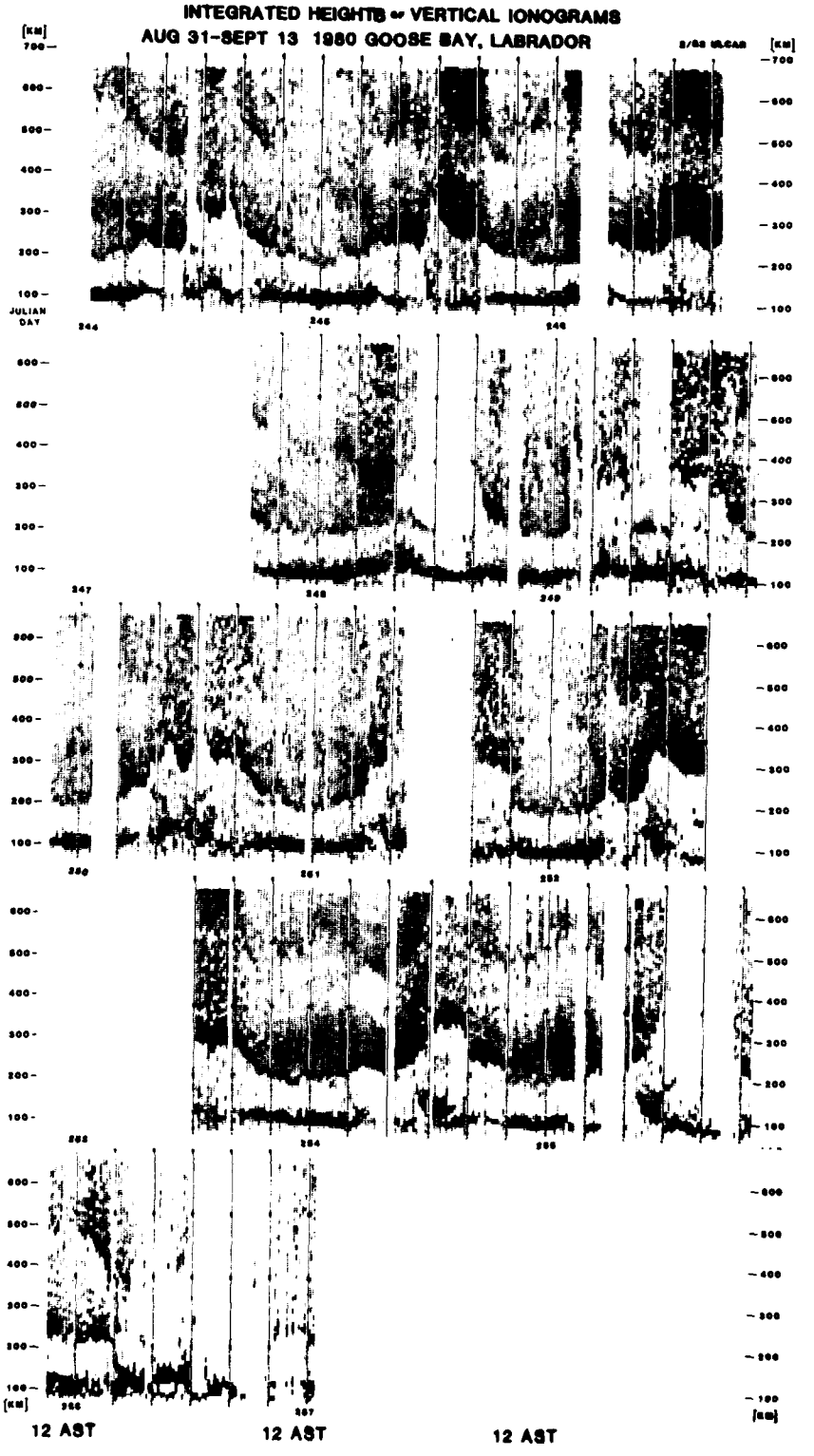
INTEGRATED HEIGHTS of VERTICAL IONOGRAMS
AUG 31-SEPT 13 1980 GOOSE BAY, LABRADOR
[KM]
JULIAN DAY
12 AST
12 AST
12 AST

Figure 36

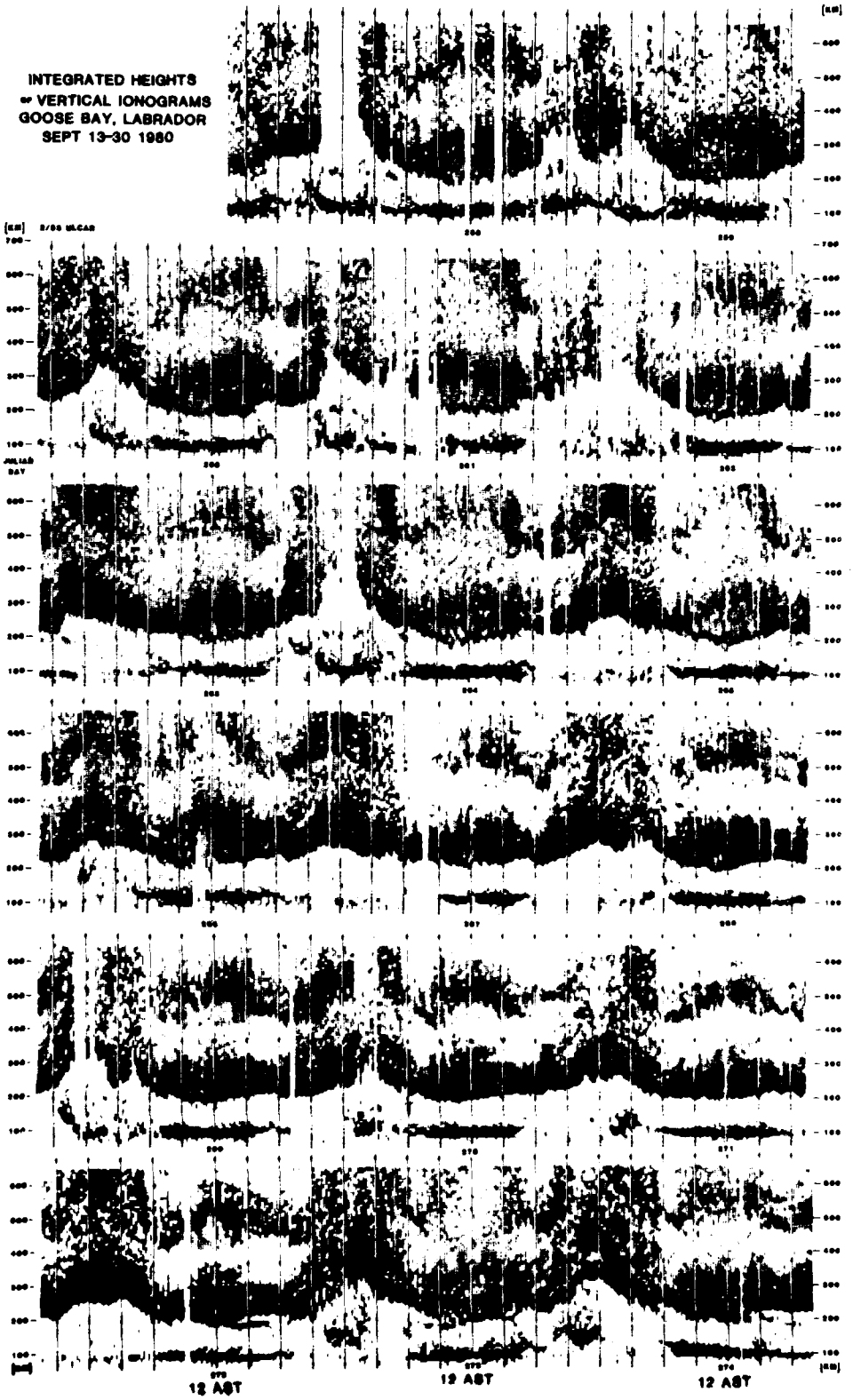
INTEGRATED HEIGHTS
of VERTICAL IONOGRAMS
GOOSE BAY, LABRADOR
SEPT 13-30 1980
12 AST
12 AST
12 AST

Figure 37

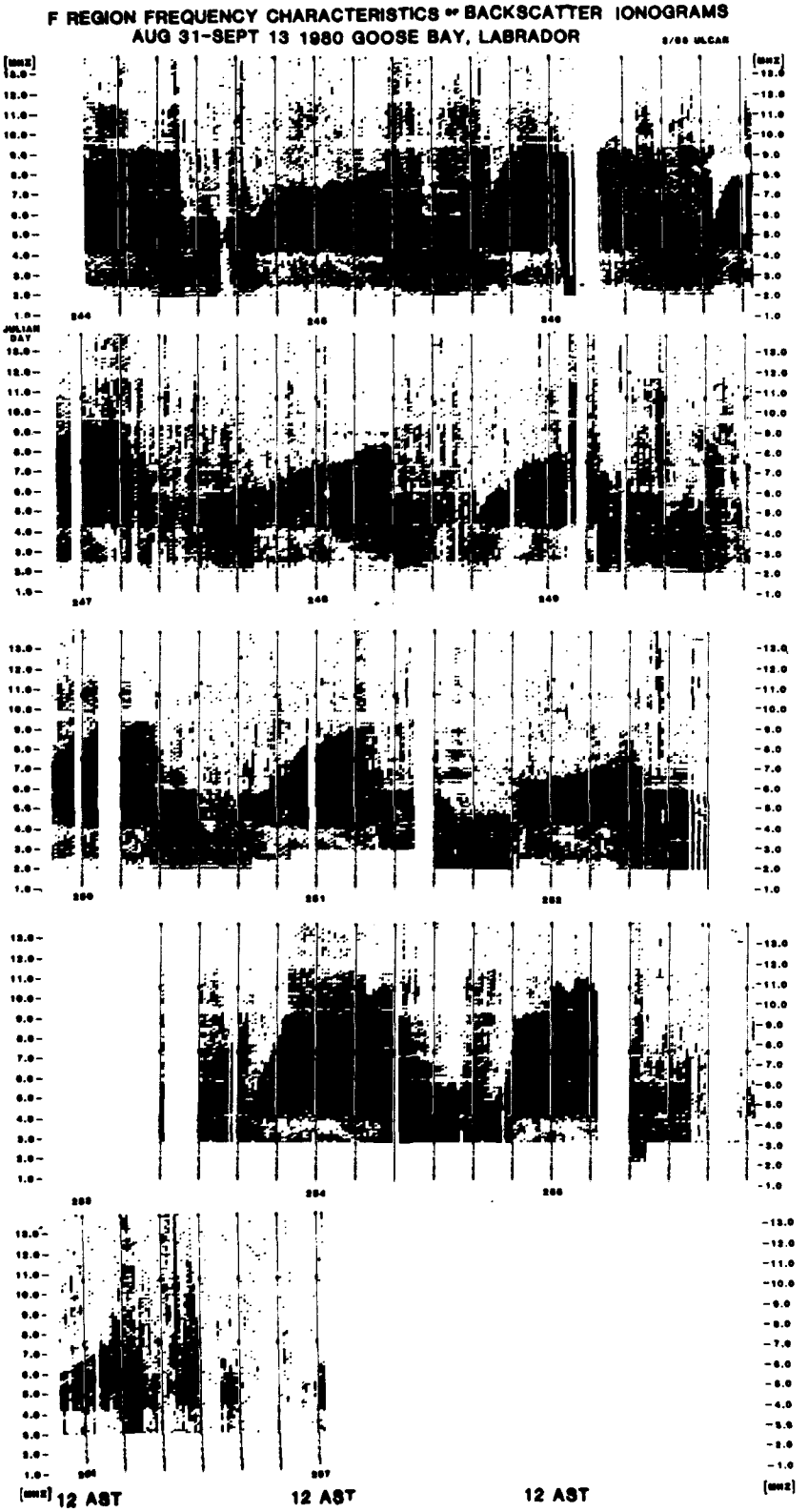
F REGION FREQUENCY CHARACTERISTICS OF BACKSCATTER IONOGRAMS
AUG 31-SEPT 13 1980 GOOSE BAY, LABRADOR
12 AST
12 AST
12 AST

Figure 38

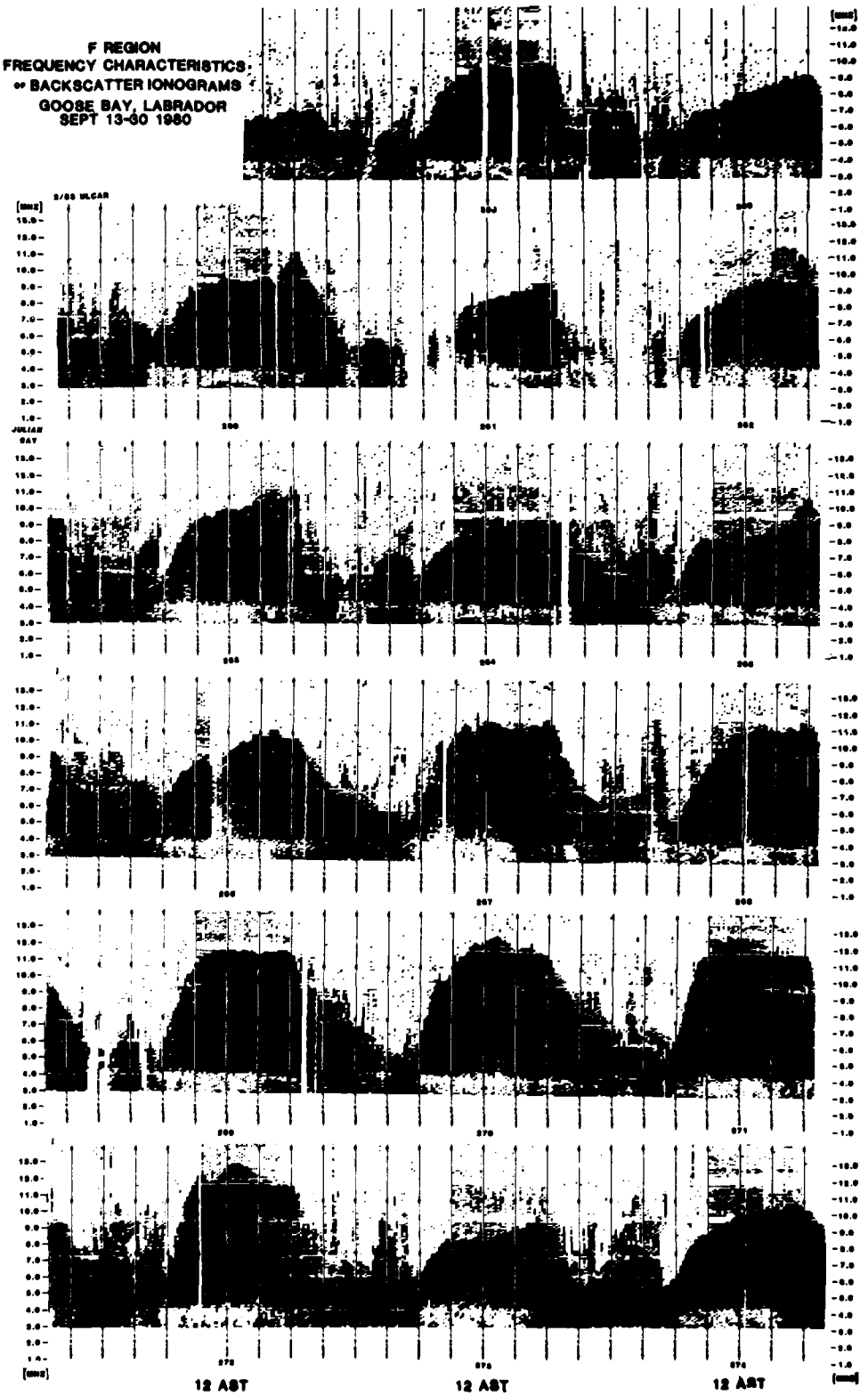
F REGION
FREQUENCY CHARACTERISTICS
of BACKSCATTER IONOGRAMS
GOOSE BAY, LABRADOR
SEPT 13-30 1980
12 AST
12 AST
12 AST

Figure 39

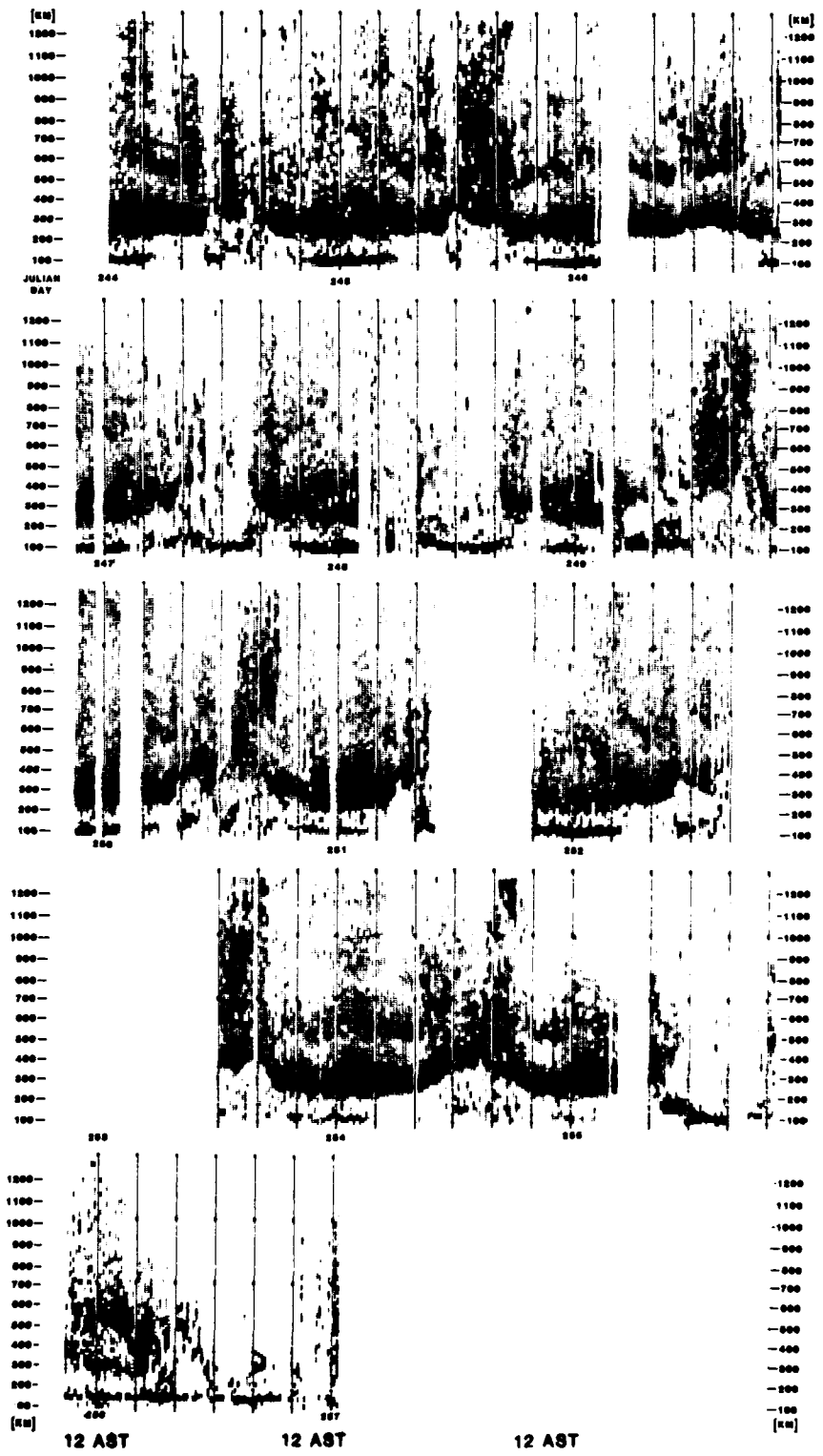
INTEGRATED HEIGHTS OF BACKSCATTER IONOGRAMS
AUG 31-SEPT 13 ,1980 GOOSE BAY, LABRADOR
S/NR WLCAR
[KM]
JULIAN DAY
12 AST
12 AST
12 AST

Figure 40

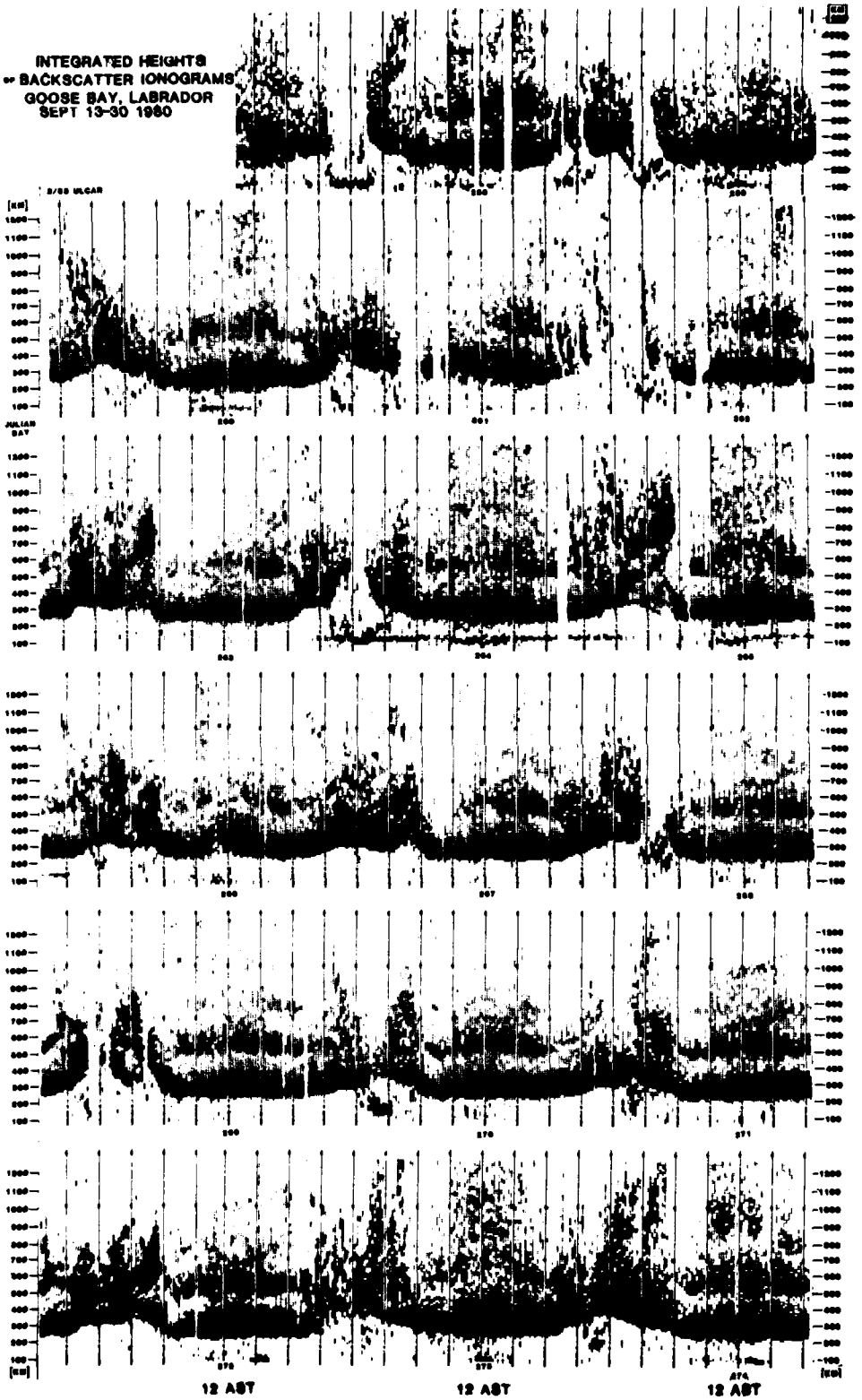
INTEGRATED HEIGHTS
of BACKSCATTER IONOGRAMS
GOOSE BAY, LABRADOR
SEPT 13-30 1980
12 AST
12 AST
12 AST

Figure 41

Goose Bay magnetometer readings for the horizontal component Y (magnetic north) and the vertical component Z. The minimum values, Y_L and Z_L, and the maximum values, Y_R and Z_R, for each 1-1/2 hour interval were available, measured in reference to fixed values Y_0 and Z_0 (Y_0 = 13,800 γ and Z_0 = 55,846 γ). From these values the monthly averages $\overline{Y}_L$, $\overline{Z}_L$, $\overline{Y}_R$ or $\overline{Z}_R$ were subtracted for each time period to eliminate the daily variation and to detrend the local K index (Mayaud, 1980).

$$Y'_L = Y_L - \overline{Y}_L;\ Z'_L = Z_L - \overline{Z}_L;\ Y'_R = Y_R - \overline{Y}_R;\ Z'_R = Z_R - \overline{Z}_R.$$

Magnetic ranges were determined for a three hour time window which was shifted along the time axis in 1-1/2 hour increments. This gives an improved time resolution in comparison with the internationally defined K value which increments the time window by three hours (without any overlapping). The ranges for a three hour window were defined as

$$\Delta Y = Y_{Rmax} - Y_{Lmin},$$

and, respectively, as

$$\Delta Z = Z_{Rmax} = Z_{Rmin}.$$

Y_{Rmax} is the maximum of two adjacent Y'_R values:

$$Y_{Rmax(t)} = \text{Max}|Y'_{R(t-1)};\ Y'_{R(t)}|.$$

Similarly:

$$Z_{Rmax(t)} = \text{Max}|Z'_{R(t-1)};\ Z'_{R(t)}|.$$

For the minima:

$$Y_{Lmin(t)} = \text{Min}|Y'_{L(t-1)};\ Y'_{L(t)}|$$

and

$$Z_{Lmin(t)} = \text{Min}|Z'_{L(t-1)};\ Z'_{L(t)}|.$$

The local K coefficient is specified in Table 2 as function of the maximum of $2\Delta Y$ and $10\Delta Z$. This local K index is not the same as the standard K index because only data from one horizontal component (in the average magnetic field direction) was available.

Although the K value is widely accepted for sorting different classes of data we were able to better relate variations in the ionospheric data to magnetic activity by looking at the magnitude of the horizontal and vertical field components. While the K parameters are equally sensitive to positive and negative magnetic bay events the Y values permit clear distinction between them. In one important local event (11 Nov 1980) studied simultaneously from an aircraft over Greenland and at Goose Bay, Labrador, we had a strong positive magnetic bay at Goose Bay and simultaneously negative bays in the Alaskan magnetometer chain recordings. The parameters $DY = Y'_L + Y'_R$ and $DZ = Z'_L + Z'_R$ have been scaled for each 1-1/2 hour period; the scaled value of DY and DZ covers the time period between t and t - 1-1/2 h, while K includes variations from the indicated time t to (t - 3) hours. Our plan is to compare the local parameters with the observed ionospheric phenomena and the planetary Kp index. The three local magnetic indices are plotted in Figures 42 to 49 for the four selected months of 1980. To facilitate comparison with the ionospheric characteristics, the same scale was used for the time axis. To compensate for the offset of magnetic data, DY and DZ were shifted by 4-1/2 hours, in the translation from UT to AST while the K values recorded in Universal Time were shifted by 5-1/4 hours.

The F-region frequency characteristics show a number of days with unexpectedly low ionization at local afternoon. These days, listed in Table 3, are marked by enhanced absorption during the day, indicated by the rugged fmin in the E-region and F-region frequency characteristics, and/or

Max [2Y, 10Z]	K
0 - 14	0
15 - 21	1-
22 - 28	1
29 - 35	1+
36 - 43	2-
44 - 53	2
54 - 66	2+
67 - 83	3-
84 - 104	3
105 - 130	3+
131 - 161	4-
162 - 198	4
199 - 241	4+
242 - 291	5-
292 - 348	5
349 - 413	5+
414 - 486	6-
487 - 568	6
569 - 660	6+
661 - 762	7-
763 - 875	7
876 - 1000	7+
1001 - 1138	8-
1139 - 1290	8
1291 - 1457	8+
1458 - 1640	9-
$\geq$ 1641	9

Table 2. Goose Bay Interpolated Local K-Values

Bi 17 Nov 82

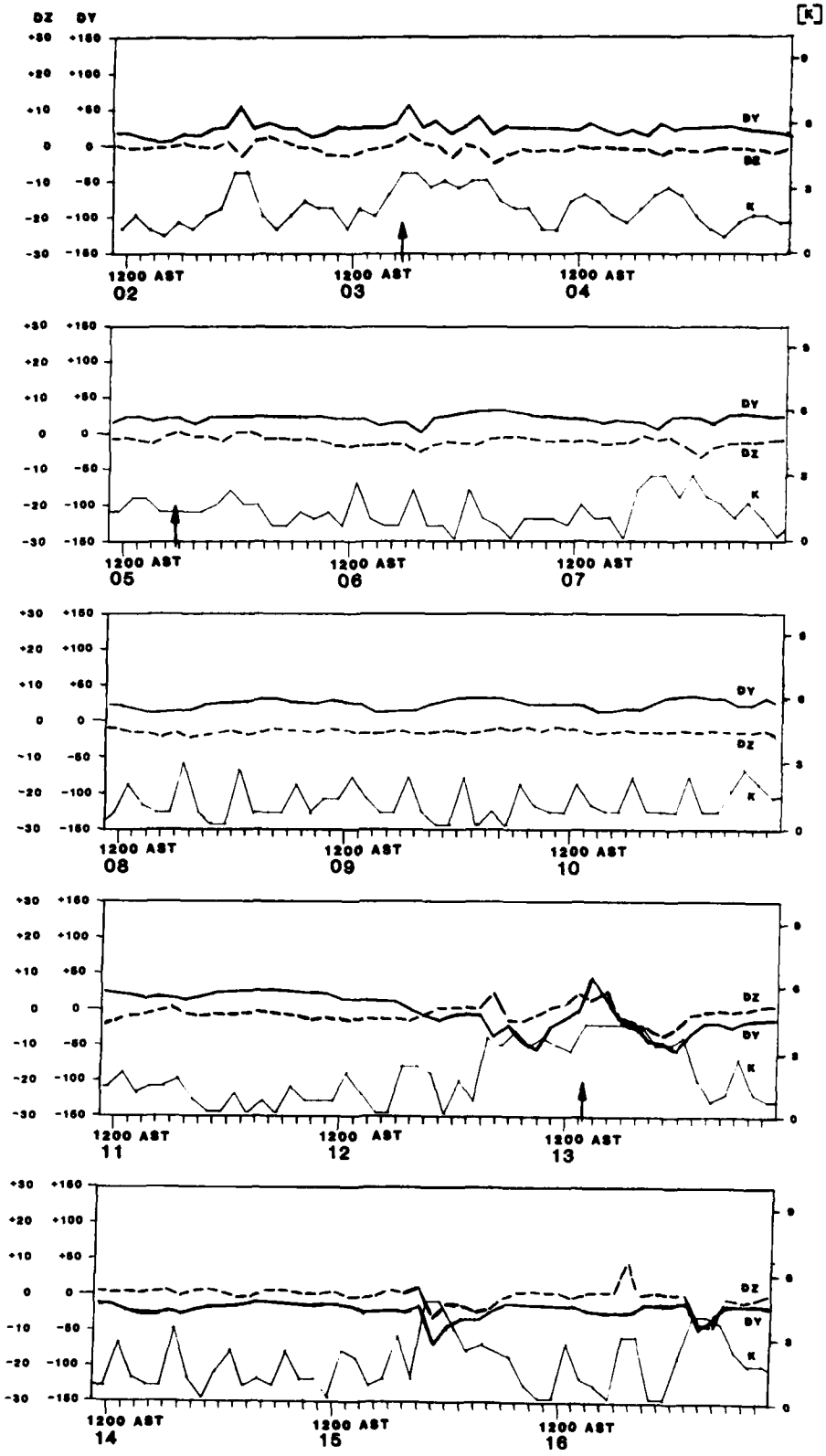

LOCAL MAGNETIC INDICES
02-16 JAN 1980 GOOSE BAY, LABRADOR

Figure 42

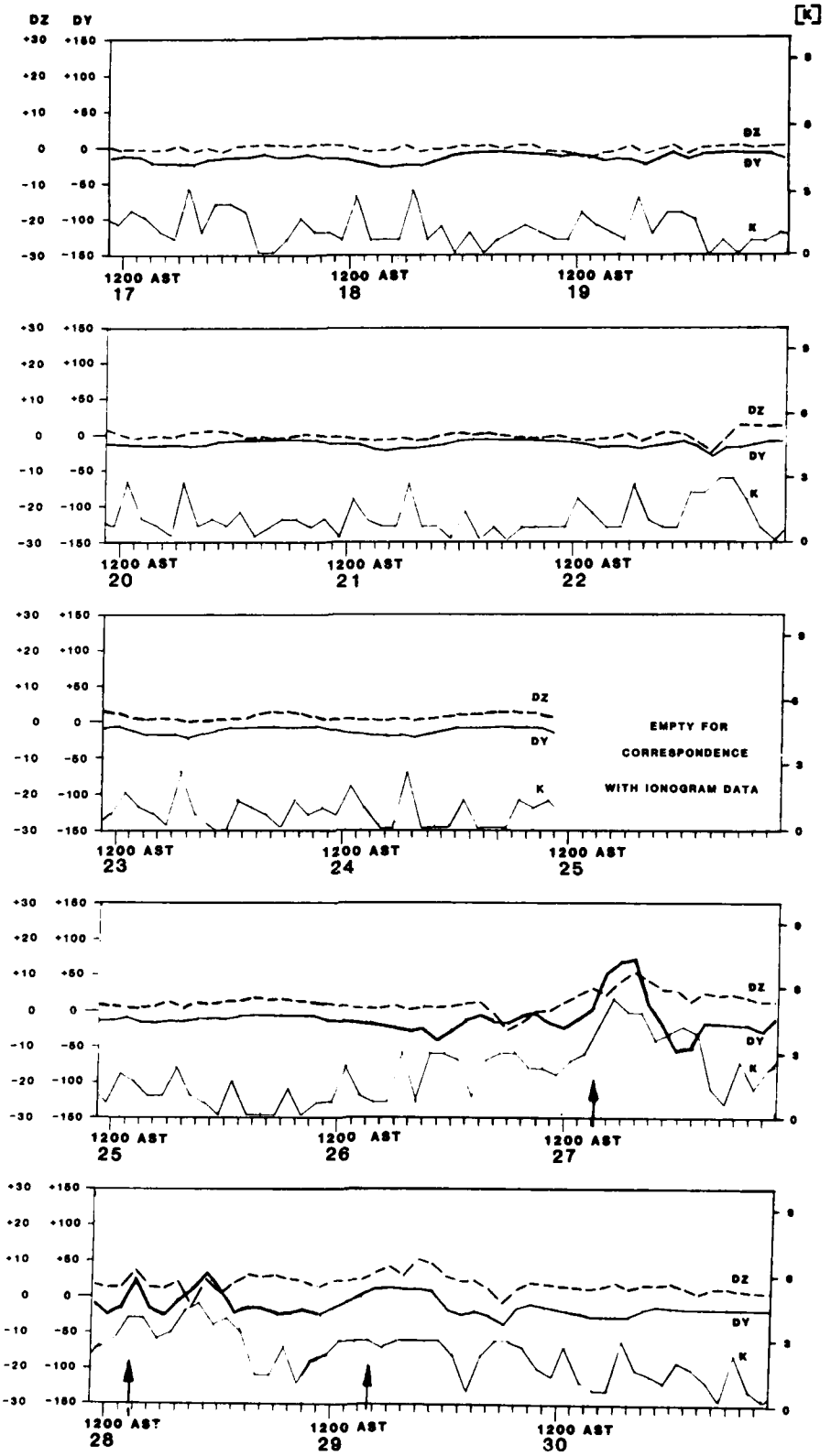

LOCAL MAGNETIC INDICES
17-30 JAN 1980 GOOSE BAY, LABRADOR

Figure 43

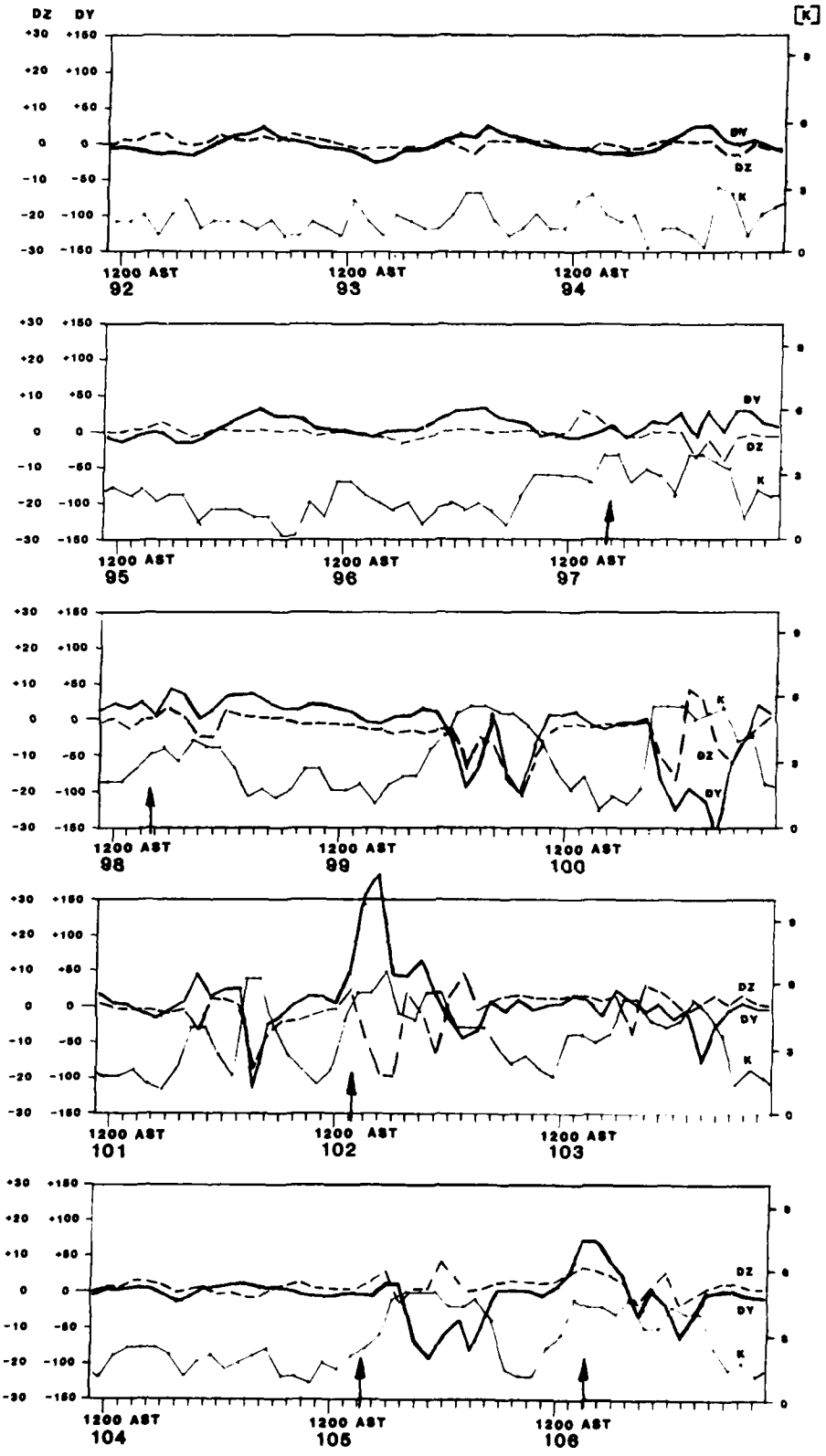

LOCAL MAGNETIC INDICES
1-15 APRIL 1980 GOOSE BAY, LABRADOR

Figure 44

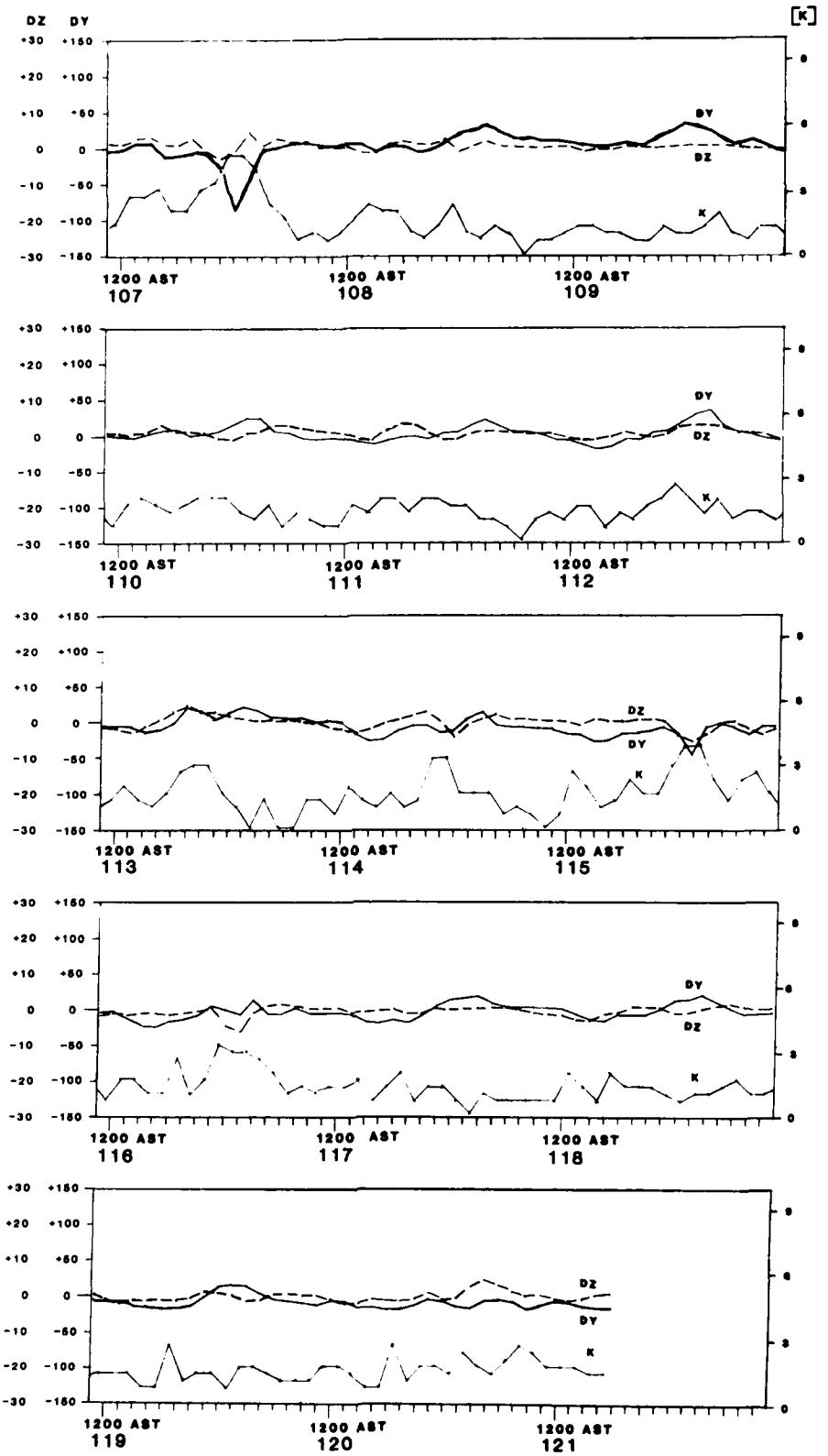

LOCAL MAGNETIC INDICES
16-30 APRIL 1980 GOOSE BAY, LABRADOR

Figure 45

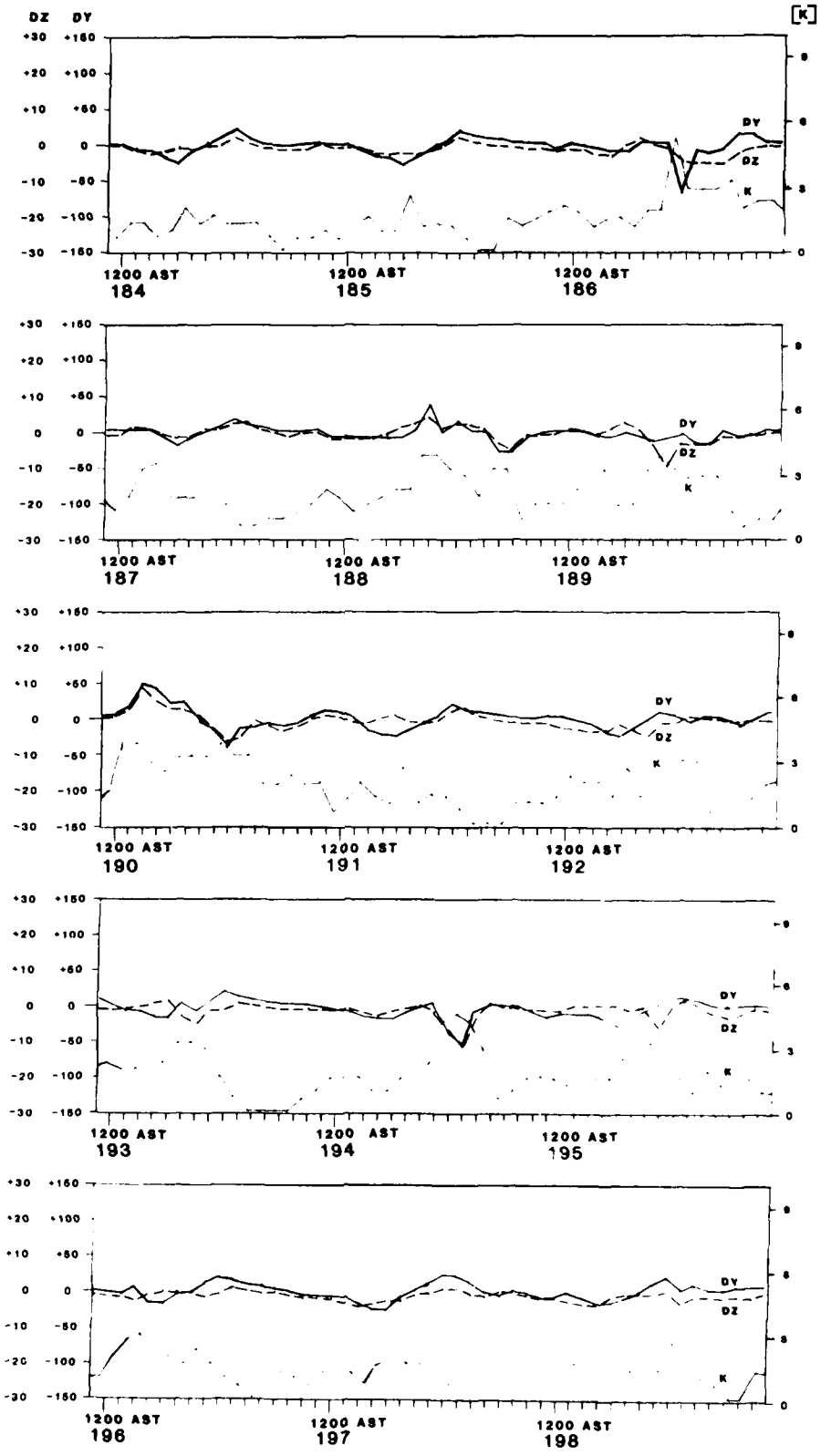

LOCAL MAGNETIC INDICES
02-16 JULY 1980 GOOSE BAY, LABRADOR

Figure 46

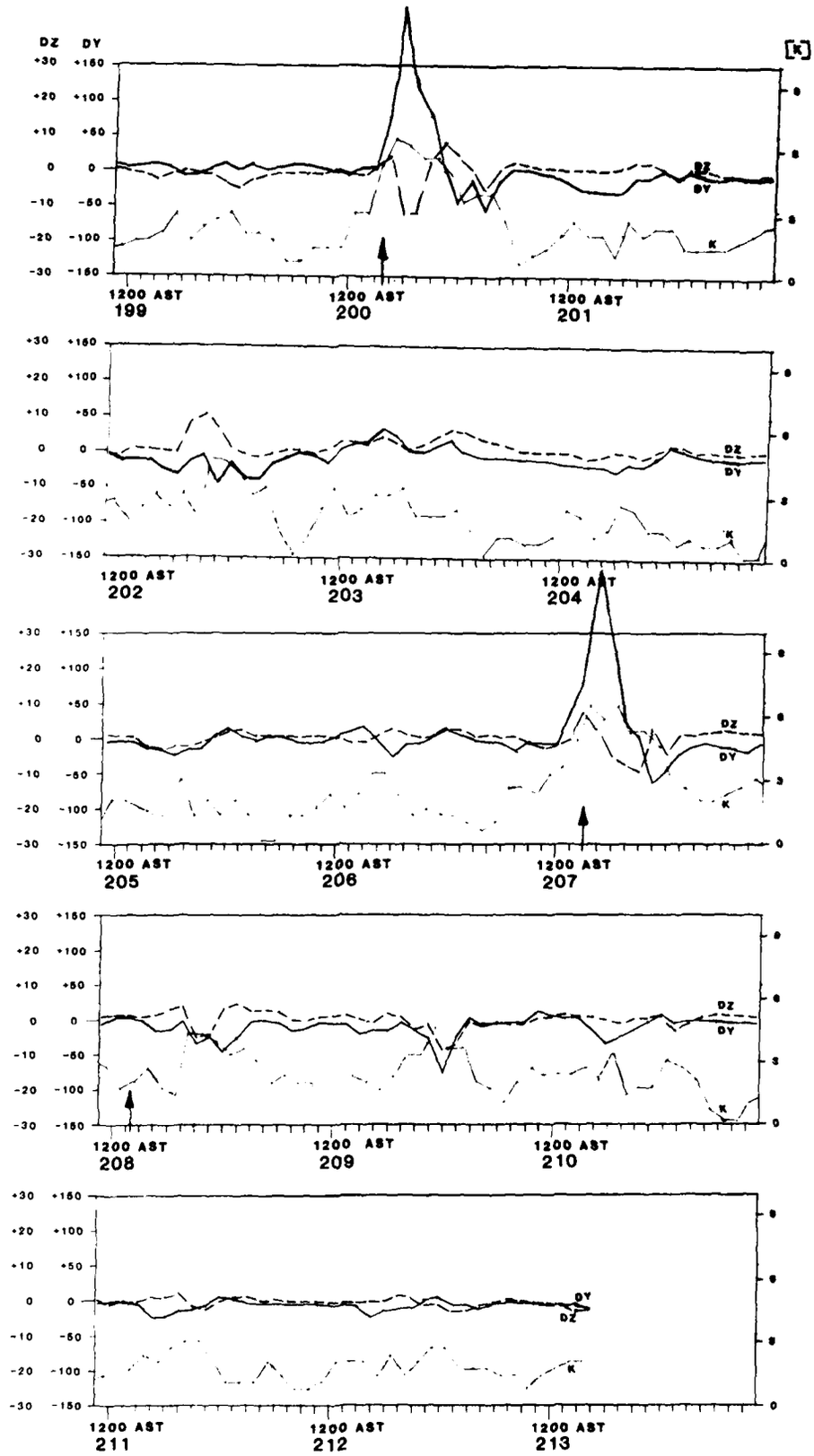

LOCAL MAGNETIC INDICES
17-31 JULY 1980 GOOSE BAY, LABRADOR

Figure 47

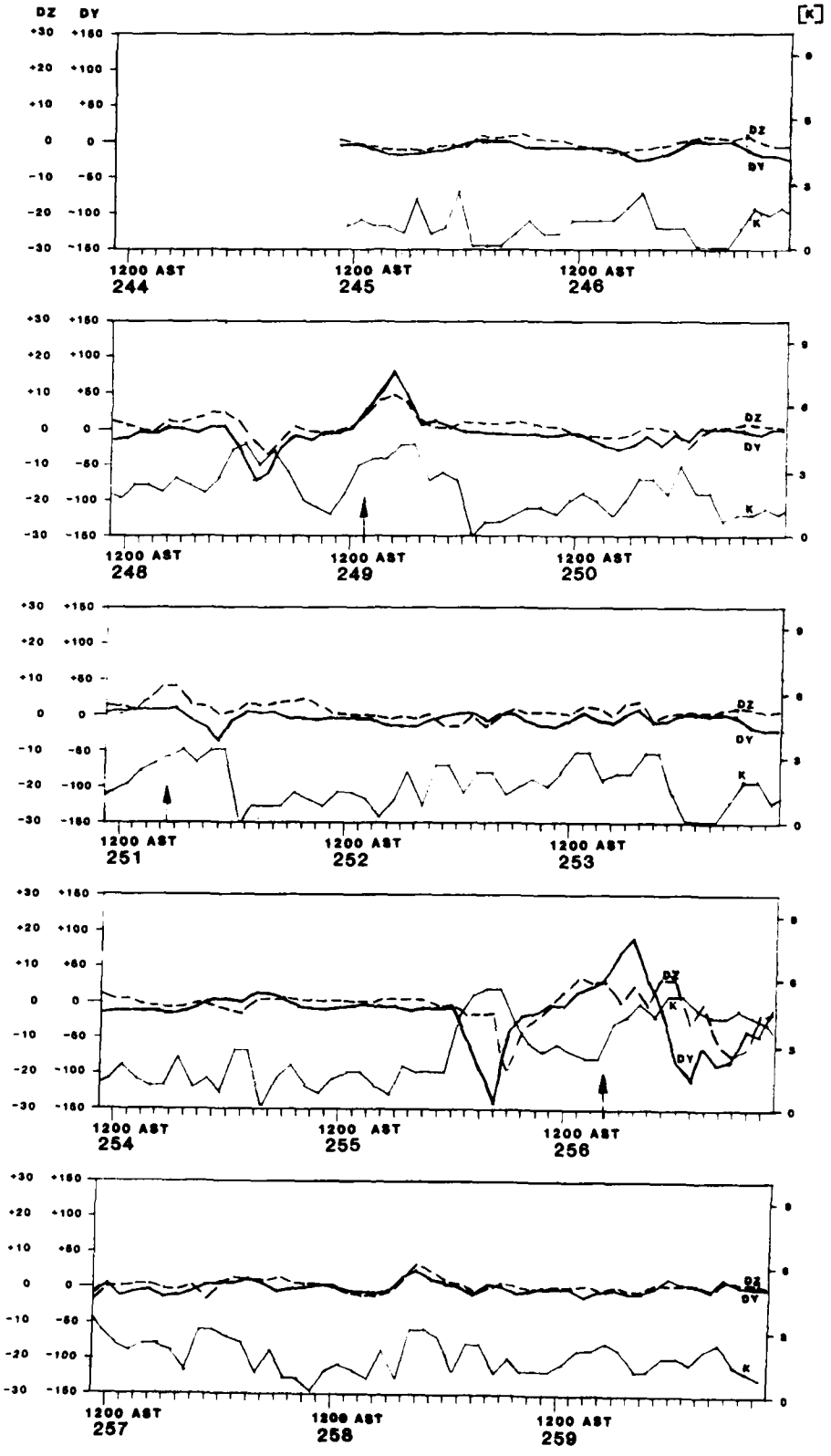

LOCAL MAGNETIC INDICES
AUG 31-SEPT 15 1980 GOOSE BAY, LABRADOR
(SEPT 8 LEFT OUT)

Figure 48

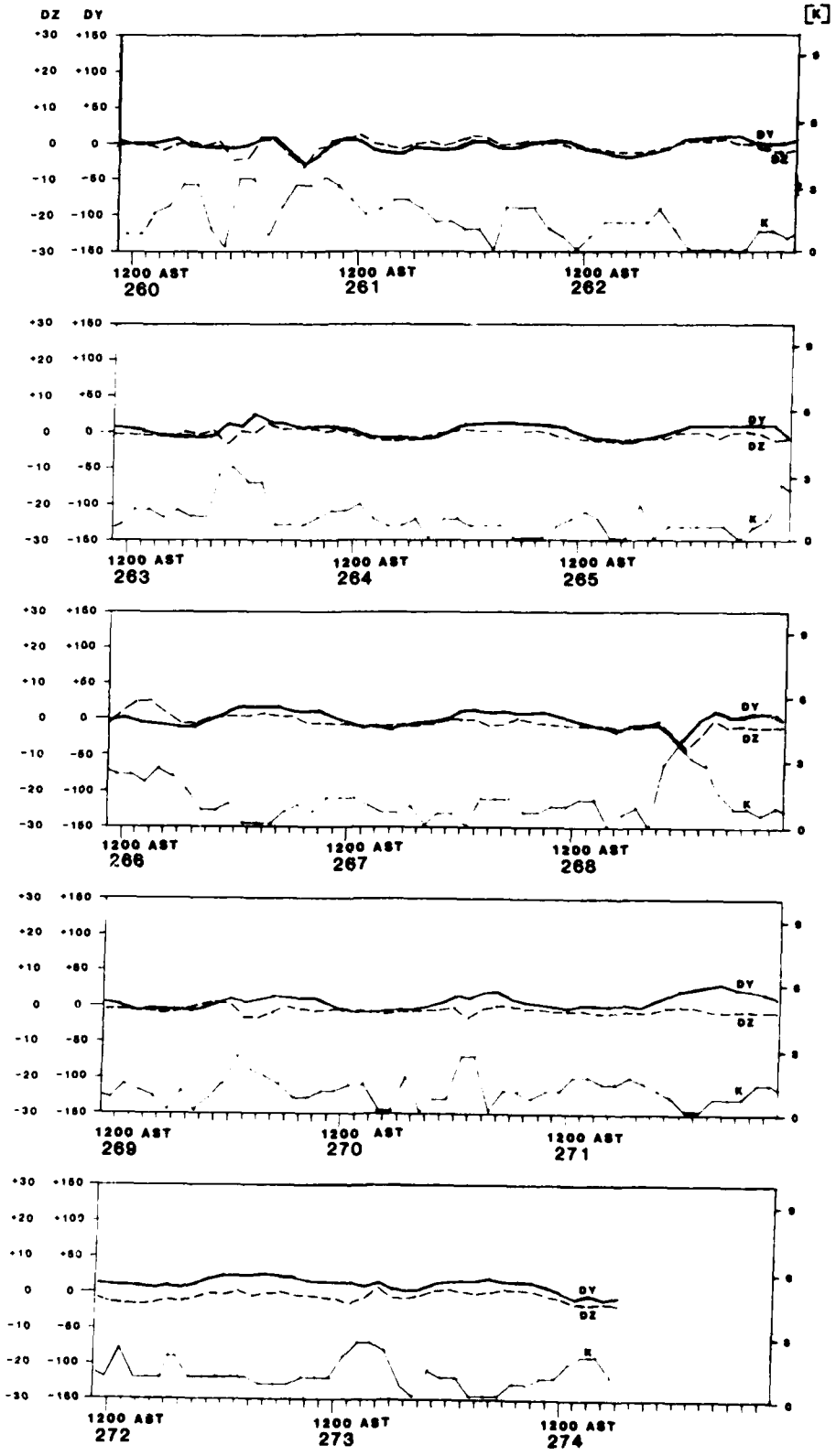

LOCAL MAGNETIC INDICES
SEPT 16 -30 1980 GOOSE BAY, LABRADOR

Figure 49

the sharp decline of the F-region critical frequency and a simultaneous rise of the virtual heights. A good illustration is the comparison of a "normal" day, January 7, 1980, with January 3, 1980, where foF2 decreased rapidly to less than 3 MHz at 1700 AST and the F-layer height increased (Figure 50). On January 7, on the other hand, the F ionization minimum is reached at 2019 AST (Figure 51). The relationship between increased absorption by enhanced particle dumping into the lower ionosphere, the formation of aurora E and the vertical motion of the F-region ionization must still be studied.

The new ionogram programs will certainly facilitate the description of these important phenomena of the auroral and subauroral ionosphere. On February 4, 1983, a very distinct event of the blowing-out of the F-region ionization has been monitored by chance in Lowell and was visible even in Digisonde 128 recording at Cape Canaveral, Florida. For one hour the F-region height increased there substantially, while h'F2 was twice as large as normal, for several hours in Lowell, Massachusetts. During this time and many hours thereafter a complete blackout alternated with strong aurora E and Es occurred in Goose Bay, Labrador. Although these events are much less pronounced during the summer season we hope to catch more of the daytime F-ionization breakdown after the recent installation of a direct warning system, triggered by Goose Bay events. A similar 'blow-out' of the F-region ionization will be described in the next section.

When the magnetic characteristics are checked for signatures one can see that on most of the selected days the horizontal component Y shows a marked increase starting between 13 and 15 h local time. The onset of the rapid decrease of the F-region ionization and the rise of the layer as presented in Table 3 in AST, are indicated as arrows in the magnetic charts of Figures 42 to 49. Even the average DY behavior, produces by overlaying the magnetic data synchronized with the ionospheric event in the superposed epochs method,

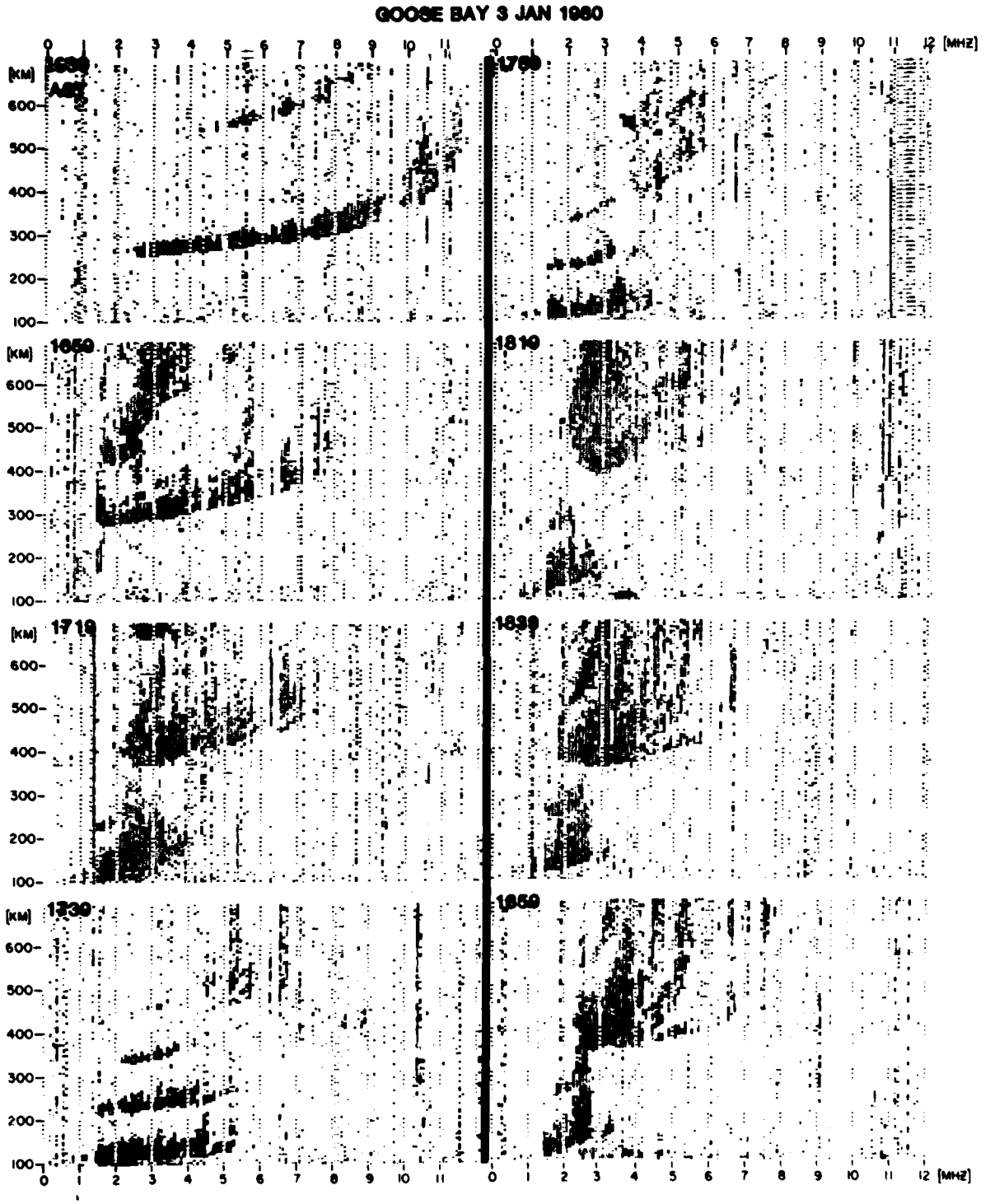

F-TROUGH AND AURORAL OVAL

Figure 50

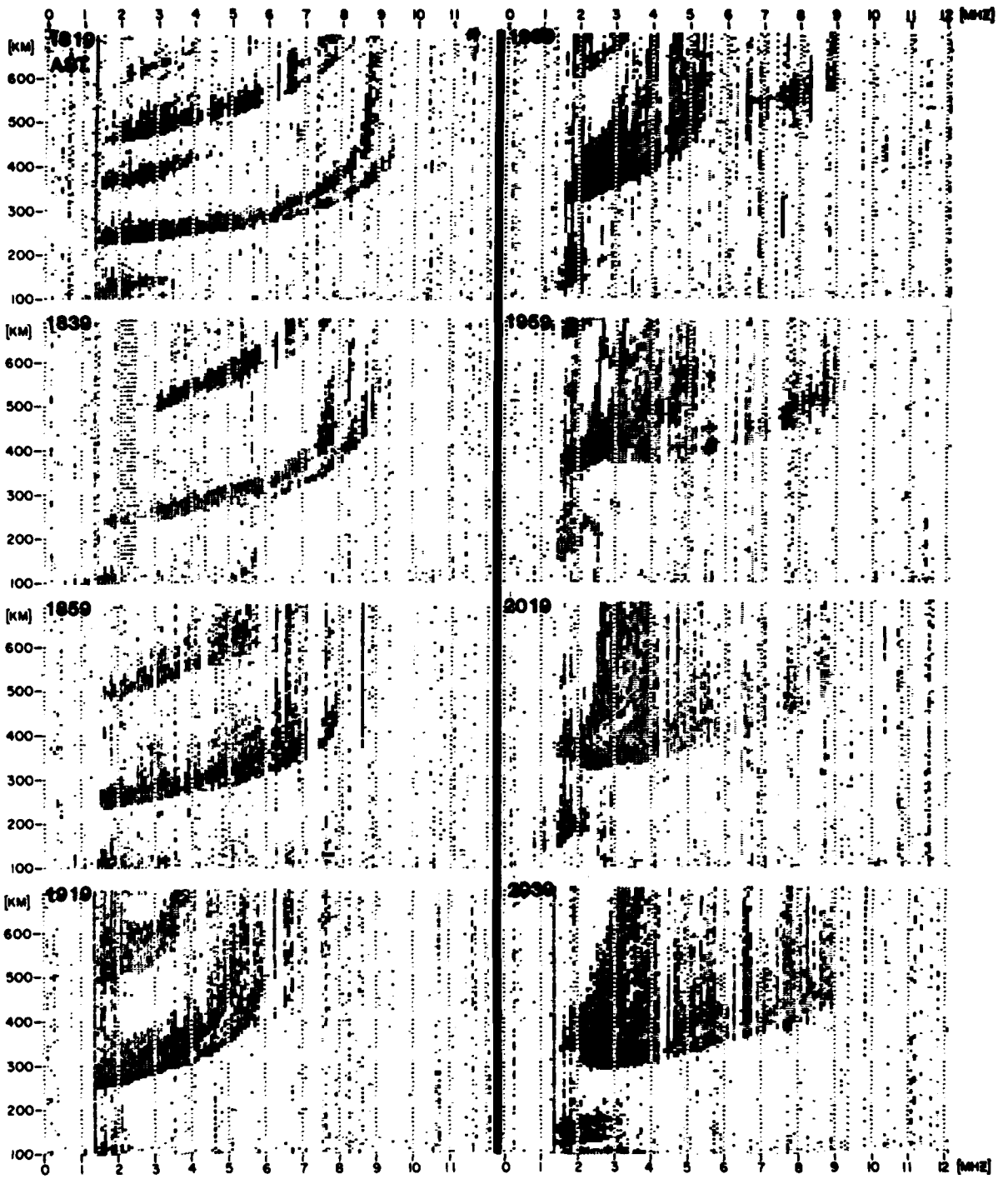

OCCURRENCE OF F-TROUGH

Figure 51

Julian Day	Positive Bay	Onset Time Date	AST
03	M	Jan 3	1645
05		Jan 5	1730
13	M	Jan 13	1415
27	MM	Jan 27	1500
28	M	Jan 28	1600
29		Jan 29	1545
97		Apr 6	1600+
98		Apr 7	1600+
102	MM	Apr 11	1400
105		Apr 14	1615
106	M	Apr 15	1500+
200	MM	Jul 18	1600
207	MM	Jul 25	1500
208		Jul 26	1400+
249	M	Sep 5	1330
251		Sep 7	1715
256	M	Sep 12	1615

+ = onset not clear

M = moderate

MM = very large

Table 3. F-Region Minima at Local Afternoon, Goose Bay, 1980

shows a distinct positive bay of the horizontal magnetic component, with the steepest slope at the onset of the ionospheric event (Figure 52). Much work remains to be done. We plan to investigate the chronological order of occurrence of the irregular magnetic variation, the F ionization change and the formation of aurora type E layers.

The following significant statements, resulting from the comparison between magnetic and ionospheric data for the four months of 1980 Goose Bay data, can be made:

1. As Figure 53 shows, the time of occurrence of positive bays with average $(Y'_L + Y'_R)/2$ maximum excursions larger than 25 [γ] is limited between 1500 to 0000 Local Mean Time (AST).
2. The time of occurrence of negative bays with the same maximum excursions is limited between 2230 and 0730 AST.
3. All significant positive bays are coinciding with fast upward motion of the F region ionization resulting in local ionization depletion.
4. Most minima in ionization are related to increases of the horizontal field components.
5. Positive bays are related to local precipitation, while the negative bays might be related to events occurring in a latitude sector of 90° to 180° towards west.

Automatic processing of the Digisonde ionograms facilitates the interpretation in terms of geophysical phenomena. A summary of such techniques is given in Scientific Report No. 1 'Processing of Digital Ionograms' by B. W. Reinisch (1981).

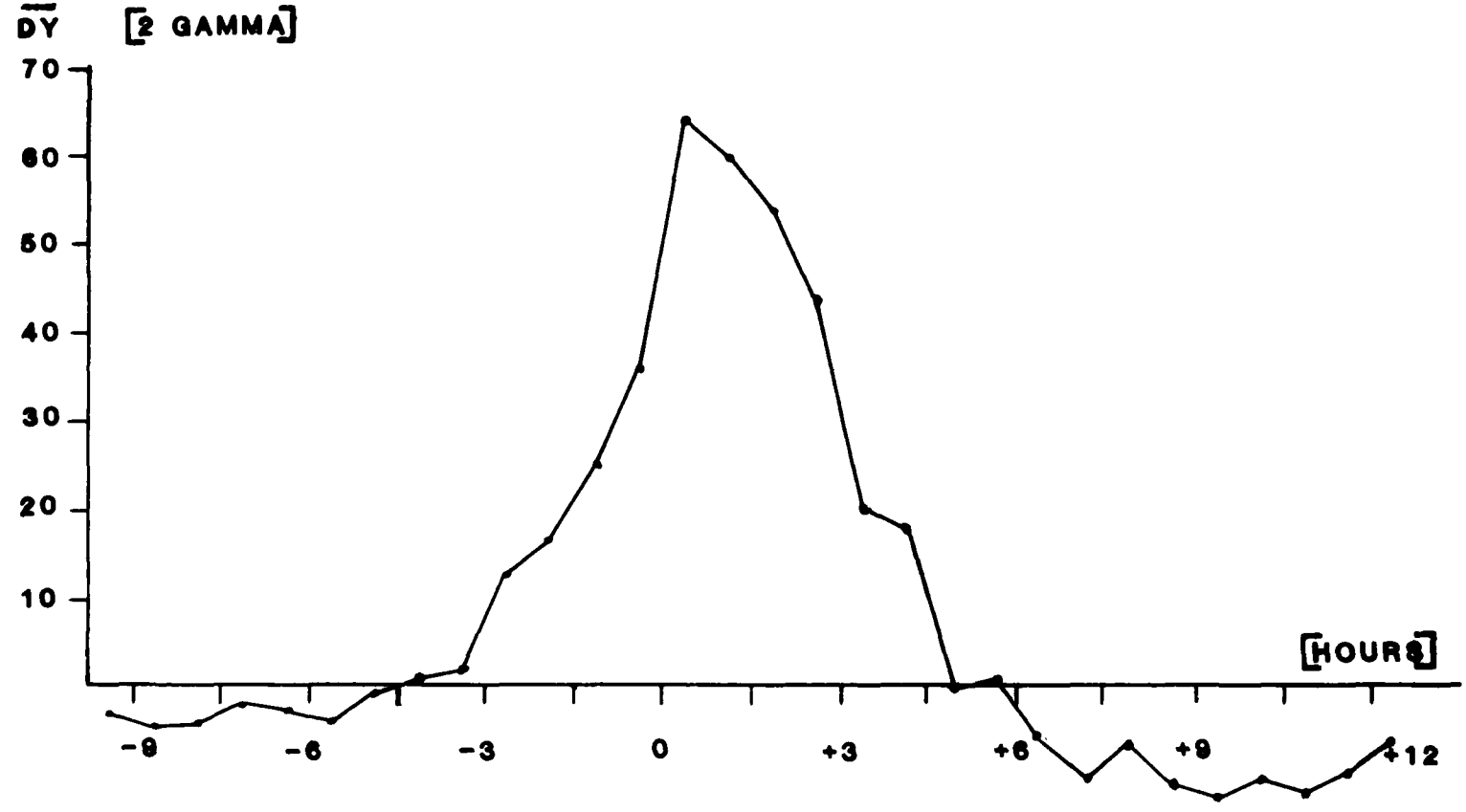

Figure 52

AVERAGE CHANGE OF HORIZONTAL MAGNETIC FIELD COMPONENT FOR 17 EVENTS OF MINIMUM F REGION IONIZATION DURING DAYTIME

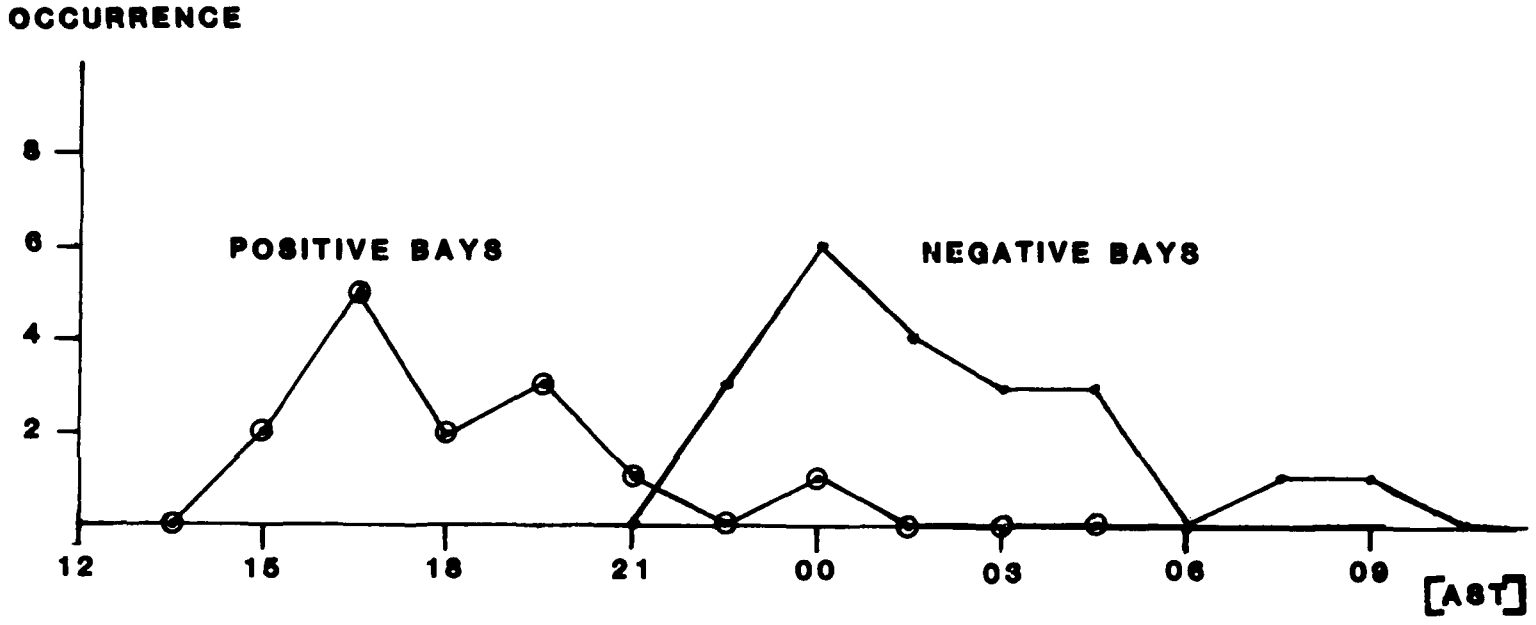

Figure 53

TIME OF OCCURRENCE FOR POSITIVE AND NEGATIVE BAYS WITH AVERAGE EXCURSIONS OVER 25 GAMMAS IN GOOSE BAY HORIZONTAL MAGNETIC FIELD

2.3 F-Region Bite-Out in the Daytime; A Case Study

On 11 November 1980, AFGL's Airborne Ionospheric Observatory (AIO) onboard a KC-135 airplane monitored a daytime collapse of the F-region ionization over the southern tip of Greenland (67° CG Latitude). The aircraft observations were combined with the ground-based ionosonde measurements at Goose Bay, Labrador (65° CGL), St. John's, Newfoundland (58° CGL), Narssarssuaq (69° CGL) and Godhaven (76° CGL) in Greenland. The results of this study were presented at the XXth URSI General Assembly in Washington, D. C., August 1981 (K. Bibl et al, 1981). Digisonde ionograms with amplitude (bottom) and Doppler (top) recorded by the AIO at 1736 UT and 1806 UT (approximately 1500 LT) are shown in Figures 54 and 55. The F-layer critical frequency decreased from 11.2 MHz (1.5×10^{12} el/m^3) to 2.7 MHz (0.9×10^{11} el/m^3), while the minimum virtual height increased from 235 to 410 km. During this time, the aircraft was zigzagging between 68° and 73° CGL (Figure 56), and changed local magnetic time, but returned to almost the same geographic location. In order to interpret the aircraft observations in terms of the larger scale ionospheric structure of the auroral dusk to midnight region we used available ground-based ionogram data from stations located between 65° CGL (Goose Bay) to 76° CGL (Godhaven). The best information was available from Goose Bay where 12 vertical and 12 backscatter ionograms were recorded per hour during the aircraft mission. A quick check of the hourly values for foF2 had not shown any unusual behavior for 11 November 1980. But the F-region frequency characteristic for this day (Figure 57) exhibits a sharp decline in foF2 starting at 1510 AST (1910 UT), although the decrease is somewhat obscured by oblique echoes. The increase in virtual range from about 270 km to 400 km within 15 minutes is clearly visible in the h' characteristic (Figure 58). The ionogram at 1504 AST (1904 UT) shows three distinct traces clearly distinguished

Figure 54

AMPLITUDE AND DOPPLER IONOGRAM

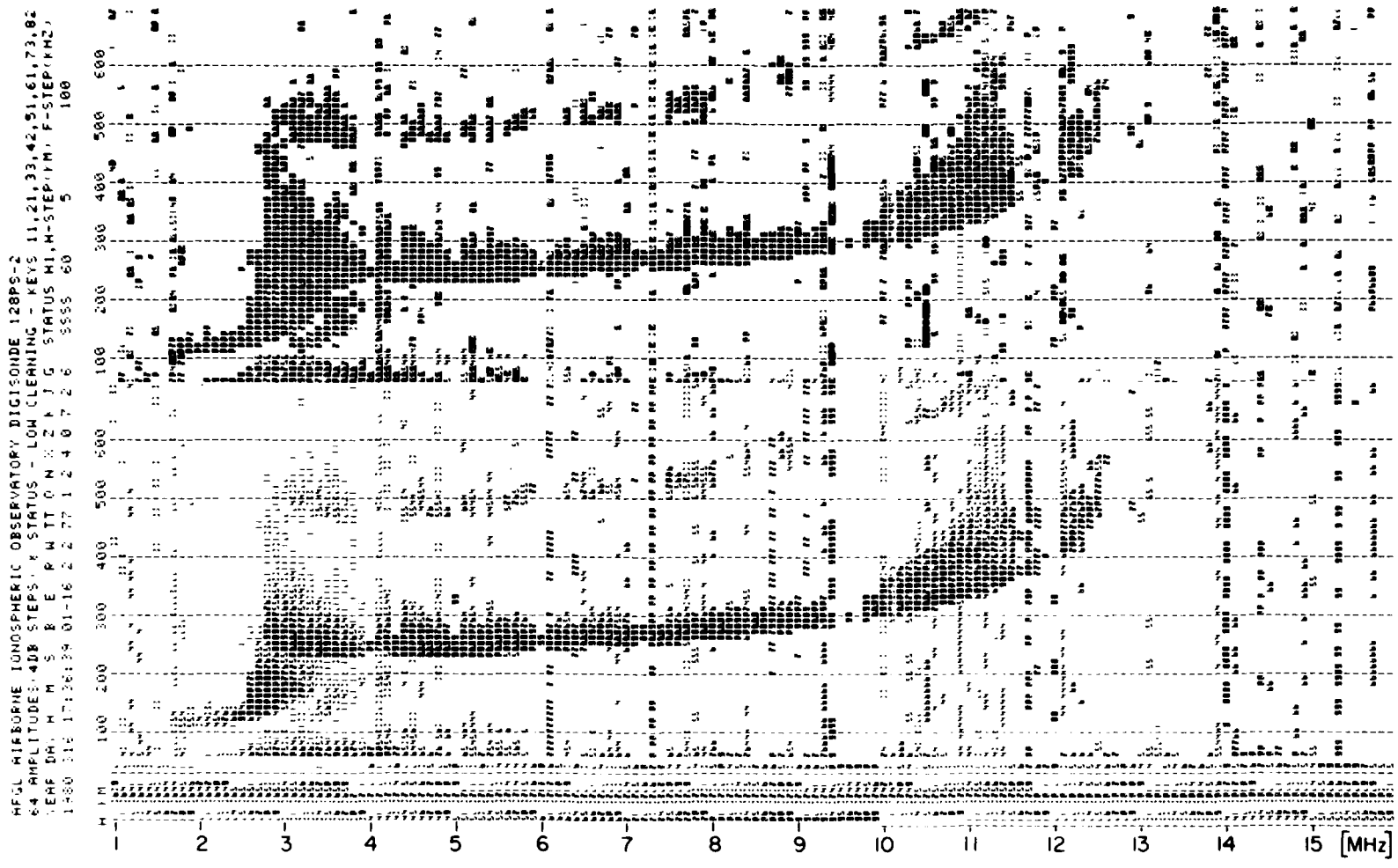

AIRCRAFT (GREENLAND WEST COAST)

11 NOV 80 1736 UT

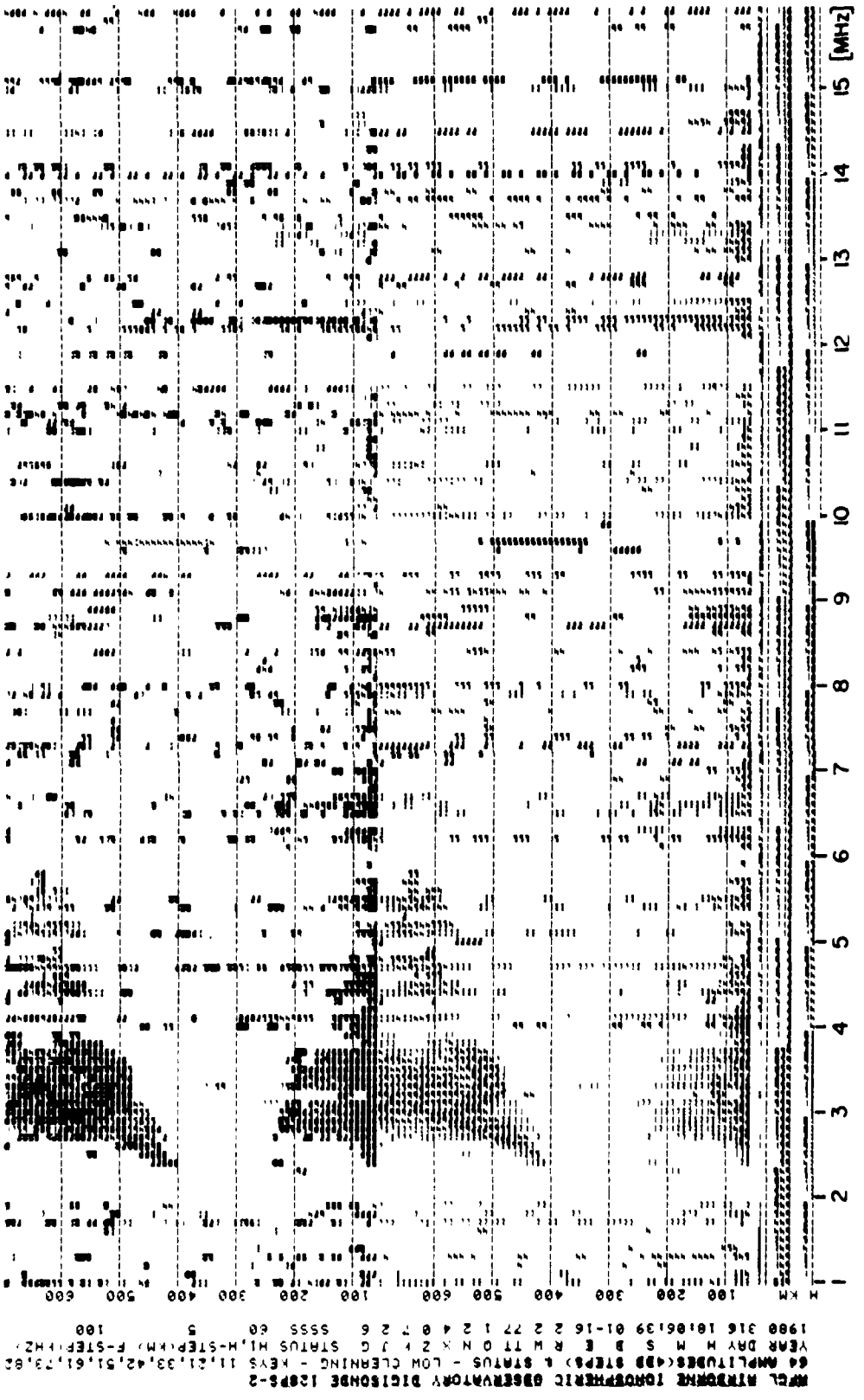
AMPLITUDE AND DOPPLER IONOGRAM
AIRCRAFT (GREENLAND WEST COAST)
11 NOV 80 1806 UT
[MHz]
KM

Figure 55

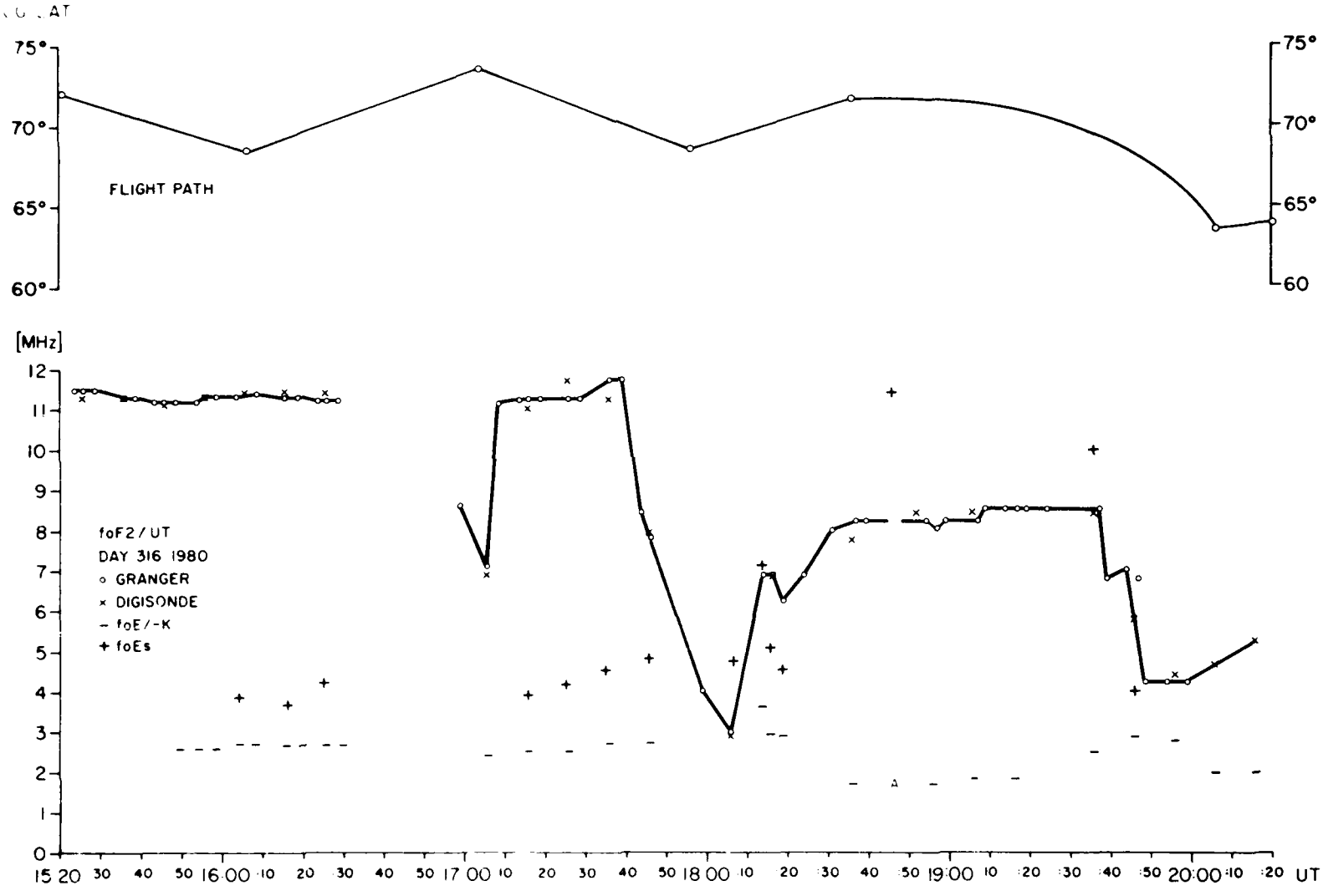

foF2 AIRCRAFT 11 NOV 80

Figure 56

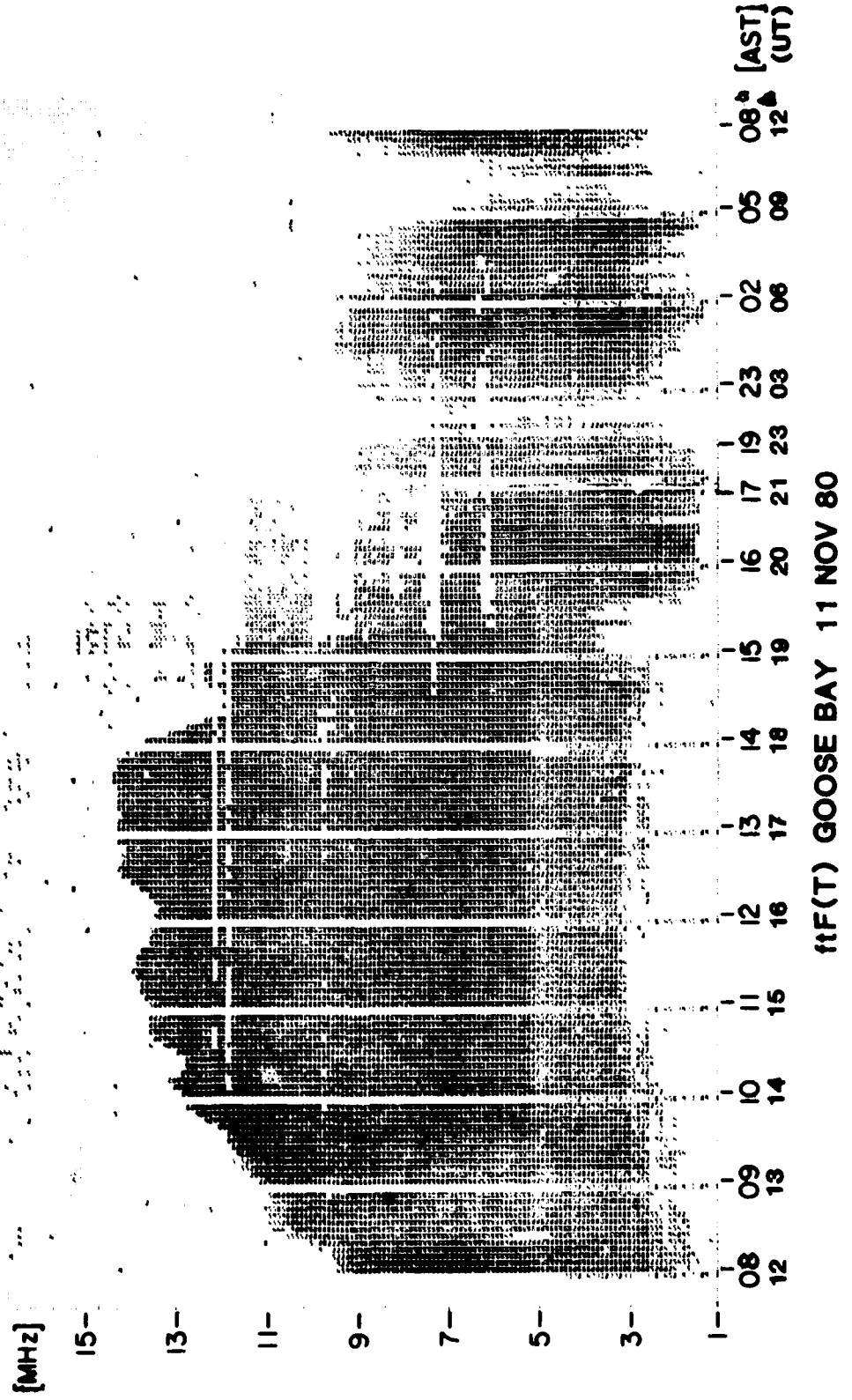
[MHz]
15
13
11
9
7
5
3
1
08 09 10 11 12 13 14 15 16 17 18 19 20 21 23 03 06 09 12
12 13 14 15 16 17 18 19 20 21 23 03 06 09 12
[AST]
(UT)
fIF(T) GOOSE BAY 11 NOV 80

Figure 57

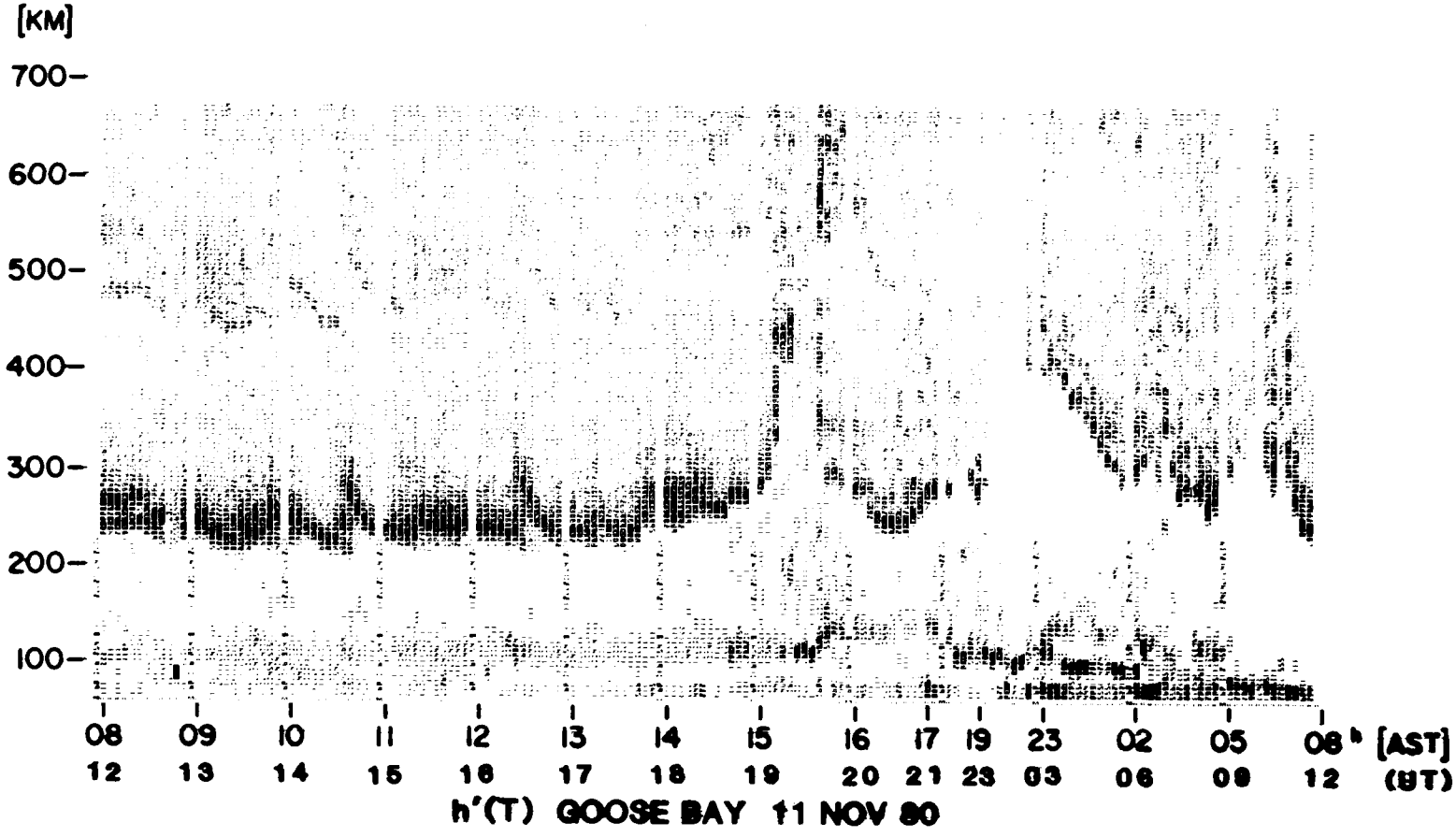
[KM]
700
600
500
400
300
200
100
08 09 10 11 12 13 14 15 16 17 19 23 02 05 08 h [AST]
12 13 14 15 16 17 18 19 20 21 23 03 06 09 12 (ST)
h'(T) GOOSE BAY 11 NOV 80

Figure 58

by different Doppler frequencies (the Doppler ionogram is at the bottom of Figure 59, the amplitudes are on top). Positive Dopplers indicate approaching and negative Dopplers receding formations. The lowest trace in the ionogram has strongly negative Dopplers, the middle one slightly positive Dopplers and the highest trace very positive Dopplers. This is the typical signature of a moving ionization hole the center of which has almost reached the station (Bibl, 1974).

The scaled peak plasma densities measured at the different locations and times where mapped in a polar corrected geomagnetic coordinate system (Whalen, 1970). Interpolation between the discrete observations resulted in the iso-density contour plot shown in Figure 60. The mid-latitude trough with plasma frequencies of 3 to 4 MHz extends from dusk to midnight. A localized F-region bite-out occurs at 1620 corrected geomagnetic local time with very steep gradients at the western wall. A quiet reference day, 26 January 1981, shows no afternoon bite-out (Figure 61).

If the trough is believed to be the result of the superposition of the corotational eastward convection and the magnetospheric polar cap convection (Knudsen, 1974; Spiro et al, 1978), then changes in the dawn to dusk magnetospheric E-field will strongly affect the shape and location of the trough. However, we do not expect the stagnation point of the convection to be at local afternoon (1600 CGLT) when the F-region is still illuminated by the sun. It is more likely that the hole is not a direct part of the premidnight trough. The observed increase in virtual height suggests an upward motion of the F ionization in a localized area, but it is not clear what physical process would explain this field aligned plasma flux.

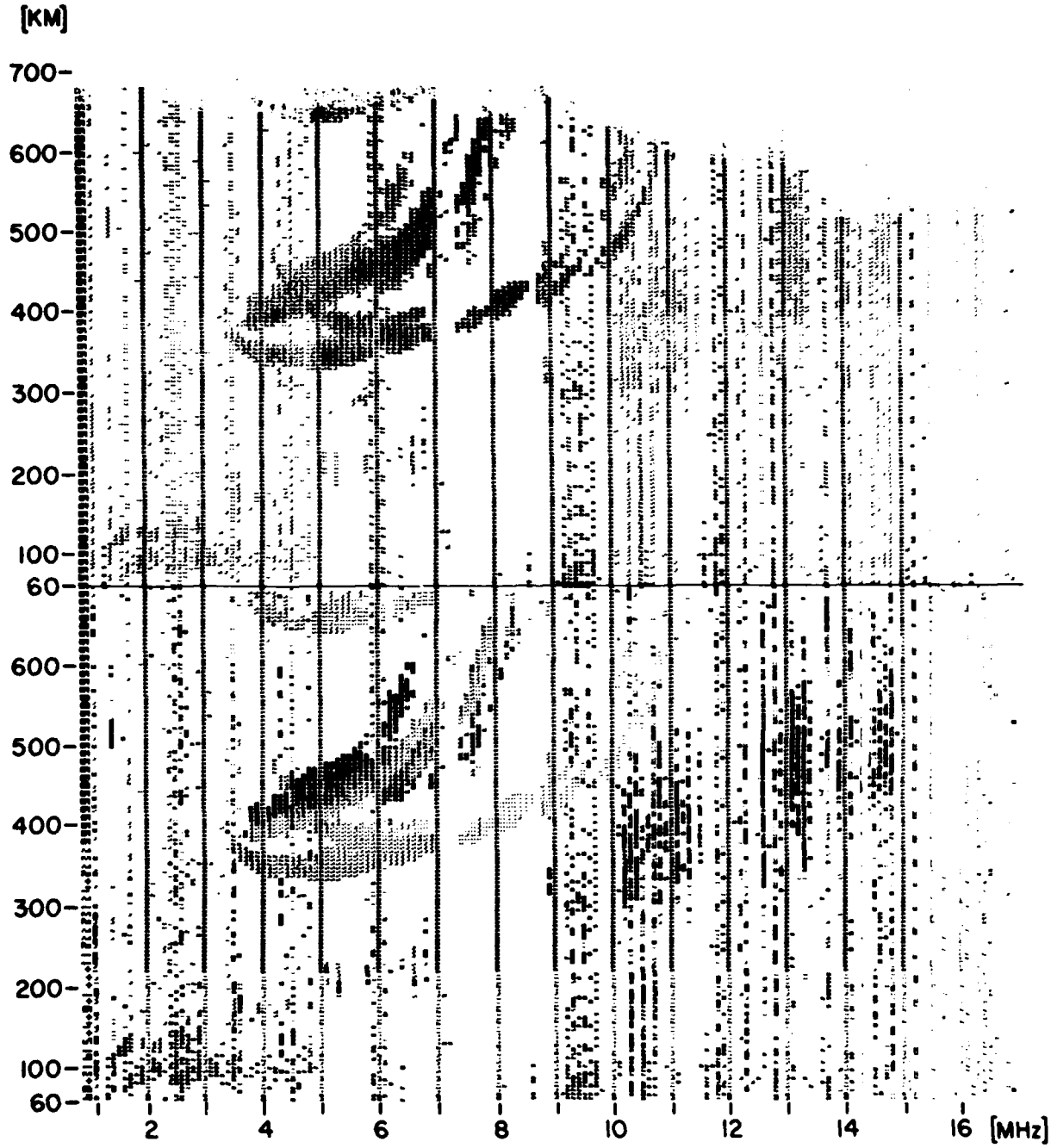
[KM]
700
600
500
400
300
200
100
60
600
500
400
300
200
100
60
2
4
6
8
10
12
14
16
[MHz]
AMPLITUDE AND DOPPLER IONOGRAM
GOOSE BAY 11 NOV 80 1504 [AST]
(UT)

Figure 59

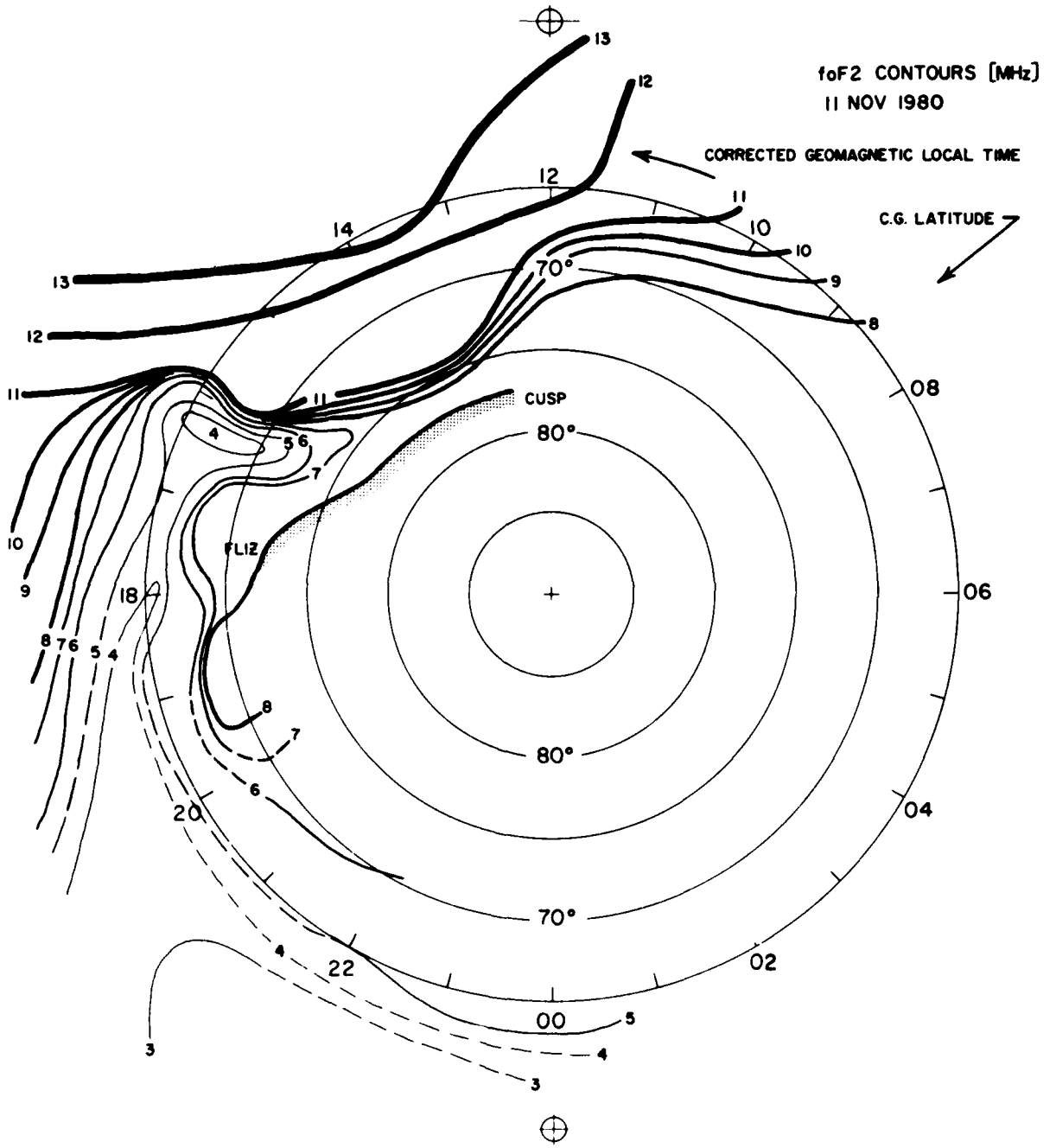
foF2 CONTOURS [MHz]
11 NOV 1980
CORRECTED GEOMAGNETIC LOCAL TIME
C.G. LATITUDE
CUSP
FLIZ
12
14
13
12
11
10
9
8
18
20
22
00
02
04
06
08
70°
80°
80°
70°

Figure 60

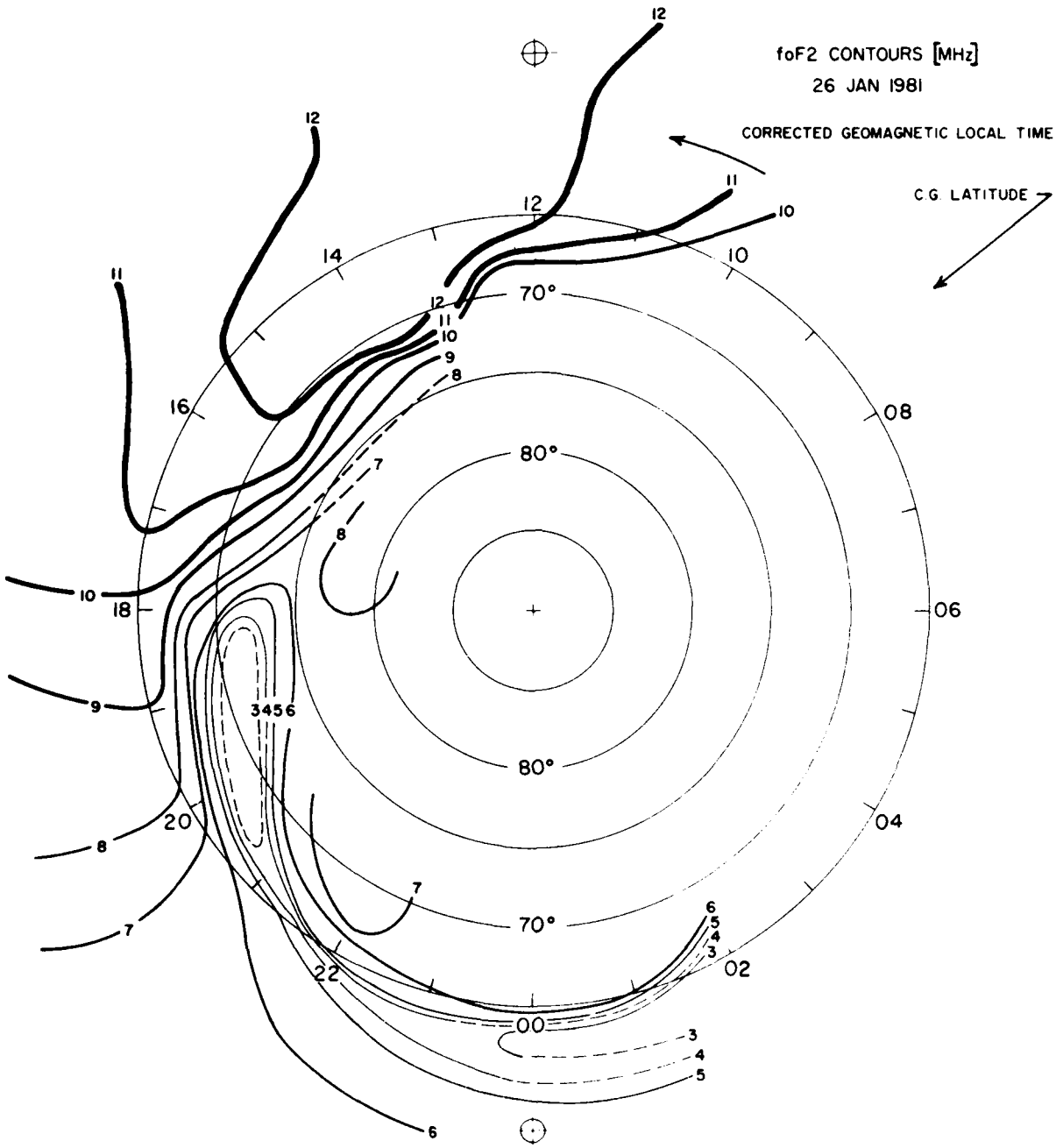
foF2 CONTOURS [MHz]
26 JAN 1981
CORRECTED GEOMAGNETIC LOCAL TIME
C.G. LATITUDE
70°
80°
80°
70°
00
02
04
06
08
10
12
14
16
18
20
22
3456

Figure 61

2.4 Routine Ionogram Scaling

The hourly vertical ionograms of Goose Bay have been scaled using URSI regulations as documented by Piggott and Rawer in the UAG Reports 23 (1972), 23A (1978) and 50 (1975) issued by the World Data Center A, Boulder, Colorado. Since these ionospheric background data serve as reference for many special studies we have scaled a complete set of ionospheric parameters.

Frequencies:

foF2	critical frequency of F2 layer
foF1	critical frequency of F1 layer
foE	critical frequency of E layer
foEs	critical frequency of Es layer
Type Es	
foEs2	critical frequency of second Es layer
Type Es2	
fbEs	critical frequency of blanketing Es
foT	critical frequency of transitory layer between E and F
frEs	cusp frequency separating E and Es
MUF(3000)F2	Max. usable frequency for F2 layer propagation on 3000 km
MUF(3000)F1	Max. usable frequency for F1 layer propagation on 3000 km
fmin	lowest frequency that shows echo
foFOB	max. frequency of oblique F echo
fminOB	min. frequency of oblique F echo

Virtual heights (ranges):

h'F2	minimum height of F2 layer
hpF2	true peak height if F layer has parabolic shape
h'F	minimum height of F1 layer (if present) or F2 layer
h'E	minimum height of E layer
h'Es	minimum height of Es layer

h'Es2	minimum height of second Es layer
h'FOB	range of oblique F echo

The oblique sporadic E and F traces are scaled to monitor irregularities moving over the station. Hourly values are not sufficient to analyze these irregularities, but at least they indicate the disturbed time periods.

Ionograms from January 1979 to September 1982 were scaled, the values were computer tabulated and stored on punch card and on magnetic tape. Actually two magnetic tapes are updated every month by adding new data. One tape is stored at AFGL, the other at the University of Lowell. Data from before 1979 are currently archived only on punch cards, and transfer onto magnetic tape will be done in the future. Table 4 shows the program required to read the tape. The computer program that sorts and error checks the scaled data also calculates the monthly medians. The median curves for foF2, foF1, foE, foEs, h'F2, h'F, h'E, h'Es and the Es occurrence distributions are shown in Appendix A for the period January 1979 to September 1982.

In winter 1979/80 the solar sunspot cycle reached its peak. This is evident by the high foF2 values between 1200 and 1500 local time. In the winter 78/79 the median values reaches a peak of 12.5 MHz (February 1979), in November 1979 the peak is 14.6 MHz, in November 1980 it is 13.5 MHz and in December 1981 13.9 MHz. In comparison, the peak median values for the winter 76/77 was 6.2 MHz (January 1977) and for winter 77/78 it was 9.1 MHz (February 1978). The highest E layer critical frequency occurred in June 1980 with foE = 3.9 MHz.

2.5 Computer Printing of Digisonde Ionograms

It is often desired to obtain computer printouts of

```
LIST

 83/07/13. 14.17.10.
PROGRAM   CLAIR

      PROGRAM,CLAIR(INPUT,OUTPUT,TAPE5=INPUT,TAPE6=OUTPUT,TAPE2,PUNCH,
     1TAPE4,TAPE11,TAPE12,TAPE13,TAPE14,TAPE15,TAPE16,TAPE17,TAPE18,
     1TAPE19,TAPE20,TAPE21,TAPE22)
      DIMENSION IFQF(12,31,24) ,IDA(12),X(31),IAV(24),NCT(24)
      DATA IDA/31,28,31,30,31,30,31,31,30,31,30,31/
      NF1=17
      NF2=18
      DO 1 K=1,24
      DO 1 I=1,12
      DO 1 J=1,31
  1   IFQF(I,J,K )=0
      DO  7 NF=NF1,NF2
      READ(NF,18)ID
      WRITE(6,30)ID
 22   CONTINUE
      READ(NF,18)ID
      IF(EOF(NF))7,8
  8   CONTINUE
      READ(NF,18)ID,IYR,MON,IDAY,IHR,IFQ
      IF(EOF(NF))7,32
 32   CONTINUE
      IF(IDAY.EQ.0)GO TO 20
      IF(MON,EQ.0)GO TO 20
      IFQF(MON,IDAY,IHR+1)=2*IFQ
  2   READ(NF,18)ID
      IF(EOF(NF))7,22
  7   CONTINUE
      IM1=NF1-10
      IM2=NF2-10
      DO 2 I=IM1,IM2
      IM=IDA(I)
      IF(IYR.EQ.76.AND.I.EQ.2)IM=IM+1
      IF(IYR.EQ.80.ANDI.EQ.2)IM=IM+1
      DO 2 J=1,IM
      WRITE(6,30)IYR,I,J,(IFQF(I,J,K),K=1,24)
  2   WRITE(4   )IYR,I,J,(IFQF(I,J,K),K=1,24)
      ENDFILE 4
      REWIND 4
 30   FORMAT(1X,30I4)
 18   FORMAT(I2,3X,4I2,43X,I3)
 19   FORMAT(I4)
      STOP
      END
```

Table 4

ionograms recorded on magnetic tape. Based on existing software we developed a special routine for this task.

The computer program prints ionograms from either Digisonde 128 or Digisonde 128PS tapes. For each ionogram, the program prints a header label with preface information, a height scale in km and amplitude data for each frequency. For each frequency line, the program prints the actual frequency (in 0.1 MHz steps) and 126 amplitude values (in 4 dB increments) followed by the noise level and the gain. This is similar to the on-line printing format in the aircraft. The user may specify whether the program will print all the ionograms on the tape, only ionograms at hourly intervals or only vertical ionograms. The program is written in FORTRAN using Control Data Corporation's FORTRAN Extended Version 4 and will need modification if used on a non-CDC computer. Figure 62 shows an example of such printout, photographically reduced to report size. The print program has been implemented on the computer of World Data Center A, Boulder, Colorado, where it is available to provide on request (Conkright, 1983) printouts of digital ionograms from Goose Bay. The total magnetic tape data base (Digisonde 128 and 128PS ionograms since January 1975) has been transferred to WDC A.

A full description of the program is given in an AFGL Research Paper (Shirley et al, 1983).

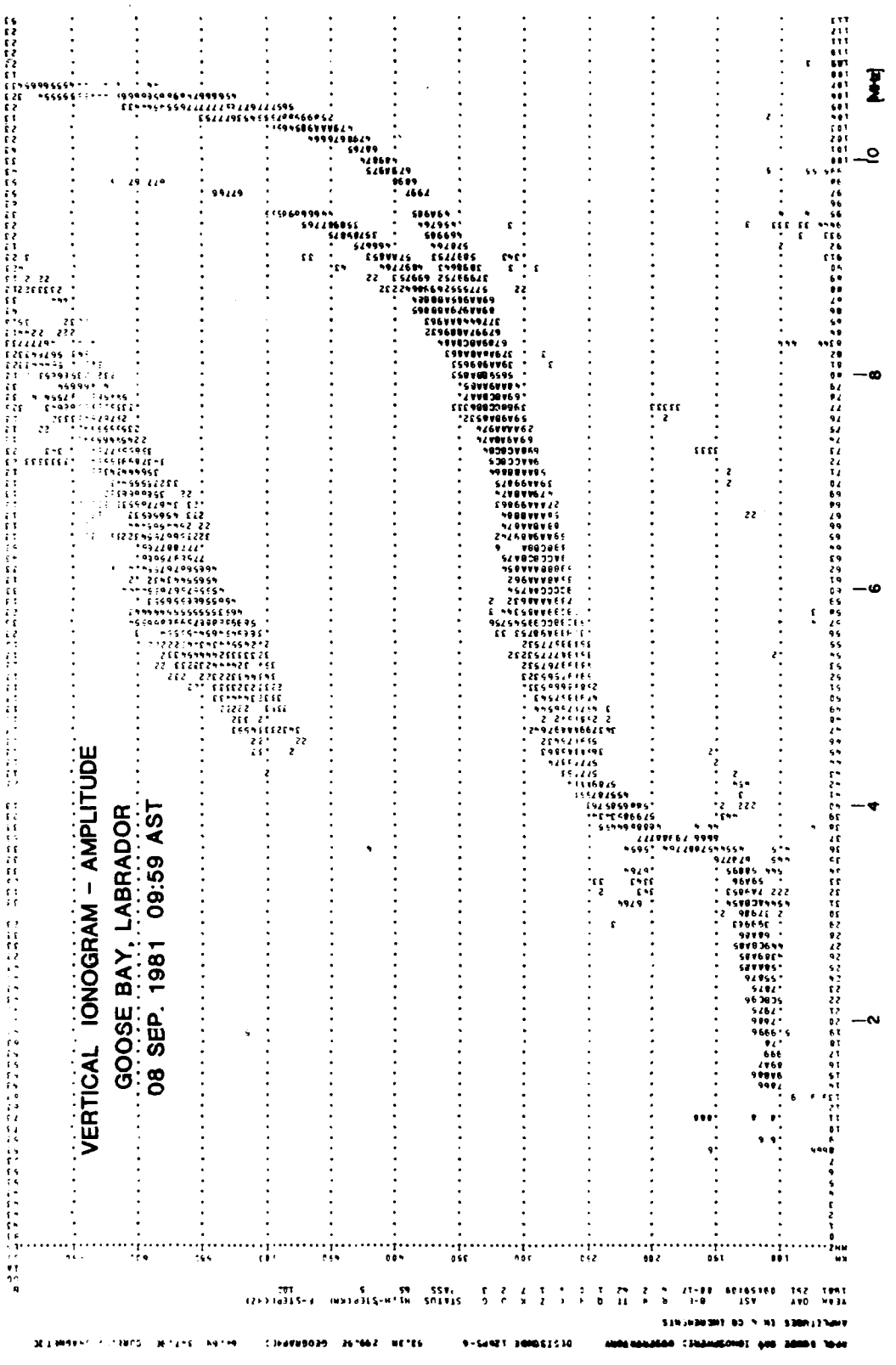
VERTICAL IONOGRAM – AMPLITUDE
GOOSE BAY, LABRADOR
08 SEP. 1981 09:59 AST

Figure 62

3.0 GROUNDBASED AND AIRBORNE IONOSONDE OBSERVATIONS IN SUPPORT OF THE OTH RADAR TESTS 1980/81

The AFGL airborne ionospheric observatory was carrying out a number of missions in 1980/81 serving as target for the OTH radar during the testing of the Experimental Radar System (ERS) and at the same time collecting ionospheric data. Vertical, bistatic (propagation) and backscatter ionograms were made at Goose Bay, the aircraft and at the OTH site in Maine. The aircraft has only one HF antenna which had to be multiplexed between the different tasks. The sounding schedule that was implemented is shown in Figure 61, listing the transmission and receiving times for the Goose Bay Digisonde, the aircraft Digisonde, the aircraft Barry sounder, and the aircraft HF transponder. The aircraft Digisonde made six vertical ionograms per hour, and the radiation was received as a propagation ionogram at Goose Bay operating its Digisonde in the receive-only mode. The Goose Bay Digisonde transmitted 16 ionograms per hour, ten of which were received at the aircraft. The Goose Bay B ionograms used vertical transmit and receive antennas to make vertical ionograms. In parallel, a log-periodic rotatable antenna was activated to transmit in the direction of the aircraft. The C ionogram was programmed for backscatter observations using transmit and receive antennas pointing toward magnetic north.

For the radar operators at Maine up-to-date information on the ionosphere in the ray path reflection region is important for frequency management and for radar range to ground range conversion. To feed complete ionograms through a dedicated telephone line to Maine ULCAR had built the Ionogram Communicator, ICOM (Reinisch and Bibl, 1981). Different ionograms can be selected for telephone transfer by operating ICOM in Mode 12, 13, 14 or 15 (Figure 63), allowing the radar

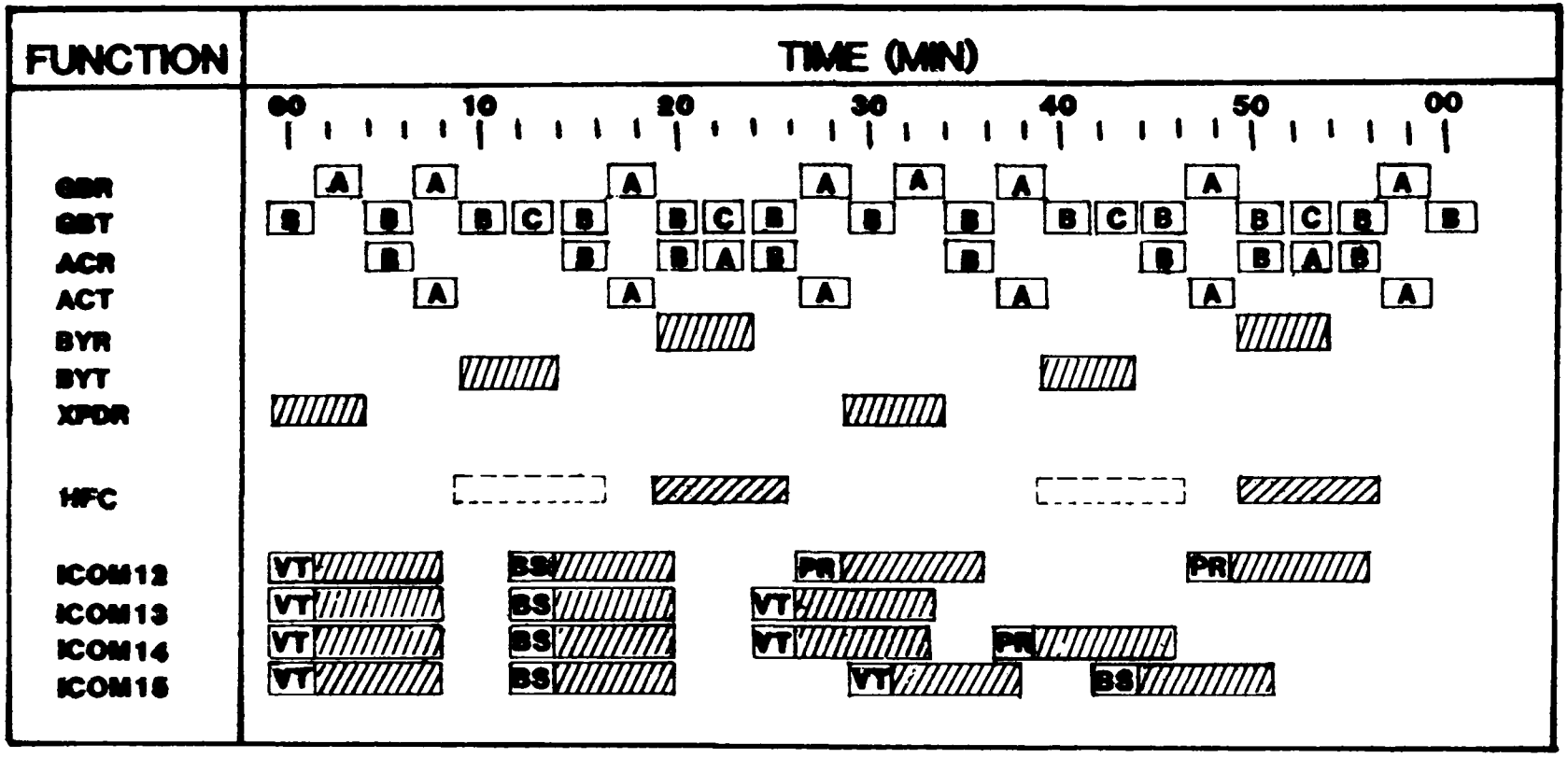

GB	Goose Bay Digisonde	R	Receive
AC	Aircraft Digisonde	T	Transmit
BY	Barry Chirp Sounder	VT	Vertical Ionogram
XPDR	Transponder	BS	Backscatter Ionogram
HFC	HF Communication	PR	Propagation Ionogram

Figure 63. HF Operations During OTH Missions

AD-A140 012 IONOSPHERIC RESEARCH USING DIGITAL IONOSONDES(U) LOWELL 2/3
UNIV MA CENTER FOR ATMOSPHERIC RESEARCH
B W REINISCH ET AL. JUL 83 ULRF-425/CAR AFGL-TR-83-0184
UNCLASSIFIED F19628-80-C-0064 F/G 4/1 NL

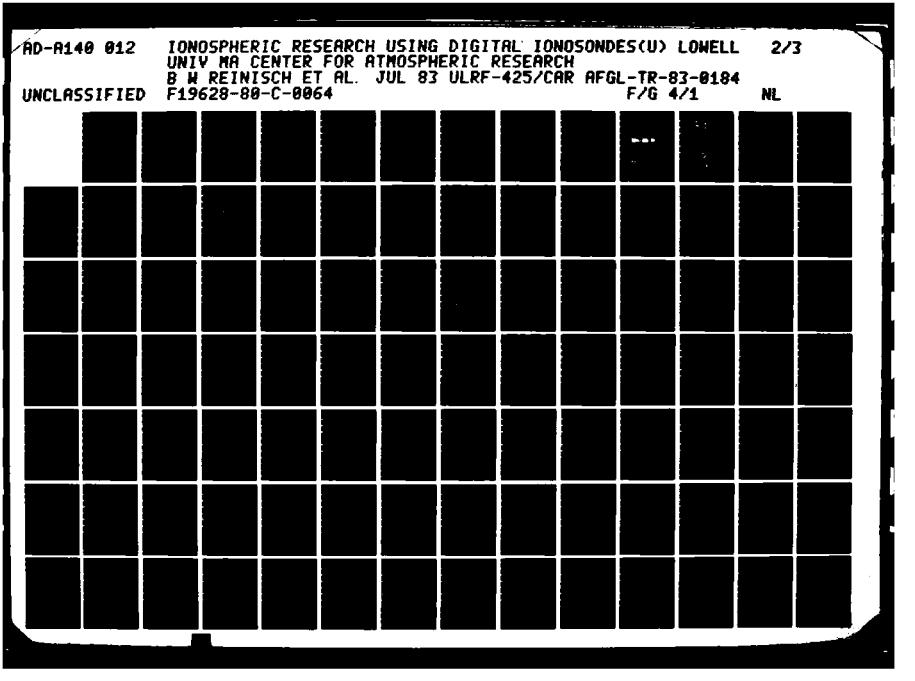

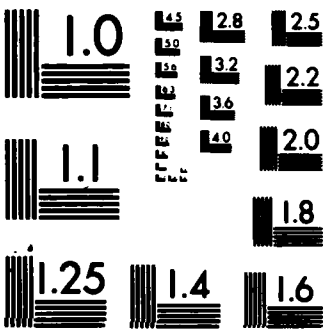

operator to consult vertical, backscatter and propagation (aircraft to Goose Bay) ionograms.

Dr. R. Penndorf analyzed a large amount of the propagation data and prepared a number of internal reports submitted to the Contract Monitor. An AFGL in-house test report summarized the results: "AFGL Airborne Ionospheric Observatory, ERS Test Report No. 2," Technical Memorandum 45, 26 January 1981 by J. Buchau, E. Weber, R. Gowell, P. Krukonis, J. Moore, K. Bibl and B. Reinisch.

4.0 IONOSPHERIC DRIFT OBSERVATIONS AT GOOSE BAY

Motions of the ionosphere can be detected and analyzed by means of the Doppler shift imposed on the radio wave by the moving reflector (Pfister and Bibl, 1972). The Digisonde 128PS (Bibl and Reinisch, 1978) in Goose Bay, when operating in the Doppler-Drift mode, measures the full Doppler spectrum of the echo signals received at each of the four receiving antennas. Cross-correlating the complex spectra (amplitude and phase) of the antenna signals results in sky maps (Bibl et al, 1975) which give the locations of the reflection points and the Doppler frequency imposed by the motion of the reflection points. Figure 64 shows on the left side the locations of the reflection points for four consecutive 18 second measurements (cases) labelled 0, 1, 2, and 3. The associated Doppler frequencies are displayed in the accompanying map on the right. It is important to stress the existence of several reflection points for each observation. The signals received at each antenna are the sum of the waves reflected at the different 'source' points. It would be meaningless to measure the phase of the composite signal since frequently the different sources have comparable amplitudes. Simple phase triangulation techniques for the determination of the source location work well only if only one source exists. Since, in general, the ionosphere is moving each reflection point has its characteristic Doppler frequency:

$$d = \frac{1}{\pi} \vec{k} \cdot \vec{v}$$

where $\vec{k}$ is the wave vector pointing from the source to the receiver and $\vec{v}$ the velocity vector of the reflector. The spectral analysis thus separates the signal contributions from the different sources, and phase comparisons between the antenna signals can be made for each spectral component.

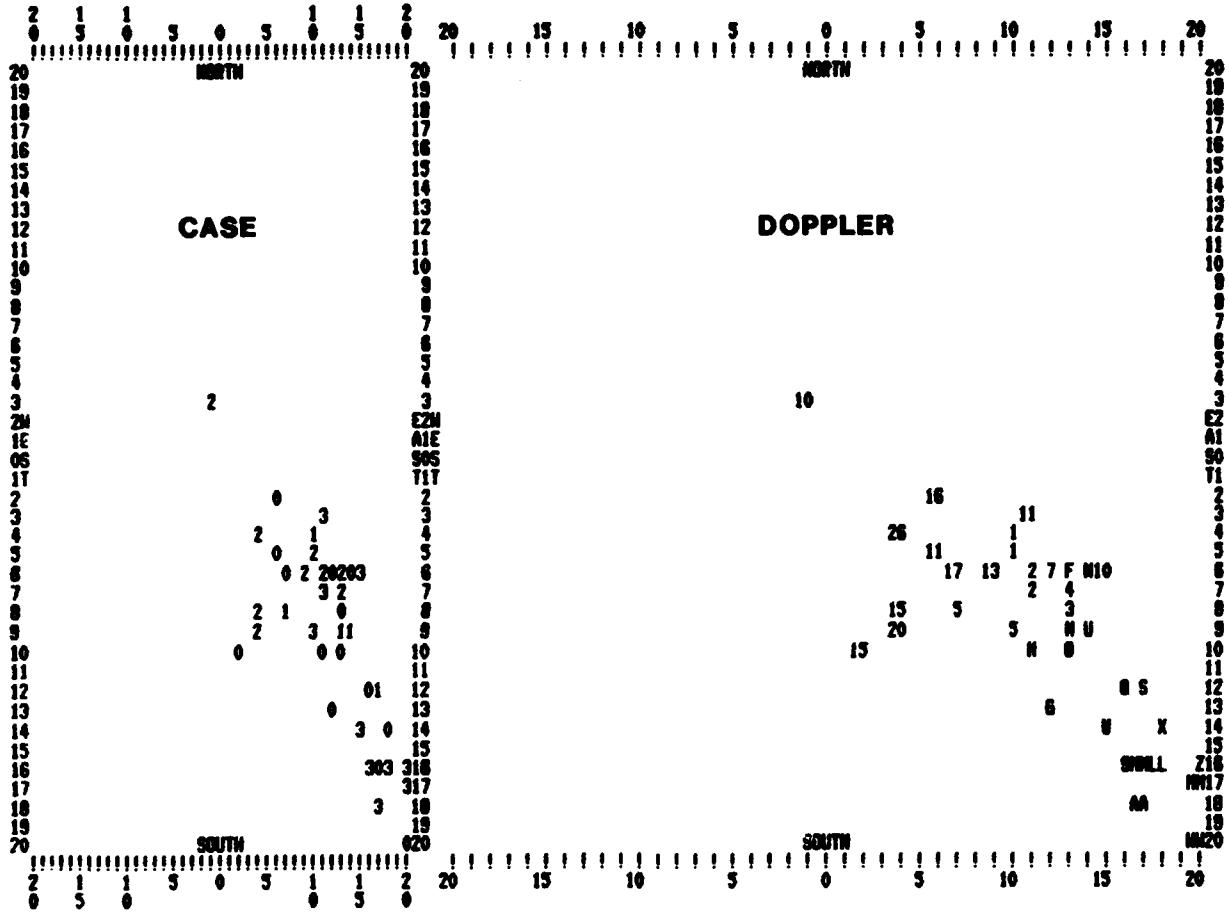

Figure 64

NEGATIVE DOPP = NUMERIC POSITIVE DOPP = ALPHA

DOPPLER RESOLUTION = .1225 HZ

SCALE: 9.4 KM/DIVISION ζ_{max} = 45°

DOPPLER SKY MAP

26 JAN 1982 GOOSE BAY, LABRADOR

20:18 AST 3 MHZ 375 KM

If a uniform drift velocity is assumed one can find the velocity vector $\vec{v}$ that best reproduces the observed Doppler frequencies for a given sky map. We have developed the computer software to the point that large data tapes, with drift data recorded at Goose Bay, can be processed efficiently outputting the three dimensional drift velocity vectors as function of time. Figure 65 is an example of the results obtained for an eleven hour observation period from 1800 AST on 26 January to 0500 AST the next morning. The azimuth (bottom) and the magnitude (top) of the horizontal component of the drift velocity are shown as solid lines. Each drift observation was conducted simultaneously at three frequencies and at the virtual heights of the corresponding plasma densities. The velocities at all three ranges are represented by numbers and letters that indicate the ranges according to the equation

$$r = 200 + 10X, \qquad X = 1, 2, 3, \ldots, 9, A, B, \ldots$$

For example between 2147 and 2200 AST the range indicators are F, G and J corresponding to ranges 350 km, 360 km and 390 km. In general, the different frequencies observe similar velocities. The solid line is the average of the three observations.

A very systematic behavior of the drift direction is seen in the azimuth display. Before local midnight the drift direction is predominantly westward, and after midnight it is mainly eastward. A similar transition is observed for January 20/21 (Figure 66). The azimuth variations are significant after midnight, when the drift speed occasionally surpasses 200 m/s. Before midnight the speed remains generally below 150 m/s with one exception around 2000 AST on 26 January. The vertical velocity component is shown in the upper panels as + and - symbols indicating upward and downward velocities. Most of the time the vertical velocity is smaller than 40 m/s,

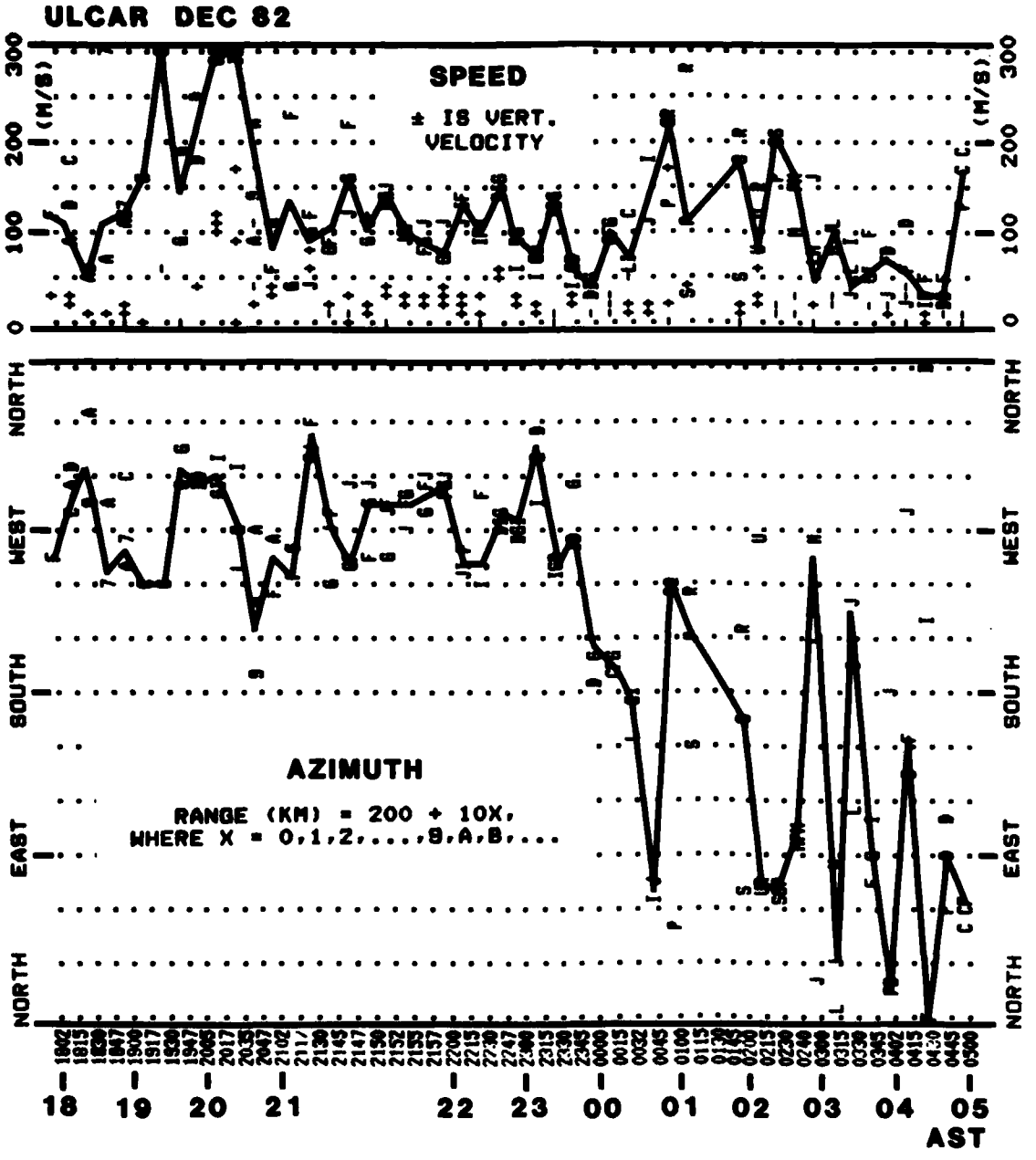

F - REGION DRIFT
DIGISONDE OBSERVATIONS AT GOOSE BAY, LABRADOR
26/27 JAN 82 18 TO 05 AST

Figure 65

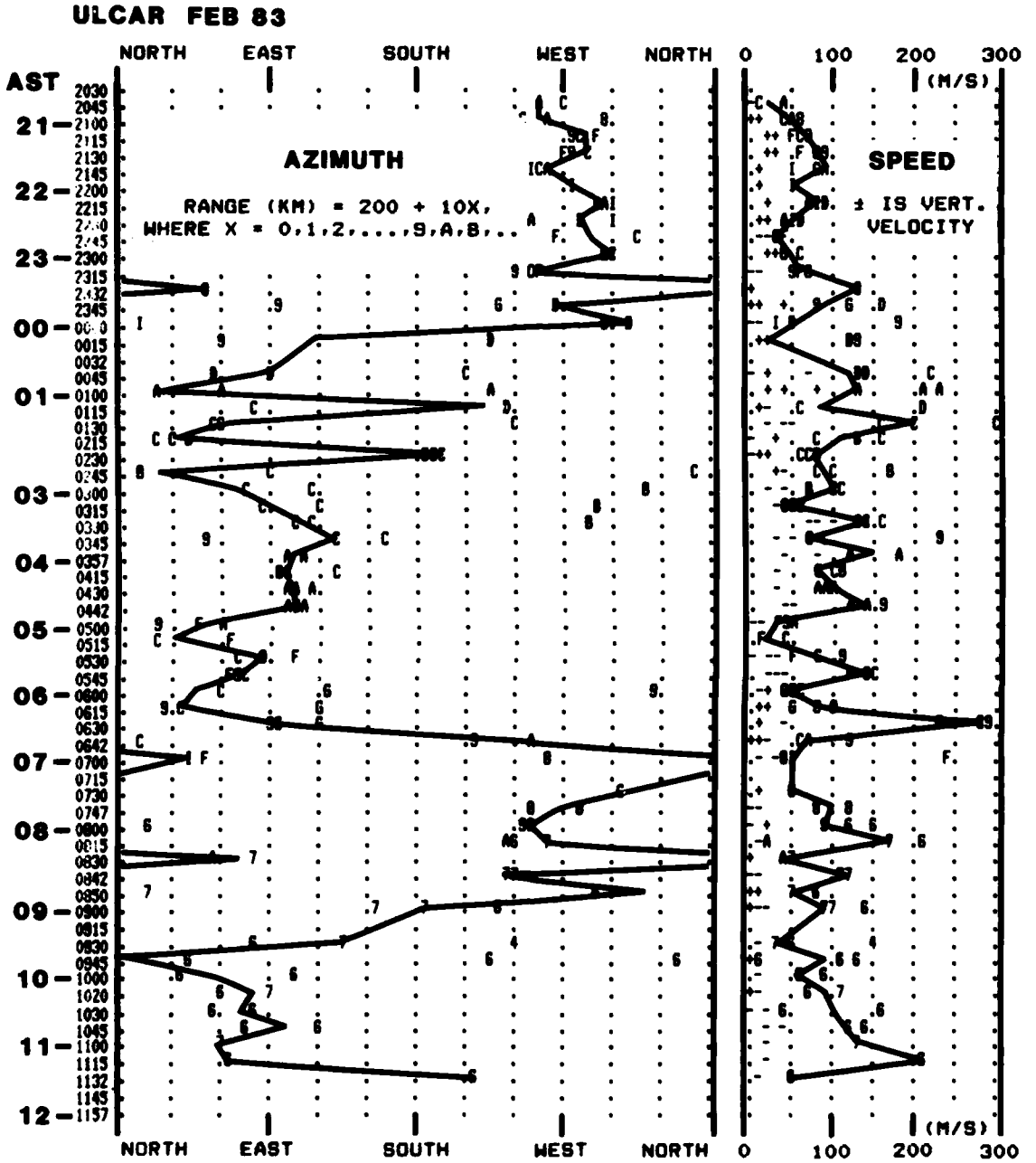

F - REGION DRIFT

DIGISONDE OBSERVATIONS AT GOOSE BAY, LABRADOR

20/21 JAN 82 20:30 TO 12 AST

Figure 66

but values up to 100 m/s are observed. The observed horizontal velocities agree in magnitude and overall directions with the statistical results recently reported by Oliver et al (1983) from Millstone Hill Incoherent Scatter Measurements.

The midnight drift reversal seems to suggest that the Goose Bay F region is part of, or at least is coupled to, the polar cap two cell convection pattern (Spiro et al, 1978). Drift measurements from January 82, January 83 and March 83 are currently analyzed to study the midnight reversal. The observational techniques and the methods of analysis are described in Scientific Report No. 6 (Dozois, 1983).

5.0 POLAR CAP IONOSPHERIC STUDIES AT THULE

In January 1982 and January 1983 AFGL's KC-135 aircraft was parked at Thule AF Base, Greenland (86° CGL) to conduct radio and optical observations of the winter polar cap ionosphere. The Digisonde operated at the aircraft HF antenna. Since no receiving antenna array was deployed we could not make incidence angle measurements on echoes received from F-region arcs and ionization patches. But all-sky photometer images (Weber et al, 1977), taken at 2 to 5 minute intervals, identified the locations of the irregularities that were seen on the Digisonde ionograms. The ionograms were recorded at 1.5 or 2.5 minute intervals. The large dynamic effects in the winter polar cap F region are illustrated by the height characteristic of 22 January 82 (Figure 67). All 160 hours of Digisonde ionograms recorded during the January 82 mission were processed with a velocity filter, based on the measured Doppler and the operational frequency, and presented as range/time characteristics; an example is shown in Figure 68. For instance, at 23:30 UT an F region irregularity approaches the station with a horizontal velocity of approximately 250 $m \cdot sec^{-1}$, since the characteristic labelled 250 $m \cdot sec^{-1}$ contains the highest signal amplitudes of the echoes trace that decreases in range as function of time. An inspection of the range change time history also reveals, that the trace best seen around 23:30 UT in the 240 $msec^{-1}$ velocity characteristic corresponds to a horizontal bulk motion of ~250 $msec^{-1}$, i.e. the bulk velocities and the simultaneous Doppler velocities are identical. A description of the data processing techniques, a summary of the observations and the conclusions are contained in the AFGL Environmental Research Paper, No. 792, by J. Buchau, B. Reinisch, E. Weber and J. Moore, "Structure and Dynamics of the Winter Polar Cap F Region." The abstract of this paper is reproduced here.

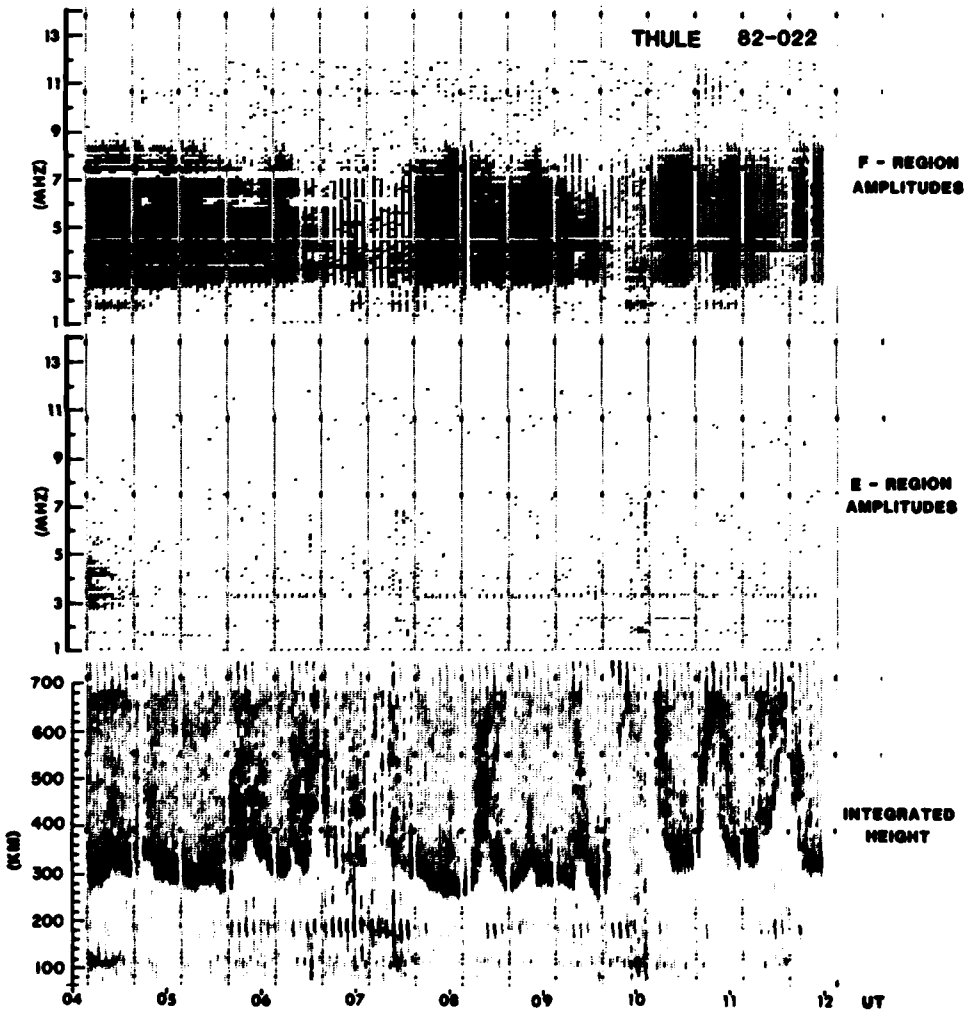
THULE 82-022
F - REGION AMPLITUDES
E - REGION AMPLITUDES
INTEGRATED HEIGHT
(MHZ)
(KM)
UT

Figure 67

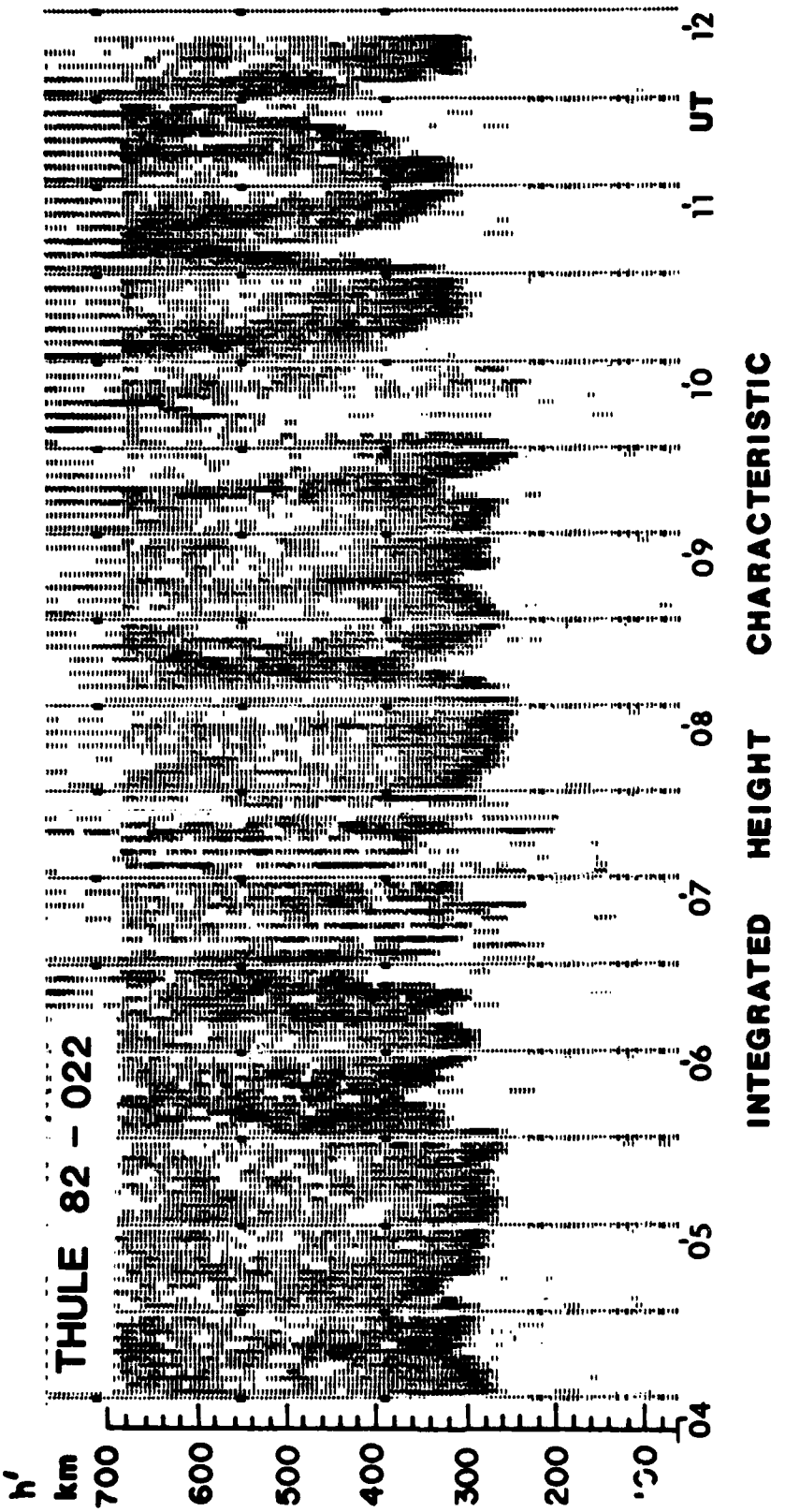
INTEGRATED HEIGHT CHARACTERISTIC
THULE 82 - 022
h'
km
700
600
500
400
300
200
04
05
06
07
08
09
10
11
12
UT

Figure 6

ABSTRACT

All-sky photometer images and ionospheric soundings taken at Thule, Greenland (86° CGL) in December 1979 and January 1982 reveal three groups of forms important in the organization of the winter polar cap ionosphere.

1) The most prominent features are sun-aligned, generally unstructured, subvisual, F-region arcs, extending for more than 1200 km (limit of all-sky camera field of view) across the polar cap. These arcs usually drift from dawn to dusk at speeds between 100 and 250 m/sec, however, stagnations of arc drift and drift reversals have been observed. The arcs are produced by soft particle precipitation.

2) During a magnetically disturbed period the arcs disappeared and large patches of enhanced F-region ionization drifted as speeds of 250 to 700 m/sec across the field of view in the antisunward direction. Although arcs are produced by soft particle precipitation, preliminary results from the Dynamics Explorer satellite do not indicate any localized soft electron precipitation into the patches.

3) On a few occasions both forms were observed simultaneously. Between F-region sun-aligned arcs drifting from dawn to dusk, small patches of ionization were observed moving at much higher speeds in the antisunward direction.

Both the arcs and the patches appear as strong localized irregularities in the ionospheric soundings. The Doppler information provided by the Digisonde 128PS was used to relate backscatter traces to individual arcs or patches and to track these features over more than 1500 km. Many observations suggest specular reflection from electron density enhancements associated with the optical forms, rather than scatter from field-aligned irregularities embedded in the arcs or patches. High velocities occurred more often during magnetically active periods.

F-region arcs are bands of enhanced ionization, imbedded in a background ionosphere with a base height h'F of approximately 250 km and a critical frequency of about 4 MHz (2×10^5 el/cm^3). The virtual heights in the ionograms did not change during transit of the arcs through the zenith. During the active periods, when the antisunward-moving patches were observed, the background ionization dropped to less than 3 MHz (10^5 el/cm^3) while the base height (h'F) moved up to heights above 400 km. The strongly ionized patches (foF2 more than 8 MHz), however, were observed to reach a minimum virtual range of about 250 km during the zenith transit, leading to rapid h'F fluctuations in the order of 200 km within minutes.

6.0 AUTOMATIC REAL TIME IONOGRAM SCALER WITH TRUE HEIGHT ANALYSIS, ARTIST

In March 1983, the ARTIST was installed at the Goose Bay Ionospheric Observatory and connected to the Digisonde 128PS. Originally conceived for the Digisonde 256, the ARTIST has been adapted to the 128PS and is now routinely scaling the Goose Bay digital ionograms in real time. After many years of development we finally succeeded in complete automatic scaling of Digisonde ionograms in real time. The difficult task was to scale ionograms for disturbed conditions. In Goose Bay about 50% of the ionograms show spread F. Goose Bay is a subauroral station and the ionograms display a large variety of features: quiet and disturbed daytime recordings, spread F during the night, the mid-latitude trough moving over the station, fast variation of the ionospheric parameters and frequent absorption events. Four months of ionograms for the high sunspot year 1980 served as data base for the evaluation of the scaling and true height algorithms. Some 8000 ionograms for January, April, July and September 1980 were processed. The autoscaled parameters for the 2000 hourly ionograms during these periods were compared with the manually scaled values. The results of this comparison are given in Scientific Report No. 7 (Reinisch et al, 1983). Table 5 shows that for 89.6% of all ionograms foF2 was autoscaled within ±0.5 MHz, and for 95.6% within ±1.0 MHz. This breakthrough in ionospheric observational techniques will be important for communication prediction as well as ionospheric research. The scaling algorithms and the scaling accuracy are described in Scientific Reports Nos. 4, 5 and 7 prepared by Reinisch et al (1982), Gamache et al (1983) and Reinisch et al (1983) under this contract. Details on the true height analysis are given in two papers by Huang and Reinisch (1983), and Reinisch and Huang (1983).

Percentage of cases for foF2, MUF3000F and M3000F where manual and automatic scalings fall within indicated limits

Table 5

1980	No. of Ionograms	foF2 ±0.5 MHz	foF2 ±1.0 MHz	MUF(3000) ±5%	MUF(3000) ±10%	M(3000) ±0.1	M(3000) ±0.2	
January	582	83.5	92.1	69.0	79.7	59.1	77.8	All Ionograms
April	546	90.3	96.2	79.5	87.7	71.6	88.0	
July	528	93.6	97.7	80.2	93.2	65.0	92.6	
September	570	91.6	97.0	80.9	92.0	65.4	81.0	
Four Months	2226	89.6	95.6	77.2	88.0	65.2	82.2	
January	267	91.0	95.1	90.8	96.3	73.8	88.0	Non-Spread
April	288	95.2	98.3	94.4	96.5	82.6	95.1	
July	133	96.2	97.7	82.8	90.3	75.2	85.7	
September	259	93.0	97.0	93.4	97.0	78.8	90.7	
Four Months	947	93.6	96.9	91.1	95.7	78.0	90.6	

As an 8086 Central Processor Unit based computer, the ARTIST is a Digisonde subunit, that is housed in a 19" × 9" × 22" chassis. It operates either in real time, connected to a Digisonde, or it reads digital ionograms from magnetic tape (9 tracks, 1600 bps). Installation and operation of the ARTIST is simple: one cable connects the ARTIST to the Processor of the Digisonde, one cable goes to the tape drive and one RS232 port drives the printer. A CRT terminal is connected to a second RS232 port. The ARTIST contains two floppy disk drives; one drive contains the floppy with the programs, the other can be used to store data and to copy disks. After activating the reset switch or after power-up the program is loaded from disk and the program options can be selected from the keyboard by answering the questions displayed on the CRT. Tables 6a, b illustrate the procedure.

It requires less than 1 minute to process one ionogram including the profile conversion. Processing starts when the ionogram scan is completed. During processing the next ionogram can be inputted, this means that a sequence of 1 minute ionograms can be handled. A typical ARTIST printout is shown in Table 6c. The top lines identify the ionogram and give the sounding parameters. The next entry lists the ionospheric parameters: foF2, foF1, h'F, h'F2, M3000, fmin, foEs, MUF(3000), fminF, fxI, fminE, foE, h'E, and h'Es. The average range spread (in km) for the F and E traces is shown under QF and QE, and the frequency spread (in MHz) under FF and FE. The complete F and E traces are listed under the heading AUTOSCALED TRACES; the virtual height (in km) is given for each sounding frequency (0.1 MHz increments). These trace data are the input to the true height routine. In the near future, the processed ionogram data will be transmitted directly to AWS and the OTH radar to support the radar range to ground range conversion algorithms of the radar.

```
                ARTIST        ULCAR 1983

ENTER INPUT. PLEASE RESPOND WITHIN 20 SECONDS,
OTHERWISE DEFAULT VALUE WILL BE CHOSEN.

EACH ENTRY MUST BE FOLLOWED BY A CARRIAGE RETURN.


*TYPE 1 FOR ONLINE PROCESSING (DEFAULT)
 TYPE 2 FOR TAPE READ

 ENTER--2



*WHERE WAS THE STATION ?
 SELECT STATION NUMBER FROM THE FOLLOWING LIST.

 1--NEW NATAL, BRAZIL DATA
 1X--OLD NATAL, BRAZIL DATA
 6--GOOSE BAY, LABRADOR, DATA TAKEN ON OR AFTER JUN 14 1980.
 6X--GOOSE BAY, LABRADOR, DATA TAKEN BEFORE JUN 14 1980.
 0--NONE OF THE ABOVE STATIONS

 ENTER--6



*ENTER SUNSPOT NUMBER (DEFAULT=90 FOR JUN 1983)

ENTER--60



*TYPE 1 FOR PROCESSING ALL INPUT IONOGRAMS(DEFAULT)
 TYPE 2 FOR PROCESSING IONOGRAMS BETWEEN SPECIFIC TIME

 ENTER--2



 ENTER START TIME:
 DAY-----74
 HOUR----16
 MINUTE--59

 ENTER END TIME:
 DAY-----75
 HOUR----0
 MINUTE--0
```

Table 6a. ARTIST Initialization

```
#SELECT PLOT IONOGRAM OPTIONS. ENTER THE NUMBER COMBINATION IN THE LIST
 BELOW FOR THE DESIRED PLOTS,
 EG.ENTER 134 OR 123456. (DEFAULT--1 )

 1--AUTOSCALED IONOGRAM
 2--OPTIFONT IONOGRAM
 3--COLOR IONOGRAM (ONLY PLOT COMPRESSED DATA)
 4--DOPPLER IONOGRAM
 5--UNDEFINED PLOT
 6--BASELINE AND AMPLITUDE

 ENTER--



#TYPE 1 TO PRINT 64 COMPRESSED BINS PER FREQUENCY (DEFAULT)
 TYPE 2 TO PRINT 128 BINS PER FREQUENCY

 ENTER--2



#THERE ARE 5 CHOICES OF PRINT OUT:
 1--ULCAR FORMAT
 2--AWS FORMAT, PARAMETERS & TRACE HEIGHTS
 3--AWS FORMAT, PARAMETER ONLY
 4--AWS FORMAT,TRACE HEIGHTS ONLY
 5--PRINT ALL(DEFAULT)

 ENTER--



#TYPE 1 TO REWIND TAPE(DEFAULT)
 TYPE 2 TO CONTINUE READ/WRITE TAPE.

 ENTER--



#ENTER 2 TO PRINT INTERMEDIATE RESULTS, OTHERWISE NO PRINT.

 ENTER--



#TO INTERRUPT ARTIST EXECUTION:
 ENTER "CONTROL C" TO RETURN CONTROL TO THE OPERATING SYSTEM
 ENTER "CONTROL A" TO RESTART ARTIST PROGRAM


    INITIALIZATIONS FINISHED, START PROCESSING
```

Table 6b. ARTIST Initialization

```
    AUTOSCALED RESULTS BY A.R.T.I.S.T.          ULCAR JUN 83
ID YEAR DAY H  M  S  B  E  R W TT Q N X Z K J G H-STEP(KM) F-STEP(KHZ)
 6 1983  74 16:59: 9 00-17 4 2 42 1 0 4 1 7 2 3    5.0       100

FOF2  FOF1  H'F   H'F2  M3000 FMIN  FOES  MUF   FMINF
 6.8  ***   238.  **** 3.04   1.6   2.3  20.7   2.3

FXI   FMINE FOE   H'E   H'ES  QF    QE    FF    FE
 7.6  1.6   2.3   120.  120.  ***   ***   ***    .3

AUTOSCALED TRACES [KM]:
-----------------------

 2. ***** ***** *****  238.  238.  238.  238.  238.  238.  238.
 3.  238.  238.  238.  238.  238.  238.  238.  238.  238.  243.
 4.  243.  248.  248.  248.  253.  253.  258.  258.  263.  263.
 5.  268.  268.  273.  273.  283.  273.  303.  308.  313.  318.
 6.  323.  328.  338.  353.  368.  393.  438.  523.  683.
 1. ***** ***** ***** ***** ***** *****  120.  125.  125.  130.
 2.  135.  140.  150.  170.

TRACE  TRANSITION  F[MHZ]   VEL.[M/S]  VEL. AT TOPF [M/S]
  F                                        -22.
  E                                         67.
 ES                                         67.

NORMALIZED AMPLITUDE AS AT REFLECTION HEIGHT 100KM IN [DB]
        TOPF    2.    3.    4.    5.    6.
  F     23.     0.   42.   42.   47.   43.
  E     16.
 ES     16.
IONOGRAM:  1
```

Table 6c. ARTIST Output

The next lines list the Doppler information contained in the echo trace and the vertical velocity component if it can be derived from the Doppler information. Since the velocity calculations are not final yet we will not further discuss them here. The last entry gives the amplitudes of the echoes in dB; a free space attenuation correction to 100 km is applied using the measured virtual heights. Around each Megahertz the echo amplitudes of three neighboring sounding frequencies are averaged. These amplitude values can be used to correlate geomagnetic activity or other parameters of relevance to radio absorption.

For demonstration and verification it proved useful to print the full ionogram together with the identified trace (defined by the leading edge of the echo pulses) on the ARTIST output printer. In Figure 69, the identified E-trace is marked by a star and the ordinary F-trace by the # symbol. The star symbol is also used to indicate X-cusp in the F2 layer. Numbers, letters and symbols are used to represent the ionogram. The amplitudes for the ordinary echoes are given in multiples of 10 dB by the numerals 1, 2, ..., 6 (positive Doppler) and the letters A, B, ..., F (negative Doppler). X echoes are simply marked by an X, and oblique echoes from the north and south by the symbols Δ and ∇. A software error in the FORTRAN operating system prevented us from linking the true height program to the scaling program. But this problem will be solved soon. We will then be able to construct isodensity contours as a function of time which makes it possible to study the time development of the electron density profiles. A sequence of profiles during sunrise period is shown in Figure 70.

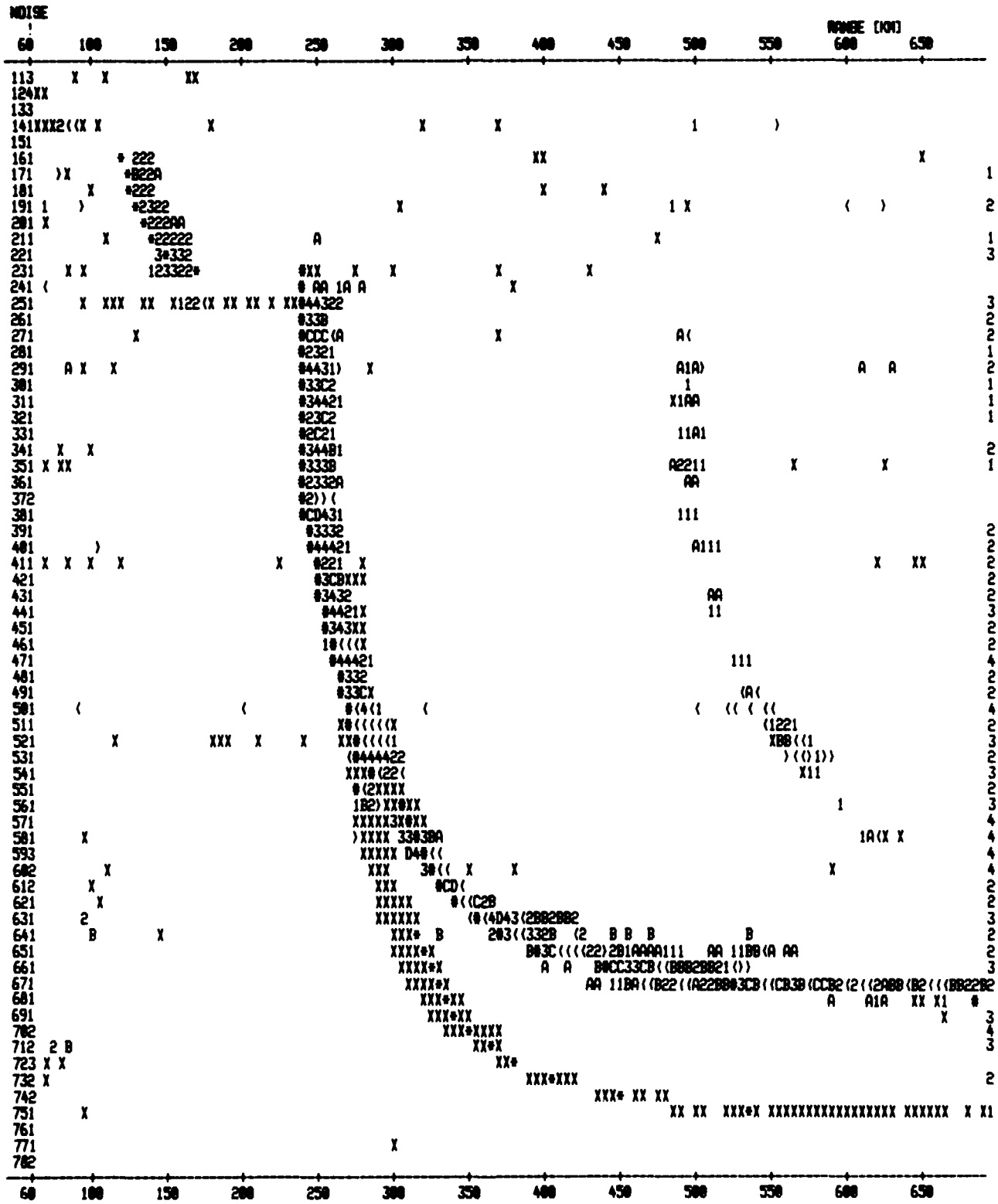

Figure 69. ARTIST Ionogram Print

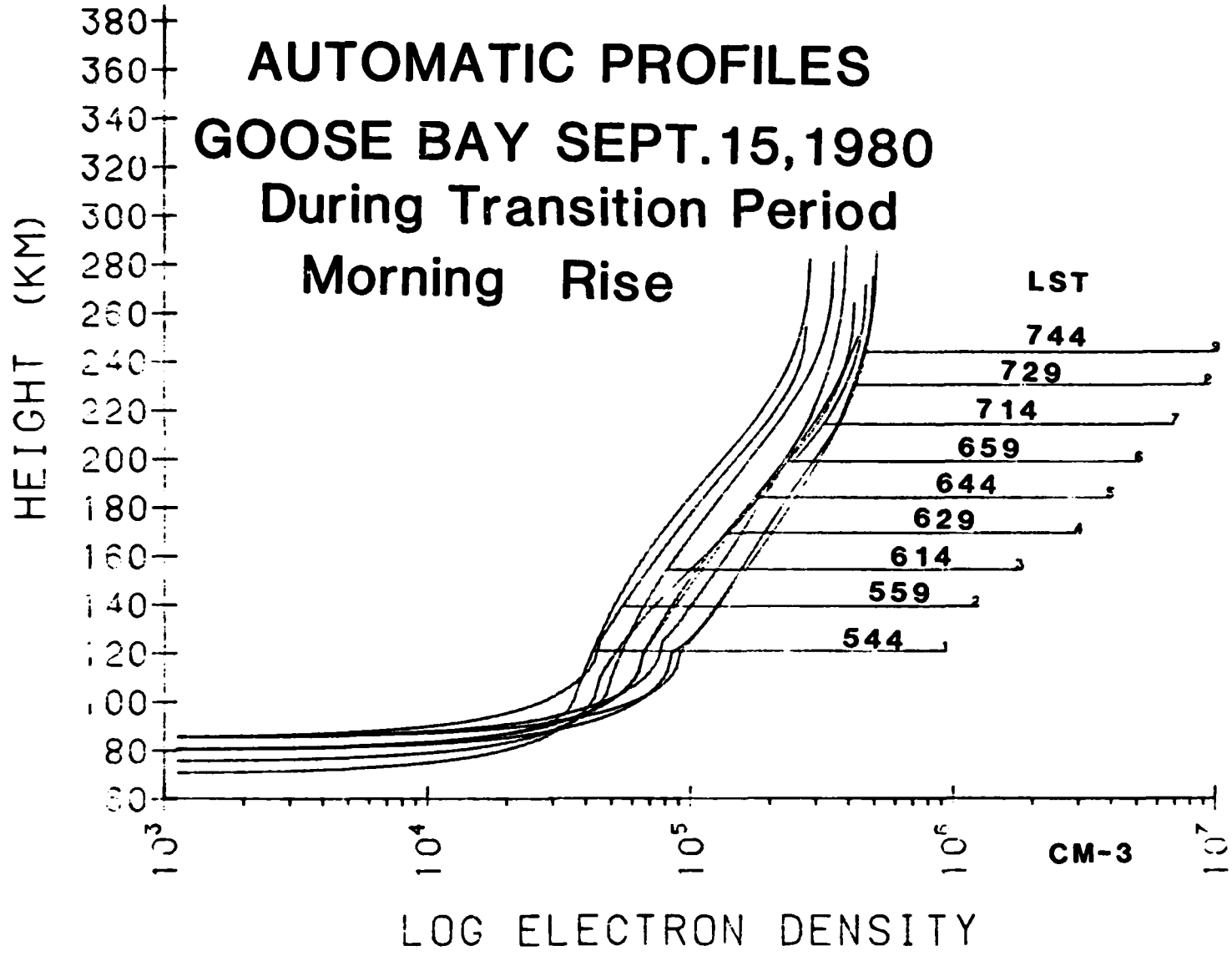
AUTOMATIC PROFILES
GOOSE BAY SEPT. 15, 1980
During Transition Period
Morning Rise
LST
744
729
714
659
644
629
614
559
544
HEIGHT (KM)
380
360
340
320
300
280
260
240
220
200
180
160
140
120
100
80
60
10^3
10^4
10^5
10^6
10^7
CM-3
LOG ELECTRON DENSITY

Figure 70

7.0 CHEMICAL RELEASE EXPERIMENTS AT NATAL

During September 1982 AFGL conducted ionospheric modification experiments near the geomagnetic equator at Natal, Brazil, in a collaborative international program to test the current theories for generating plasma instabilities in the equatorial ionosphere. Rocket borne explosive releases of H_2O, CO_2 and N_2 created plasma depletions at the ionospheric F-region ledge. Barium releases produced depletions at electrical polarization fields. ULCAR participated in these experiments with Digisonde observations from the ground and from AFGL's KC-135 aircraft. An overview of the different observations and the preliminary conclusions drawn are contained in the Proceeding of the 3-5 March 1983 BIME/ Coloured Bubbles Preliminary Data Review Meeting, issued by R. Narcisi, AFGL, in April 1983. ULCAR scientists presented or coauthored a number of papers during this meeting (Szuszczewicz et al, 1983; Buchau et al, 1983; Reinisch et al, 1983a; Buchau et al, 1983a; Reinisch and Buchau, 1983).

In June 1982, ULCAR's Digisonde was installed at the West Catre AFB (5° 55'S, 35° 15'W, -6.4° ML) near Natal to collect background information on ionospheric conditions at Natal. A seven antenna crossed-loop array was deployed permitting the identification of the polarization of the echo returns and their approximate angle of arrival. Amplitude, angle of arrival and Doppler information made it possible to identify and track the effects of the chemical releases.

The day to day variations of the height of the F ledge is shown in Figure 71 which displays the diurnal variation of h' for 4 MHz (2×10^5 cm^{-3}) from 13 August to 18 September 1982. The dashed section indicates the presence of spread F. The $\sum$Kp for each day is given on the right of each diurnal curve. The four rocket releases are shown as arrows on days 251, 256, 260 and 261. The electron density profiles

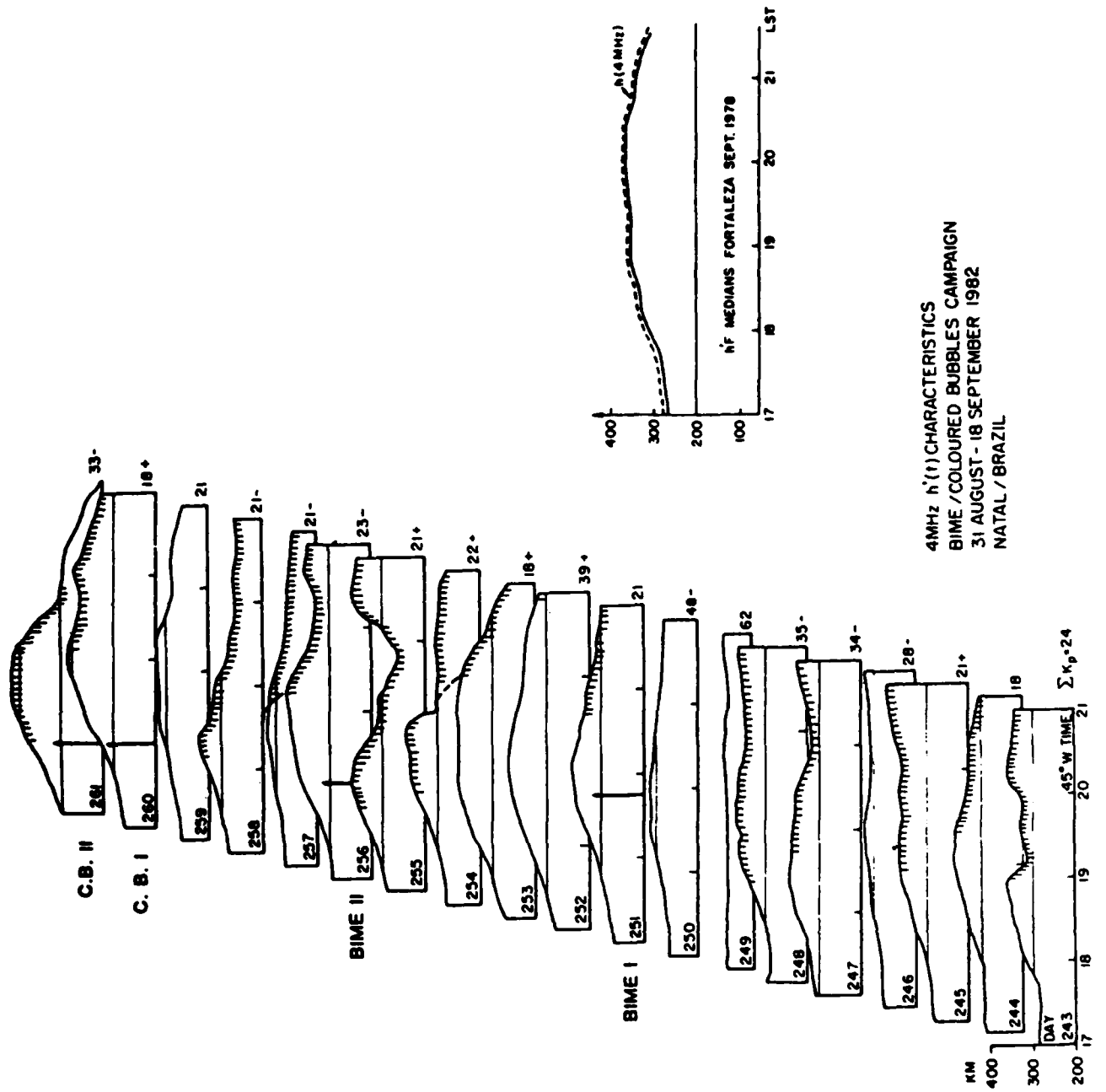
4MHz h'(t) CHARACTERISTICS
BIME/COLOURED BUBBLES CAMPAIGN
31 AUGUST - 18 SEPTEMBER 1982
NATAL/BRAZIL
h'F MEDIANS FORTALEZA SEPT. 1978
h'(4MHz)
LST
C.B. II
C.B. I
BIME II
BIME I
KM
DAY
45°W TIME
$\Sigma K_p \cdot 24$

Figure 71

and their changes have been calculated for the sunset periods to determine the rise velocity of the F-region ledge. Figures 72 through 75 illustrate the profile changes for the four launch days. Similar plots were prepared for the aircraft location from the AIO ionograms. For the BIME I launch the rise velocity decreases from 1.4 km/min 1830 LST to 0.6 km/min at release time (Figure 76). No spread F development was triggered by the H_2O/CO_2 release. For BIME II the rise velocity of the F-layer at time of release was 1.7 km/min at Natal (Figure 77) which according to current theories should permit development of instabilities and spread F. However, no clear indication for such development was observed. By comparing the Natal and AIO profiles we found a substantial east-west tilt of the F-region with a gradient in ionization of about 9%. The rise velocity of the F-layer over the aircraft, i.e. in the neighborhood of the rocket release, was also smaller than at Natal.

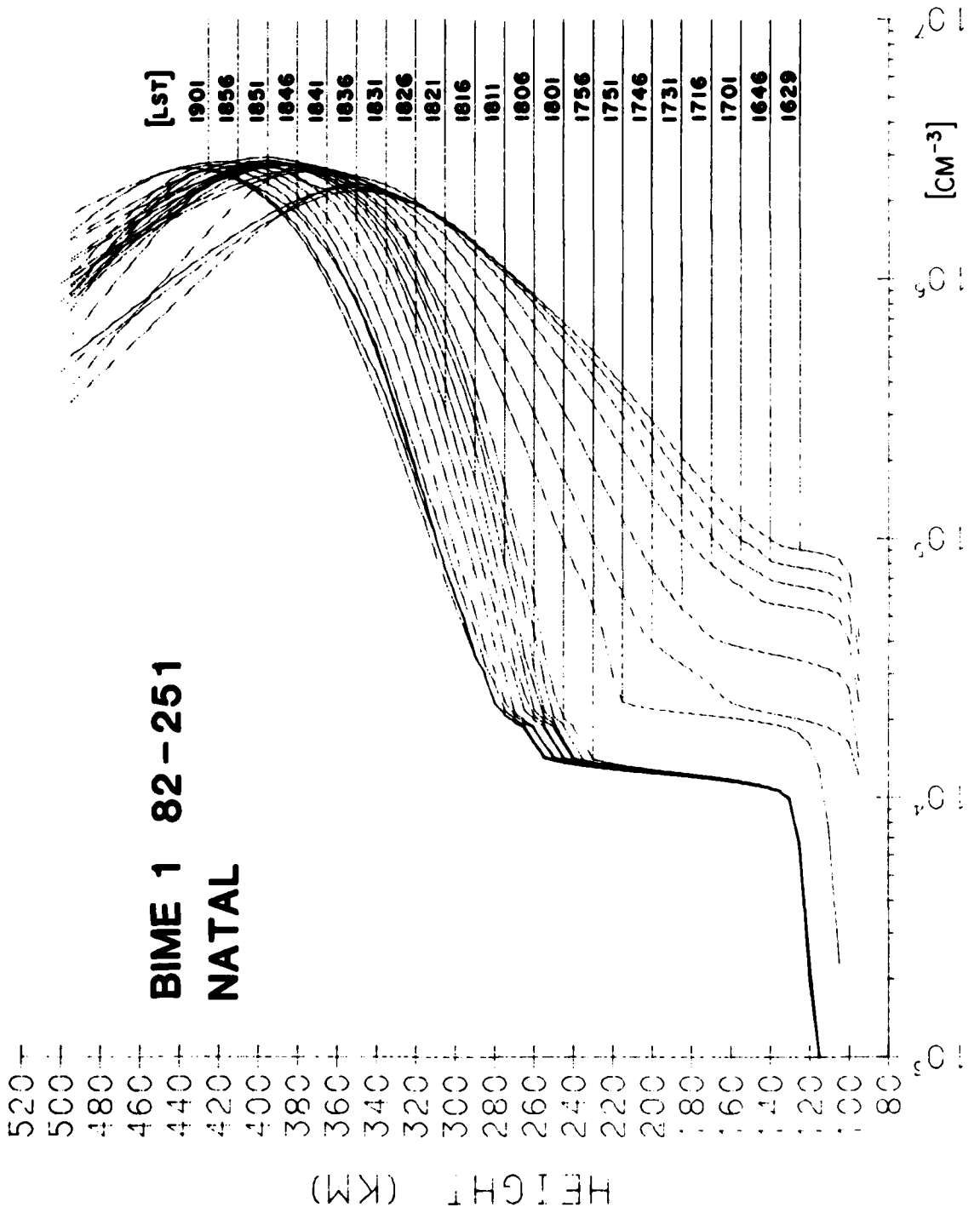
BIME 1 82-251
NATAL
[LST]
1901
1856
1851
1846
1841
1836
1831
1826
1821
1816
1811
1806
1801
1756
1751
1746
1731
1716
1701
1646
1629
LOG ELECTRON DENSITY
[CM-3]
HEIGHT (KM)

Figure 72

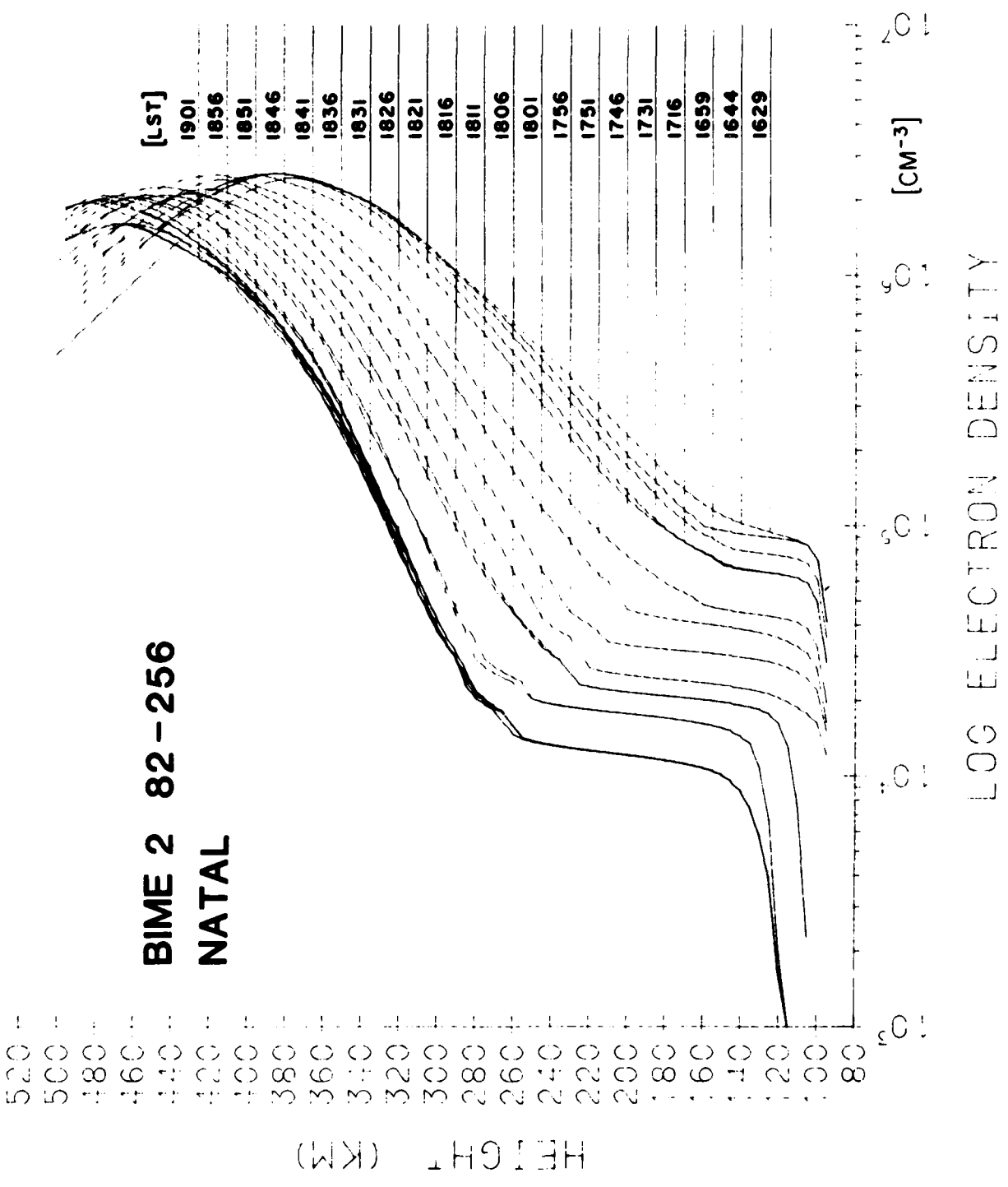
BIME 2 82-256
NATAL
[LST]
1901
1856
1851
1846
1841
1836
1831
1826
1821
1816
1811
1806
1801
1756
1751
1746
1731
1716
1659
1644
1629
LOG ELECTRON DENSITY
[CM-3]
HEIGHT (KM)

Figure 73

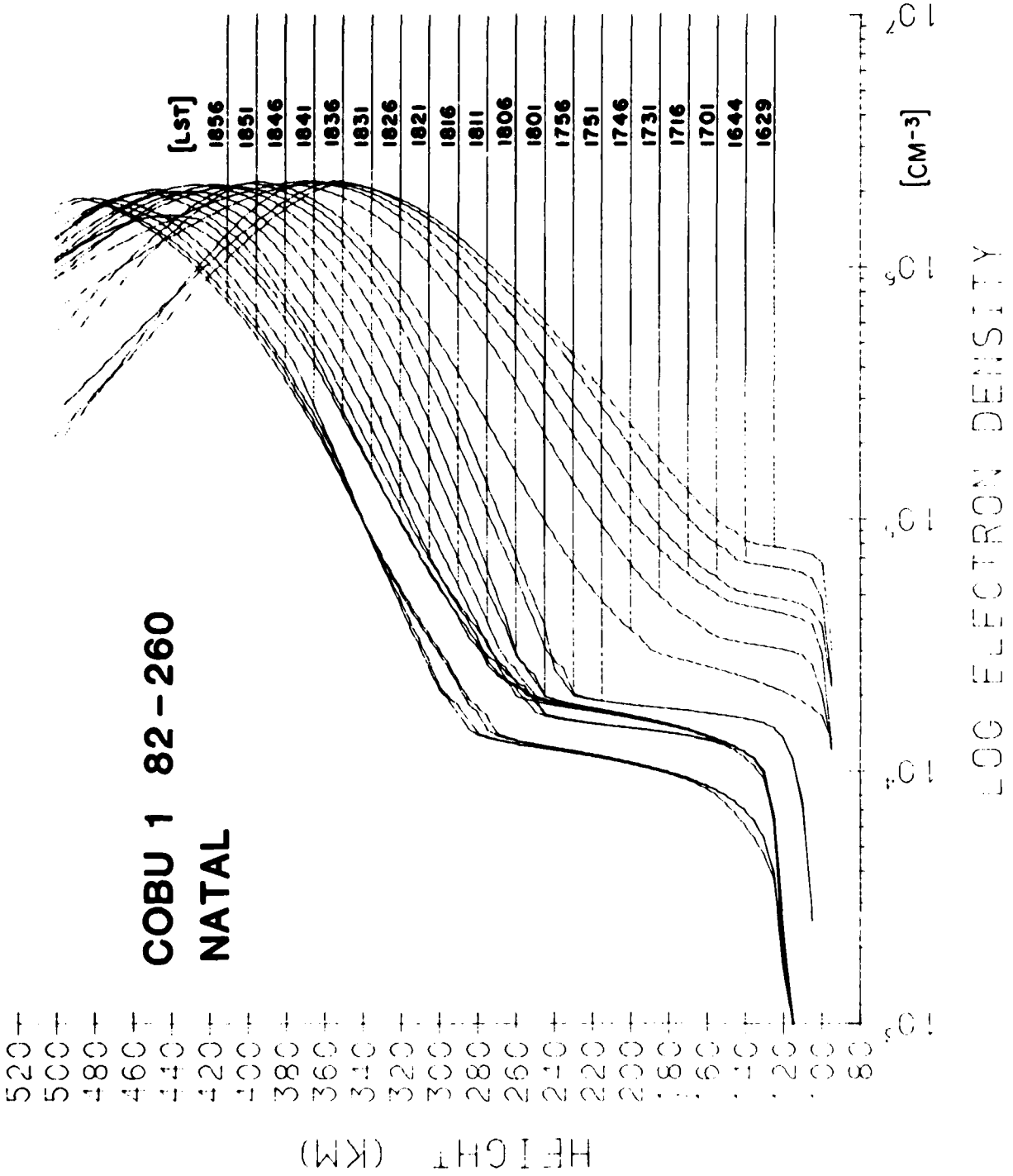
COBU 1 82-260
NATAL
[LST]
1856
1851
1846
1841
1836
1831
1826
1821
1816
1811
1806
1801
1756
1751
1746
1731
1716
1701
1644
1629
LOG ELECTRON DENSITY
[CM-3]
HEIGHT (KM)

Figure 74

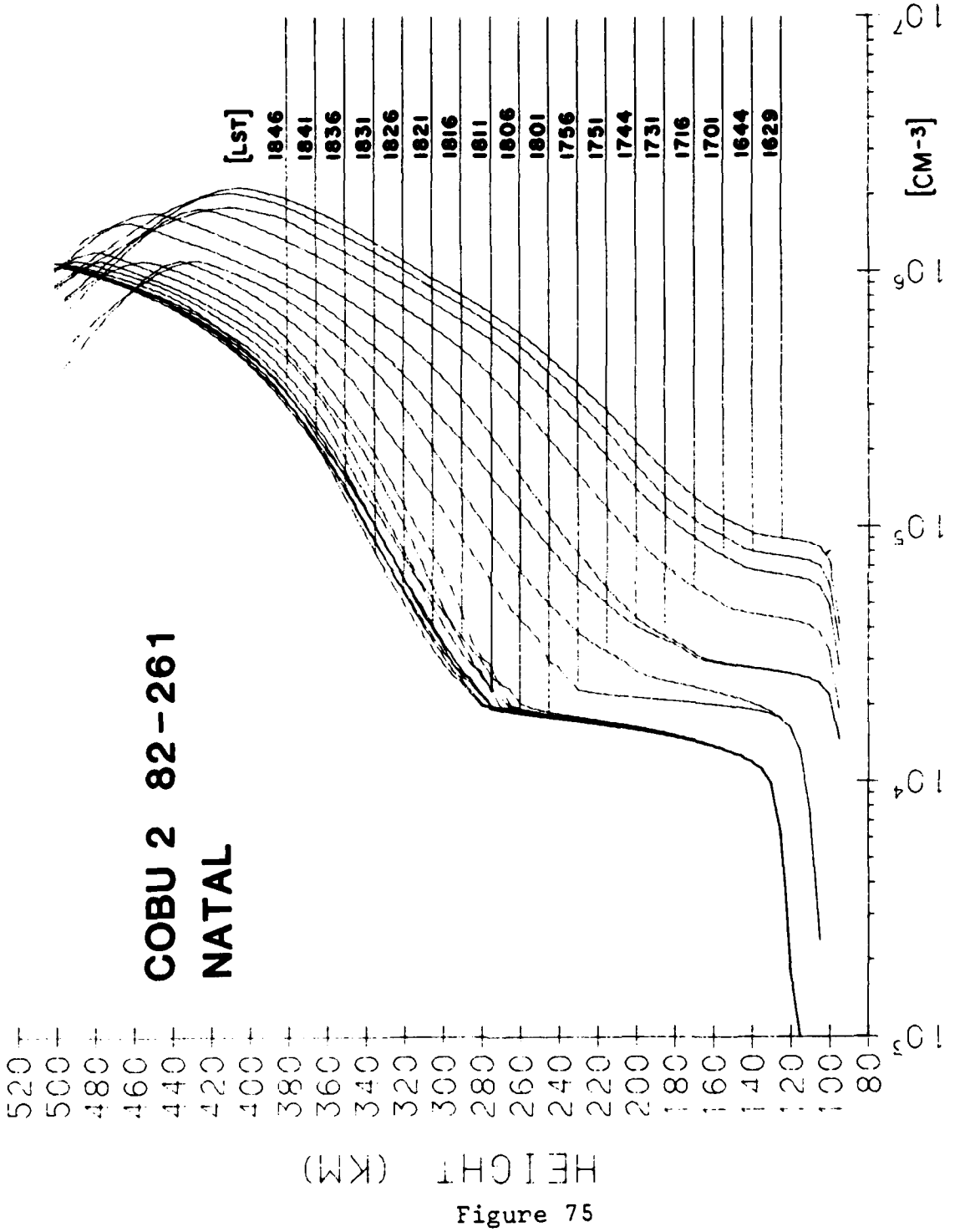
COBU 2 82-261
NATAL
[LST]
1846
1841
1836
1831
1826
1821
1816
1811
1806
1801
1756
1751
1744
1731
1716
1701
1644
1629
LOG ELECTRON DENSITY
[CM-3]
HEIGHT (KM)

Figure 75

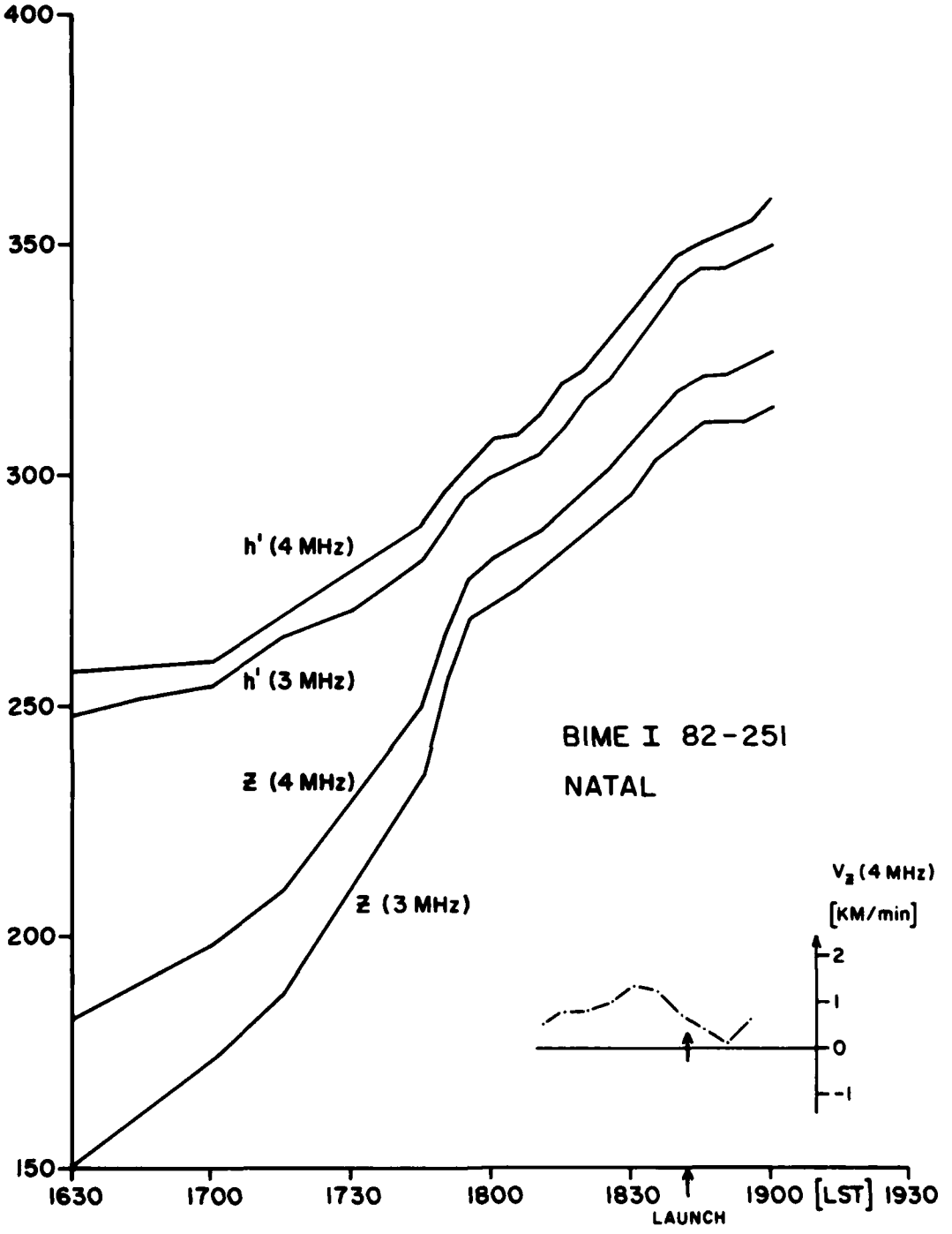

VIRTUAL AND TRUE HEIGHTS
for plasma densities 3 and 4 MHz
NATAL, 8 Sep 82

Figure 76

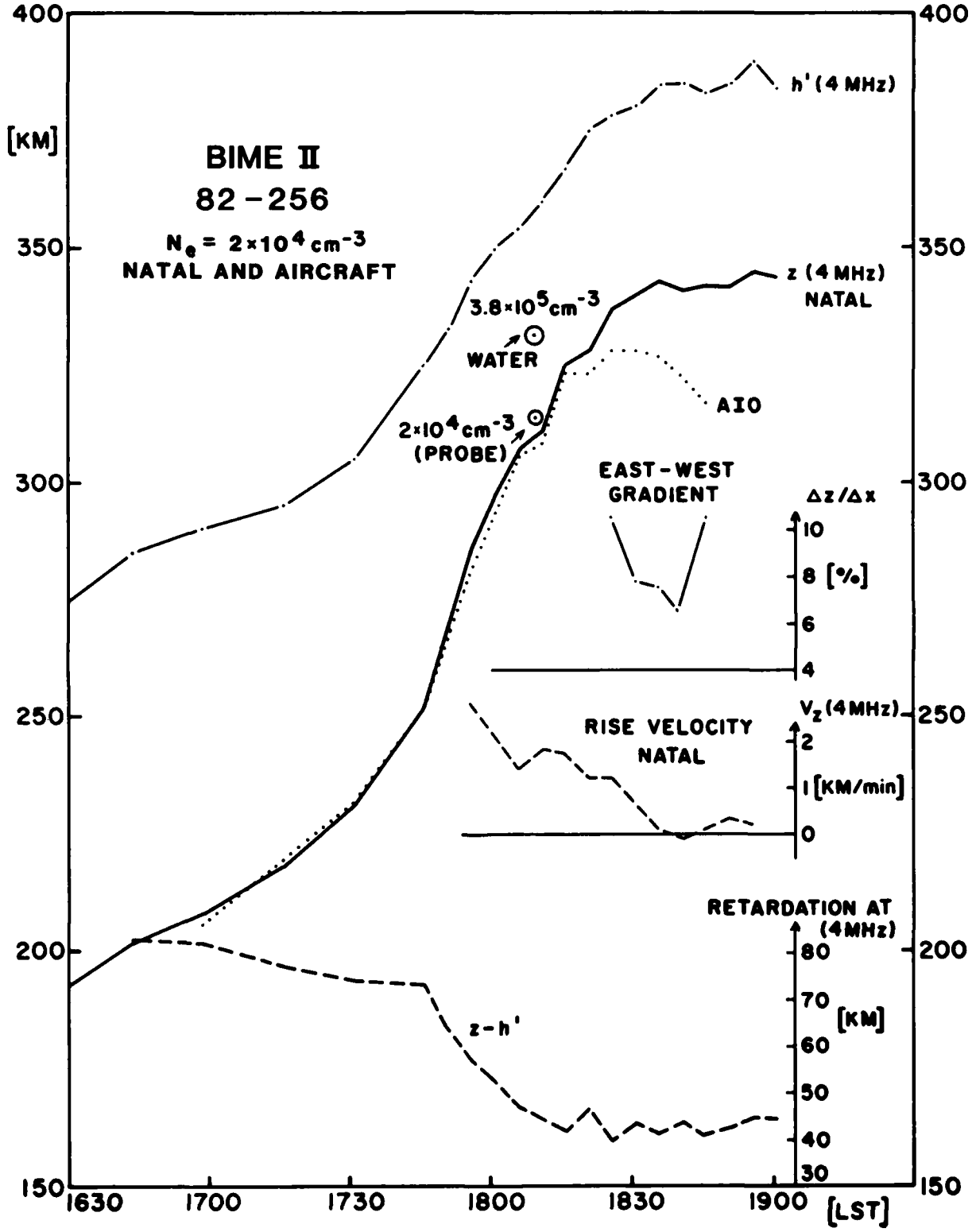
400
350
300
250
200
150
[KM]
BIME II
82 - 256
$N_e = 2 \times 10^4 cm^{-3}$
NATAL AND AIRCRAFT
h' (4 MHz)
z (4 MHz)
NATAL
$3.8 \times 10^5 cm^{-3}$
WATER
AIO
$2 \times 10^4 cm^{-3}$
(PROBE)
EAST - WEST
GRADIENT
$\Delta z / \Delta x$
10
8 [%]
6
4
RISE VELOCITY
NATAL
V_z (4MHz)
2
1 [KM/min]
0
RETARDATION AT
(4MHz)
80
70
[KM]
60
50
40
30
z - h'
1630
1700
1730
1800
1830
1900
[LST]

Figure 77

8.0 IONOSPHERIC HEATING EXPERIMENTS AT ARECIBO

In September 1981 AFGL's Airborne Ionospheric Observatory participated in ionospheric heating experiments at Arecibo. The HF heater antenna is located some 20 km north of the Arecibo Observatory in Puerto Rico. The antenna array was driven by transmitters outputting up to 400 kW of RF power. Frequencies of 7.3 and 5.1 MHz were selected for the experiments, that were conducted at night. Optical and sounder observations were made from the aircraft which was shuttling back and forth on a magnetic meridian (approximately) in order to map the heated volume with a ray path to a geostationary satellite, which was providing the signal for 250 MHz scintillation measurements. No scintillations were observed, probably because of the low power level of the heater's RF emission. The optical instruments also did not show airglow signatures that could be attributed to the heating. The foF2 values for the five round-robin flights are shown in Figure 78. It was expected that the HF heating would cause development of spread F. However, no large scale spread F was seen during these nights.

At certain aircraft locations (see tick marks in Figure 78) the Digisonde observed oblique echoes which seemed to originate in the heated volume. This was verified later by playing back the tape recorded ionograms through a Doppler filter. The oblique echoes have the correct Doppler shifts expected for waves reflected in the heated region and received on the moving aircraft. The aircraft Digisonde showed oblique echoes each time when the plane defined by the normal onto the magnetic field direction and the location of the aircraft was intersecting the heated volume. This suggests that the heating generates field aligned irregularities (F.A.I.) which form a reflecting grid for the radio waves.

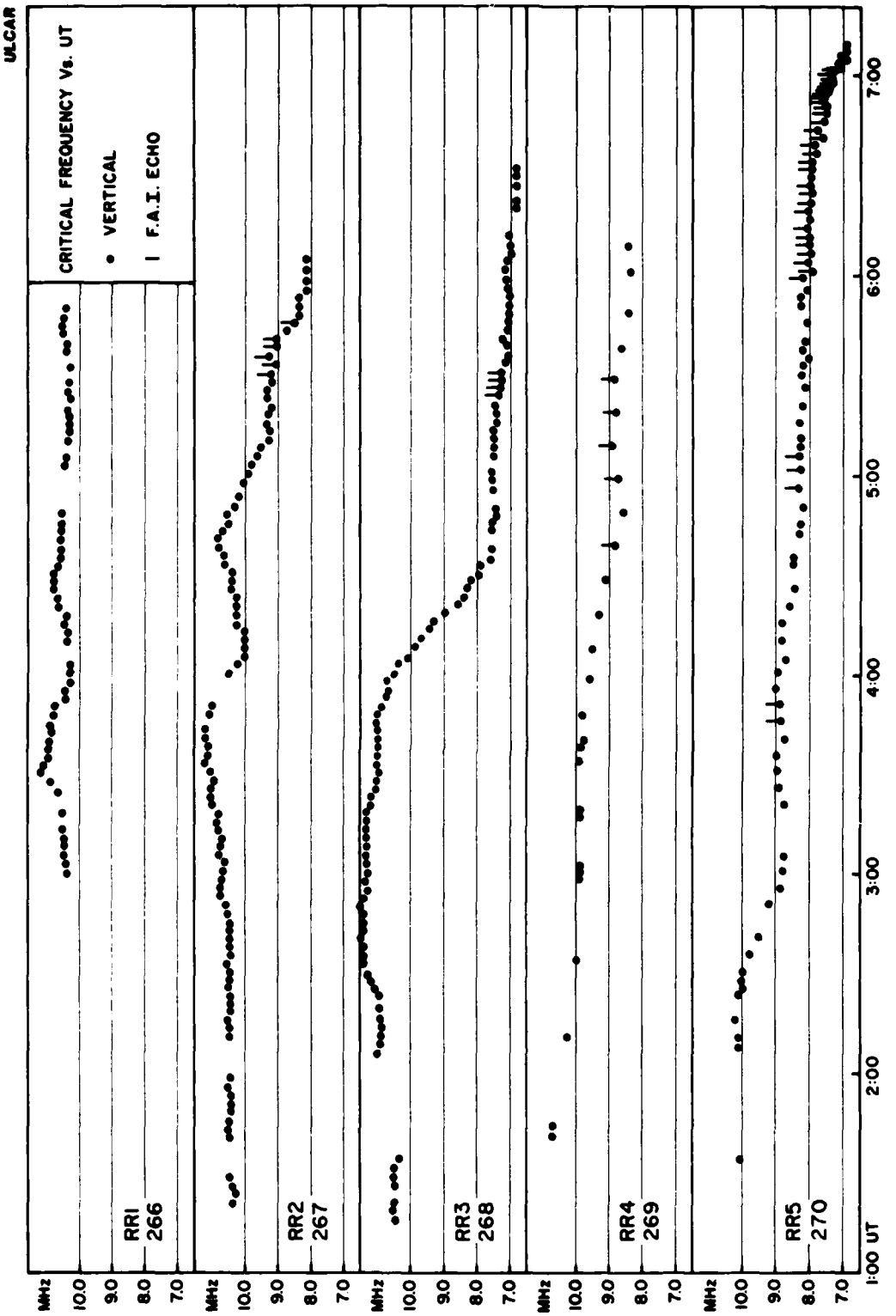

PUERTO RICO SEP 1981 "HEATER" EXPERIMENT

Figure 78

Figure 79 shows a sequence of four ionograms recorded during round-robin #3 when the aircraft was crossing the critical location. Only the second and third ionogram (lower left and upper right) show the echoes, the first and fourth ionogram has only vertical echoes. The ionograms in Figure 79 show the Doppler frequencies rather than the usually presented amplitudes of the echoes. It is interesting to note that the F.A.I. echoes have zero Doppler shift which is expected since the aircraft was flying in the magnetic meridian plane, i.e. the aircraft velocity vector was at right angle to the wave propagation vector. During round-robin #5 the aircraft was flying normal to this plane toward and away from the heated volume, and the F.A.I. echoes showed alternatingly positive and negative Doppler frequencies.

On September 28, the aircraft flew over the heater antenna array with the Digisonde operating in the fixed frequency mode at 5.1 MHz (the heater frequency) to perform antenna calibration measurements. The results from these measurements are discussed in Scientific Report No. 3 (Reinisch et al, 1982).

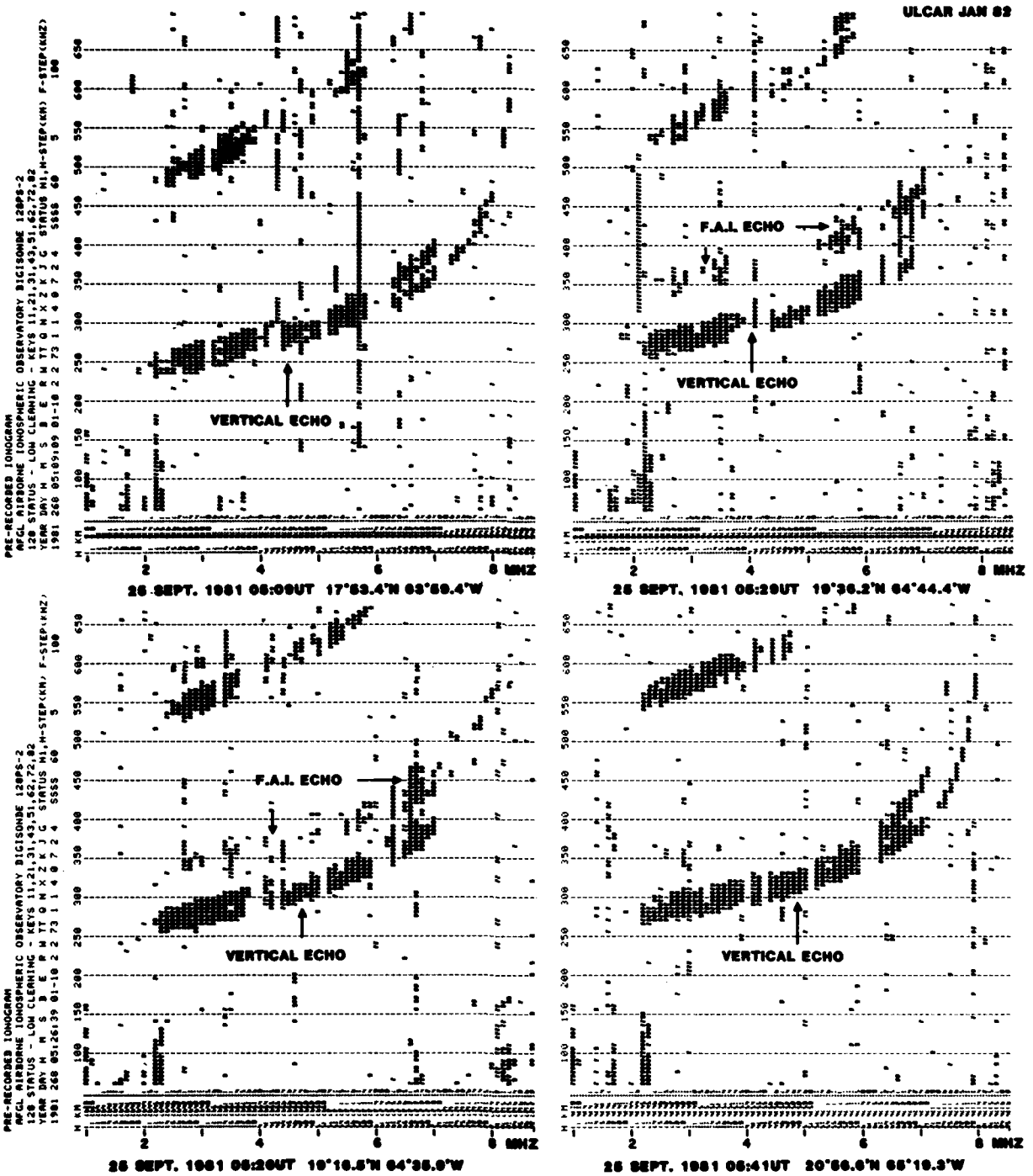

AIRCRAFT DOPPLER IONOGRAMS
PUERTO RICO HEATING EXPERIMENT

Figure 79

9.0 DIGISONDE 128 INSTALLATION AT KENNEDY SPACE CENTER WITH REMOTE DATA LINK

A Digisonde 128 which had been operated by AFGL near Keflavik, Iceland, had been sent to Lowell for a thorough check-up and for installation of a new Olivetti Thermal Dot Printer. This printer is driven by a microcomputer built into the Digisonde 128, similar to the design of the output interfaces of the new Digisonde 256.

In September 1982 the modified Digisonde 128 was installed at Kennedy Space Center, Florida, replacing the old prototype Digisonde 128, operated at this location for several years. Although the Olivetti printer did not fulfill the expectation in reliability, as it had achieved in Belgium with the new Digisonde 256, the replacement system was a substantial improvement compared to the old sounder. A telephone link for data transfer was installed between Kennedy Space Center and the Air Weather Station at Patrick AFB. A remote printer provides all pertinent information of the ionogram and facilitates with its frequency and range grid and a MUF3000 overlay the fast scaling of the most important ionospheric parameters by AWS personnel. The Digisonde system is operated by RCA maintenance personnel who also have erected the small vertical rhombus transmitter antenna and a single turnstile loop antenna for reception following the advice of ULCAR. After installation of the system an introductory lecture on data analysis was given for the AWS personnel.

10.0 PAPERS, REPORTS AND PRESENTATIONS

A number of publications were based on or related to work done under this contract.

10.1 Papers

Reinisch, B. W. and X. Huang, "Automatic Calculation of Electron Density Profiles from Digital Ionograms. 1. Automatic O and X Trace Identification for Topside Ionograms," Radio Sci., 17, 2, pp. 421-434, March-April 1982.

Huang, X. and B. W. Reinisch, "Automatic Calculation of Electron Density Profiles from Digital Ionograms. 2. True Height Inversion of Topside Ionograms with the Profile-Fitting Method," Radio Sci., 17, 4, pp. 837-844, July-August 1982.

Reinisch, B. W. and X. Huang, "Automatic Calculation of Electron Density Profiles from Digital Ionograms. 3. Processing of Bottomside Ionograms," Radio Sci., 18, 3, pp. 477-492, May-June 1983.

Reinisch, B. W., J. Tang and X. Huang, "Seasonal Variations in the Aurora Ionosphere," IES 81 Symposium, Alexandria, Virginia, April 1981.

Buchau, J., B. W. Reinisch, E. J. Weber and J. Moore, "Structure and Dynamics of the Winter Polar Cap Ionosphere," Radio Science, 1983 (in press).

Weber, E. J., J. Buchau, J. G. Moore, J. R. Sharber, R. C. Livingston, J. D. Winningham and B. W. Reinisch, "F-Layer Ionization Patches in the Polar Cap," submitted to JGR, 1983.

10.2 Reports

Reinisch, B. W., "Processing of Digital Ionograms," Scientific Report No. 1, AFGL-TR-81-0085, ULRF-414/CAR, 1981, ADA125831.

Reinisch, B. W., J. Tang, W. N. Hall and J. Buchau, "Automated Ionogram Processing Shows Seasonal Variations in the Aurora Ionosphere," Scientific Report No. 2, AFGL-TR-82-0122, ULRF-420/CAR, 1982, ADA119911.

Reinisch, B. W., R. W. Gowell, J. G. Moore, J. B. Waaramaa and R. R. Gamache, "Measuring the Antenna Pattern of the HF Heater Antenna in Puerto Rico," Scientific Report No. 3, AFGL-TR-82-0123, ULRF-419/CAR, 1982, ADA119963.

Reinisch, B. W., J. S. Tang and R. R. Gamache, "Automatic Scaling of Digisonde Ionograms, Test and Evaluation Report," Scientific Report No. 4, AFGL-TR-82-0324, ULRF-421/CAR, 1982, ADA125830.

Gamache, R. R., B. W. Reinisch and J. Tang, "Automatic Scaling of Digisonde Ionograms Computer Program and Numerical Analysis Documentation," Scientific Report No. 5, AFGL-TR-83-0052, ULRF-422/CAR, 1983, ADA128934.

Dozois, C. G., B. W. Reinisch and K. Bibl, "A High Frequency Radio Technique for Measuring Plasma Drifts in the Ionosphere," Scientific Report No. 6, AFGL-TR-83-0202, ULRF-424/CAR, 1983 (in press).

Reinisch, B. W., R. R. Gamache, J. S. Tang and D. F. Kitrosser, "Automatic Real Time Ionogram Scaler with True Height Analysis - ARTIST," Scientific Report No. 7, AFGL-TR-83-0209, ULRF-426/CAR, 1983 (in press).

Bibl, K., "Symmetric Four Antenna Array Resolves Multiple Reflectors with Complex Spectrum Analysis of Multiplexed Closely Spaced Frequency Soundings," Scientific Report No. 8, ULRF-428/CAR, 1983.

Shirley, M. A., B. W. Reinisch and J. Buchau, "Computer Printing of Digisonde Ionograms," AFGL Research Paper, ULRF-423/CAR, (in press).

10.3 Presentations at Scientific Meetings

Reinisch, B. W. and X. Huang, "Automatic Evaluation of Topside Ionograms," Programs and Abstracts of National Radio Science Meeting, G1-3, p. 45, Boulder, Colorado, January 1981.

Huang, X. and B. W. Reinisch, "Automatic Calculation of Topside Electron Density Profiles," Programs and Abstracts of National Radio Science Meeting, G1-4, p. 46, Boulder, Colorado, January 1981.

Reinisch, B. W., J. Tang and X. Huang, "Automatic Ionogram Evaluation," IES 81 Symposium, Alexandria, Virginia, April 1981.

Reinisch, B. W. and J. Tang, "Seasonal Variations in the Aurora Ionosphere," IES 81 Symposium, Alexandria, Virginia, April 1981.

Reinisch, B. W., X. Huang and J. Tang, "Automatic Electron Density Profiles from Digital Topside and Bottomside Ionograms," Abstracts of URSI XXth General Assembly, G1-3, p. 163, Washington, D. C., August 1981.

Bibl, K., J. Buchau and B. W. Reinisch, "F-Region Bite-Out in the Day-Time Icnosphere Over Greenland," Abstracts of URSI XXth General Assembly, GH7-4, p. 435, Washington, D. C., August 1981.

Buchau, J., E. J. Weber, B. W. Reinisch and K. Bibl, "Polar Cap F-Region Structure Determined from Digital Doppler Ionograms and Photometric All Sky Images," Abstracts of URSI XXth General Assembly, GH7-5, p. 436, Washington, D. C., August 1981.

Basu, S. (Emanuel College, Boston, MA), Basu, Sunanda (Emmanuel College, Boston, MA), Weber, E. J., Moore, J. G., Buchau, J., Gordon, W. E. (Rice University, Houston, TX), Lee, M. C. (Regis College, Weston, MA), Livingston, R. C. (SRI International, Menlo Park, CA), Reinisch, B. W. (Univ. of Lowell, Lowell, MA), Behnke, R. A., "Multitechnique Probing of the Artificially Modified Ionosphere Over Arecibo," presented at National Radio Science Meeting, Boulder, CO, January 1982.

Buchau, J., B. W. Reinisch, E. J. Weber and J. Moore, "Structure and Dynamics of the Winter Polar Cap Ionosphere," URSI International Symposium on Radio Probing of the High-Latitude Ionosphere and Atmosphere: New Techniques and New Results, Fairbanks, Alaska, August 1982.

Bibl, K., "Symmetric Four Antenna Array Resolves Multiple Reflectors with Complex Spectrum Analysis of Multiplexed Closely Spaced Frequency Soundings," Proceedings of International URSI Commission F 1983 Symposium, Louvain-La Neure, Belgium, June 1983.

Reinisch, B. W., R. R. Gamache and J. S. Tang, "Automatic Electron Density Profiles from Digital Ionograms," NATO AGARD/EPP Symposium on Propagation Factors Affecting Remote Sensing, Oberammergau, Germany, May 1983.

Szuszczewicz, D. N. Walker, J. C. Holmes, R. S. Narcisi, J. Buchau and B. W. Reinisch, "Real-Time In Situ Targeting of Geoplasma Domains for Purposes of Chemical Injection and Artificial Triggering of Equatorial Spread-F," Proceedings of the 3-5 March 1983 BIME/Coloured Bubbles Preliminary Data Review Meeting, p. 23, April 1983.

Reinisch, B. W., J. Buchau and W. T. Kersey, "True Height Analysis of Equatorial Ionograms as Input to the Launch Decisions," Proceedings of the 3-5 March 1983 BIME/Coloured Bubbles Preliminary Data Review Meeting, p. 92, April 1983.

Buchau, J., B. W. Reinisch, K. Bibl and J. B. Waaramaa, "Overview of the Ionospheric Conditions at Natal During the September 1982 BIME/Coloured Bubbles Campaign," Proceedings of the 3-5 March 1983 BIME/Coloured Bubbles Preliminary Data Review Meeting, p. 110, April 1983.

Reinisch, B. W. and J. Buchau, "Ground Based/Airborne Ionospheric Observations During BIME I and II," Proceedings of the 3-5 March 1983 BIME/Coloured Bubbles Preliminary Data Review Meeting, p. 129, April 1983.

Buchau, J., B. W. Reinisch and M. Shirley, "Ground-Based/Aircraft Ionospheric Observations During Coloured Bubbles I and II," Proceedings of the 3-5 March 1983 BIME/Coloured Bubbles Preliminary Data Review Meeting, p. 145, April 1983.

11.0 REFERENCES

Bibl, K., "Automatic Recording of Ionospheric Characteristics," J.A.T.P. 8, p. 295, 1956.

Bibl, K., "Font of Digital, or other, Characters and Method for Pattern Printing Thereof," U.S. Patent No. 3,810,095, 1974.

Bibl, K., "Velocity of the Reflection Points Reveals Structure and Motions in the Ionosphere," COSPAR Symposium 1973 on Methods of Measurements and Results of Lower Ionosphere Structure, pp. 369-375, 1974.

Bibl, K., W. Pfister, B. W. Reinisch and G. S. Sales, "Velocities of Small and Medium Scale Ionospheric Irregularities Deduced from Doppler and Arrival Angle Measurements," COSPAR, Space Research XV, pp. 405-411, 1975.

Bibl, K. and B. W. Reinisch, "The Universal Digital Ionosonde," Radio Sci., 13, 3, pp. 519-530, May-June 1978.

Buchau, J., W. N. Hall, B. W. Reinisch and S. Smith, "Remote Ionospheric Monitoring," Proceedings of 1978 Symposium on the Effects of the Ionosphere on Space and Terrestrial Systems, Paper 5-5, 1978.

Buchau, J., B. W. Reinisch, E. J. Weber and J. G. Moore, "Structure and Dynamics of the Winter Polar Cap F Region," AFGL-TR-82-0258, Environmental Research Papers, No. 792, 1982, ADA123706.

Buchau, J., B. W. Reinisch, K. Bibl and J. B. Waaramaa, "Overview of the Ionospheric Conditions at Natal During the September 1982 BIME/Coloured Bubbles Campaign," Proceedings of the 3-5 March 1982 BIME/Coloured Bubbles Preliminary Data Review Meeting, p. 110, April 1983.

Conkright, R. (private communication), NOAA, Boulder, CO, 1983.

Dozois, C. G., "A High Frequency Radio Technique for Measuring Plasma Drifts in the Ionosphere," Scientific Report No. 6, AFGL-TR-83-0202, ULRF-424/CAR, 1983.

Gamache, R. R., B. W. Reinisch and J. Tang, "Automatic Scaling of Digisonde Ionograms Computer Program and Numerical Analysis Documentation," Scientific Report No. 5, AFGL-TR-83-0052, ULRF-422/CAR, 1983, ADA128934.

Huang, X. and B. W. Reinisch, "Automatic Calculation of Electron Density Profiles from Digital Ionograms. 2. True Height Inversion of Topside Ionograms with the Profile-Fitting Method," Radio Sci., 17, 4, pp. 837-844, July-August 1982.

Knudsen, W. C., "Magnetospheric convection and the high-latitude F2 ionosphere," JGR, 79, pp. 1046-1055, 1974.

Mayaud, P. N., "Derivation, Meaning and Use of Geomagnetic Indices," Geophysical Monograph 22, American Geophysical Union, 1980.

Narcisi, R. (ed.), "Proceedings of the 3-5 March 1983 BIME/ Coloured Bubbles Preliminary Data Review Meeting, April 1983.

Oliver, W. L., J. M. Holt, R. H. Wand and J. V. Evans, "Millstone Hill Incoherent Scatter Observations of Auroral Convection over 60° < λ > 75°, 3, Average Patterns Versus Kp," J. Geophys. Res., 88, 5505-5516, 1983.

Patenaude, J., K. Bibl and B. W. Reinisch, "Direct Digital Graphics, The Display of Large Data Fields," American Laboratory, pp. 95-101, 1973.

Pfister, W. and K. Bibl, "A Modernized Technique for Ionospheric Drifts with Spectral Analysis," Space Research XII, p. 975, 1972.

Piggott, W. R. and K. Rawer, URSI Handbook of Ionogram Interpretation and Reduction, Rep. UAG-23, 2nd ed., World Data Center A, National Oceanic and Atmos. Admin., Boulder, Colorado, 1972.

Piggott, W. R. and K. Rawer, URSI Handbook of Ionogram Interpretation and Reduction, Rep. UAG-23A, 2nd ed., World Data Center A, National Oceanic and Atmos. Admin., Boulder, Colorado, 1978.

Piggott, W. R., High-Latitude Supplement to the URSI Handbook on Ionogram Interpretation and Reduction, Rep. UAG-50, World Data Center A, National Oceanic and Atmos. Admin., Boulder, Colorado, 1975.

Reinisch, B. W. and K. Bibl, "Digital Ionospheric Sounding in the Arctic," Final Report, AFGL-TR-81-0022, ULRF-412/CAR, 1981.

Reinisch, B. W., J. S. Tang and R. R. Gamache, "Automatic Scaling of Digisonde Ionograms, Test and Evaluation Report," Scientific Report No. 4, AFGL-TR-82-0324, ULRF-421/CAR, 1982a.

Reinisch, B. W. and X. Huang, "Automatic Calculation of Electron Density Profiles from Digital Ionograms. 1. Automatic O and X Trace Identification for Topside Ionograms," Radio Sci., 17, 2, pp. 421-434, March-April 1982b.

Reinisch, B. W. and X. Huang, "Automatic Calculation of Electron Density Profiles from Digital Ionograms. 3. Processing of Bottomside Ionograms," Radio Sci., 18, 3, pp. 477-492, May-June 1983.

Reinisch, B. W. and J. Buchau, "Ground Based/Airborne Ionospheric Observations During BIME I and II," Proceedings of the 3-5 March 1983 BIME/Coloured Bubbles Preliminary Data Review Meeting, p. 129, April 1983.

Reinisch, B. W., R. R. Gamache, J. S. Tang and D. F. Kitrosser, "Automatic Real Time Ionogram Scaler with True Height Analysis - ARTIST," Scientific Report No. 7, ULRF- /CAR, 1983.

Shirley, M. A., B. W. Reinisch and J. Buchau, "Computer Printing of Digisonde Ionograms," AFGL Research Paper, ULRF-423/CAR, 1983 (in press).

Spiro, R. W., R. A. Heelis and W. B. Hanson, "Ion Convection and the Formation of the Midlatitude F Region Ionization Trough," JGR, 83, pp. 4255-4264, 1978.

Szuszczewicz, E. P., D. N. Walker, J. C. Holmes, R. S. Narcisi, J. Buchau and B. W. Reinisch, "Real-Time In Situ Targeting of Geoplasma Domains for Purposes of Chemical Injection and Artificial Triggering of Equatorial Spread-F," Proceedings of the 3-5 March 1983 BIME/Coloured Bubbles Preliminary Data Review Meeting, p. 23, April 1983.

Weber, E. J., J. Buchau, R. H. Eather and J. W. F. Lloyd, "Large Scale Optical Mapping of the Ionosphere," AFGL-TR-77-0236, ADA051122, 1977.

Whalen, J. A., "Auroral Oval Plotter and Nomograph for Determining Corrected Geomagnetic Local Time, Latitude, and Longitude for High Latitudes in the Northern Hemisphere," AFGL-70-0422, Environmental Research Papers, No. 327, 1970.

A P P E N D I X A

MONTHLY MEDIAN VALUES FOR JANUARY 1979 TO SEPTEMBER 1982

MEDIAN VALUES OF h' AND f_0 AT GOOSEBAY, LABRADOR FOR JANUARY 1979

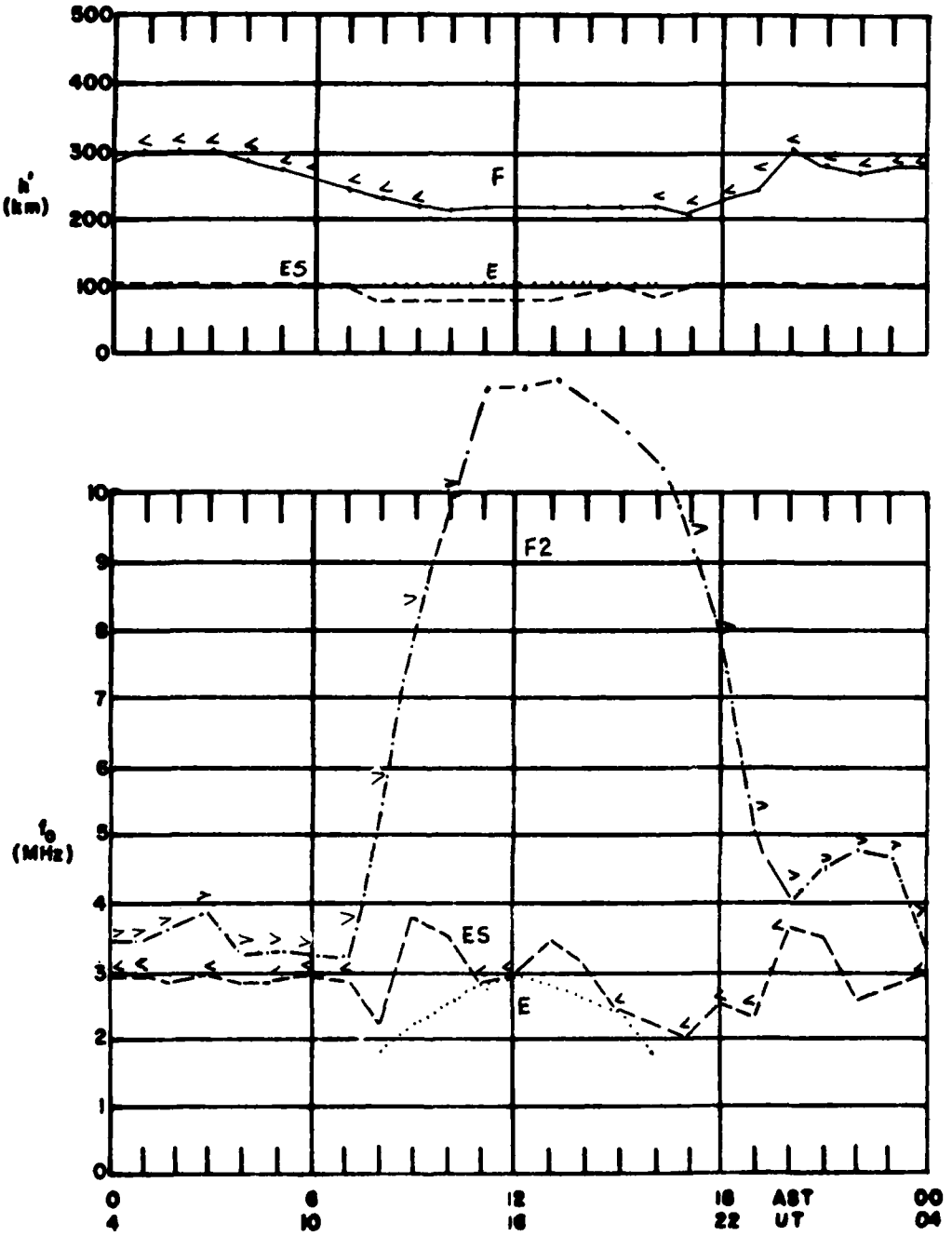

FEBRUARY 1979

GOOSE BAY, LABRADOR

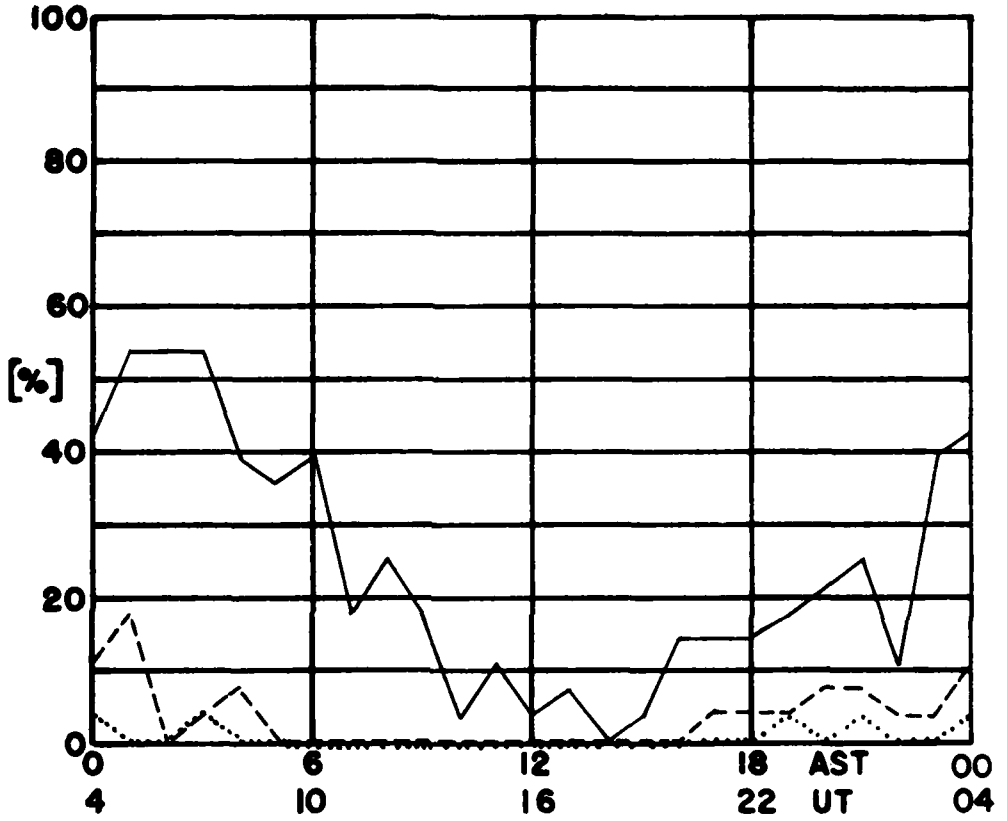

LIMITING FREQUENCY = 3MHz ————————

LIMITING FREQUENCY = 5MHz — — — — —

LIMITING FREQUENCY = 7MHz .....

PERCENTAGE OF TOTAL TIME DURING WHICH
f_0E_s IS GREATER THAN THE LIMITING FREQUENCY

MEDIAN VALUES OF h' AND f_0 AT GOOSEBAY, LABRADOR FOR FEBRUARY 1979

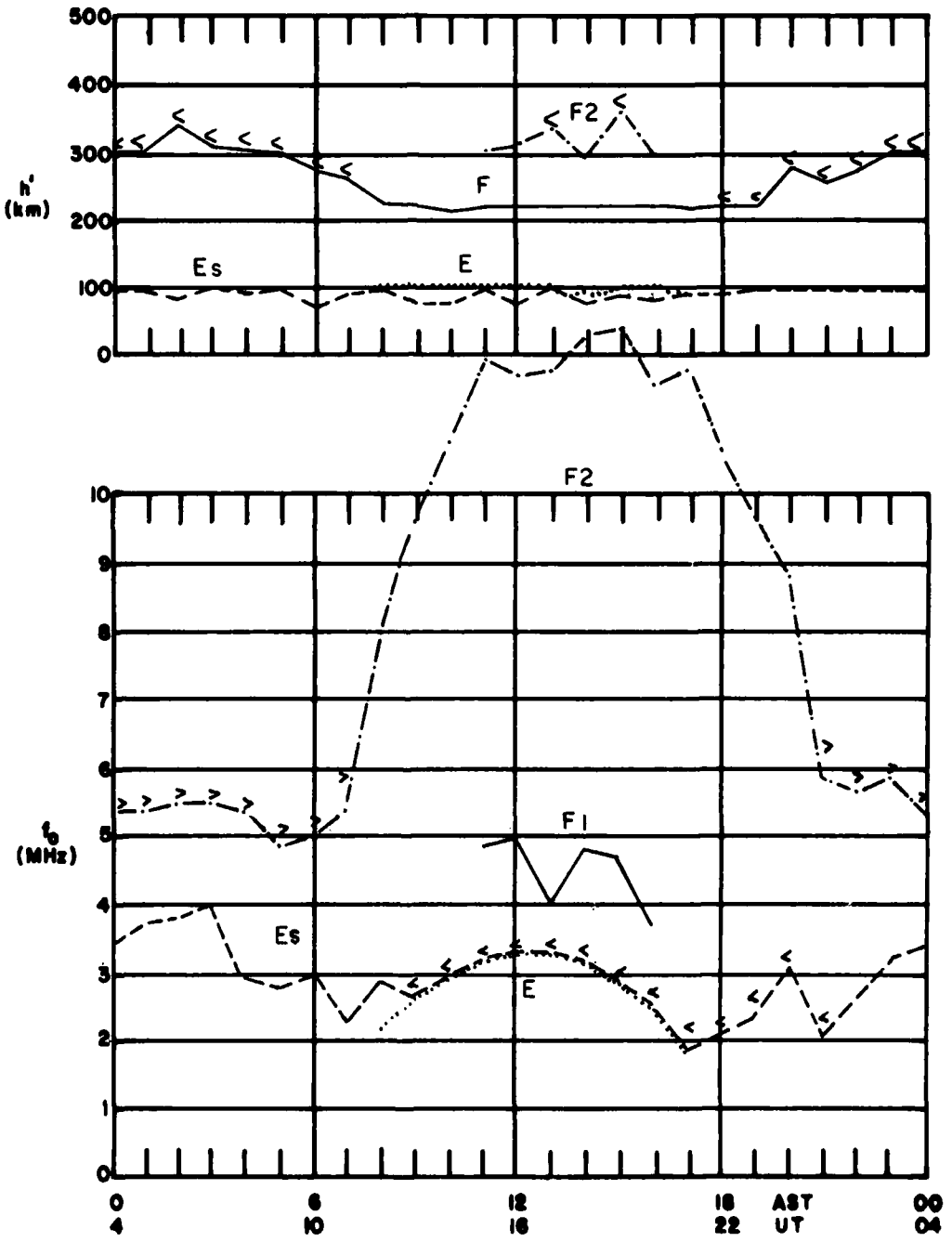

MARCH 1979

GOOSE BAY, LABRADOR

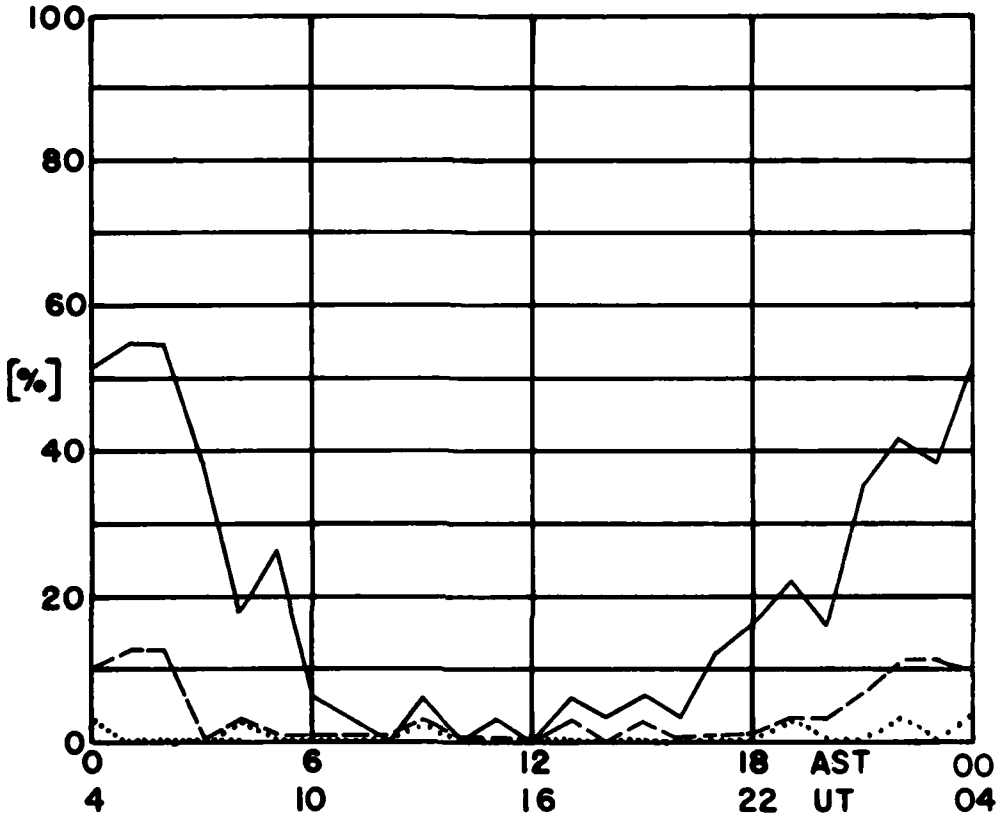

LIMITING FREQUENCY = 3MHz ————————

LIMITING FREQUENCY = 5MHz — — — — — —

LIMITING FREQUENCY = 7MHz .....

PERCENTAGE OF TOTAL TIME DURING WHICH
$f_0 E_s$ IS GREATER THAN THE LIMITING FREQUENCY

MEDIAN VALUES of h' AND f_0 AT GOOSE BAY, LABRADOR FOR MARCH 1979

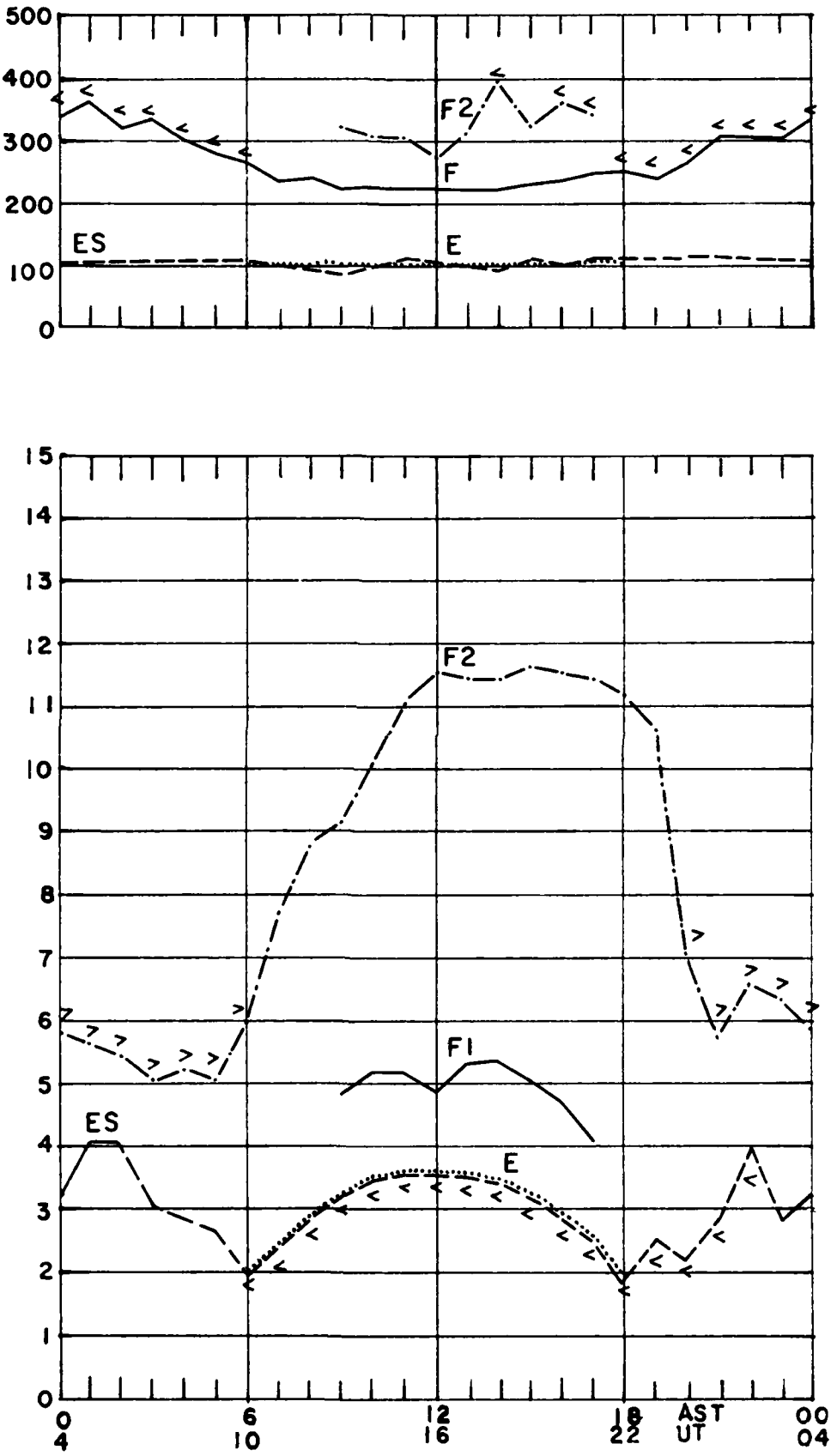

APRIL 1979

GOOSE BAY, LABRADOR

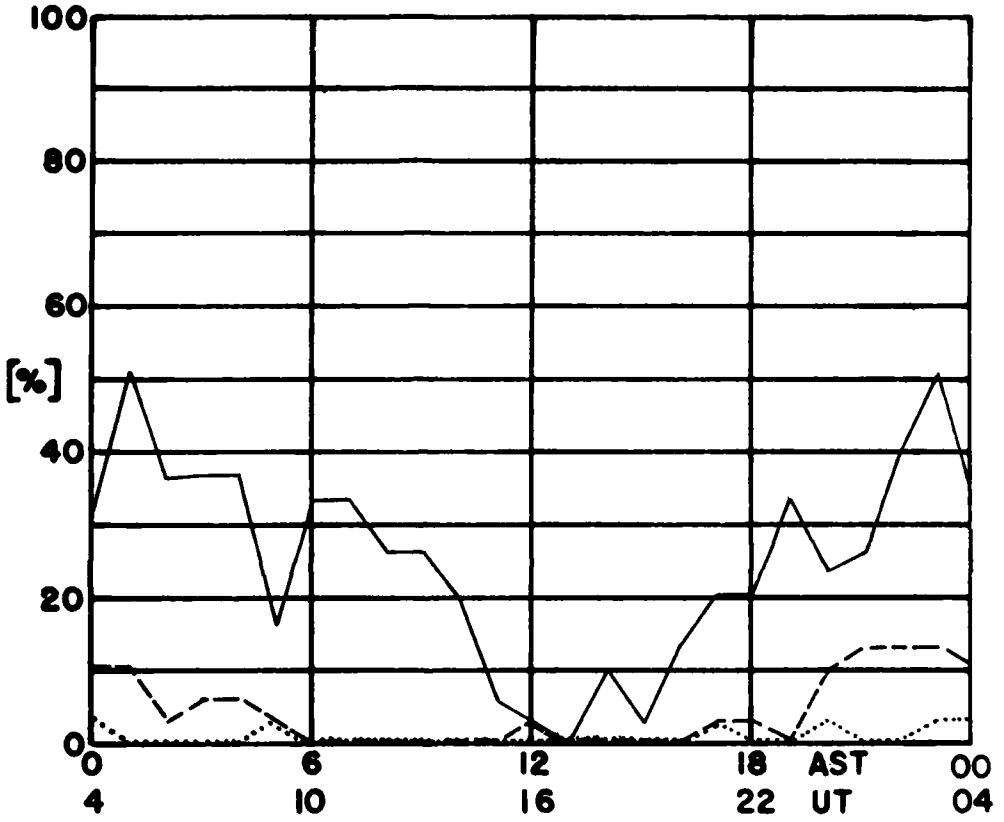

LIMITING FREQUENCY = 3MHz ————————

LIMITING FREQUENCY = 5MHz — — — — — —

LIMITING FREQUENCY = 7MHz .....

PERCENTAGE OF TOTAL TIME DURING WHICH
$f_0 E_s$ IS GREATER THAN THE LIMITING FREQUENCY

MEDIAN VALUES of h' AND f_0 AT GOOSE BAY, LABRADOR FOR

APRIL 1979

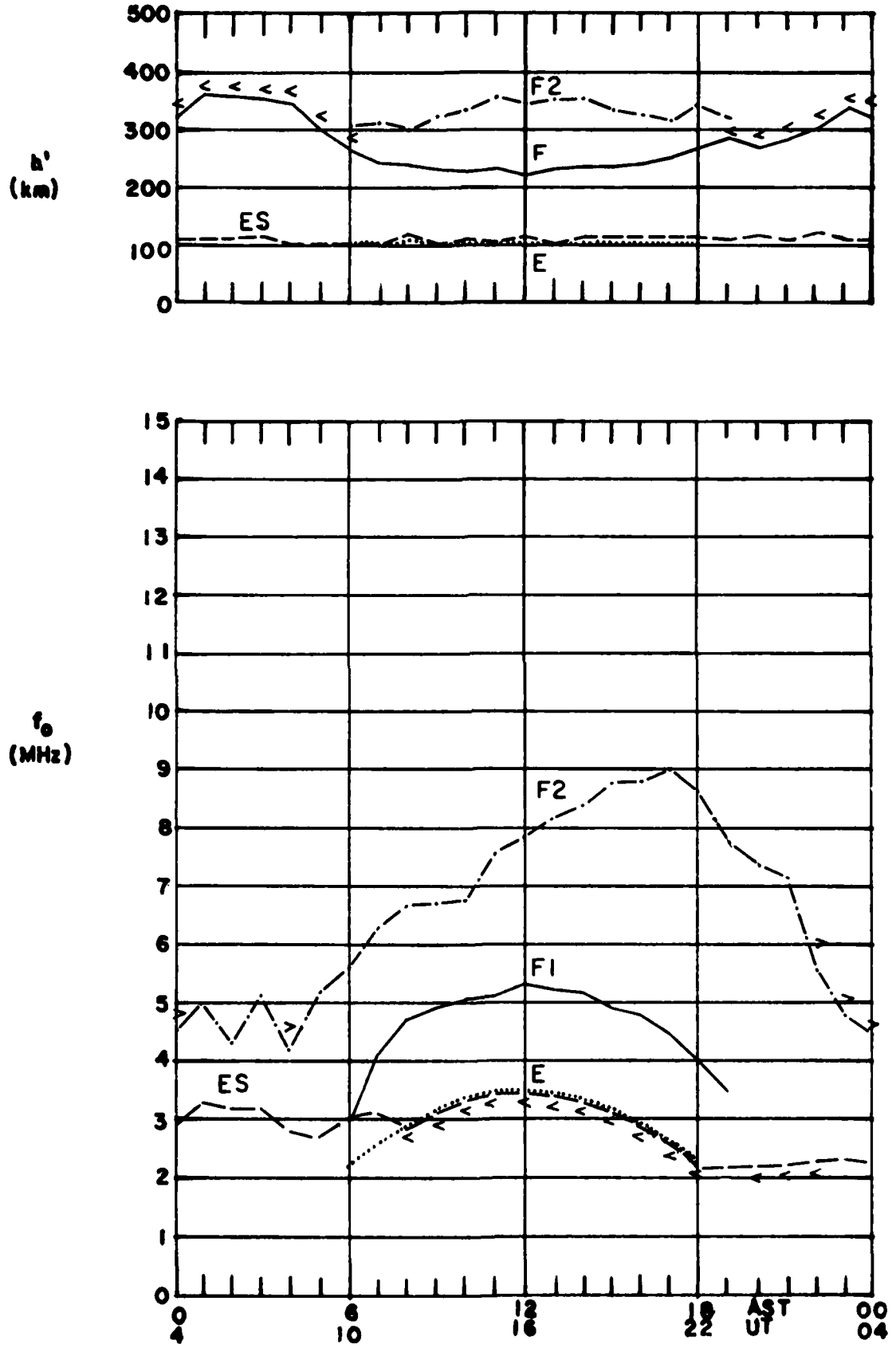

MAY 1979

GOOSE BAY, LABRADOR

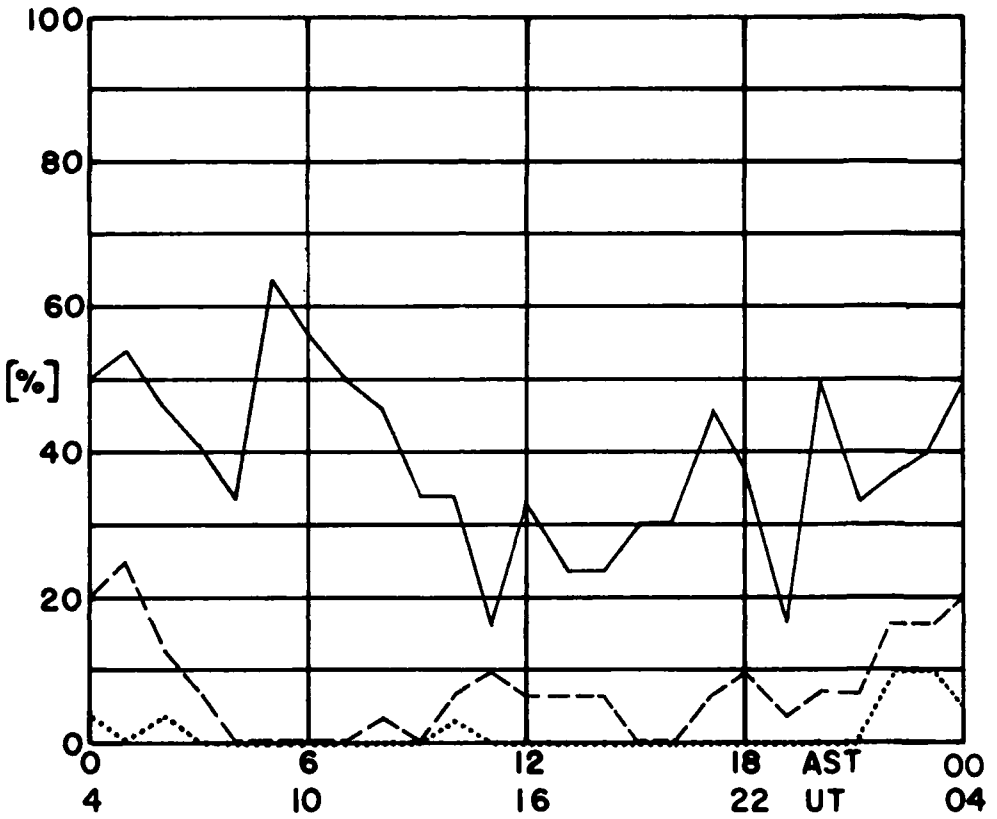

LIMITING FREQUENCY = 3MHz ————————

LIMITING FREQUENCY = 5MHz – – – – – –

LIMITING FREQUENCY = 7MHz .....

PERCENTAGE OF TOTAL TIME DURING WHICH
$f_0 E_s$ IS GREATER THAN THE LIMITING FREQUENCY

MEDIAN VALUES of h' AND f_0 AT GOOSE BAY, LABRADOR FOR

MAY 1979

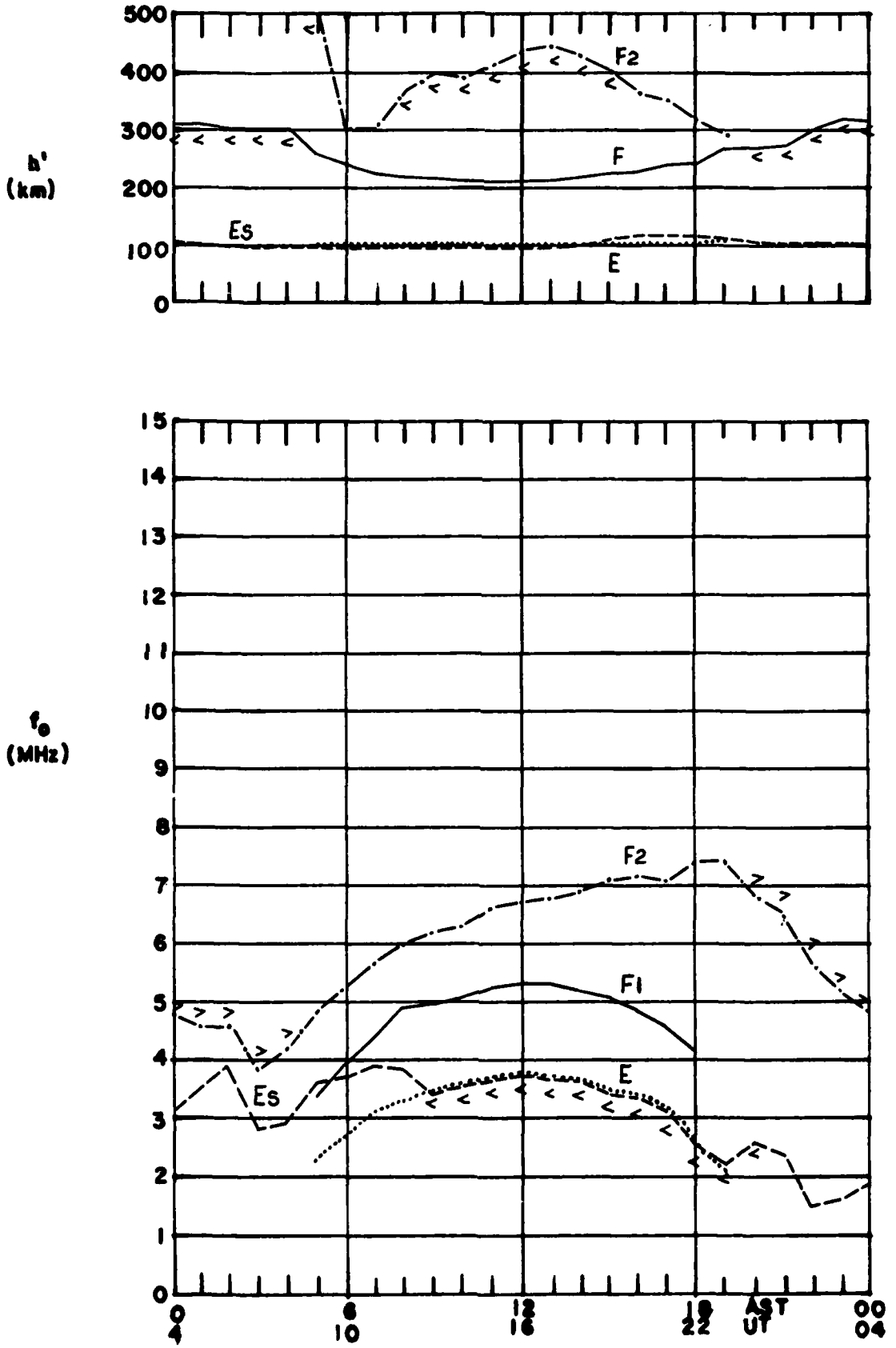

JUNE 1979

GOOSE BAY, LABRADOR

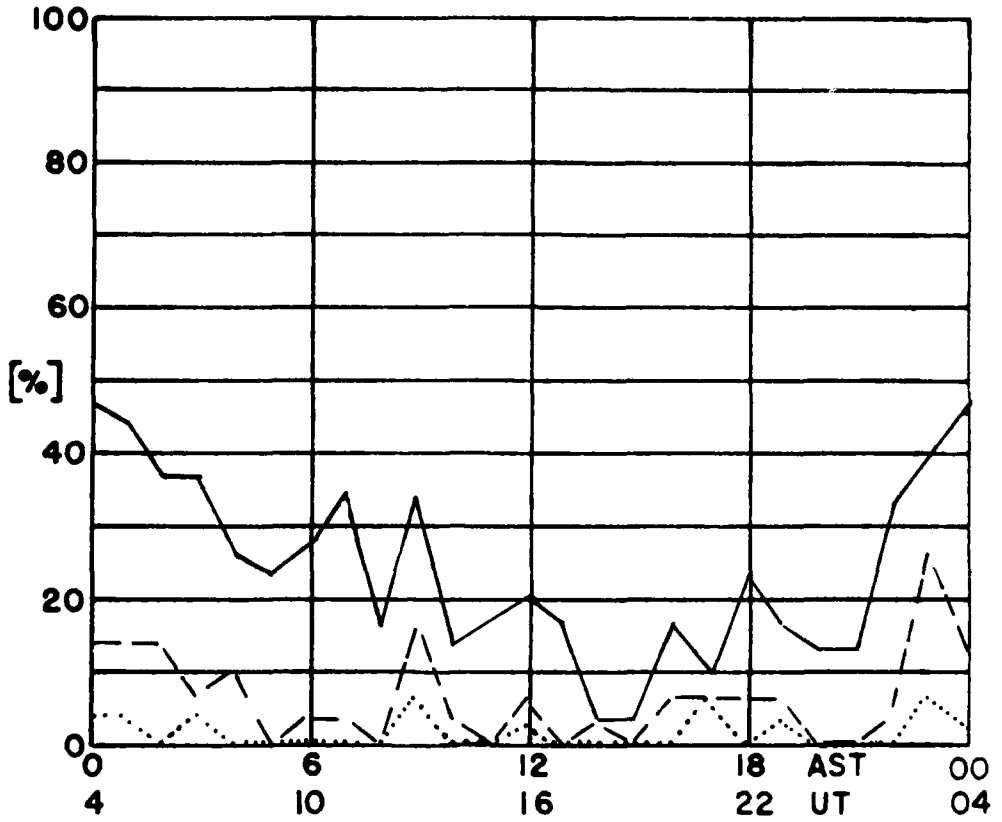

LIMITING FREQUENCY = 3MHz ————————

LIMITING FREQUENCY = 5MHz — — — — — —

LIMITING FREQUENCY = 7MHz .....

PERCENTAGE OF TOTAL TIME DURING WHICH
$f_0 E_s$ IS GREATER THAN THE LIMITING FREQUENCY

MEDIAN VALUES of h' AND f_0 AT GOOSE BAY, LABRADOR FOR

JUNE 1979

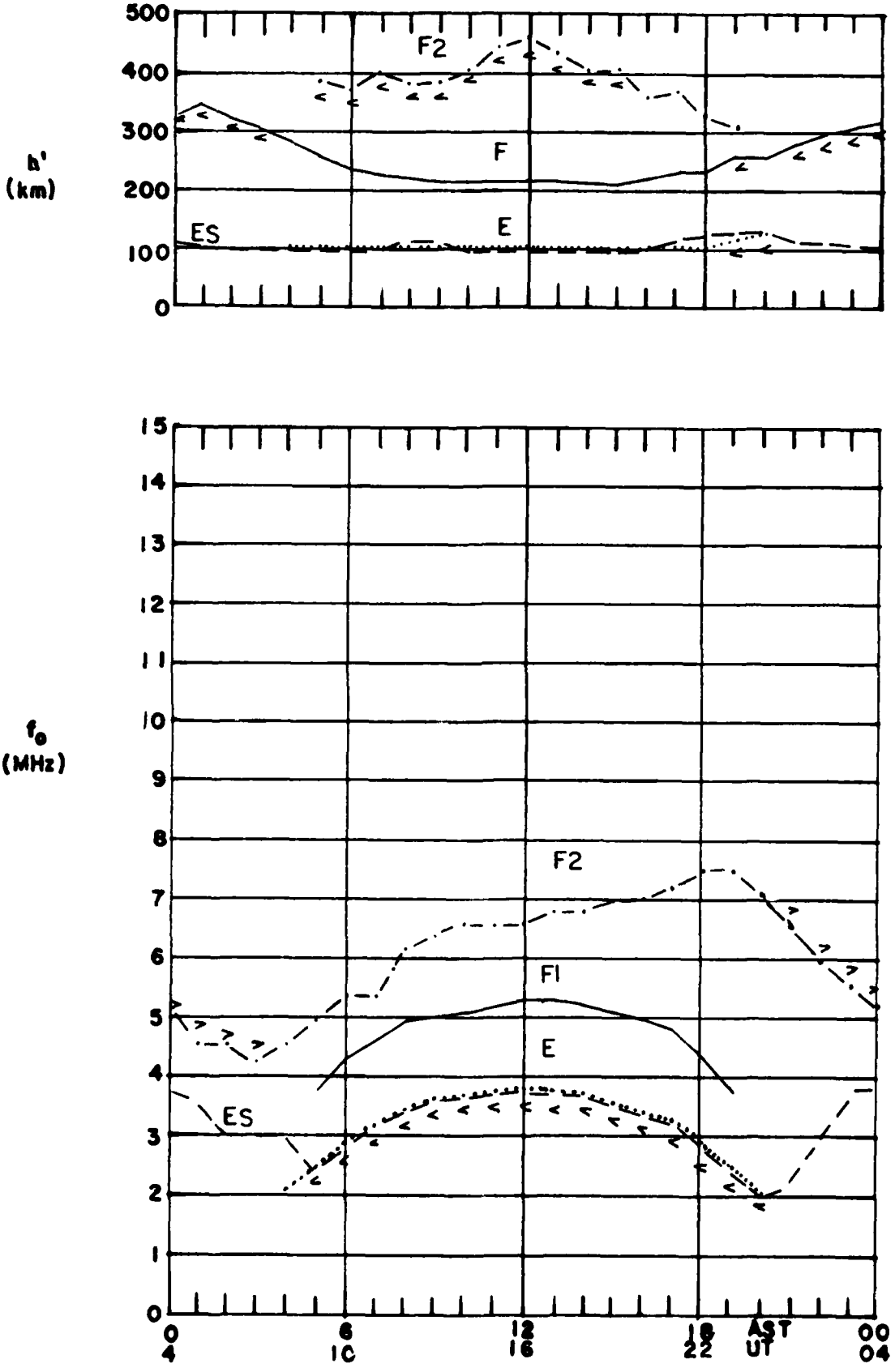

JULY 1979

GOOSE BAY, LABRADOR

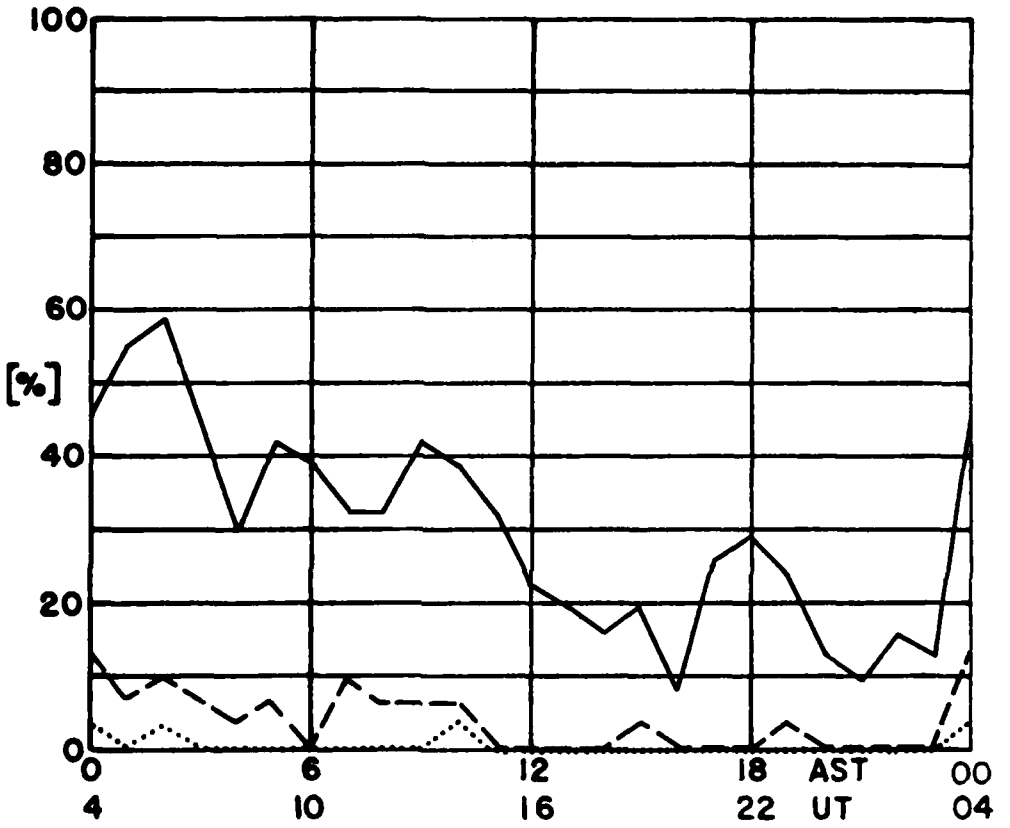

LIMITING FREQUENCY = 3MHz ————————

LIMITING FREQUENCY = 5MHz — — — — — —

LIMITING FREQUENCY = 7MHz .....

PERCENTAGE OF TOTAL TIME DURING WHICH
$f_0 E_s$ IS GREATER THAN THE LIMITING FREQUENCY

MEDIAN VALUES of h' AND f_0 AT GOOSE BAY, LABRADOR FOR

JULY 1979

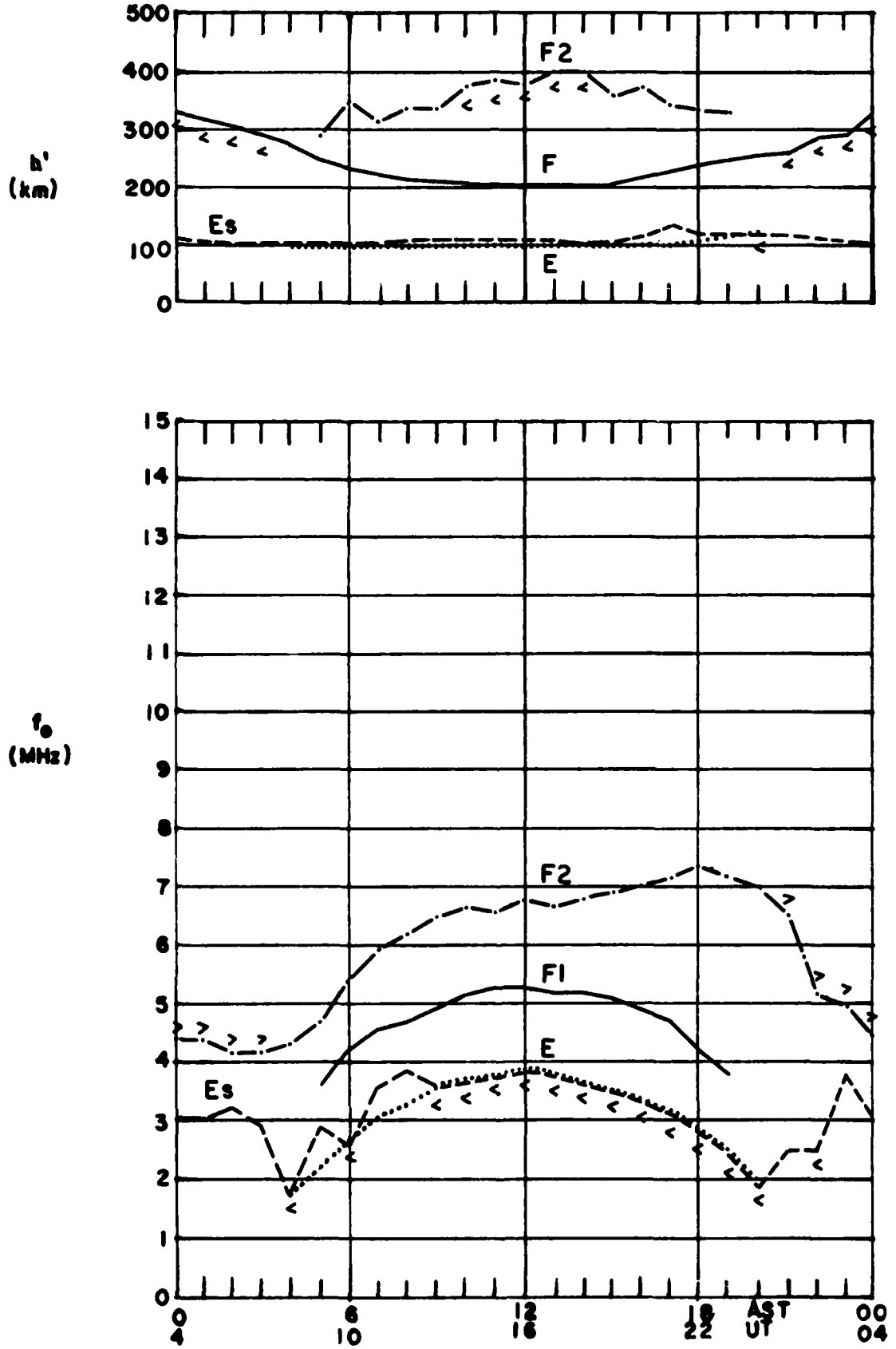

AUGUST 1979

GOOSE BAY, LABRADOR

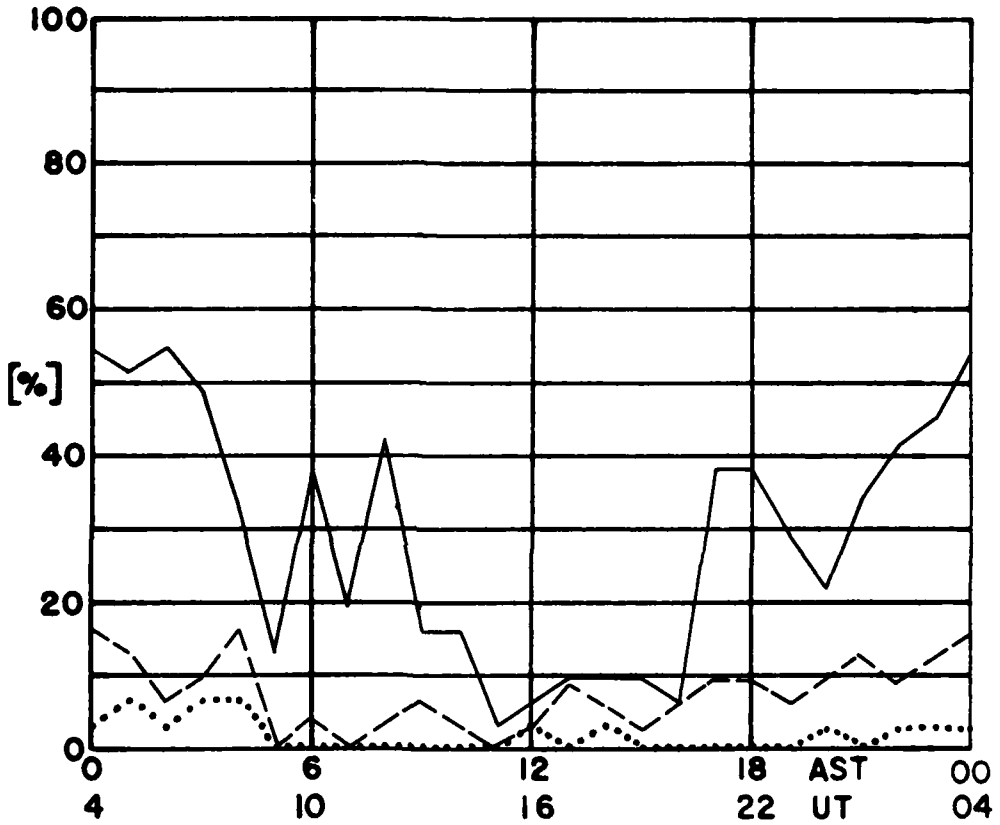

LIMITING FREQUENCY = 3MHz ——————

LIMITING FREQUENCY = 5MHz — — — — —

LIMITING FREQUENCY = 7MHz .....

PERCENTAGE OF TOTAL TIME DURING WHICH
$f_0 E_s$ IS GREATER THAN THE LIMITING FREQUENCY

MEDIAN VALUES of h' AND f_0 AT GOOSE BAY, LABRADOR FOR AUGUST 1979

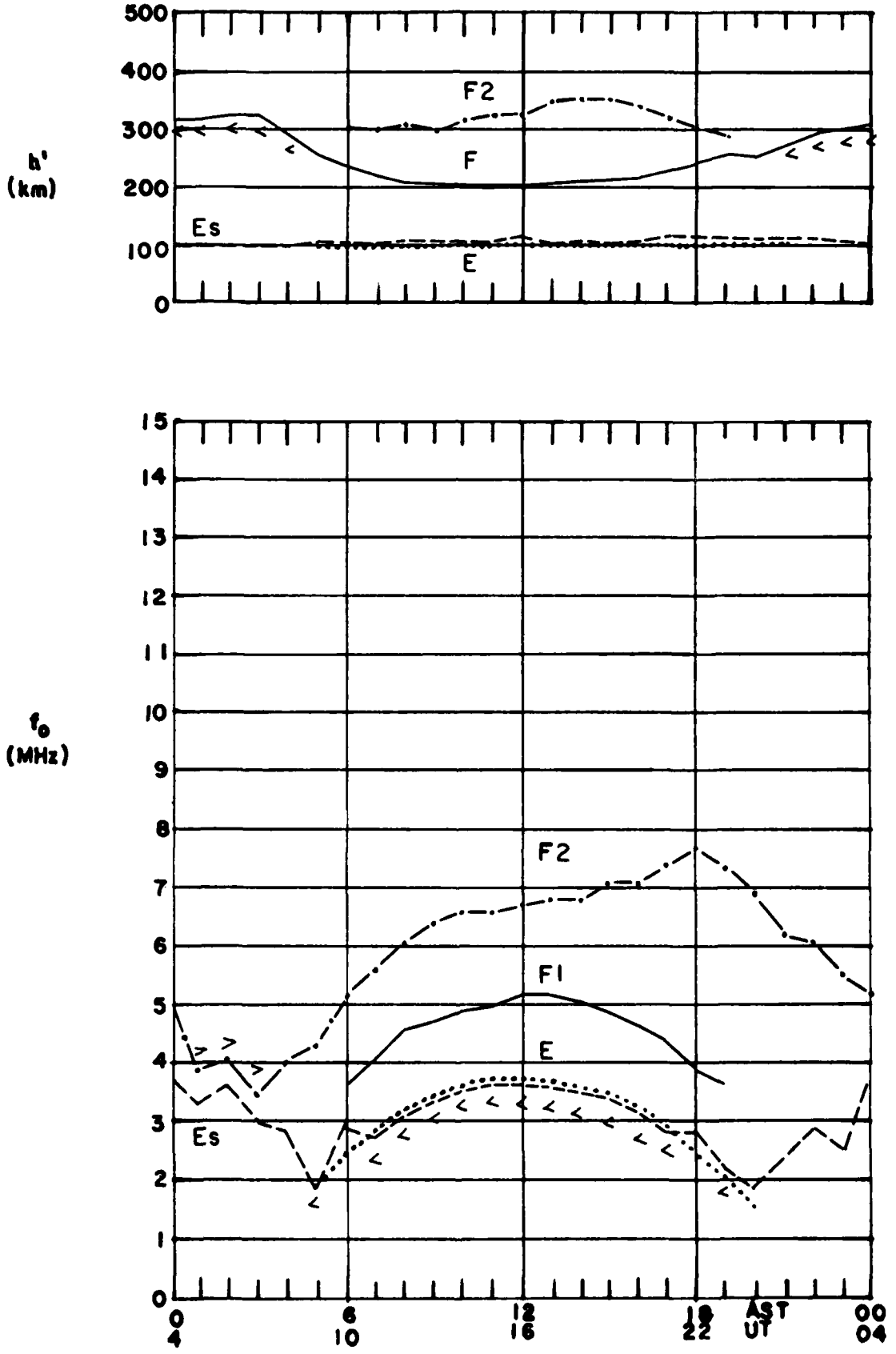

SEPTEMBER 1979

GOOSE BAY, LABRADOR

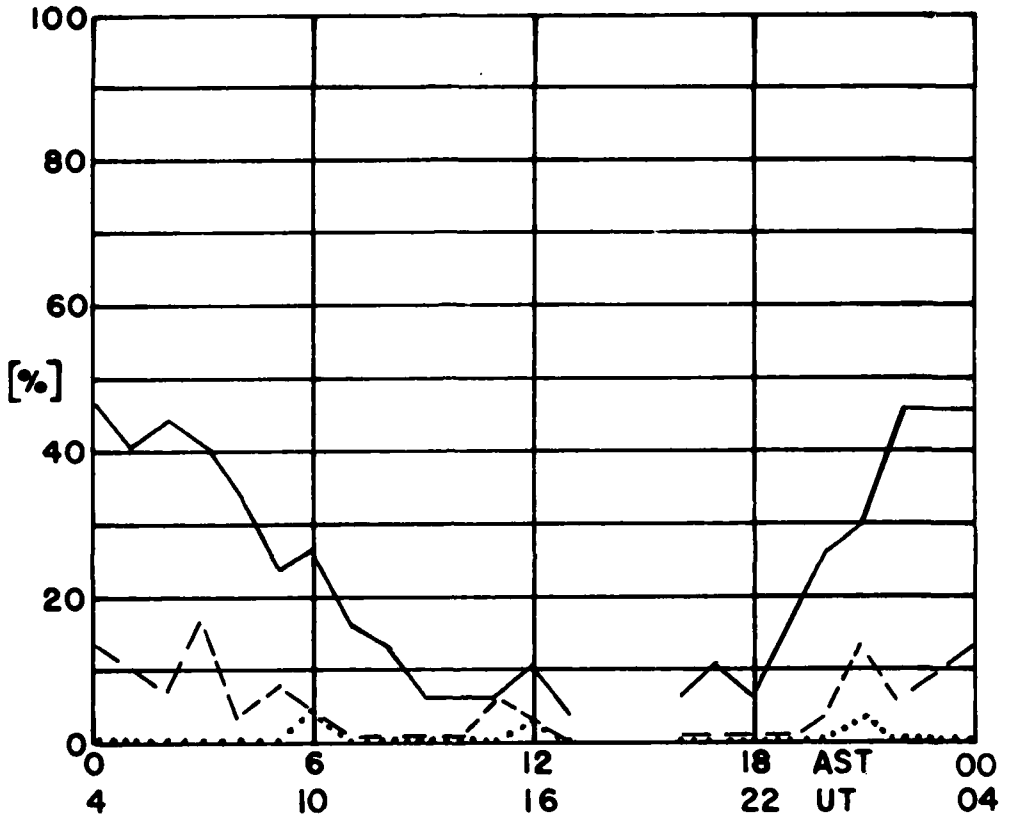

LIMITING FREQUENCY = 3MHz ——————

LIMITING FREQUENCY = 5MHz — — — — —

LIMITING FREQUENCY = 7MHz .....

PERCENTAGE OF TOTAL TIME DURING WHICH
$f_0 E_s$ IS GREATER THAN THE LIMITING FREQUENCY

MEDIAN VALUES of h' AND f_0 AT GOOSE BAY, LABRADOR FOR

SEPTEMBER 1979

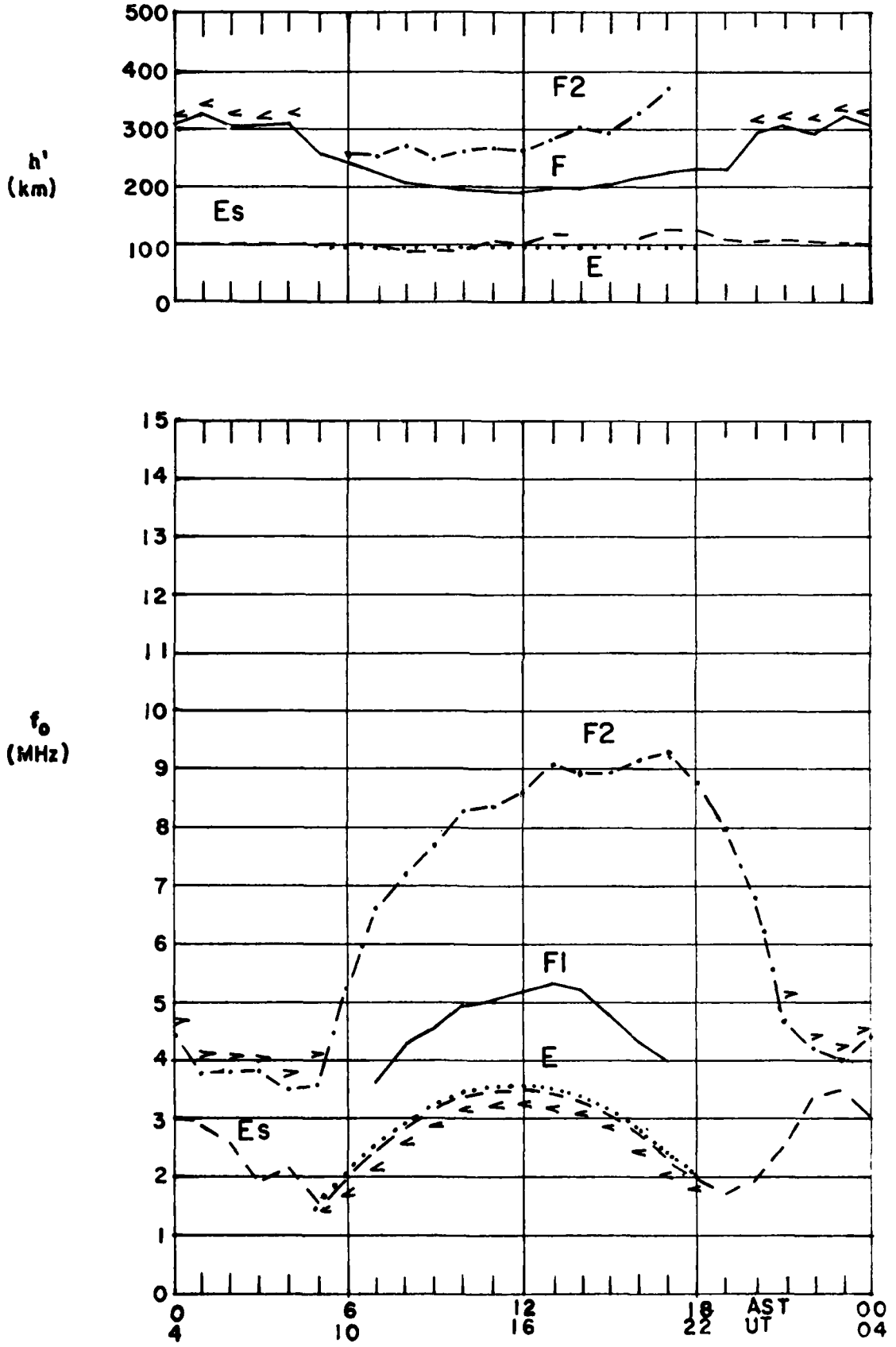

OCTOBER 1979

GOOSE BAY, LABRADOR

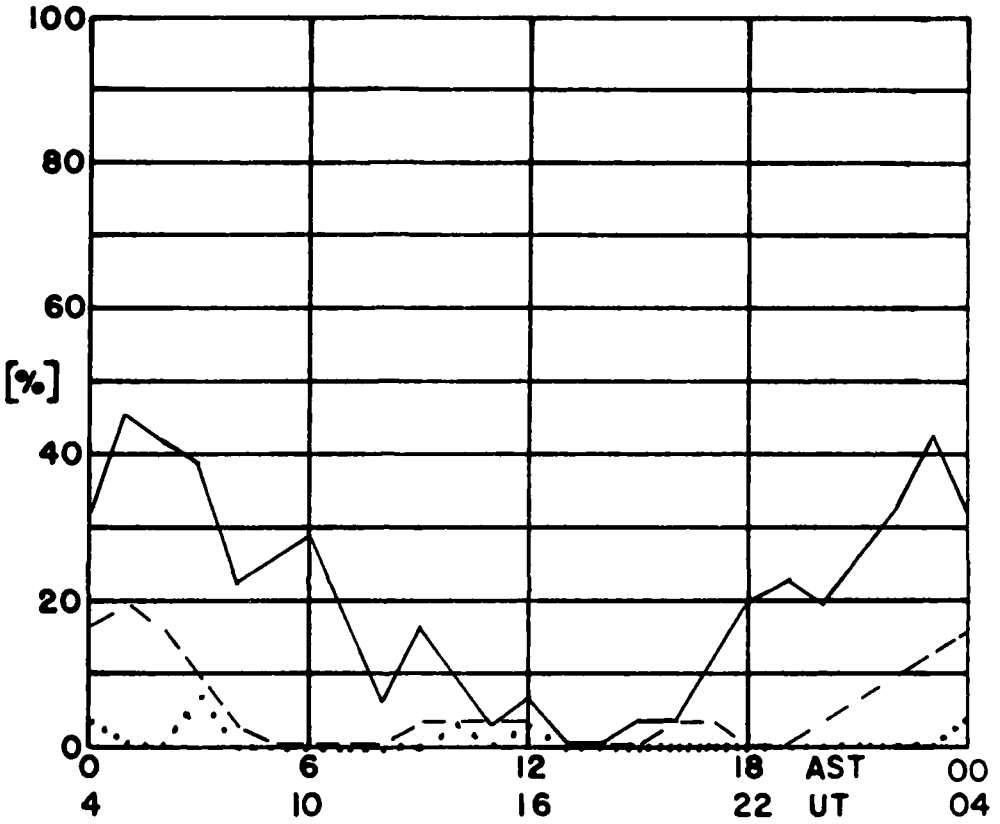

LIMITING FREQUENCY = 3MHz ————————

LIMITING FREQUENCY = 5MHz — — — — — —

LIMITING FREQUENCY = 7MHz .....

PERCENTAGE OF TOTAL TIME DURING WHICH
$f_0 E_s$ IS GREATER THAN THE LIMITING FREQUENCY

MEDIAN VALUES of h' AND f_0 AT GOOSE BAY, LABRADOR FOR OCTOBER 1979

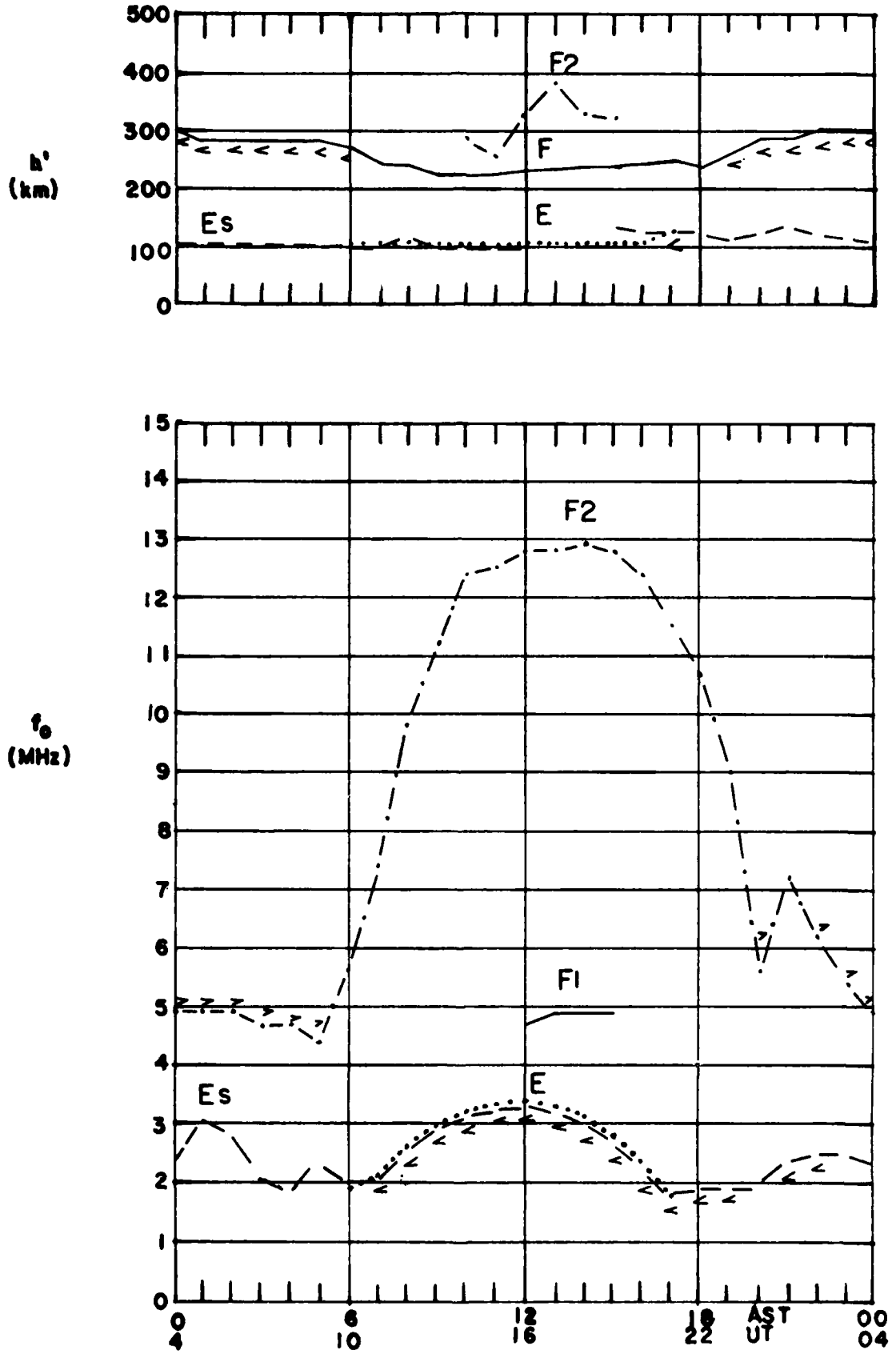

NOVEMBER 1979

GOOSE BAY, LABRADOR

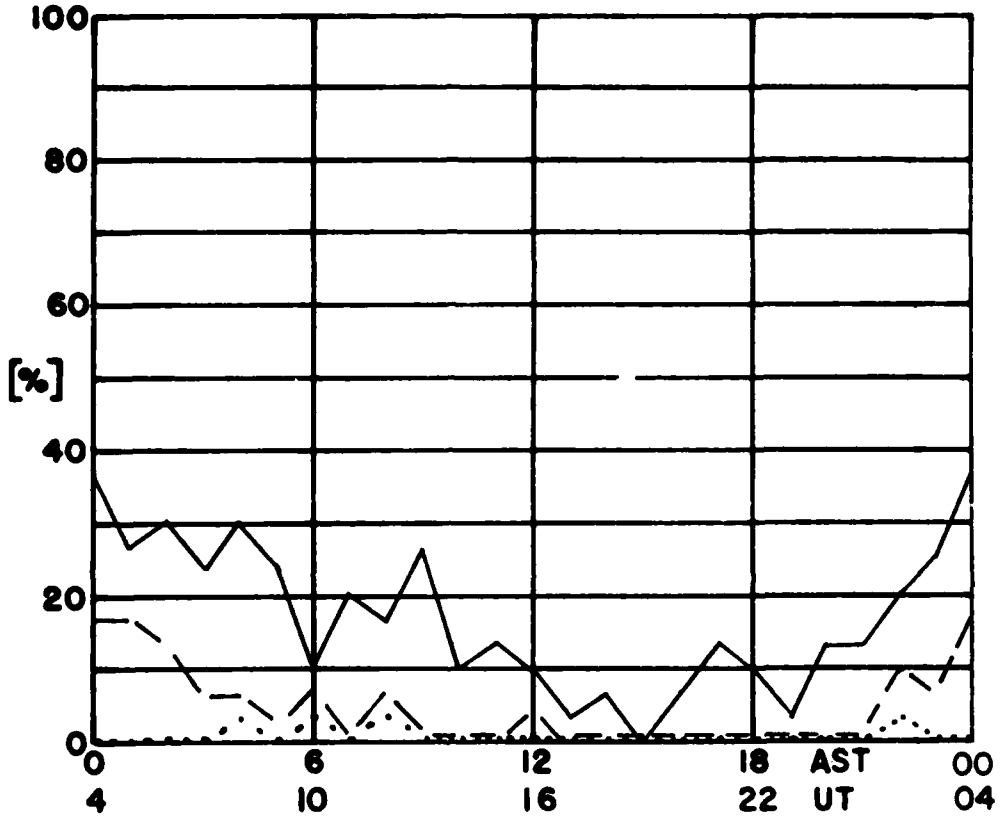

LIMITING FREQUENCY = 3MHz ————————

LIMITING FREQUENCY = 5MHz — — — — — —

LIMITING FREQUENCY = 7MHz .....

PERCENTAGE OF TOTAL TIME DURING WHICH
$f_0 E_s$ IS GREATER THAN THE LIMITING FREQUENCY

MEDIAN VALUES of h' AND fo AT GOOSE BAY, LABRADOR FOR

NOVEMBER 1979

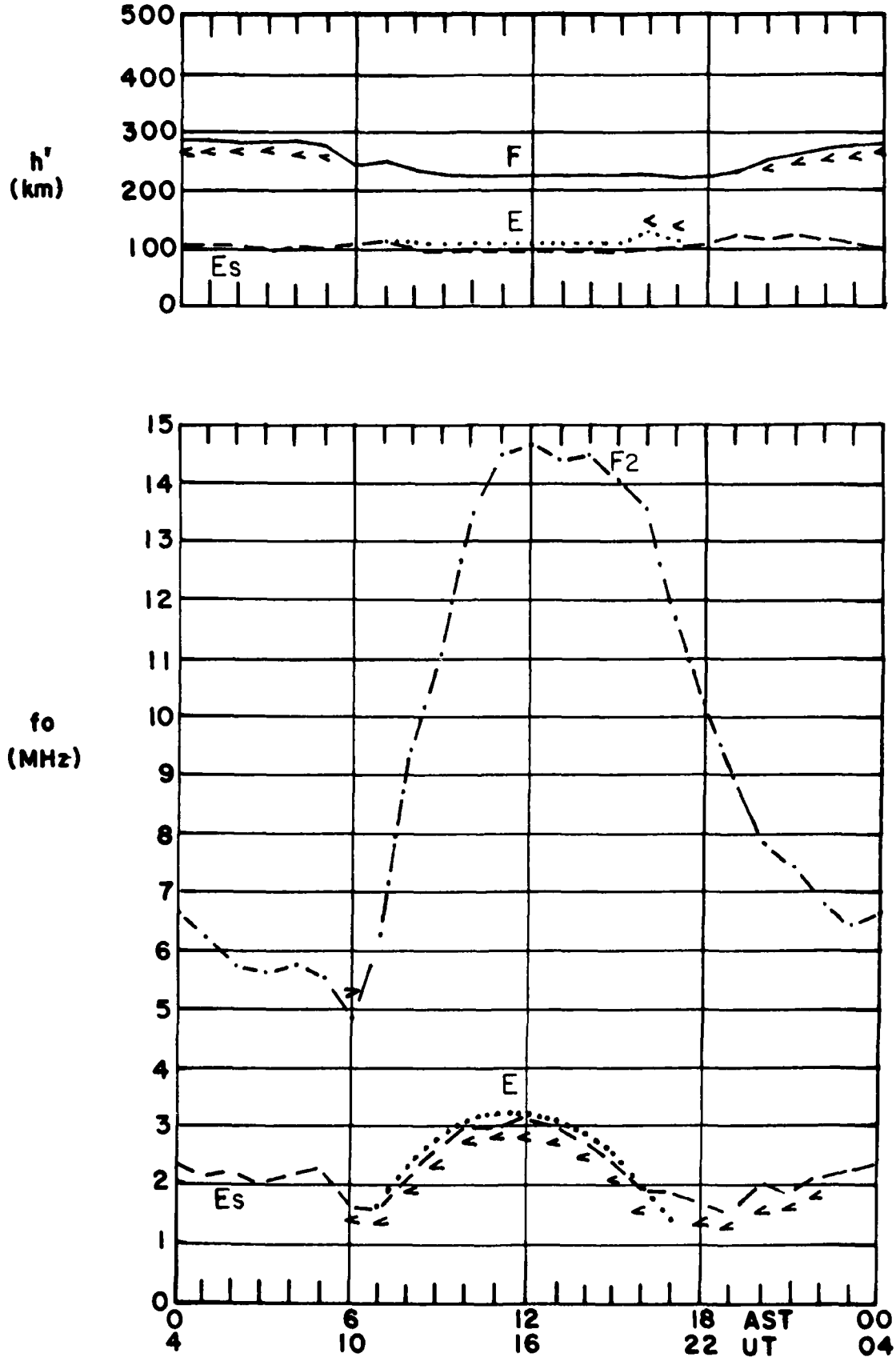

DECEMBER 1979

GOOSE BAY, LABRADOR

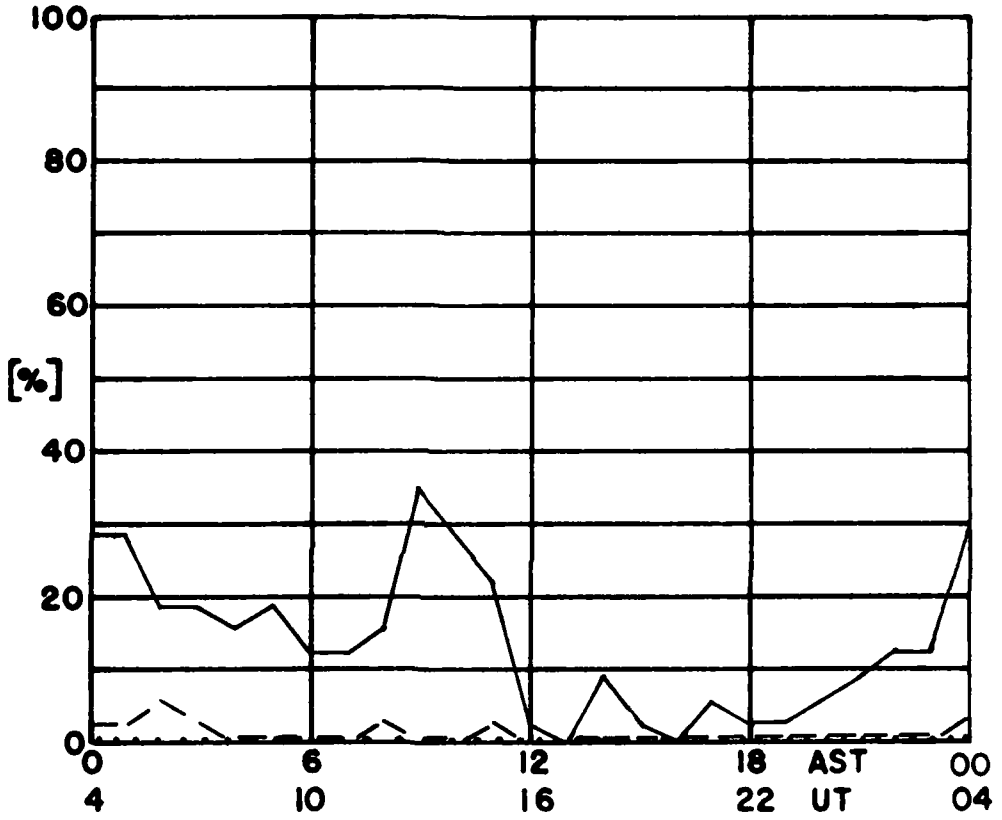

LIMITING FREQUENCY = 3MHz ————————

LIMITING FREQUENCY = 5MHz – – – – – –

LIMITING FREQUENCY = 7MHz .....

PERCENTAGE OF TOTAL TIME DURING WHICH
$f_0 E_s$ IS GREATER THAN THE LIMITING FREQUENCY

MEDIAN VALUES of h' AND fo AT GOOSE BAY, LABRADOR FOR DECEMBER 1979

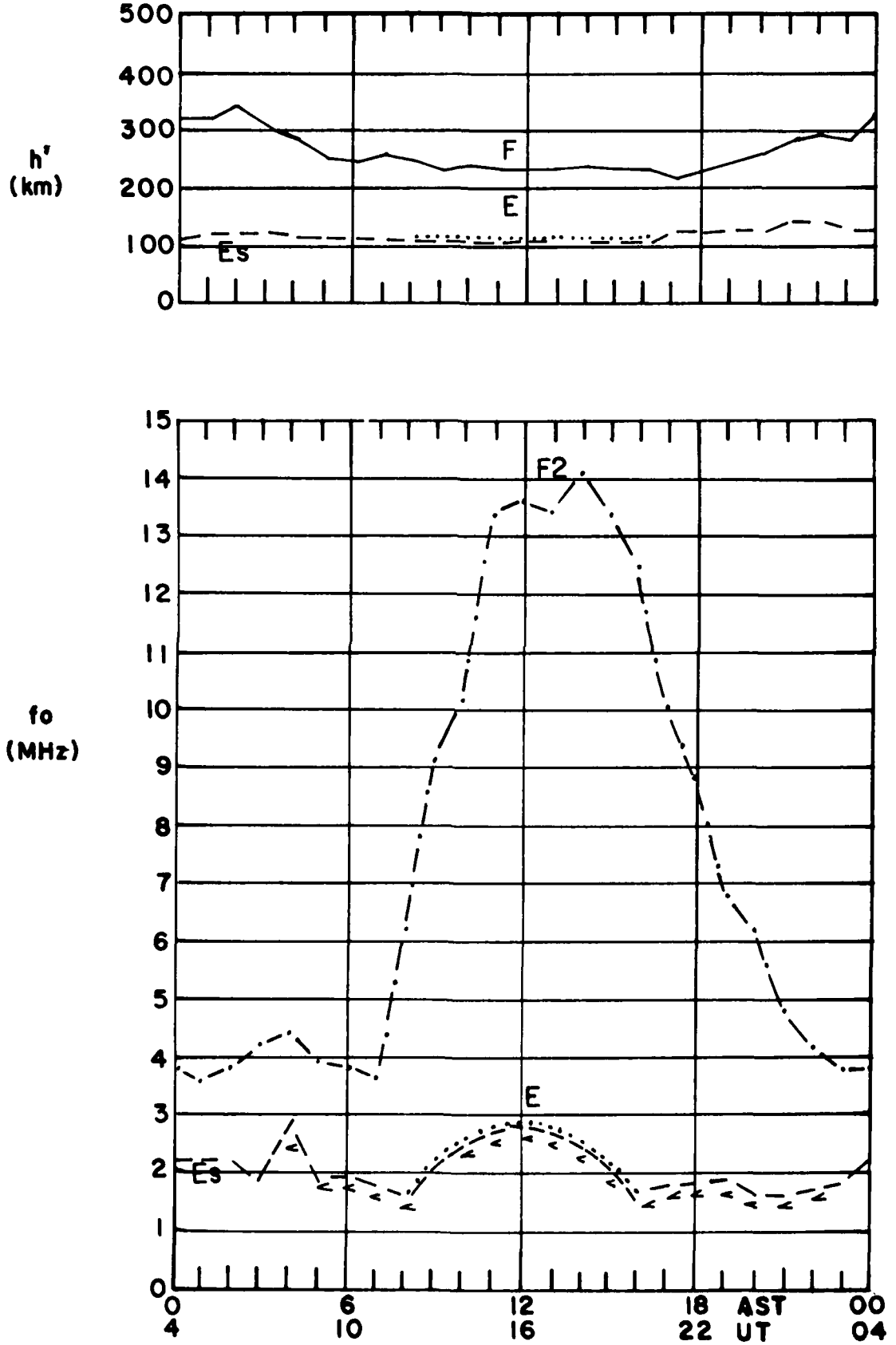

JANUARY 1980

GOOSE BAY, LABRADOR

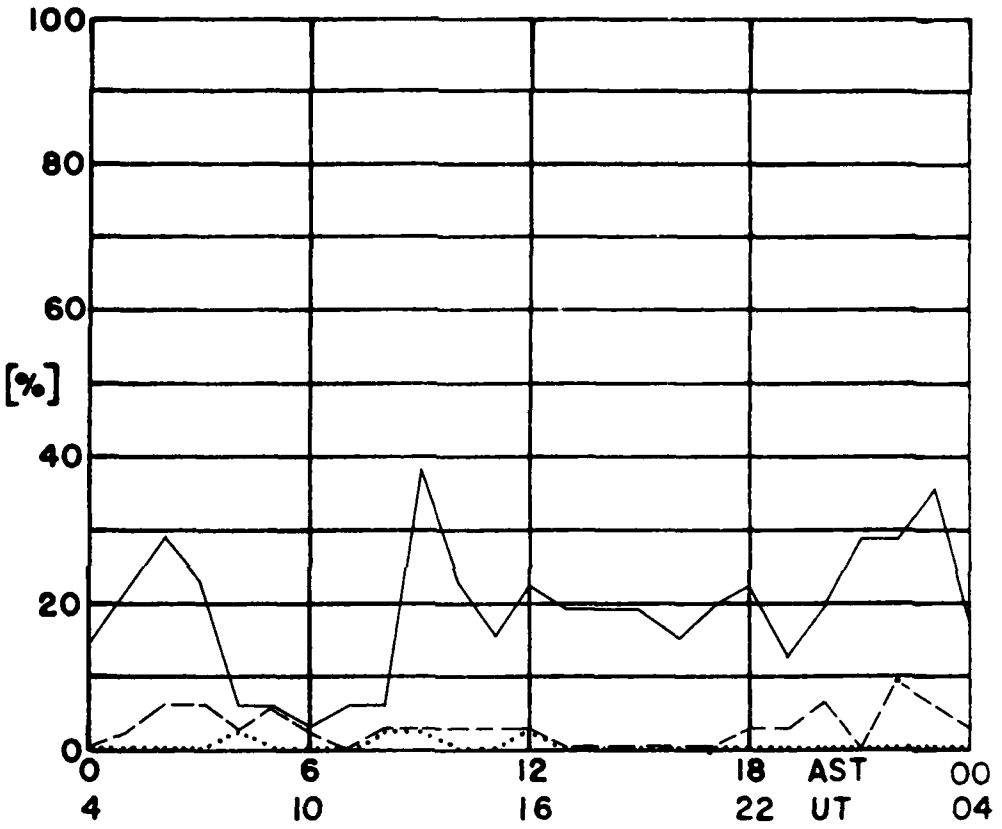

LIMITING FREQUENCY = 3MHz ——————

LIMITING FREQUENCY = 5MHz — — — — —

LIMITING FREQUENCY = 7MHz .....

PERCENTAGE OF TOTAL TIME DURING WHICH
$f_0 E_s$ IS GREATER THAN THE LIMITING FREQUENCY

MEDIAN VALUES of h' AND f_0 AT GOOSE BAY, LABRADOR FOR JANUARY 1980

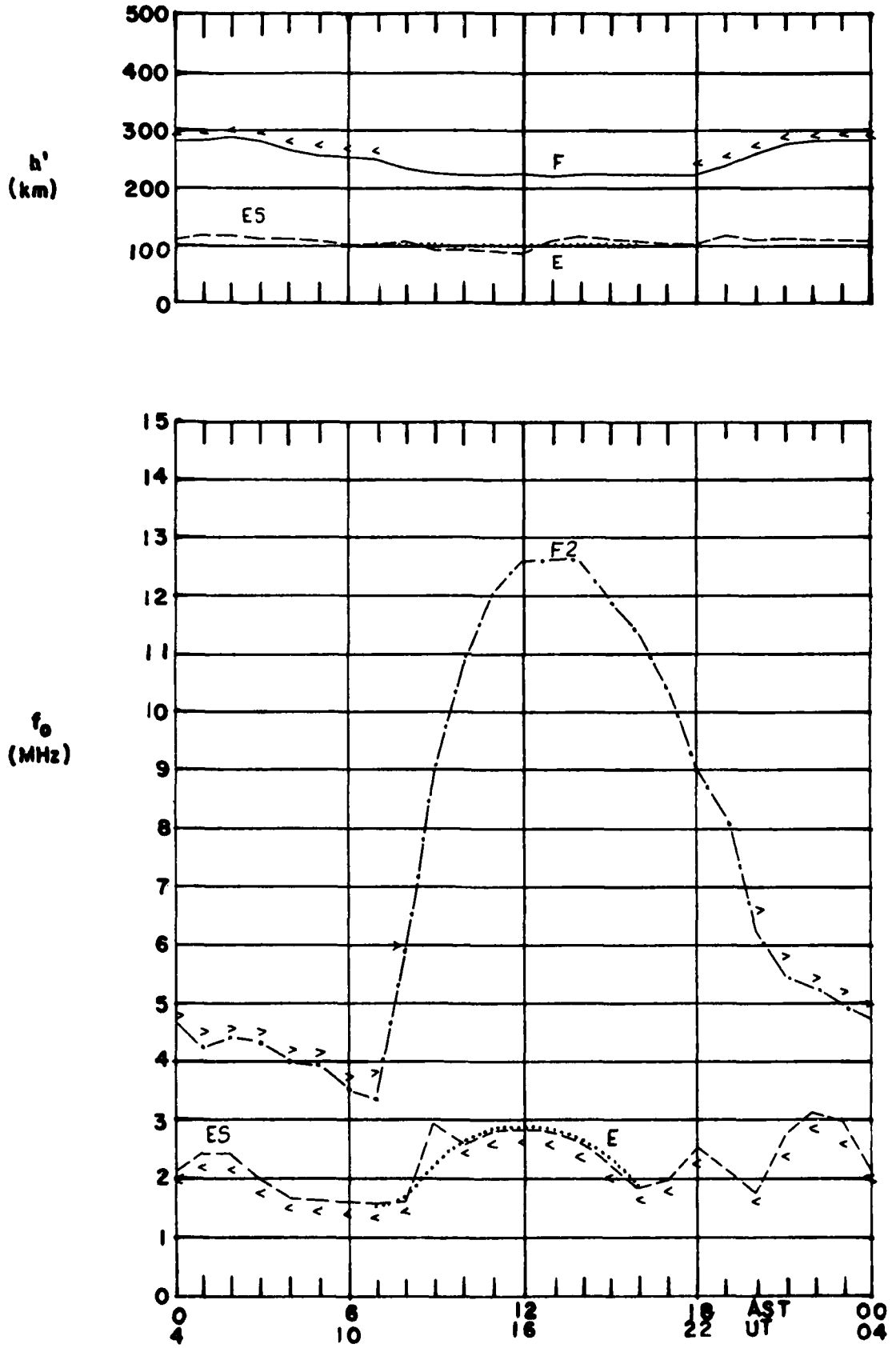

FEBRUARY 1980

GOOSE BAY, LABRADOR

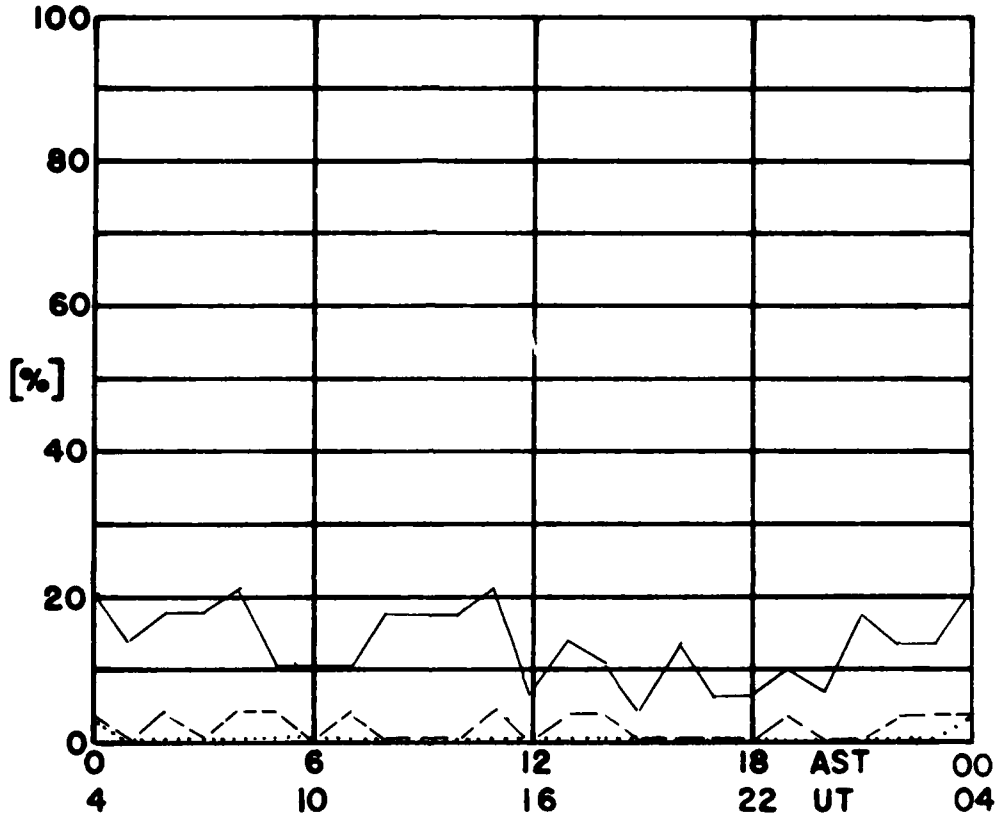

LIMITING FREQUENCY = 3MHz ————————

LIMITING FREQUENCY = 5MHz — — — — —

LIMITING FREQUENCY = 7MHz .....

PERCENTAGE OF TOTAL TIME DURING WHICH
$f_0 E_s$ IS GREATER THAN THE LIMITING FREQUENCY

MEDIAN VALUES of h' AND f_0 AT GOOSE BAY, LABRADOR FOR FEBRUARY 1980

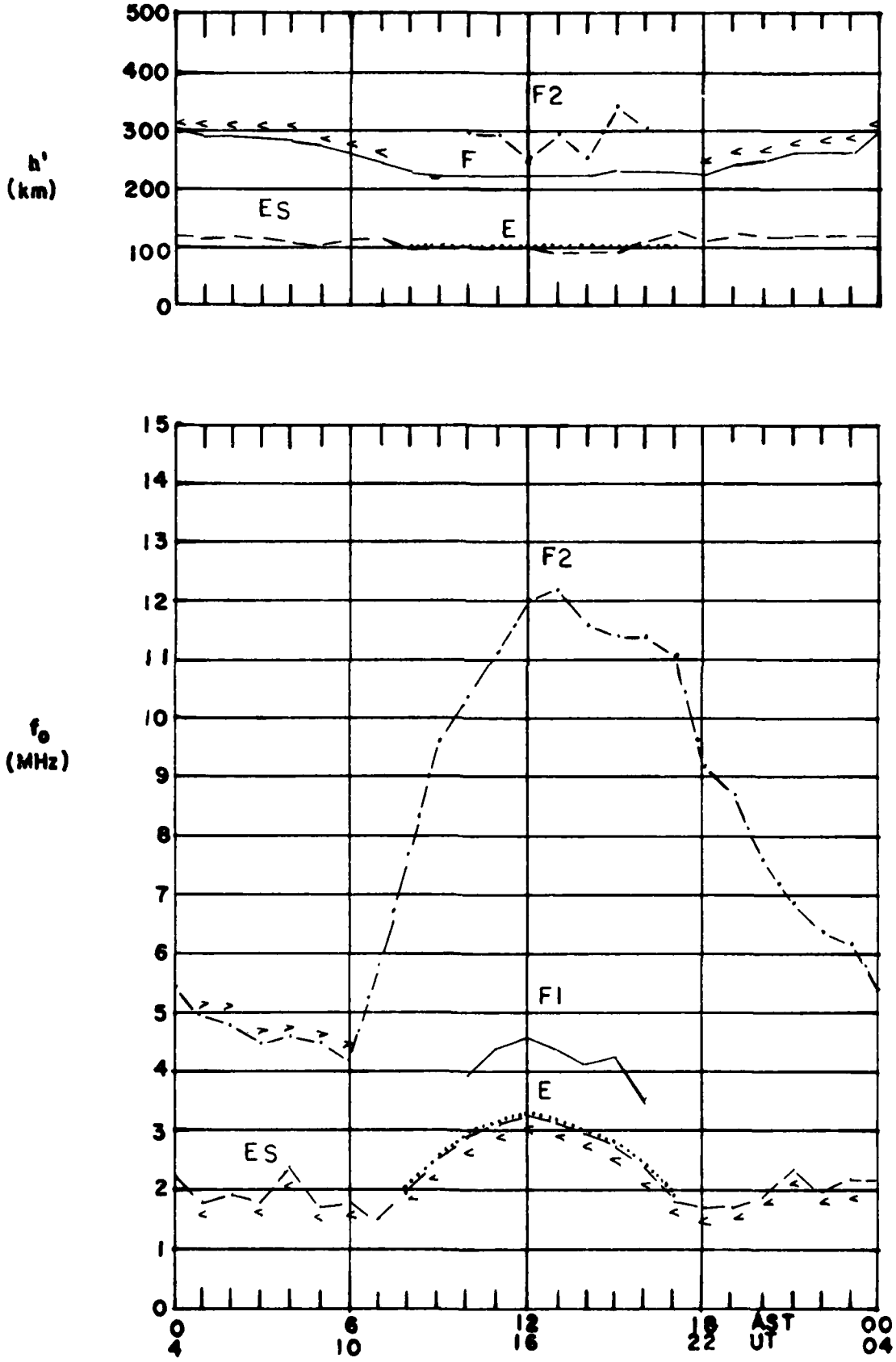

MARCH 1980

GOOSE BAY, LABRADOR

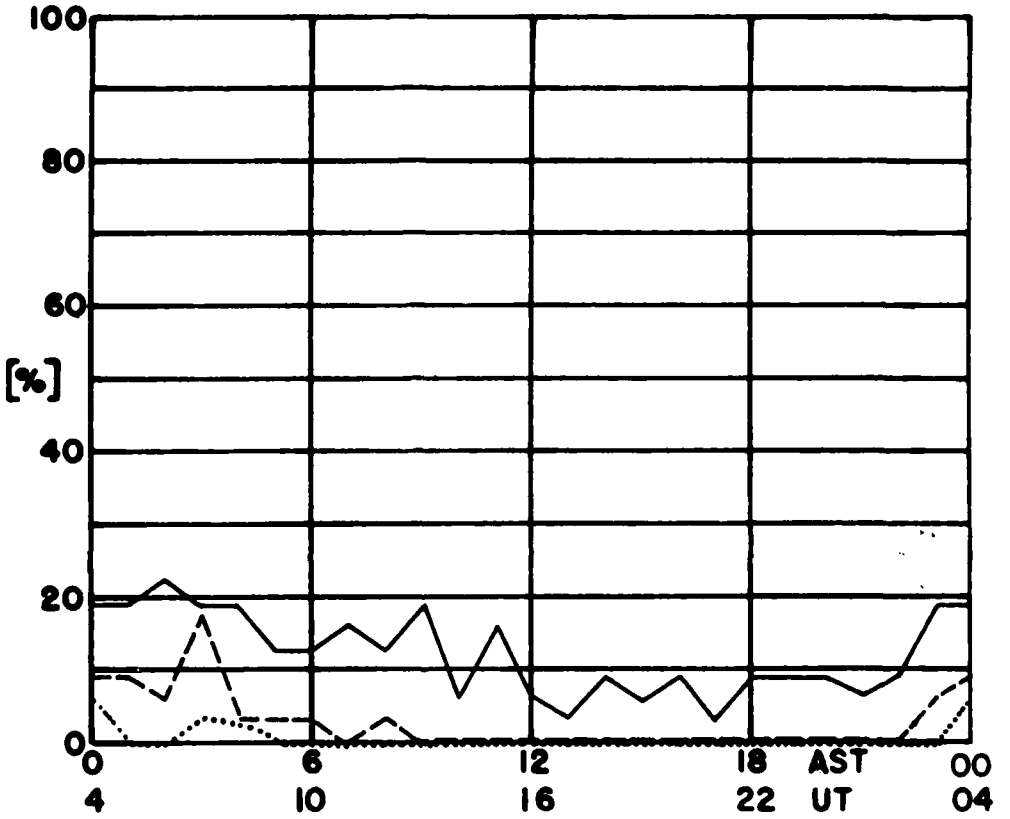

LIMITING FREQUENCY = 3MHz ————————

LIMITING FREQUENCY = 5MHz — — — — — —

LIMITING FREQUENCY = 7MHz .....

PERCENTAGE OF TOTAL TIME DURING WHICH
$f_0 E_s$ IS GREATER THAN THE LIMITING FREQUENCY

MEDIAN VALUES of h' AND f_0 AT GOOSE BAY, LABRADOR FOR

MARCH 1980

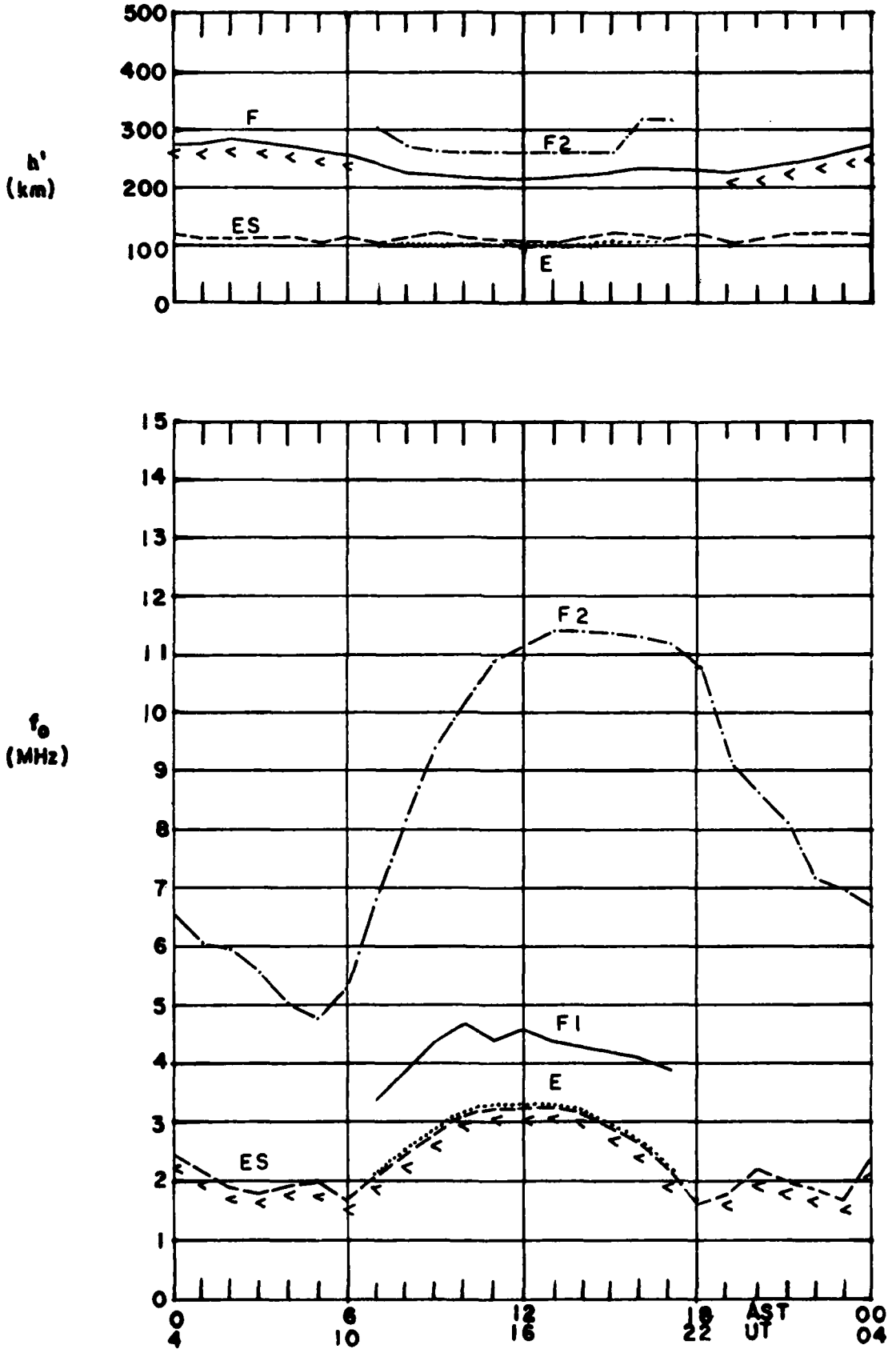

APRIL 1980

GOOSE BAY, LABRADOR

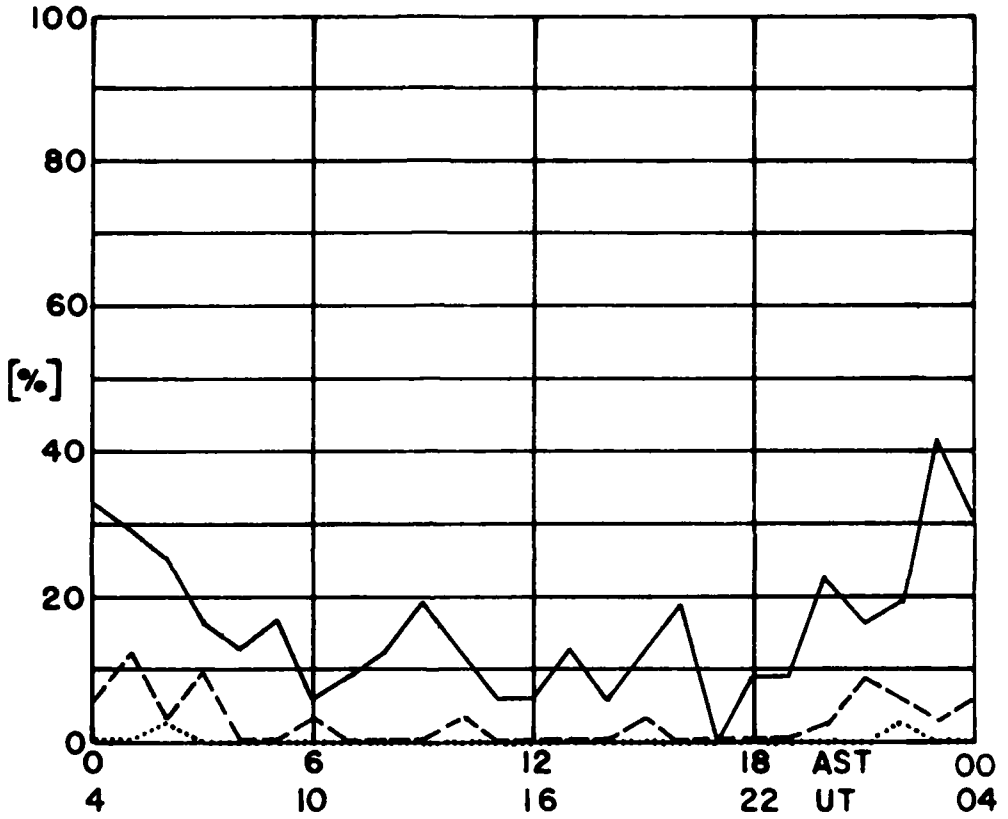

LIMITING FREQUENCY = 3MHz ——————

LIMITING FREQUENCY = 5MHz — — — — —

LIMITING FREQUENCY = 7MHz .....

PERCENTAGE OF TOTAL TIME DURING WHICH
$f_0 E_s$ IS GREATER THAN THE LIMITING FREQUENCY

MEDIAN VALUES of h' AND f_0 AT GOOSE BAY, LABRADOR FOR

APRIL 1980

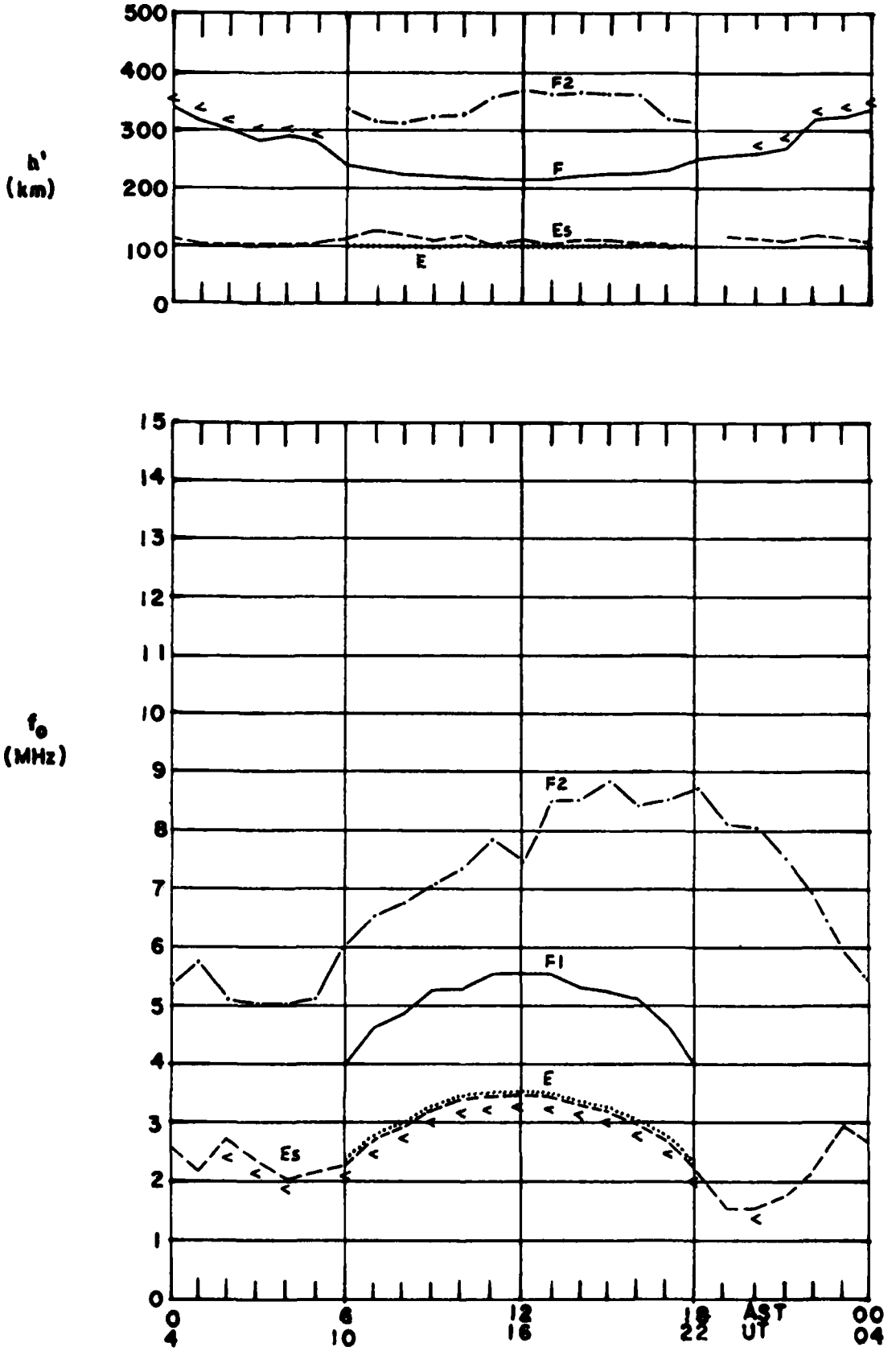

MAY 1980

GOOSE BAY, LABRADOR

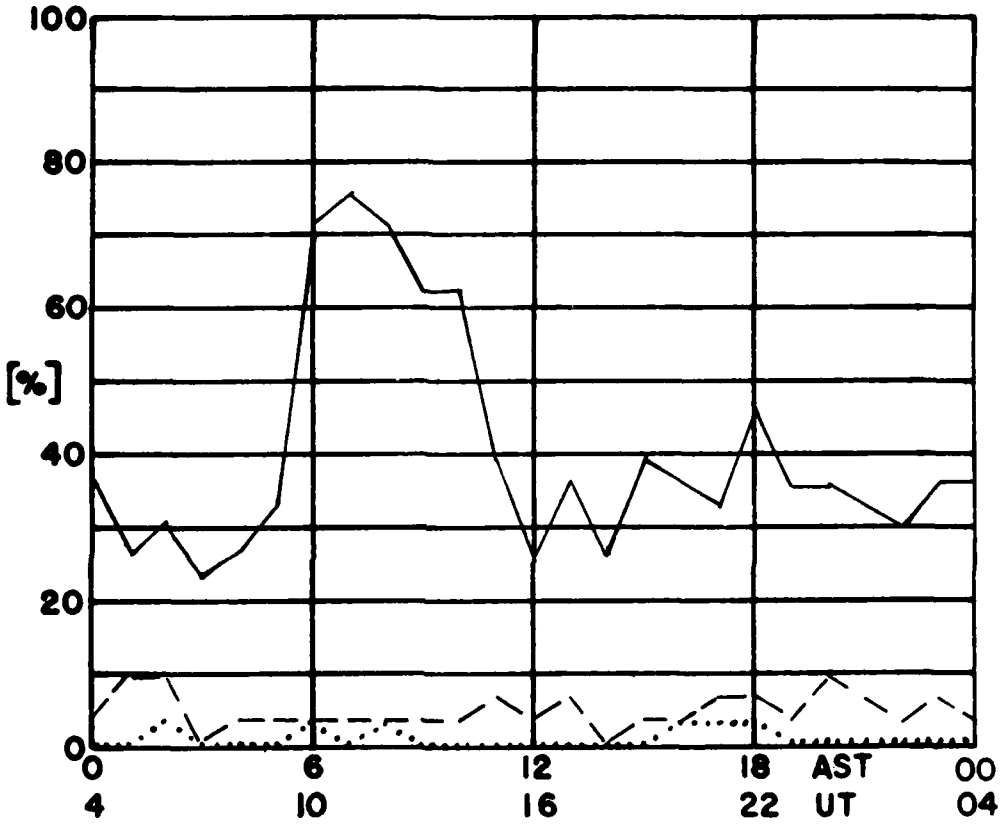

LIMITING FREQUENCY = 3MHz ————————

LIMITING FREQUENCY = 5MHz — — — — —

LIMITING FREQUENCY = 7MHz .....

PERCENTAGE OF TOTAL TIME DURING WHICH
$f_0 E_s$ IS GREATER THAN THE LIMITING FREQUENCY

MEDIAN VALUES of h' AND f_o AT GOOSE BAY, LABRADOR FOR

MAY 1980

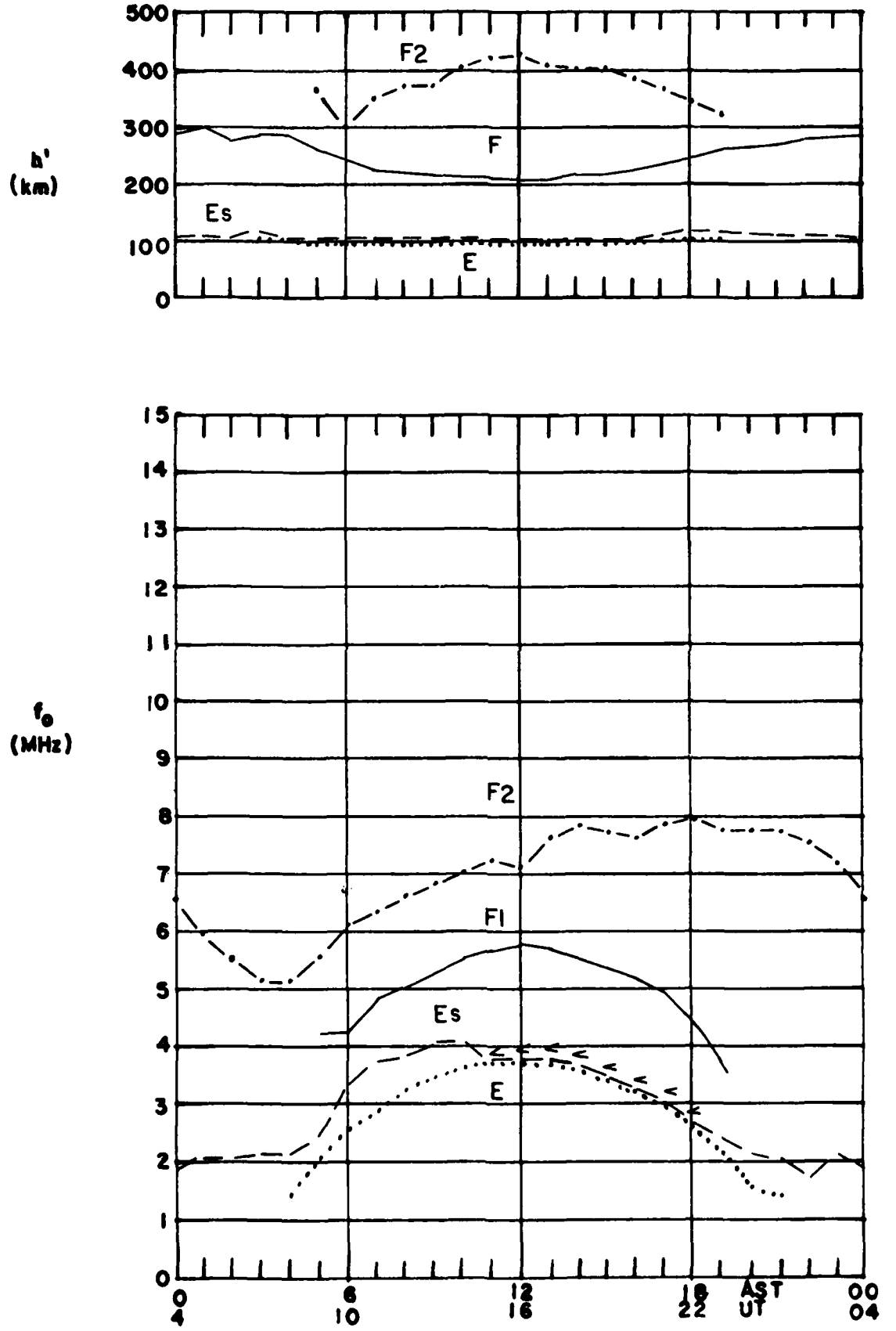

JUNE 1980

GOOSE BAY, LABRADOR

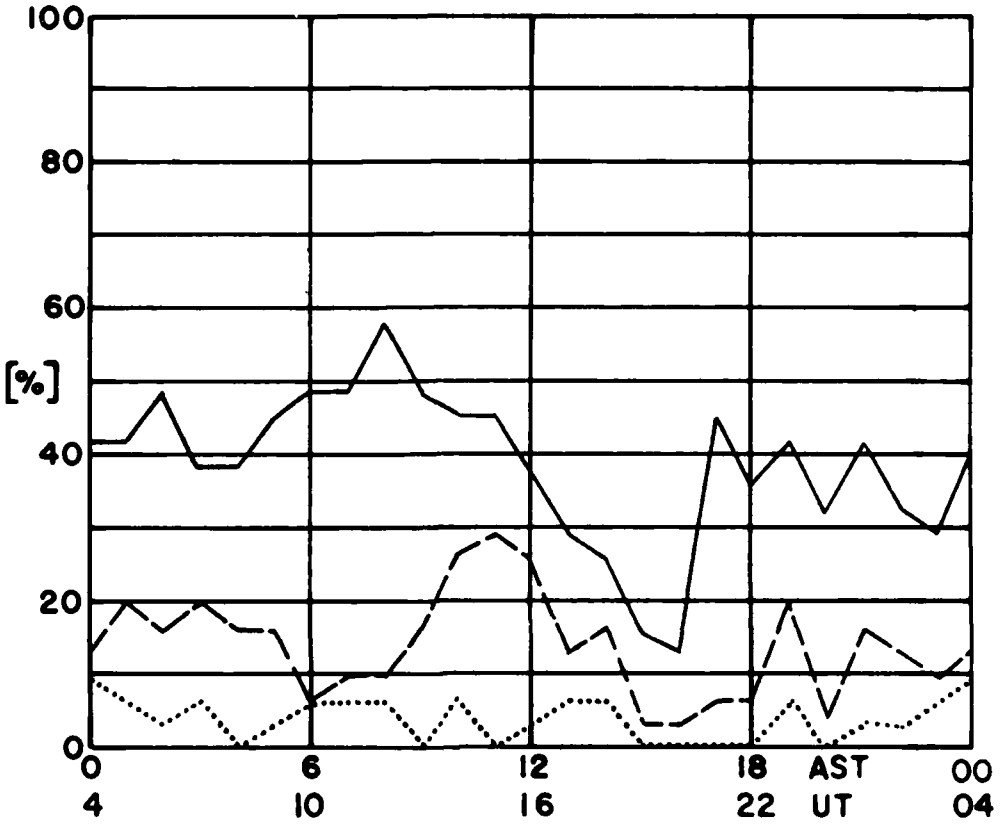

LIMITING FREQUENCY = 3MHz ————————

LIMITING FREQUENCY = 5MHz — — — — —

LIMITING FREQUENCY = 7MHz .....

PERCENTAGE OF TOTAL TIME DURING WHICH
$f_0 E_s$ IS GREATER THAN THE LIMITING FREQUENCY

MEDIAN VALUES of h' AND f_0 AT GOOSE BAY, LABRADOR FOR

JUNE 1980

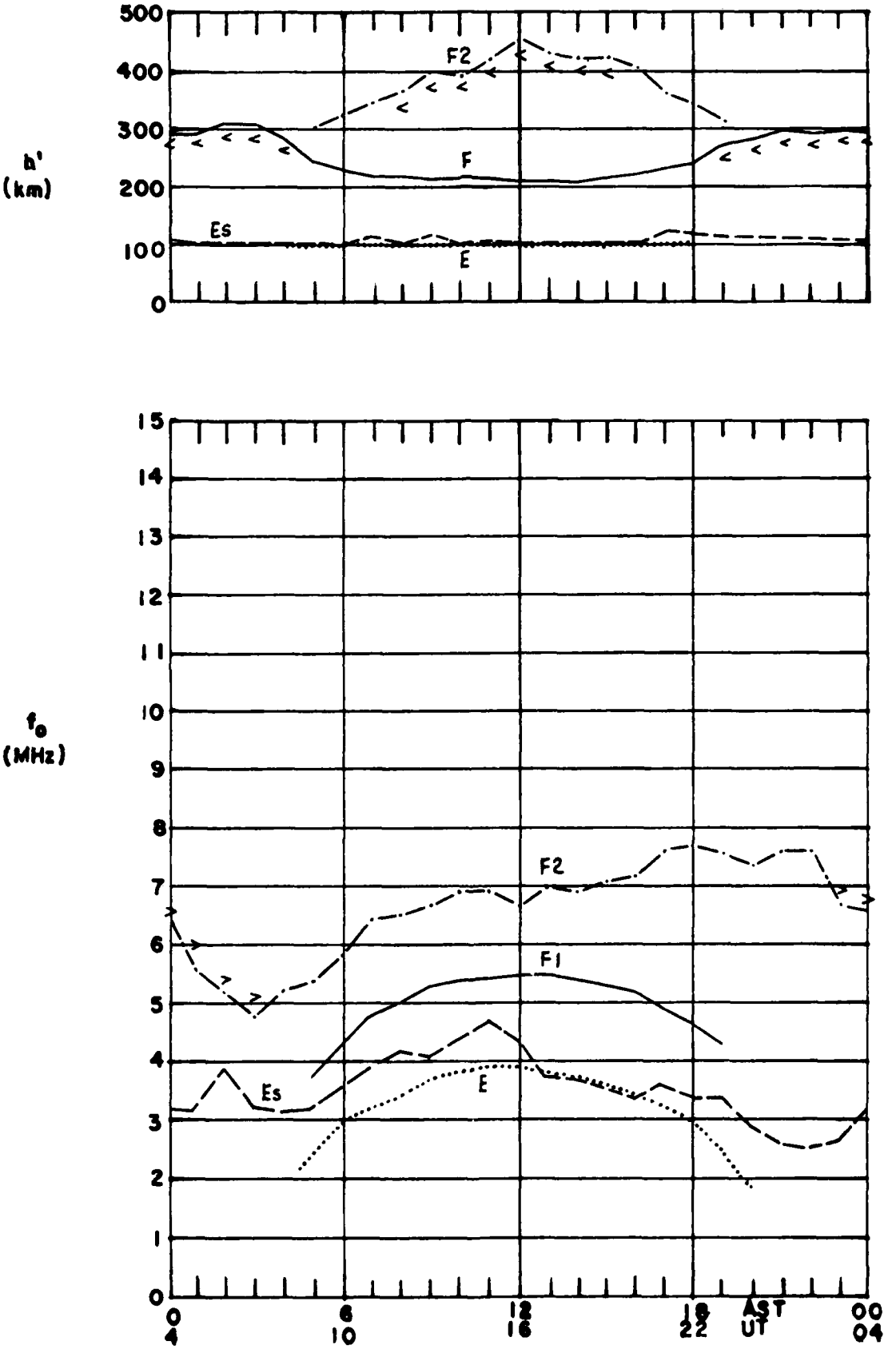

JULY 1980

GOOSE BAY, LABRADOR

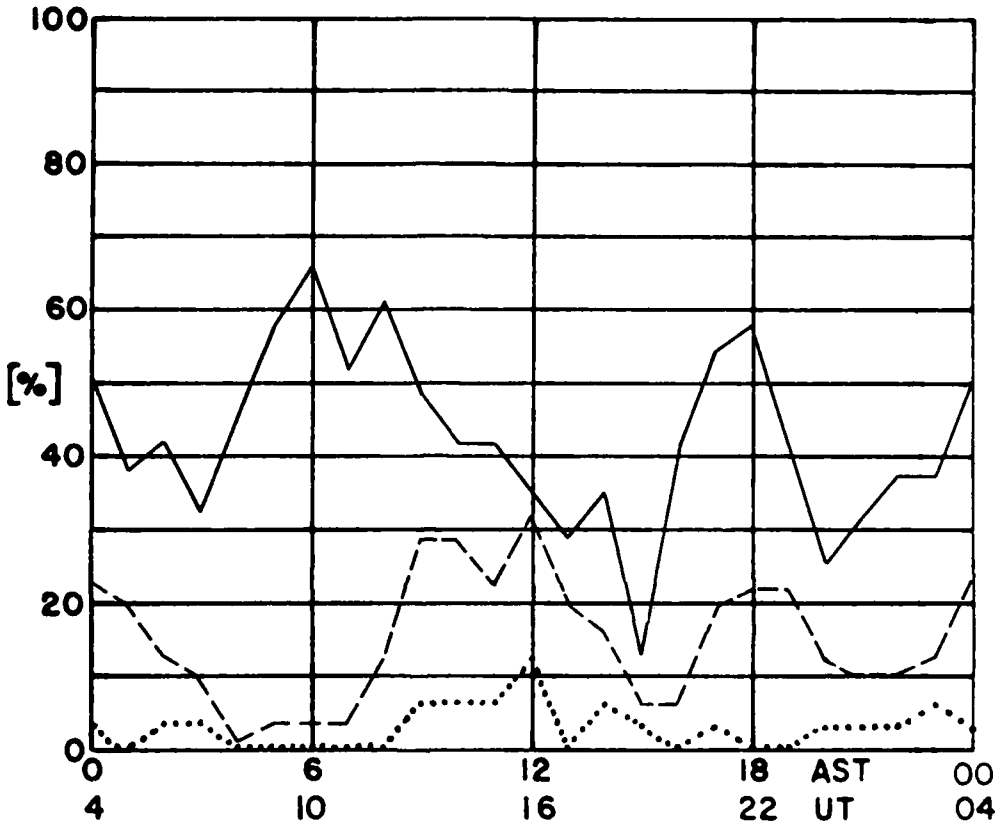

LIMITING FREQUENCY = 3MHz ————————

LIMITING FREQUENCY = 5MHz — — — — — —

LIMITING FREQUENCY = 7MHz .....

PERCENTAGE OF TOTAL TIME DURING WHICH
$f_0 E_s$ IS GREATER THAN THE LIMITING FREQUENCY

MEDIAN VALUES of h' AND f_0 AT GOOSE BAY, LABRADOR FOR

JULY 1980

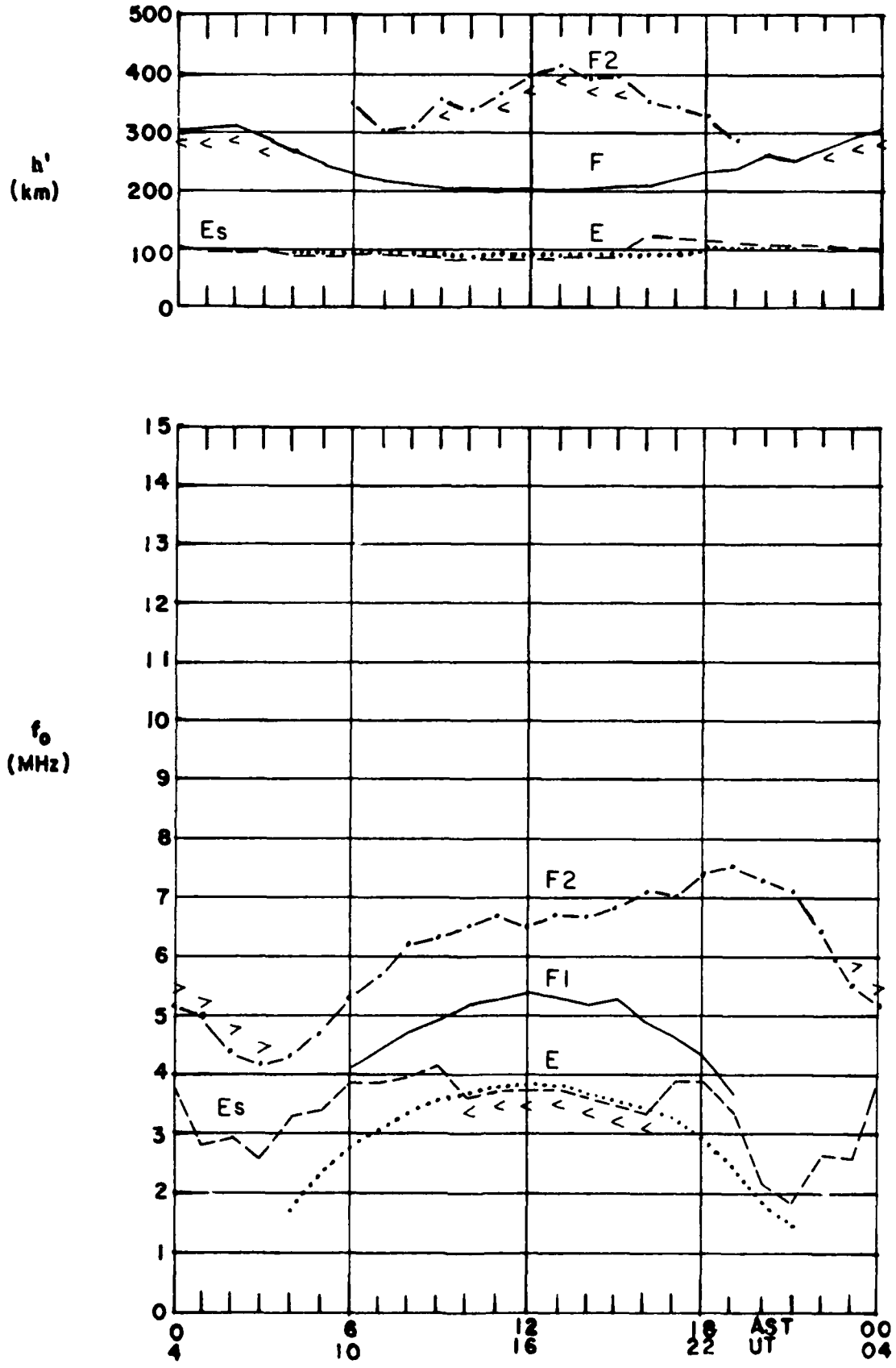

AUGUST 1980

GOOSE BAY, LABRADOR

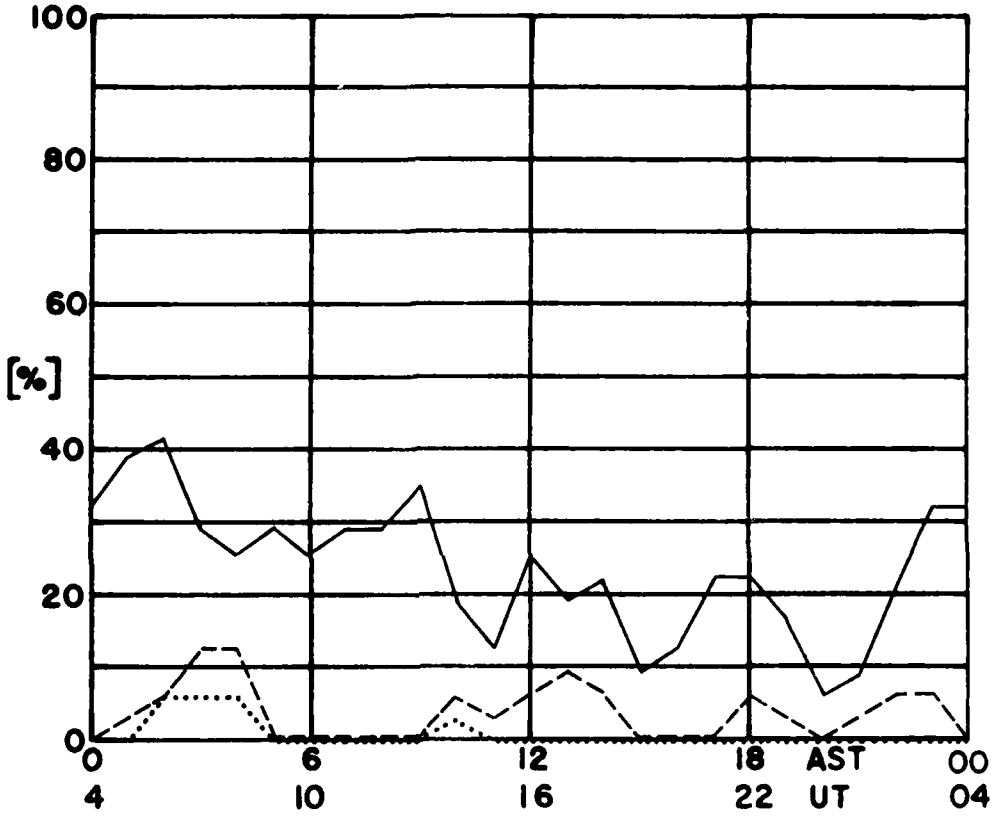

LIMITING FREQUENCY = 3MHz ————————

LIMITING FREQUENCY = 5MHz — — — — — —

LIMITING FREQUENCY = 7MHz .....

PERCENTAGE OF TOTAL TIME DURING WHICH
$f_0 E_s$ IS GREATER THAN THE LIMITING FREQUENCY

MEDIAN VALUES of h' AND f_0 AT GOOSE BAY, LABRADOR FOR

AUGUST 1980

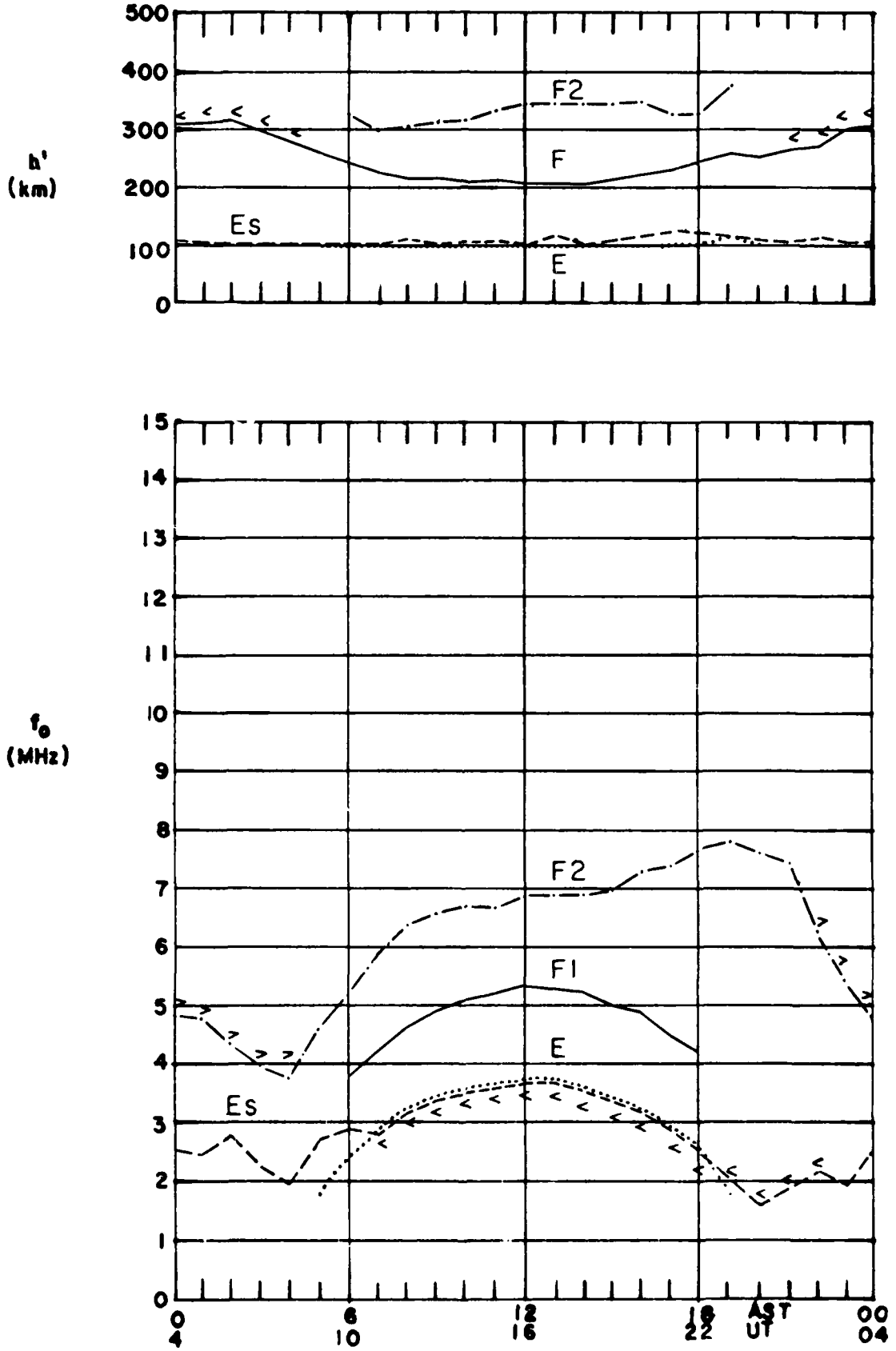

SEPTEMBER 1980

GOOSE BAY, LABRADOR

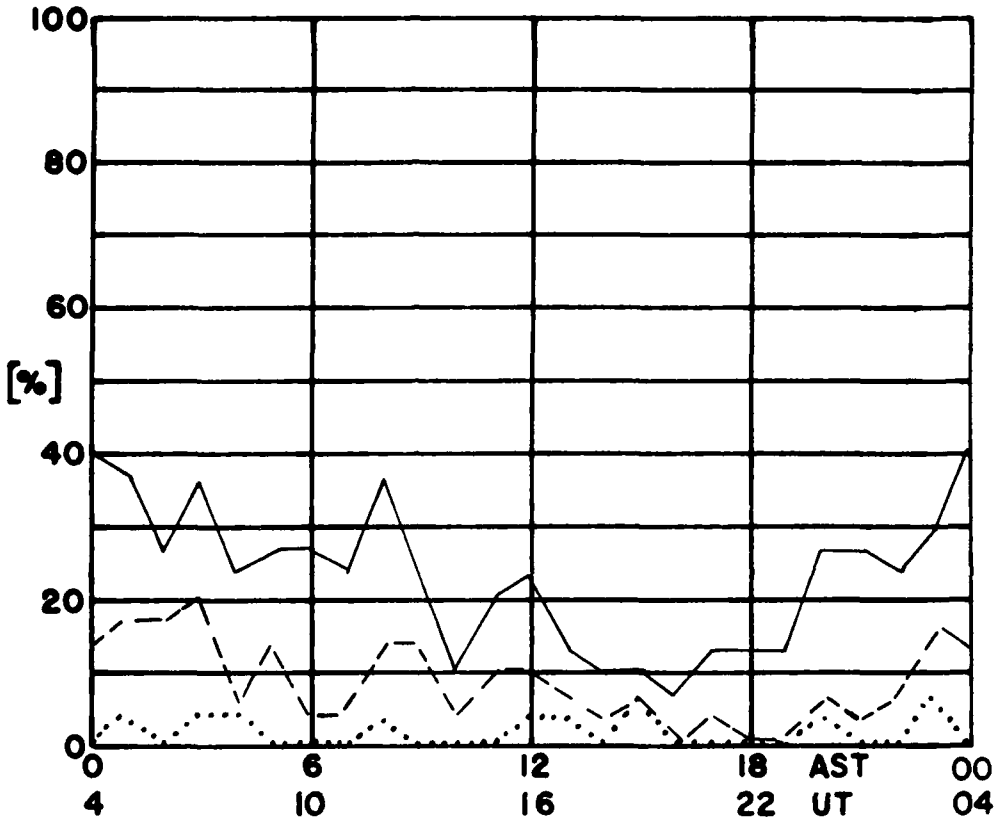

LIMITING FREQUENCY = 3MHz ————————

LIMITING FREQUENCY = 5MHz — — — — — —

LIMITING FREQUENCY = 7MHz .....

PERCENTAGE OF TOTAL TIME DURING WHICH
$f_0 E_s$ IS GREATER THAN THE LIMITING FREQUENCY

MEDIAN VALUES of h' AND f_0 AT GOOSE BAY, LABRADOR FOR

SEPTEMBER 1980

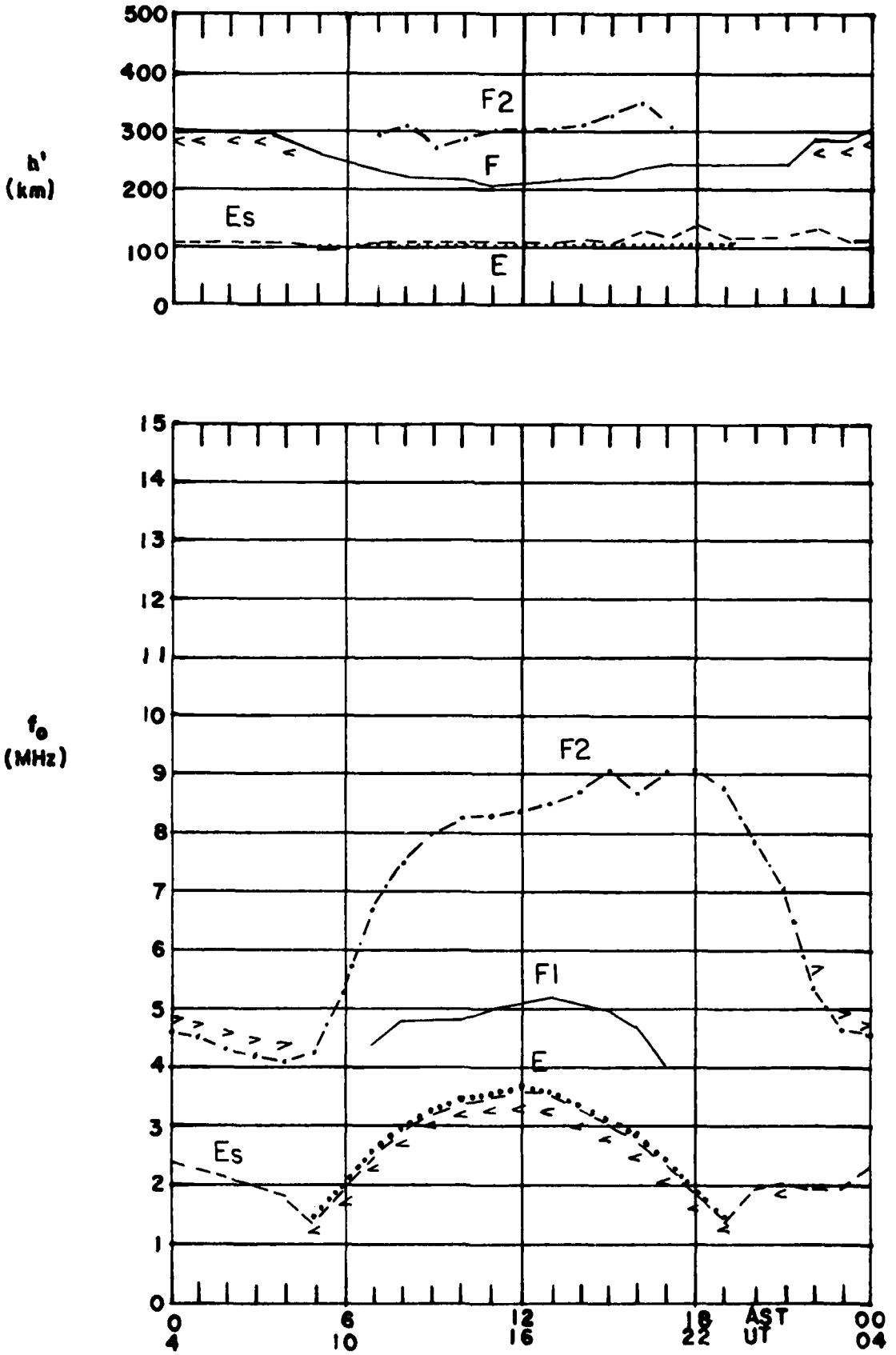

OCTOBER 1980

GOOSE BAY, LABRADOR

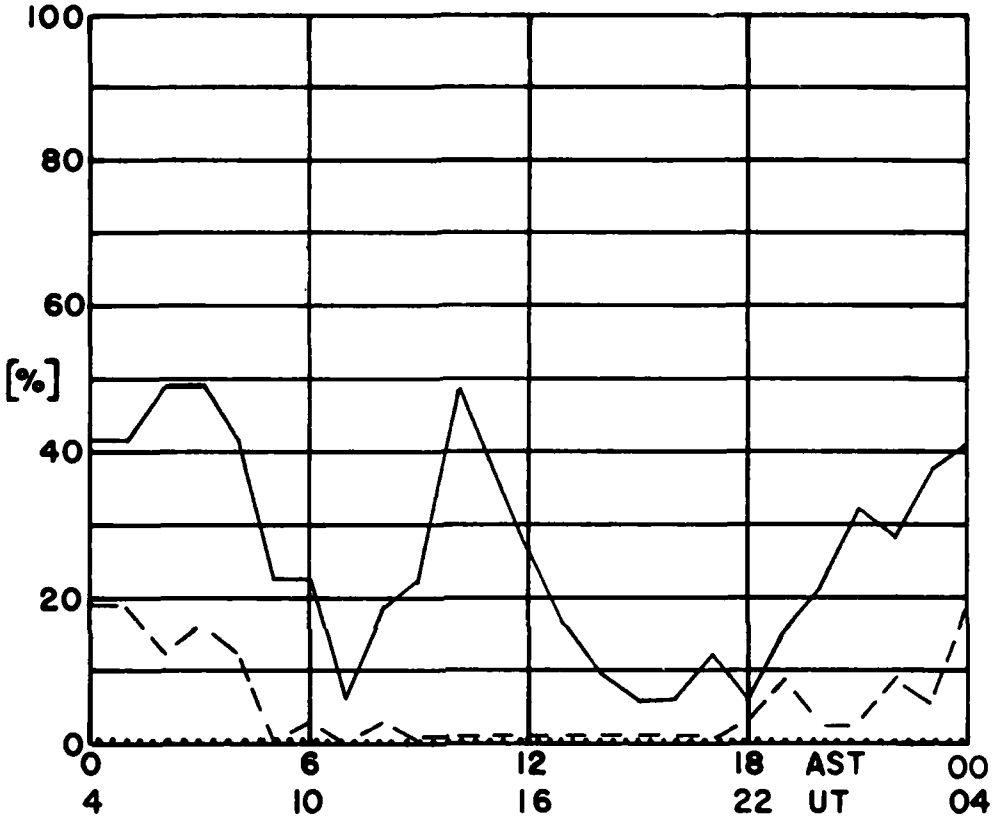

LIMITING FREQUENCY = 3MHz ——————

LIMITING FREQUENCY = 5MHz — — — — —

LIMITING FREQUENCY = 7MHz .....

PERCENTAGE OF TOTAL TIME DURING WHICH
$f_0 E_s$ IS GREATER THAN THE LIMITING FREQUENCY

MEDIAN VALUES of h' AND f_0 AT GOOSE BAY, LABRADOR FOR

OCTOBER 1980

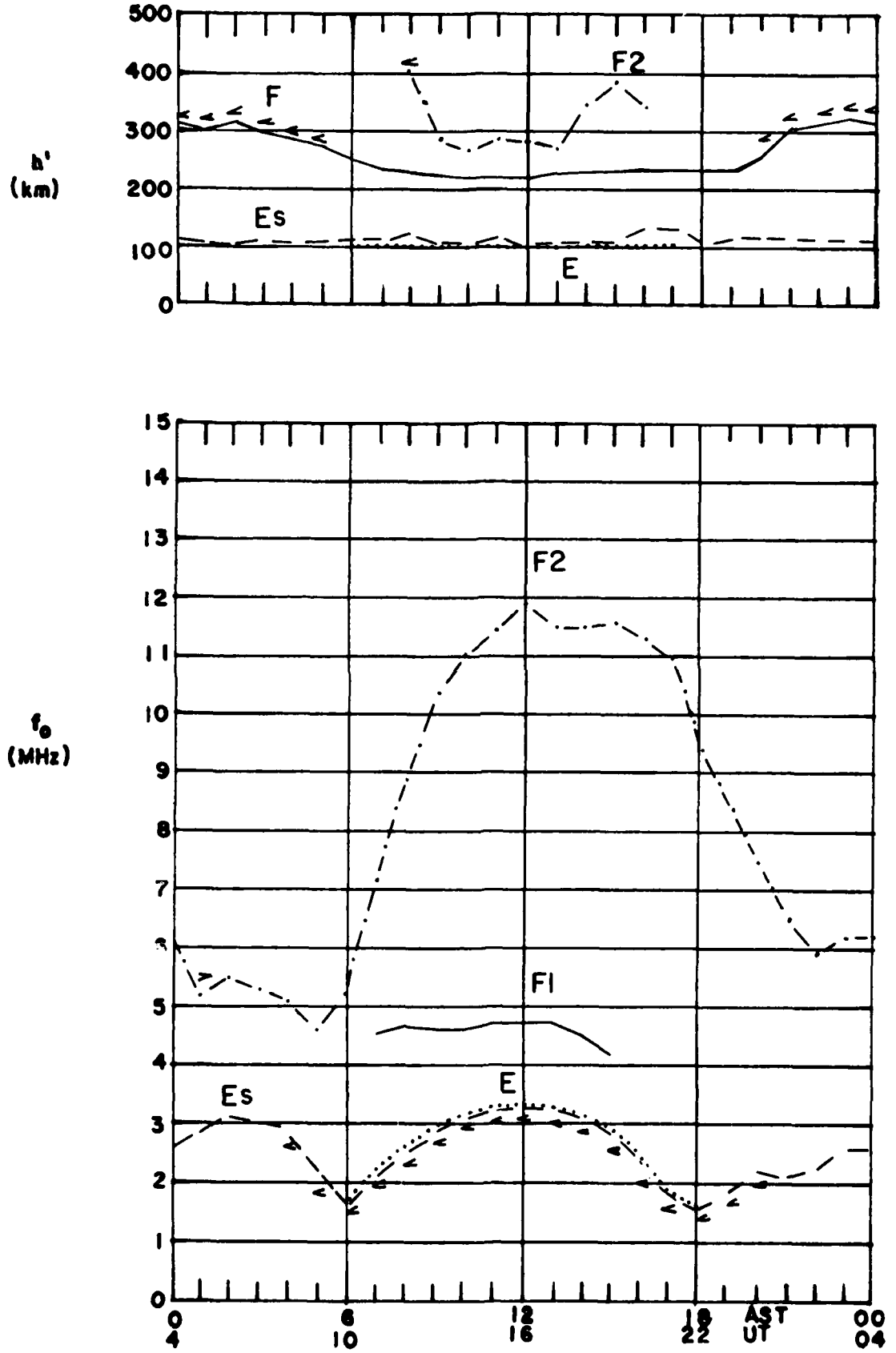

NOVEMBER 1980

GOOSE BAY, LABRADOR

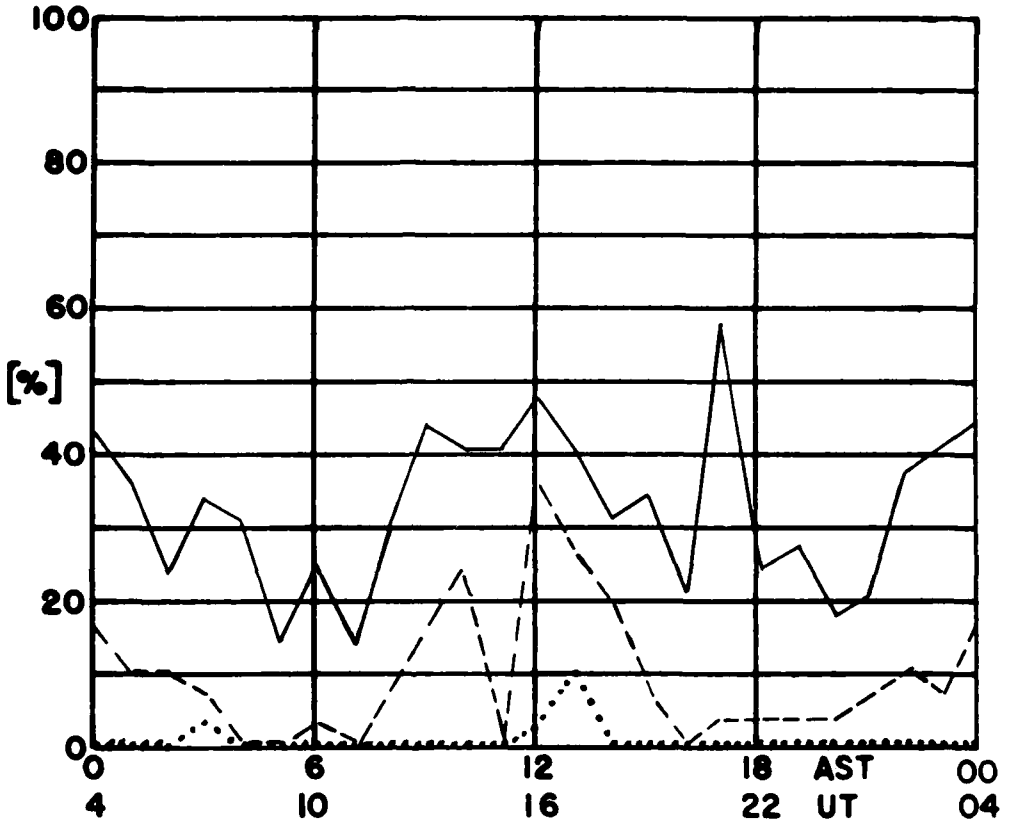

LIMITING FREQUENCY = 3MHz ————————

LIMITING FREQUENCY = 5MHz — — — · — — —

LIMITING FREQUENCY = 7MHz .....

PERCENTAGE OF TOTAL TIME DURING WHICH
$f_0 E_s$ IS GREATER THAN THE LIMITING FREQUENCY

MEDIAN VALUES of h' AND f_0 AT GOOSE BAY, LABRADOR FOR NOVEMBER 1980

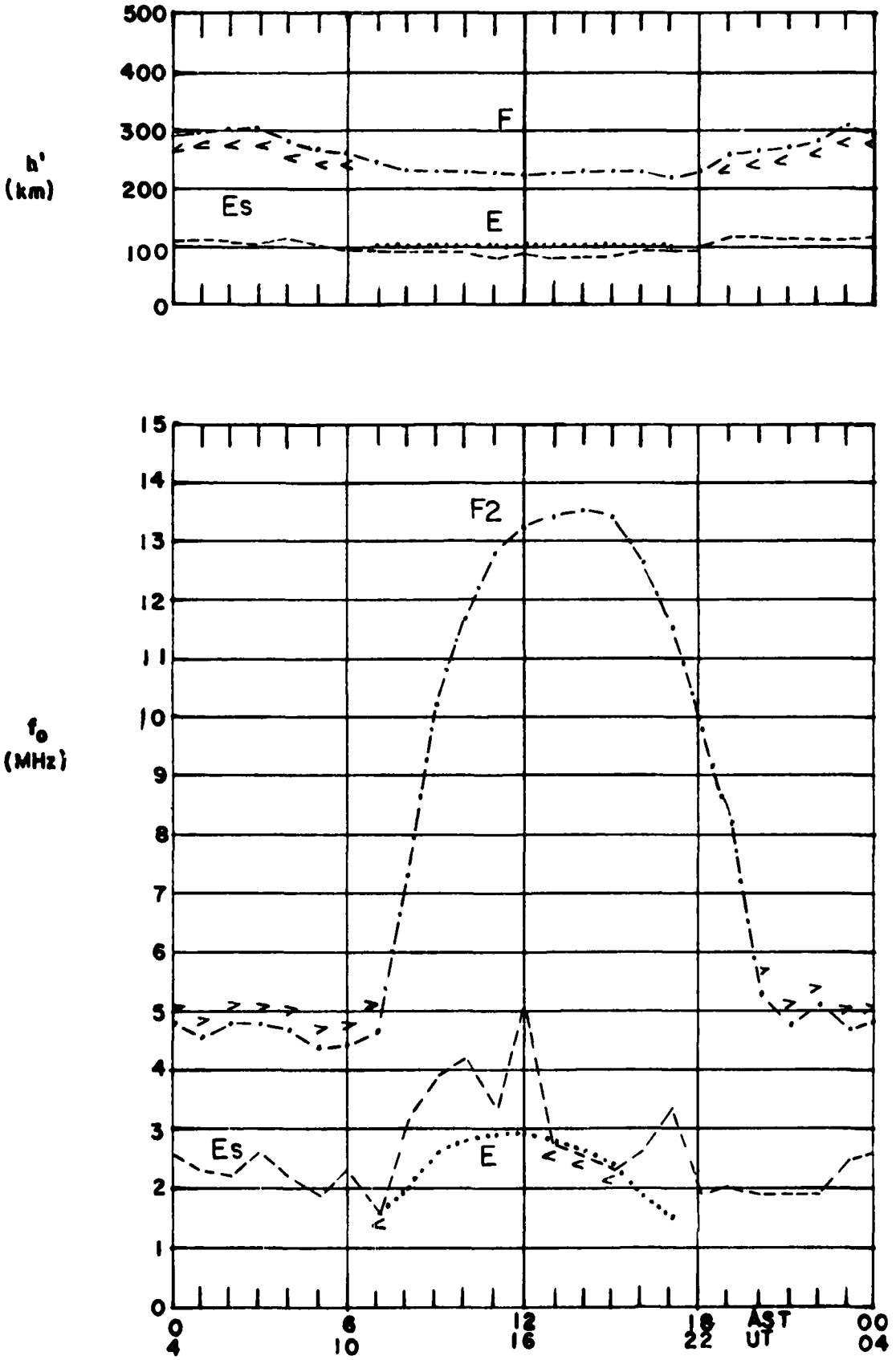

DECEMBER 1980

GOOSE BAY, LABRADOR

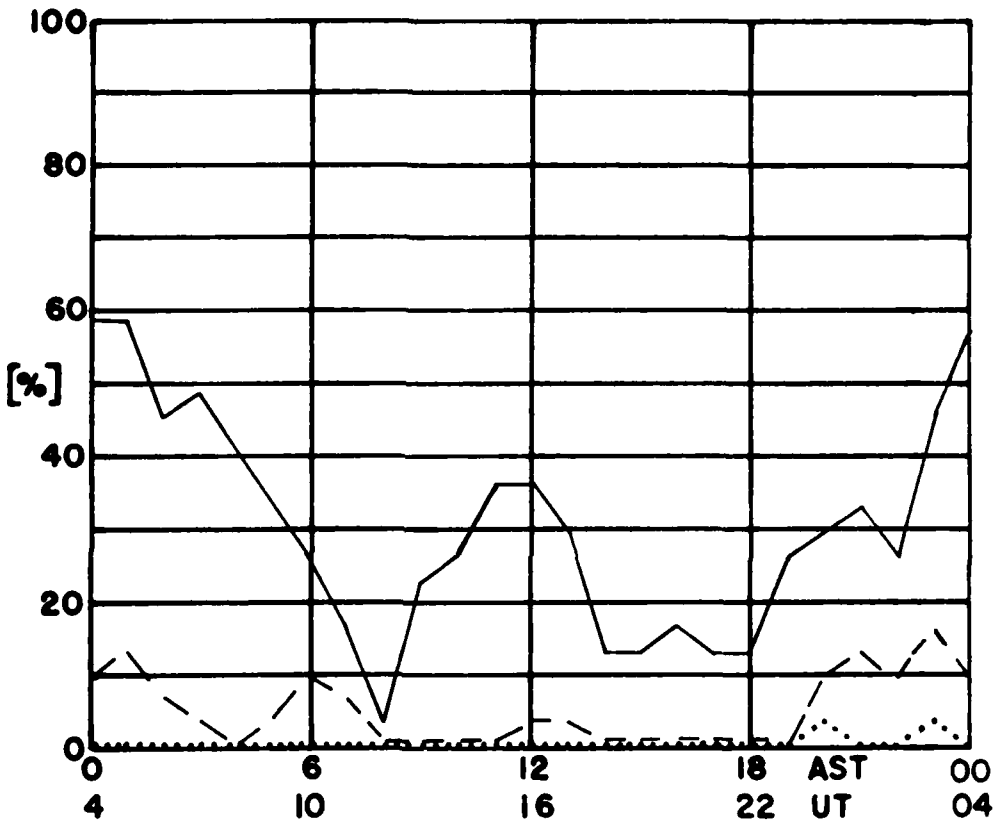

LIMITING FREQUENCY = 3MHz ————————

LIMITING FREQUENCY = 5MHz – – – – – –

LIMITING FREQUENCY = 7MHz .....

PERCENTAGE OF TOTAL TIME DURING WHICH
$f_0 E_s$ IS GREATER THAN THE LIMITING FREQUENCY

MEDIAN VALUES of h' AND f_0 AT GOOSE BAY, LABRADOR FOR

DECEMBER 1980

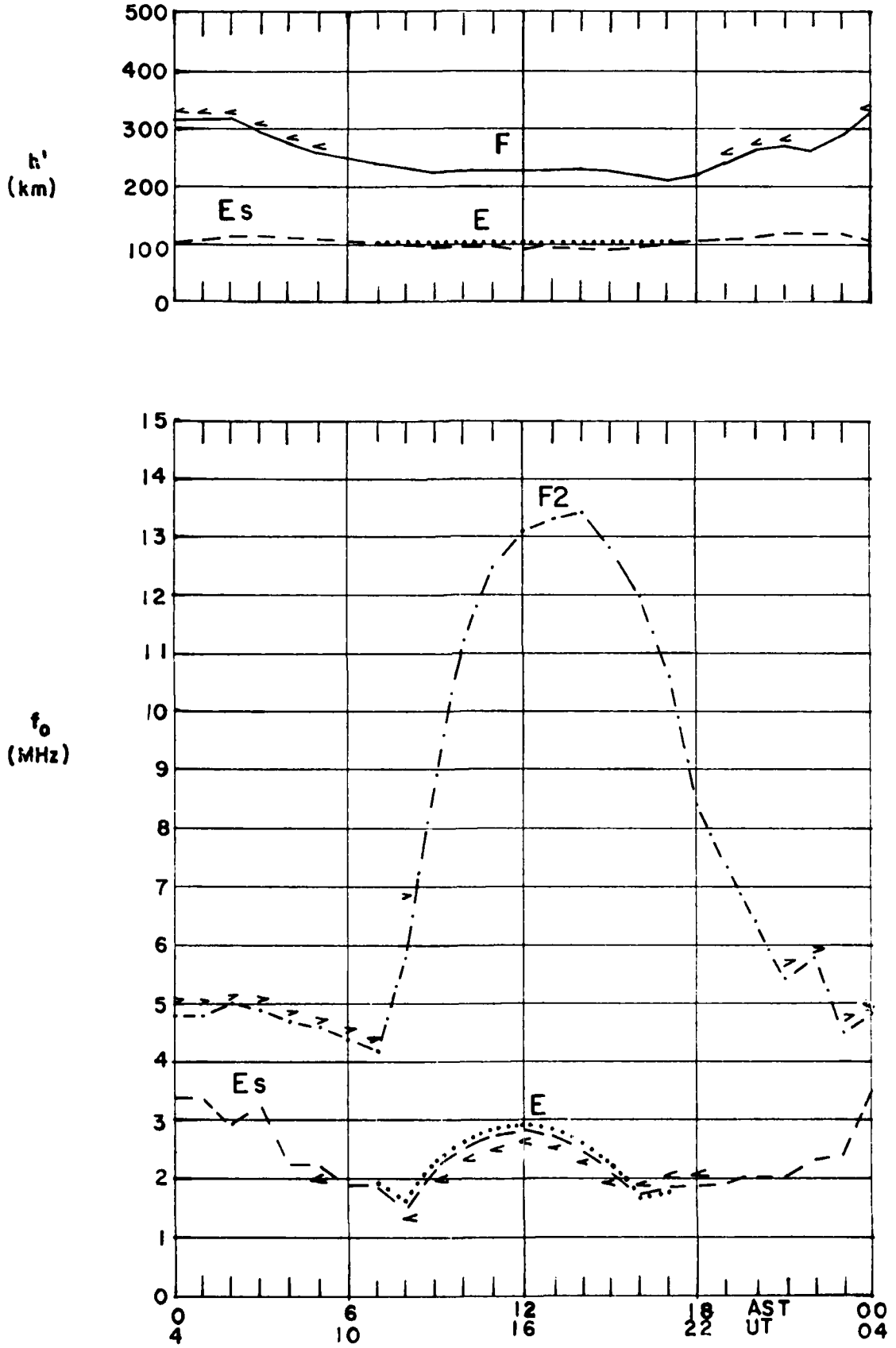

JANUARY 1981

GOOSE BAY, LABRADOR

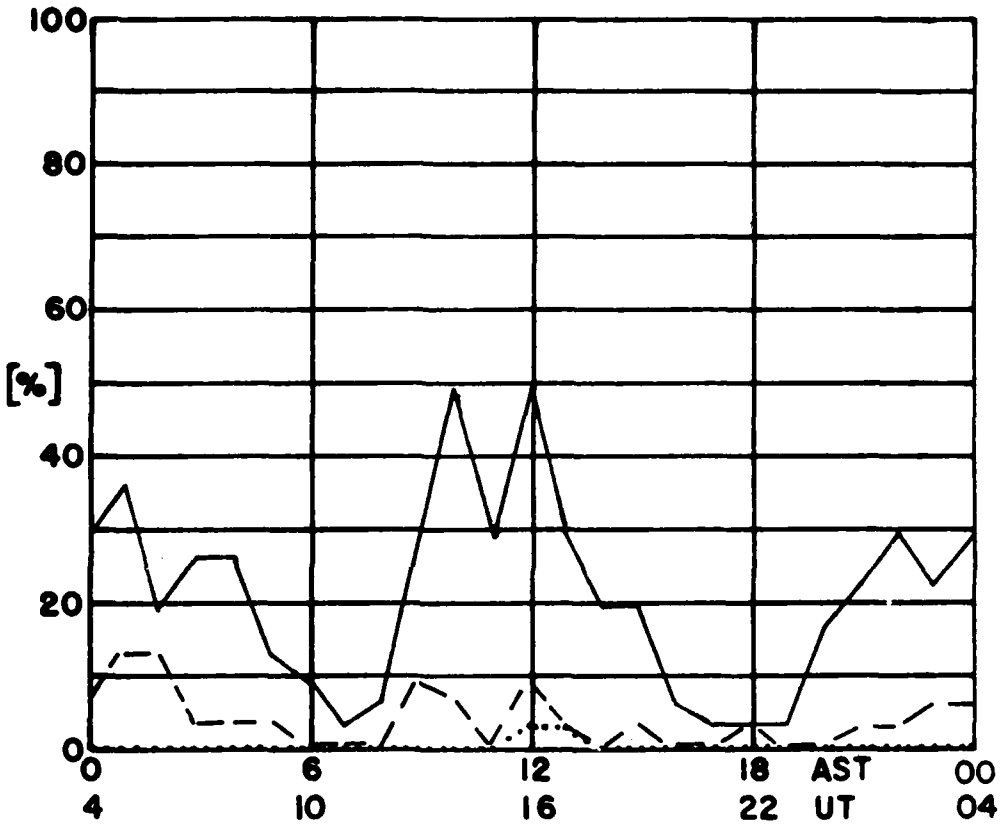

LIMITING FREQUENCY = 3MHz ————————

LIMITING FREQUENCY = 5MHz – – – – – –

LIMITING FREQUENCY = 7MHz .....

PERCENTAGE OF TOTAL TIME DURING WHICH
$f_0 E_s$ IS GREATER THAN THE LIMITING FREQUENCY

MEDIAN VALUES of h' AND fo AT GOOSE BAY, LABRADOR FOR JANUARY 1981

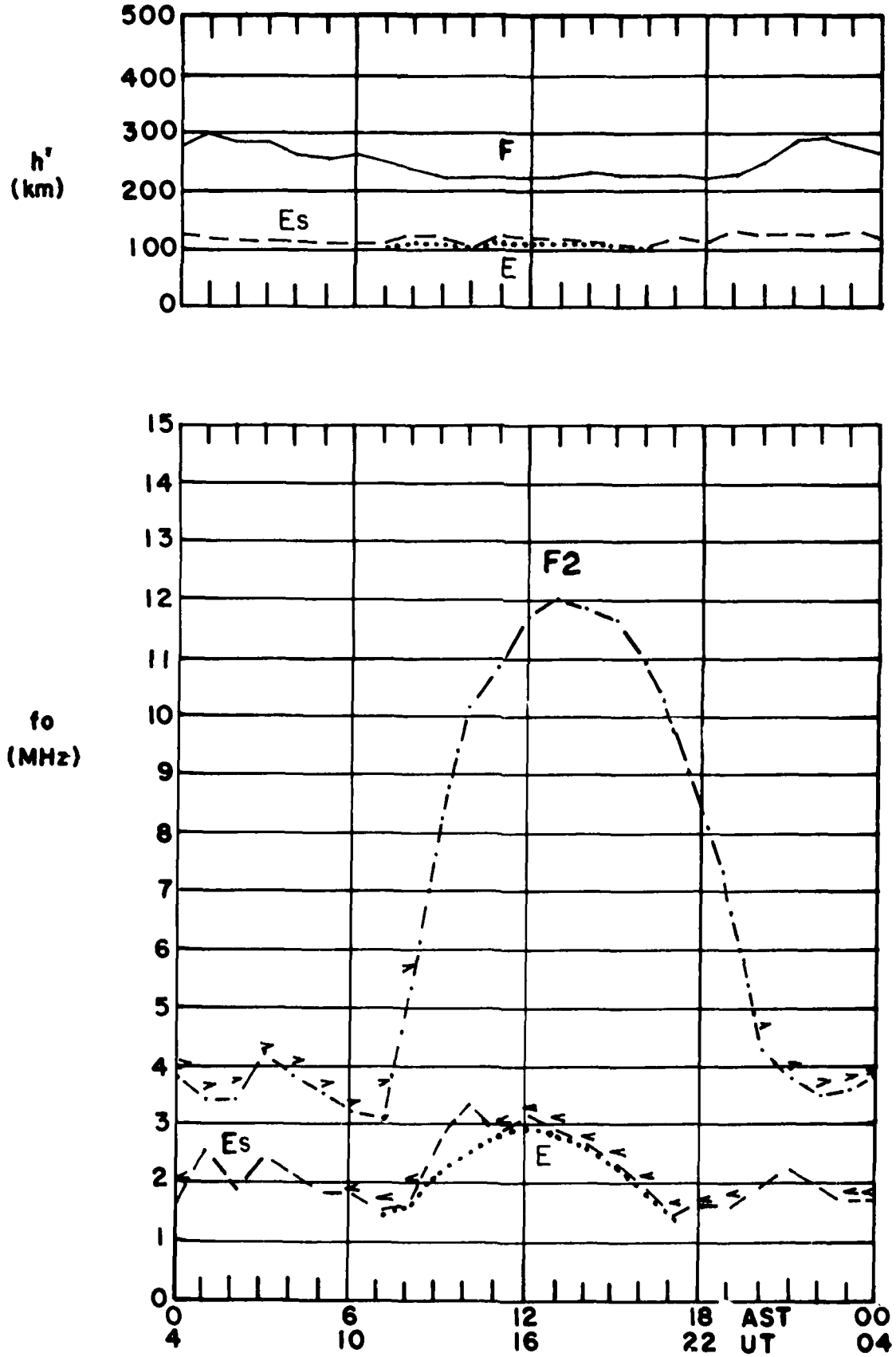

FEBRUARY 1981

GOOSE BAY, LABRADOR

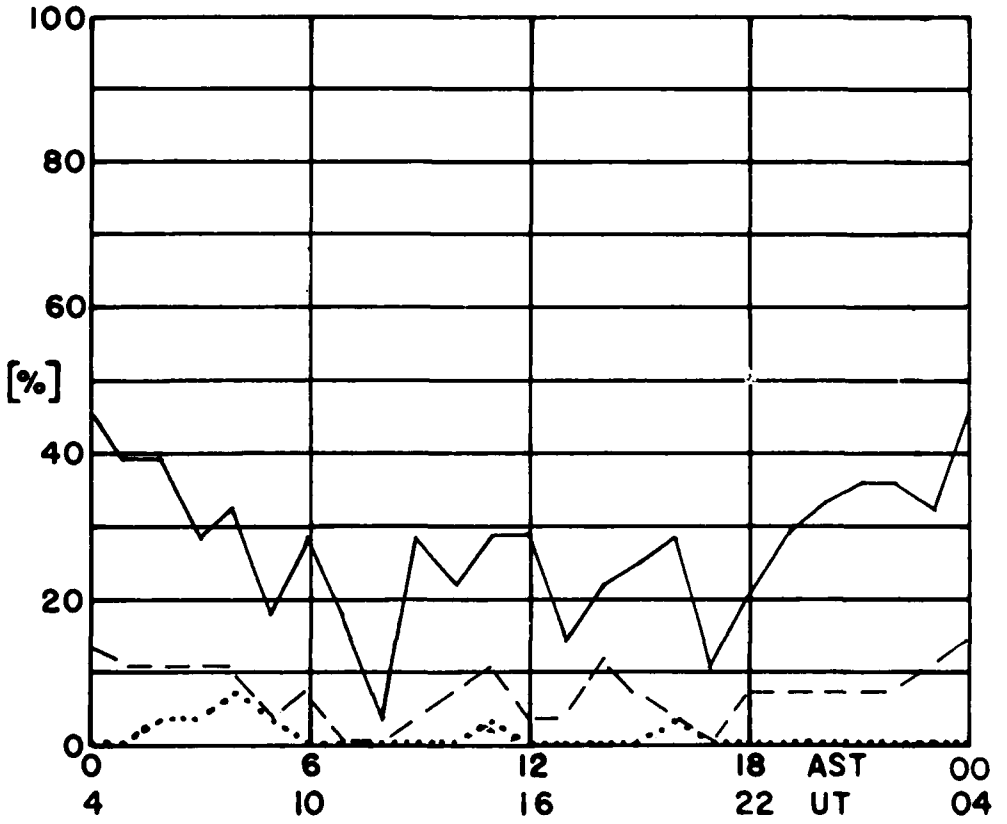

LIMITING FREQUENCY = 3MHz ————————

LIMITING FREQUENCY = 5MHz – – – – – –

LIMITING FREQUENCY = 7MHz .....

PERCENTAGE OF TOTAL TIME DURING WHICH
$f_0 E_s$ IS GREATER THAN THE LIMITING FREQUENCY

MEDIAN VALUES of h' AND f_0 AT GOOSE BAY, LABRADOR FOR FEBRUARY 1981

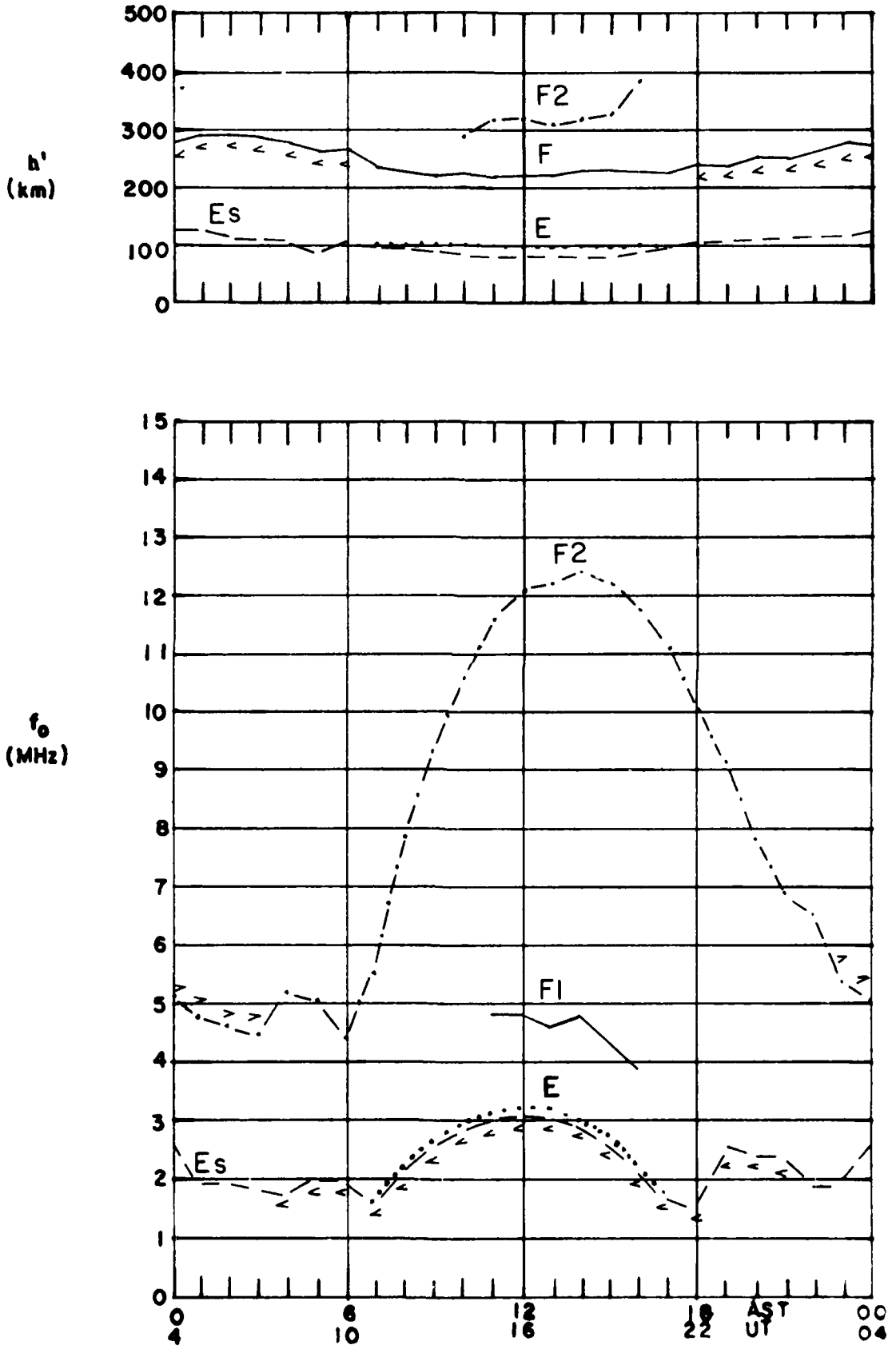

AD-A140 012 IONOSPHERIC RESEARCH USING DIGITAL IONOSONDES(U) LOWELL 3/3
UNIV MA CENTER FOR ATMOSPHERIC RESEARCH
B W REINISCH ET AL. JUL 83 ULRF-425/CAR AFGL-TR-83-0184
UNCLASSIFIED F19628-80-C-0064 F/G 4/1 NL

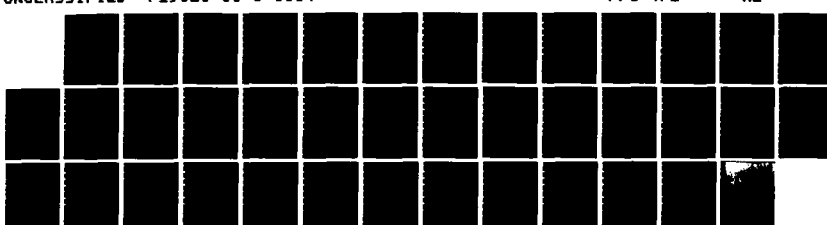

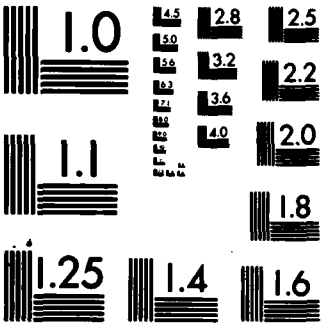

MARCH 1981

GOOSE BAY, LABRADOR

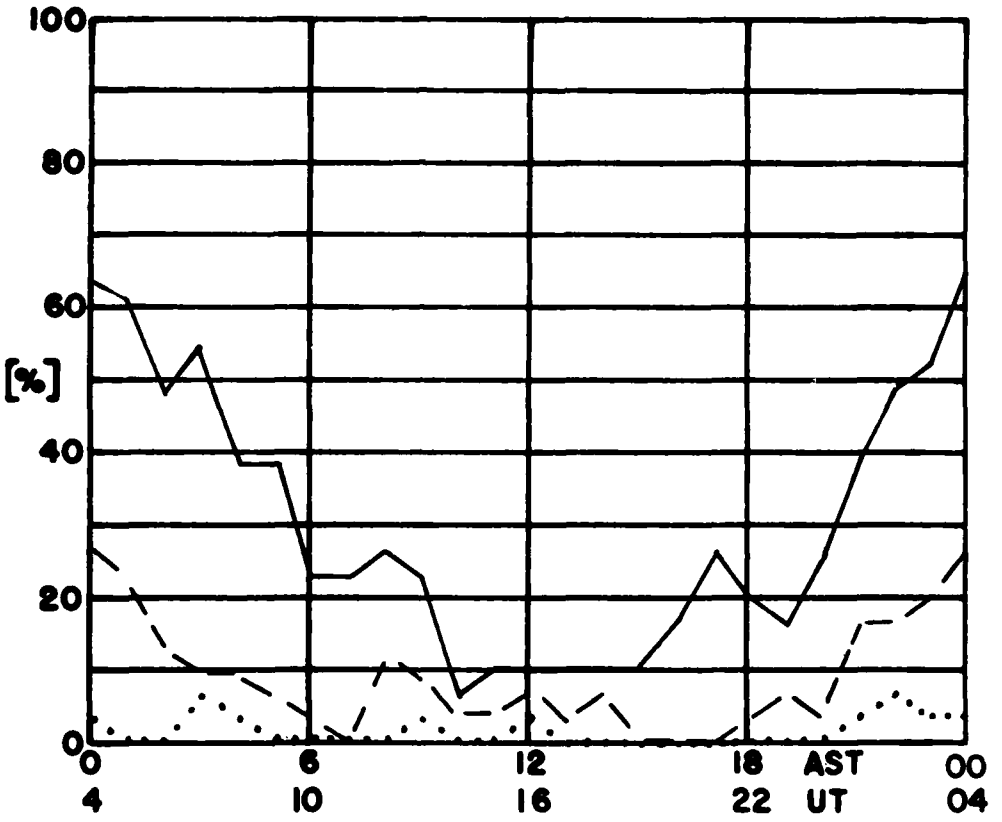

LIMITING FREQUENCY = 3MHz ————————

LIMITING FREQUENCY = 5MHz — — — — —

LIMITING FREQUENCY = 7MHz .....

PERCENTAGE OF TOTAL TIME DURING WHICH
$f_0 E_s$ IS GREATER THAN THE LIMITING FREQUENCY

MEDIAN VALUES of h' AND fo AT GOOSE BAY, LABRADOR FOR MARCH 1981

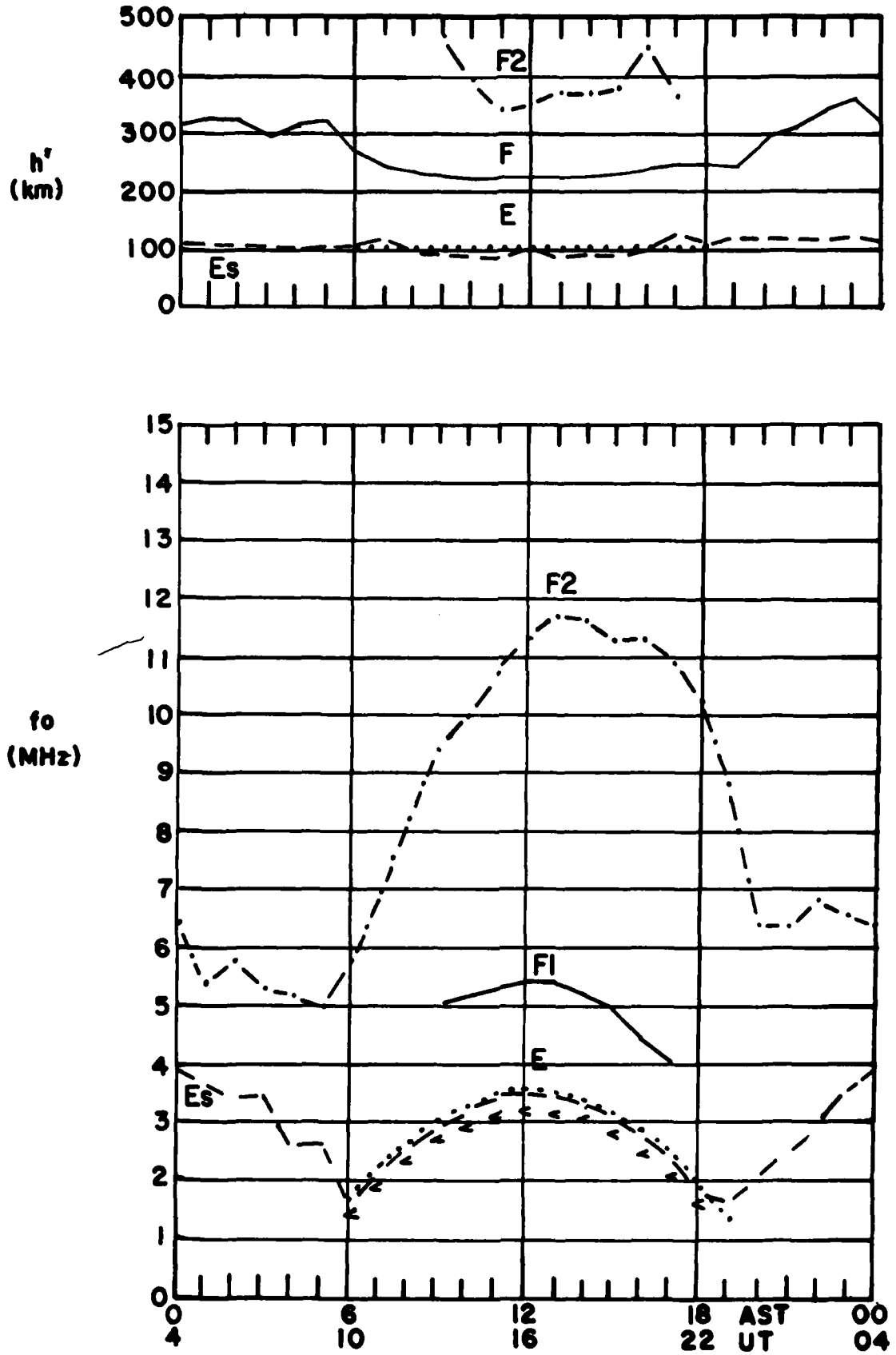

APRIL 1981

GOOSE BAY, LABRADOR

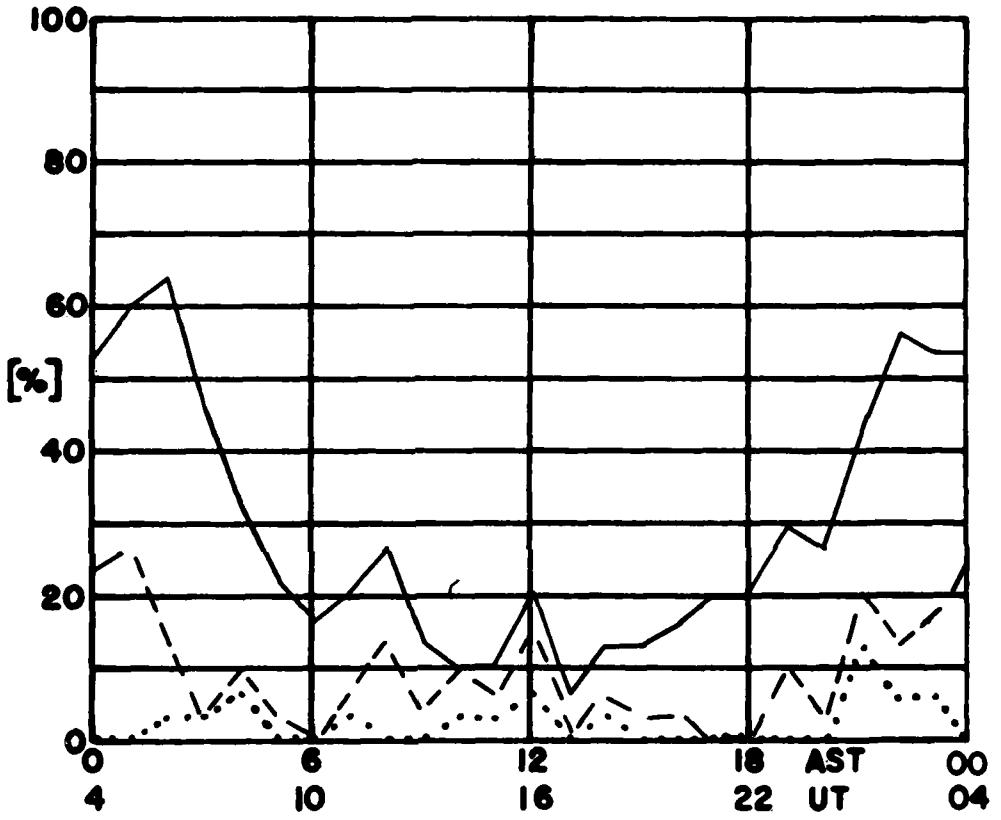

LIMITING FREQUENCY = 3MHz ————————

LIMITING FREQUENCY = 5MHz — — — — —

LIMITING FREQUENCY = 7MHz .....

PERCENTAGE OF TOTAL TIME DURING WHICH
$f_0 E_s$ IS GREATER THAN THE LIMITING FREQUENCY

MEDIAN VALUES of h' AND fo AT GOOSE BAY, LABRADOR FOR APRIL 1981

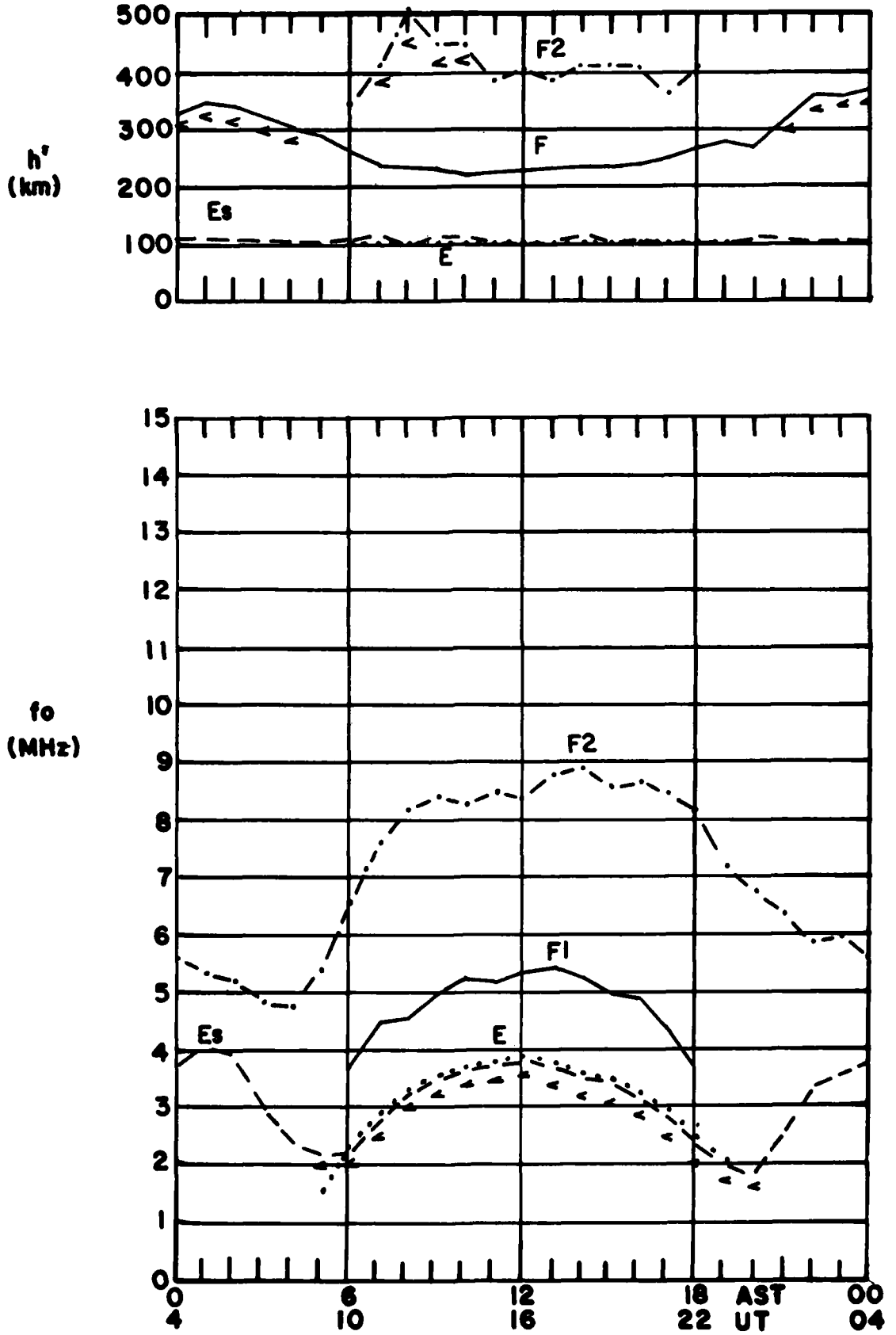

MAY 1981
GOOSE BAY, LABRADOR

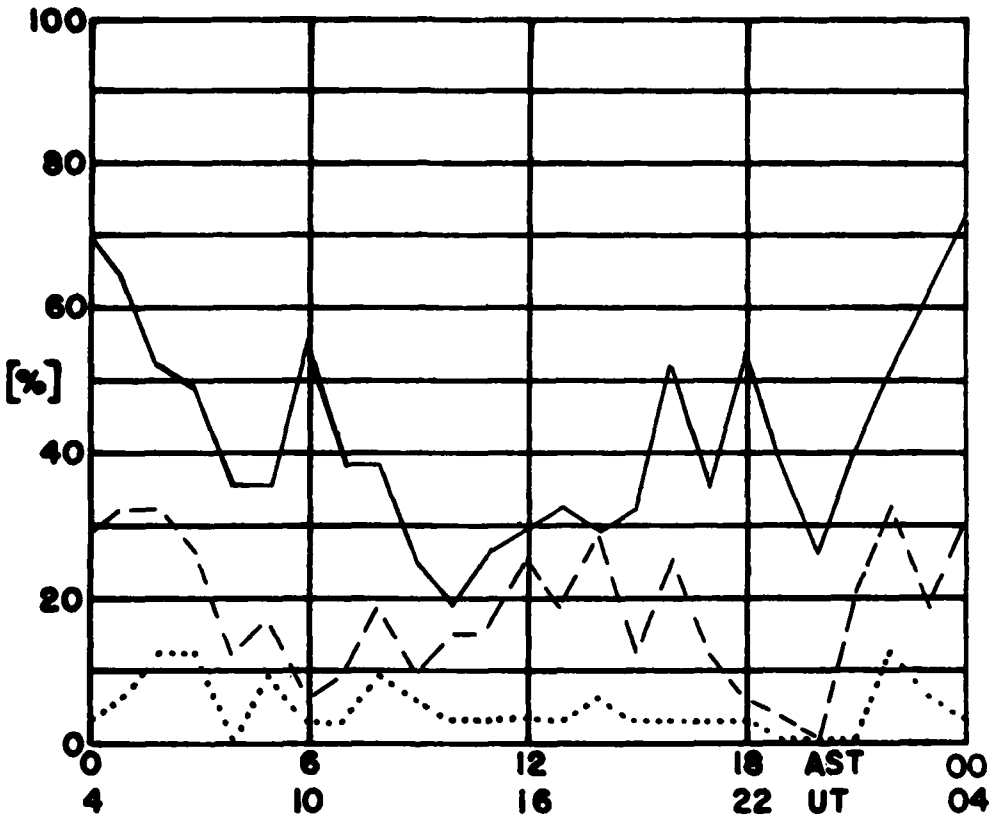

LIMITING FREQUENCY = 3MHz ————————
LIMITING FREQUENCY = 5MHz — — — — — —
LIMITING FREQUENCY = 7MHz .....

PERCENTAGE OF TOTAL TIME DURING WHICH
$f_o E_s$ IS GREATER THAN THE LIMITING FREQUENCY

MEDIAN VALUES of h' AND f_0 AT GOOSE BAY, LABRADOR FOR MAY 1981

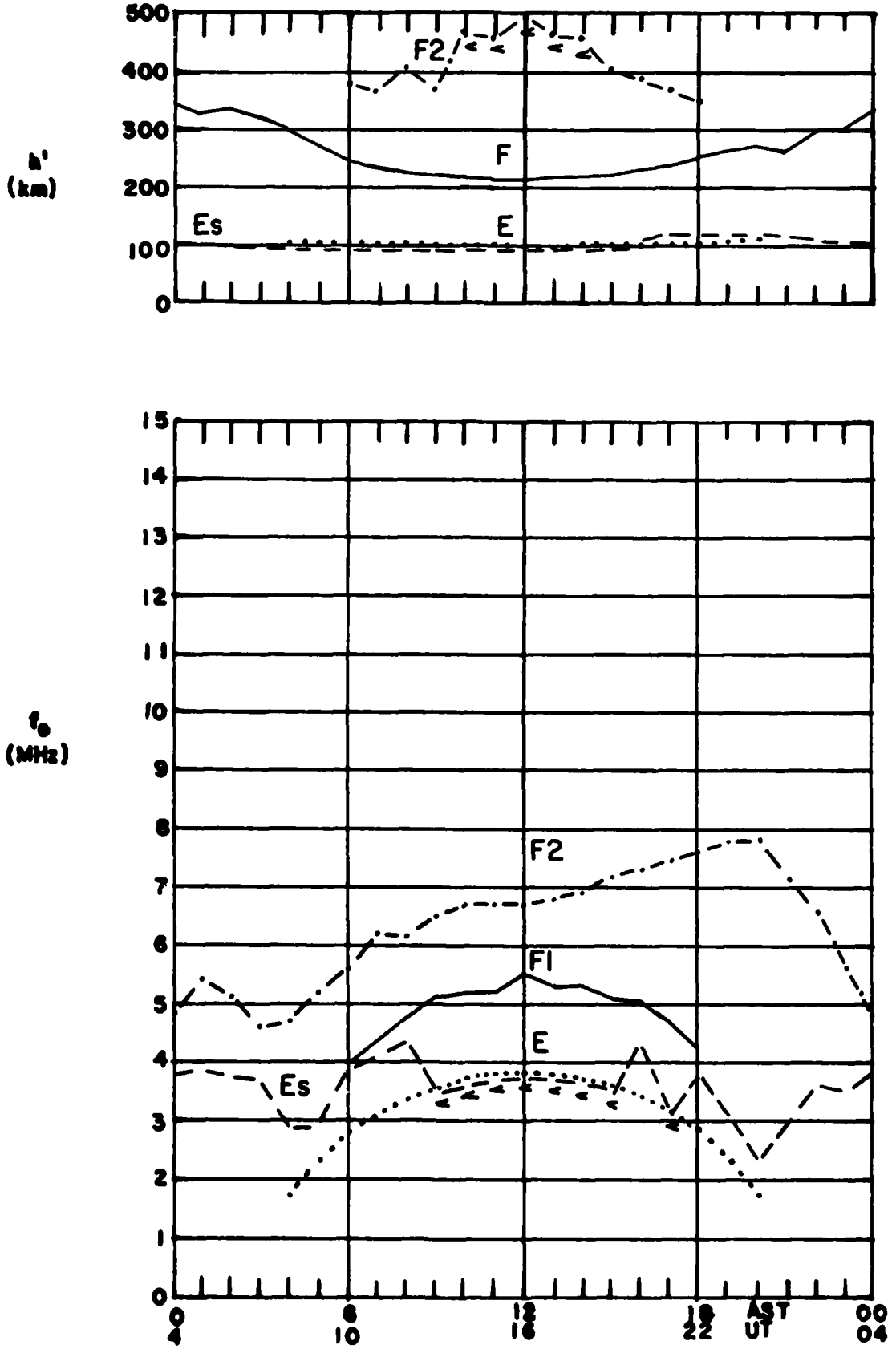

JUNE 1981

GOOSE BAY, LABRADOR

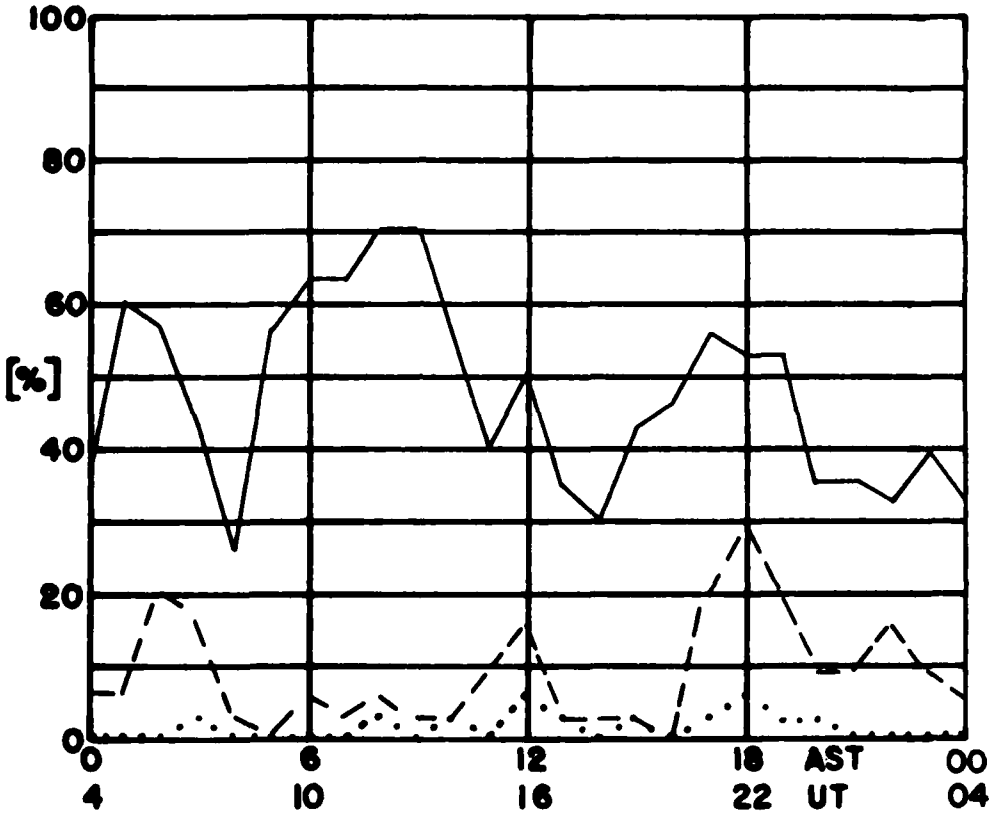

LIMITING FREQUENCY = 3MHz ————————

LIMITING FREQUENCY = 5MHz — — — — —

LIMITING FREQUENCY = 7MHz .....

PERCENTAGE OF TOTAL TIME DURING WHICH
f_0E_s IS GREATER THAN THE LIMITING FREQUENCY

MEDIAN VALUES of h' AND fo AT GOOSE BAY, LABRADOR FOR JUNE 1981

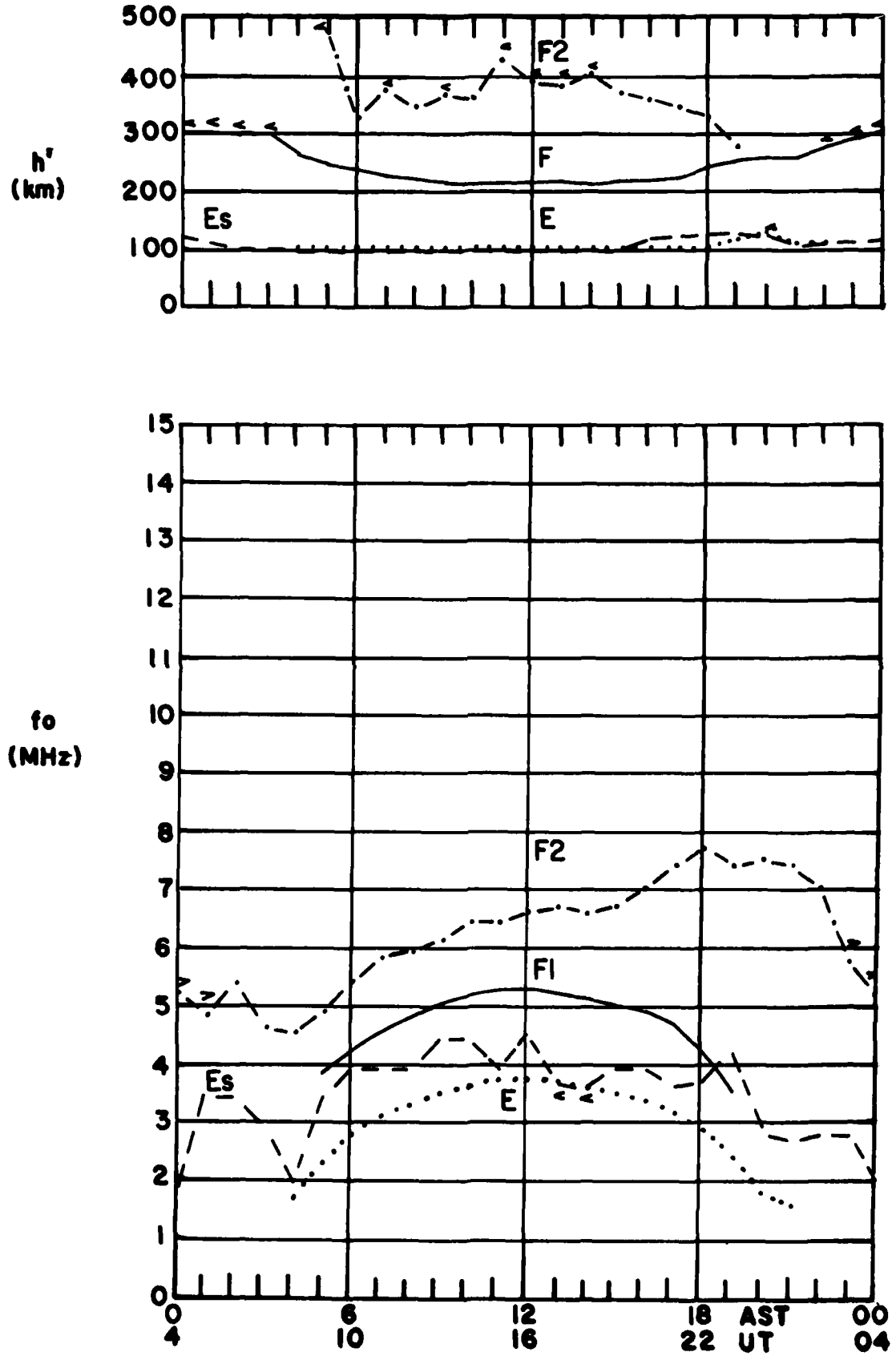

JULY 1981

GOOSE BAY, LABRADOR

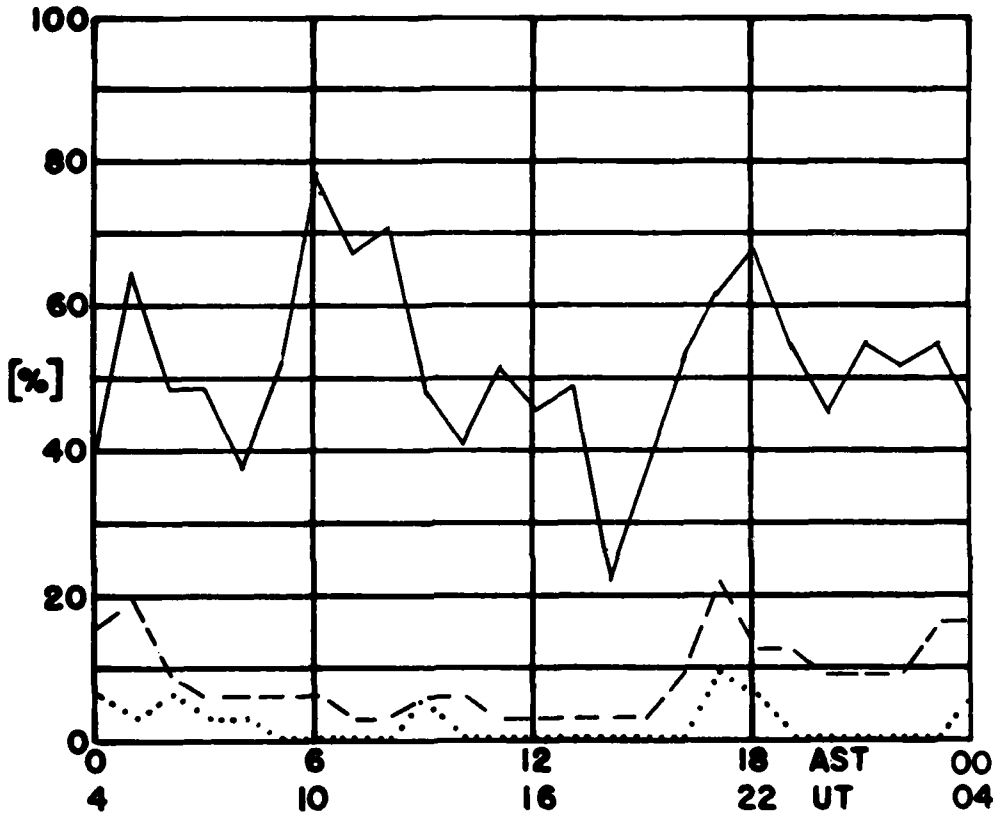

LIMITING FREQUENCY = 3MHz ——————

LIMITING FREQUENCY = 5MHz — — — — —

LIMITING FREQUENCY = 7MHz .....

PERCENTAGE OF TOTAL TIME DURING WHICH
f_0E_s IS GREATER THAN THE LIMITING FREQUENCY

MEDIAN VALUES of h' AND f_0 AT GOOSE BAY, LABRADOR FOR

JULY 1981

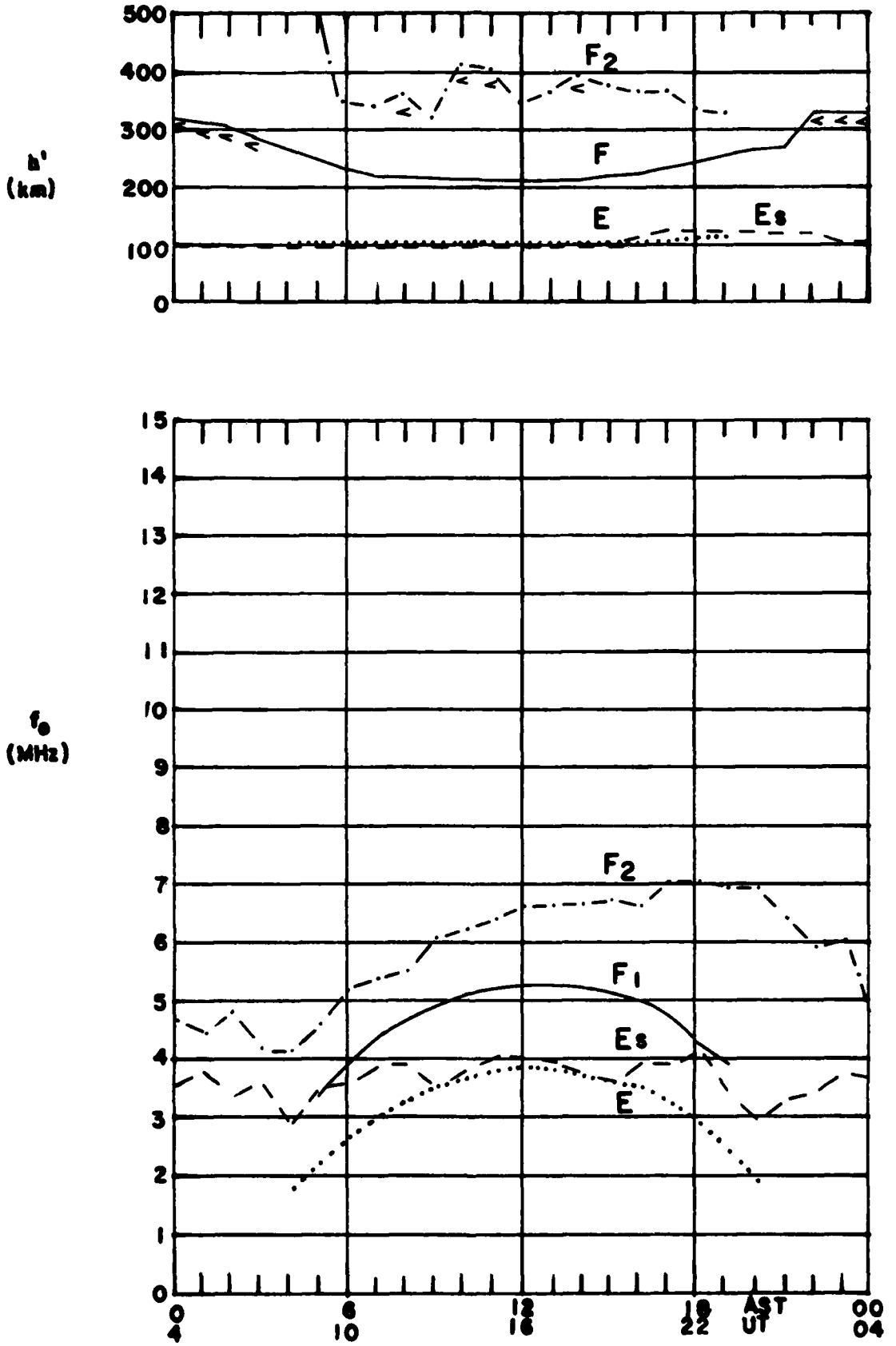

AUGUST 1981

GOOSE BAY, LABRADOR

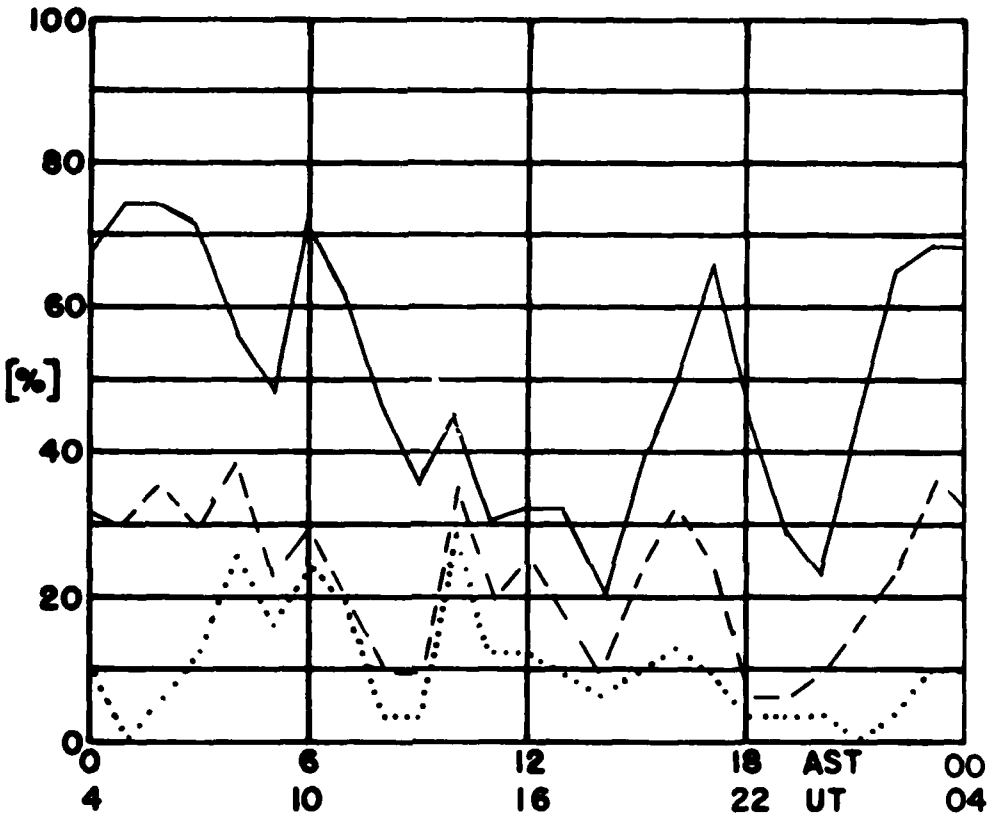

LIMITING FREQUENCY = 3MHz ————————

LIMITING FREQUENCY = 5MHz - - - - - - -

LIMITING FREQUENCY = 7MHz .....

PERCENTAGE OF TOTAL TIME DURING WHICH
$f_0 E_s$ IS GREATER THAN THE LIMITING FREQUENCY

MEDIAN VALUES of h' AND fo AT GOOSE BAY, LABRADOR FOR AUGUST 1981

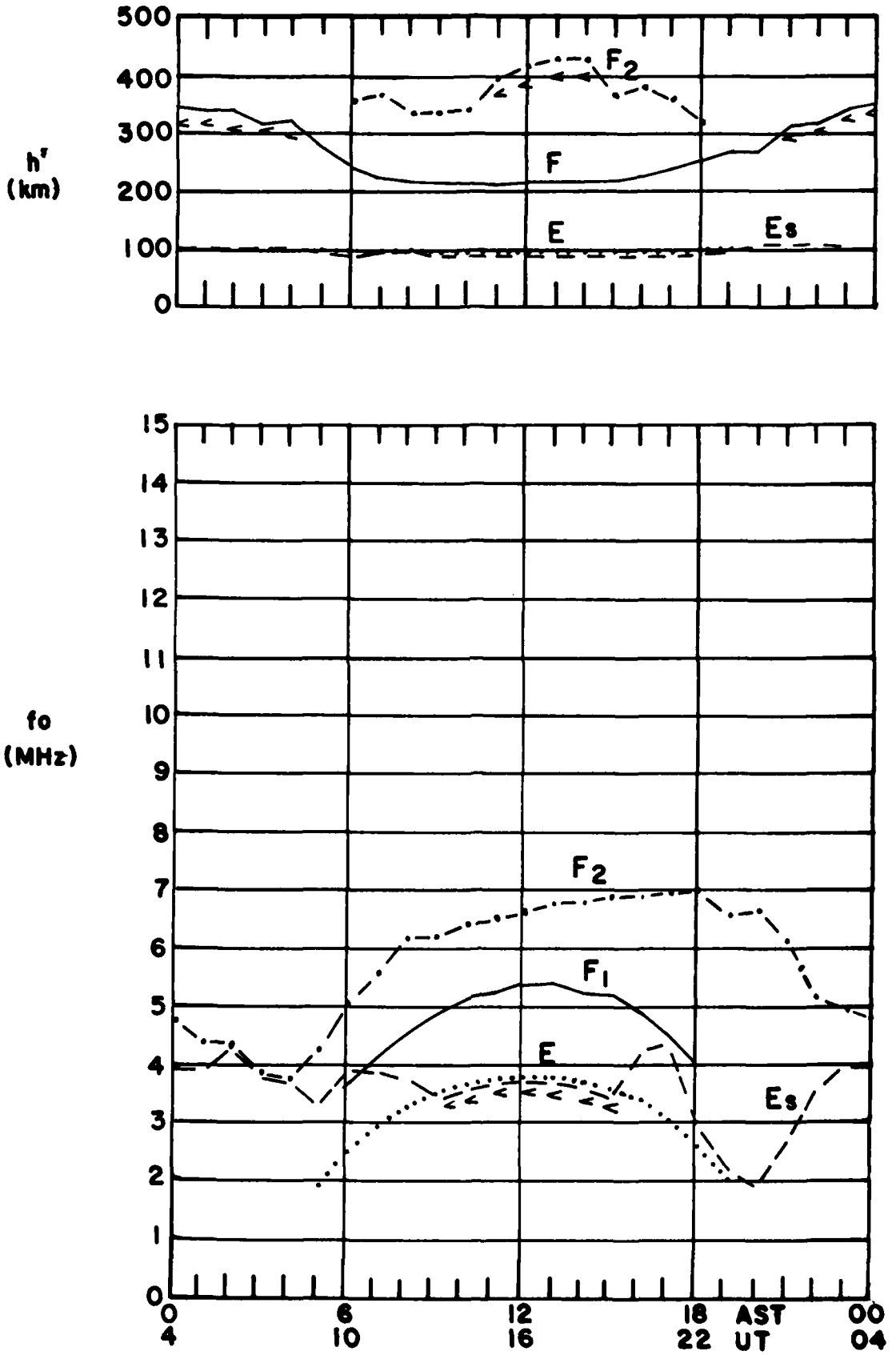

SEPTEMBER 1981

GOOSE BAY, LABRADOR

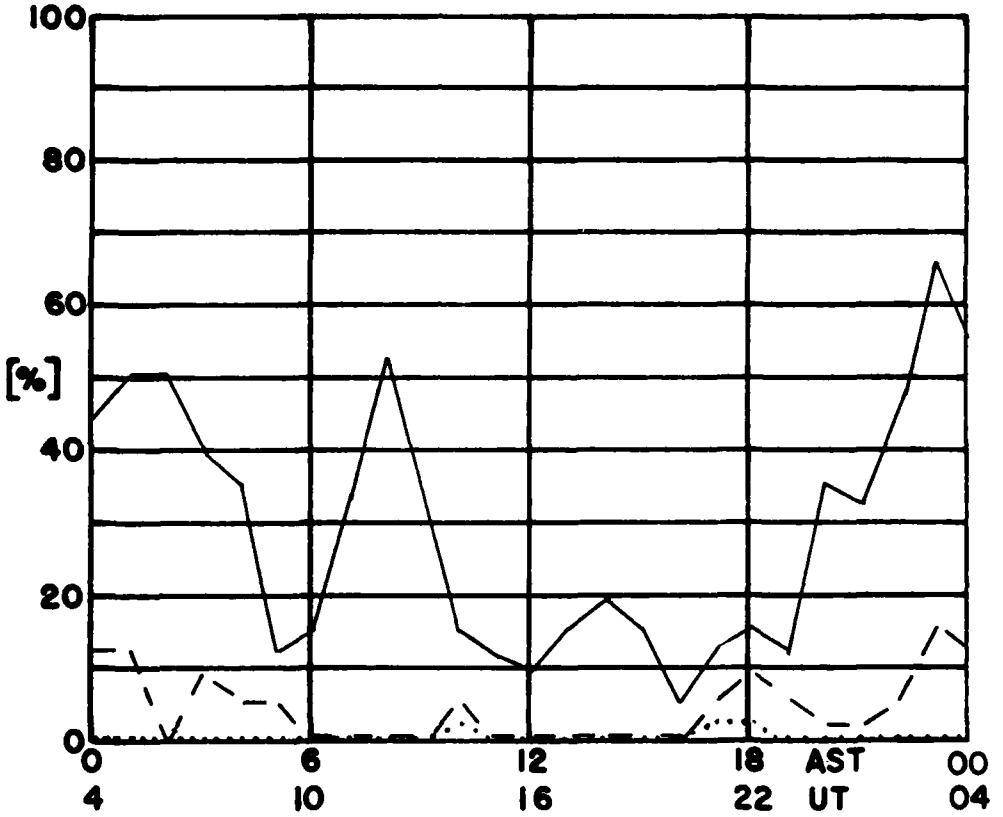

LIMITING FREQUENCY = 3MHz ——————

LIMITING FREQUENCY = 5MHz — — — — —

LIMITING FREQUENCY = 7MHz .....

PERCENTAGE OF TOTAL TIME DURING WHICH
$f_0 E_s$ IS GREATER THAN THE LIMITING FREQUENCY

MEDIAN VALUES of h' AND f_0 AT GOOSE BAY, LABRADOR FOR SEPTEMBER 1981

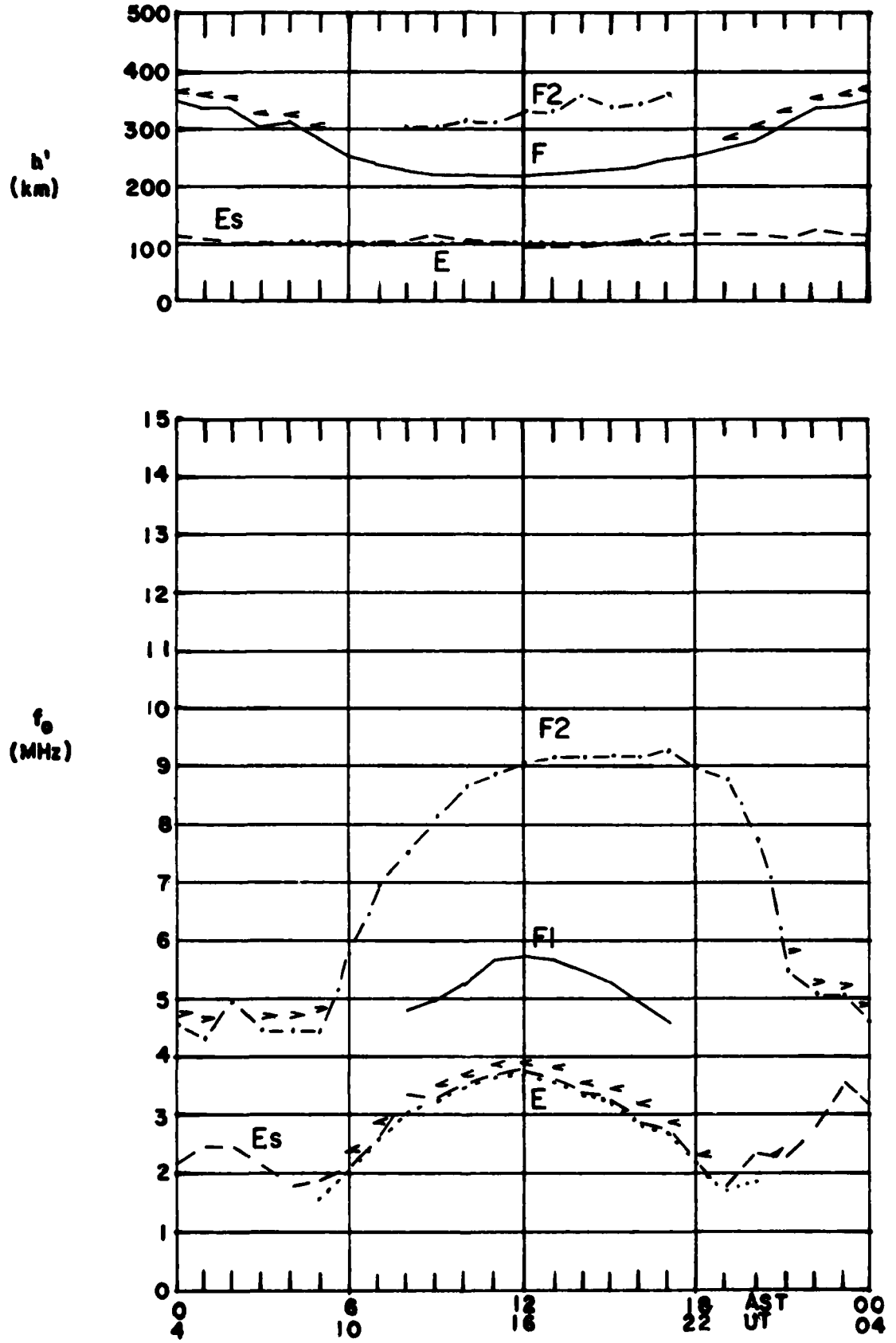

OCTOBER 1981

GOOSE BAY, LABRADOR

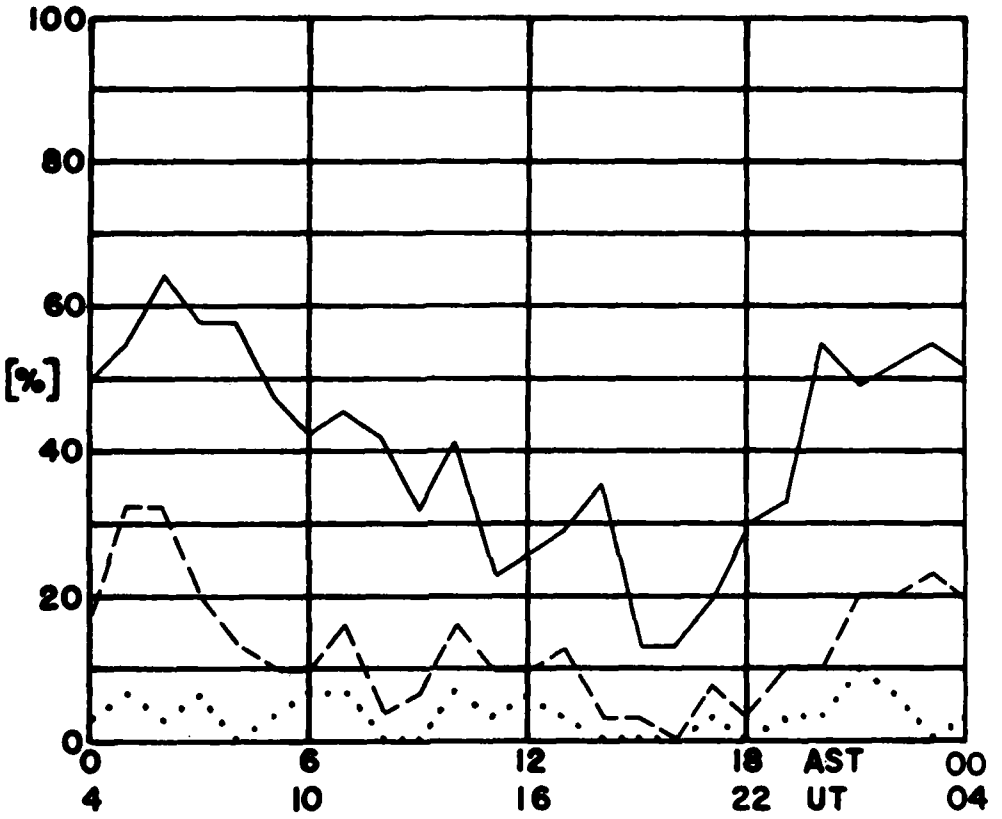

LIMITING FREQUENCY = 3MHz ——————

LIMITING FREQUENCY = 5MHz — — — — —

LIMITING FREQUENCY = 7MHz .....

PERCENTAGE OF TOTAL TIME DURING WHICH
$f_0 E_s$ IS GREATER THAN THE LIMITING FREQUENCY

MEDIAN VALUES of h' AND fo AT GOOSE BAY, LABRADOR FOR OCTOBER 1981

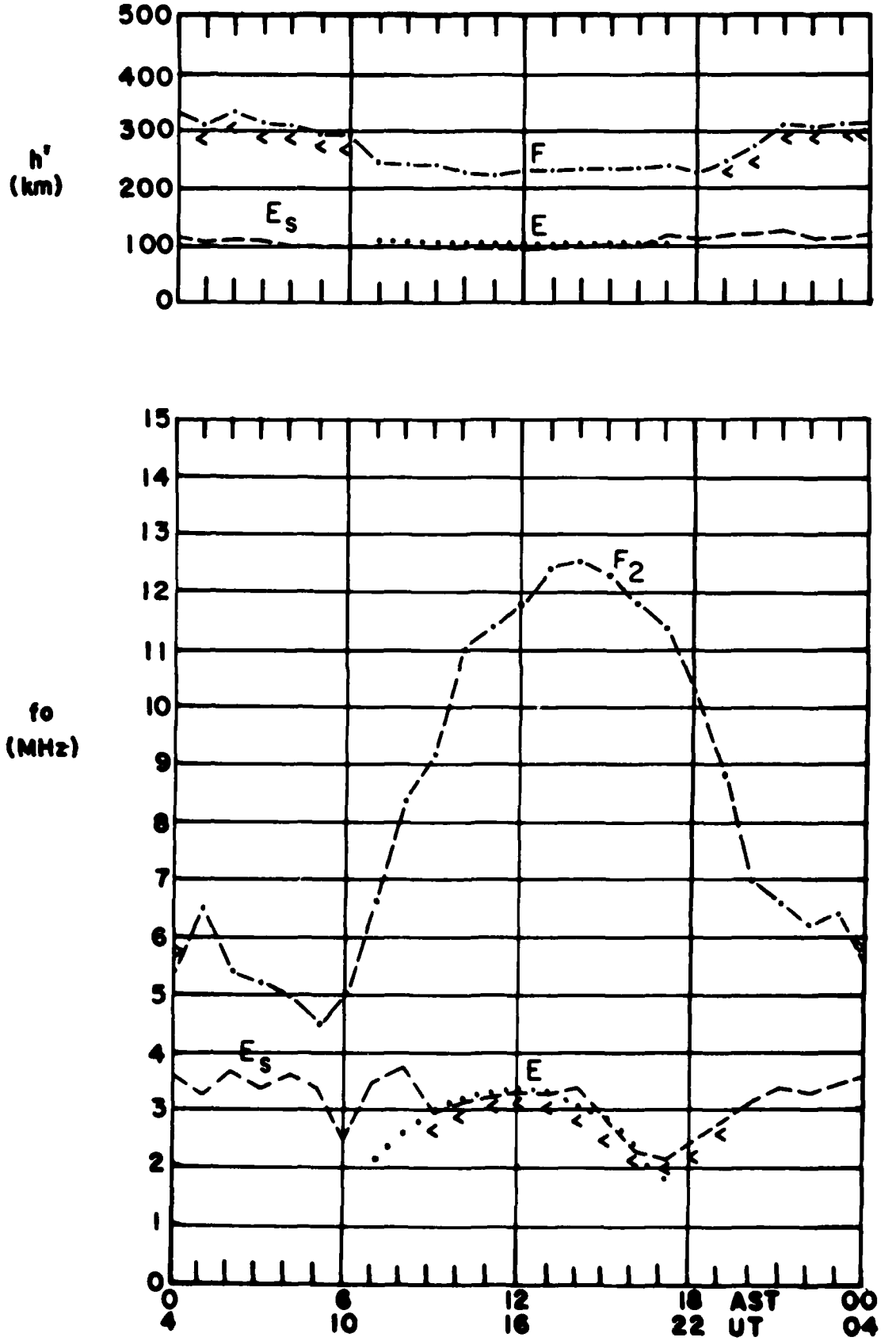

NOVEMBER 1981

GOOSE BAY, LABRADOR

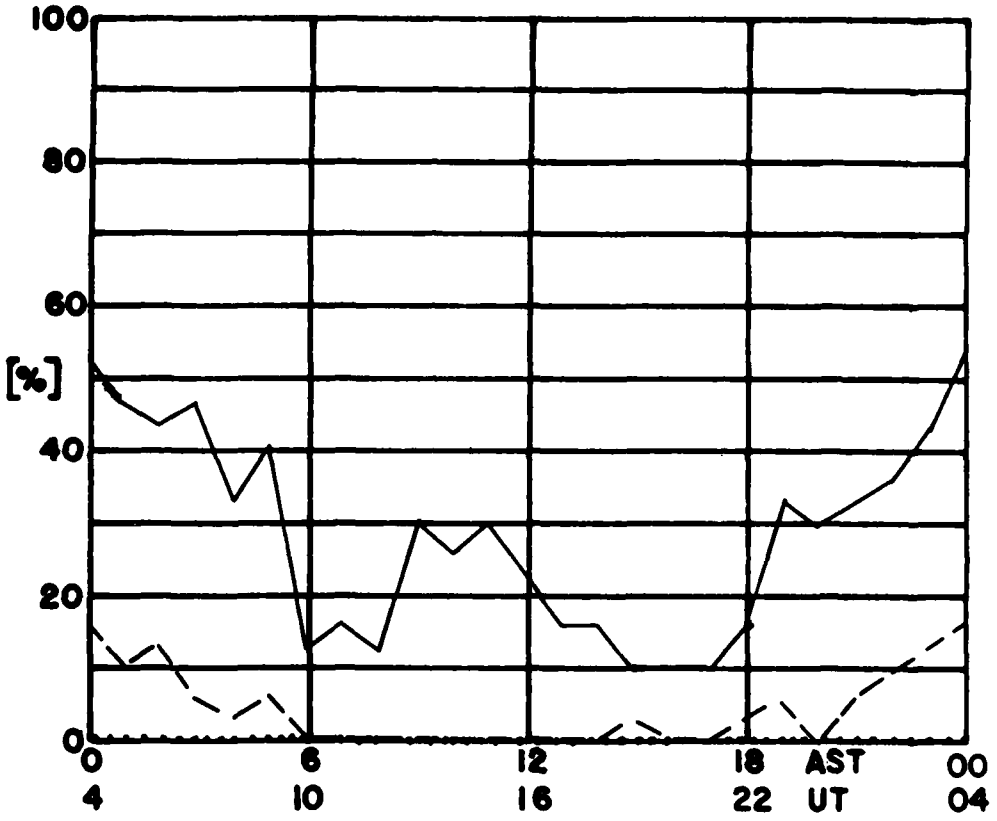

LIMITING FREQUENCY = 3MHz ————————

LIMITING FREQUENCY = 5MHz – – – – – –

LIMITING FREQUENCY = 7MHz .....

PERCENTAGE OF TOTAL TIME DURING WHICH
f_0E_s IS GREATER THAN THE LIMITING FREQUENCY

MEDIAN VALUES of h' AND fo AT GOOSE BAY, LABRADOR FOR NOVEMBER 1981

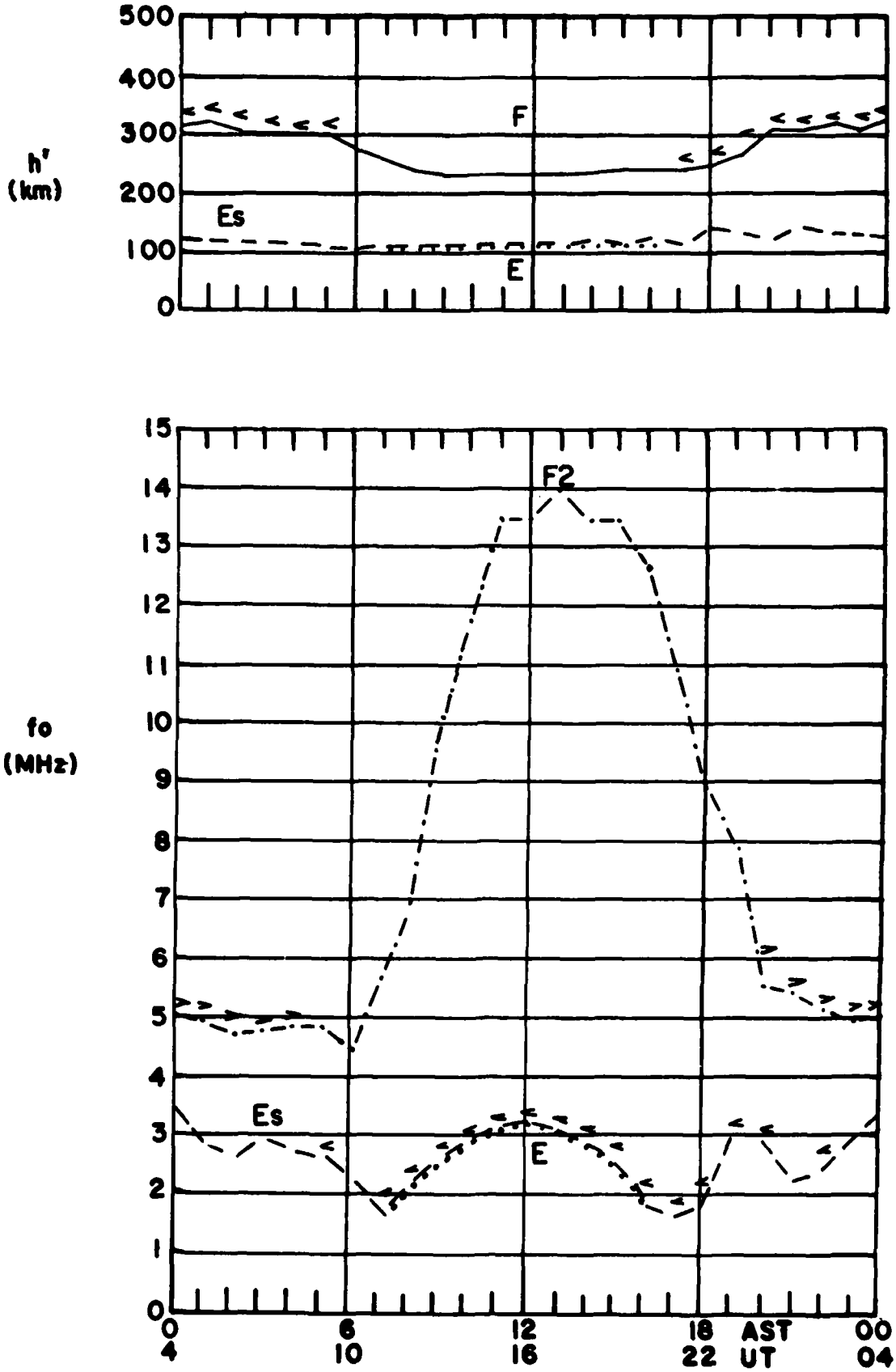

DECEMBER 1981

GOOSE BAY, LABRADOR

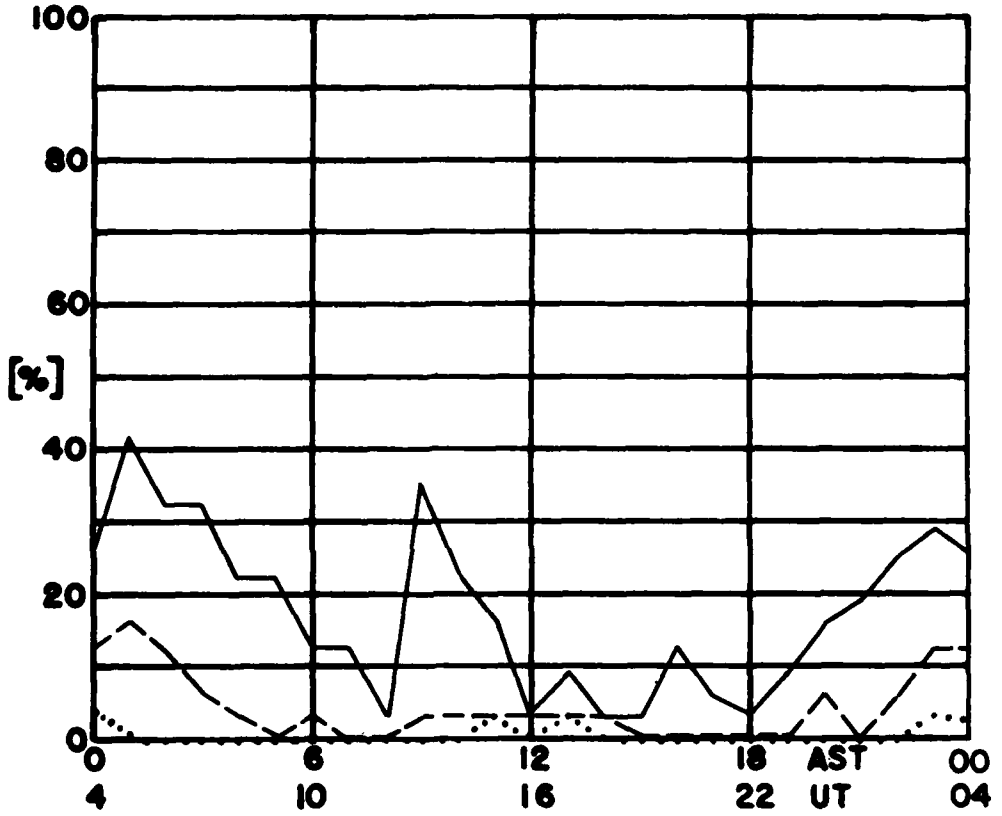

LIMITING FREQUENCY = 3MHz ————————

LIMITING FREQUENCY = 5MHz – – – – – –

LIMITING FREQUENCY = 7MHz .....

PERCENTAGE OF TOTAL TIME DURING WHICH
f_0E_s IS GREATER THAN THE LIMITING FREQUENCY

MEDIAN VALUES of h' AND f_0 AT GOOSE BAY, LABRADOR FOR

DECEMBER 1981

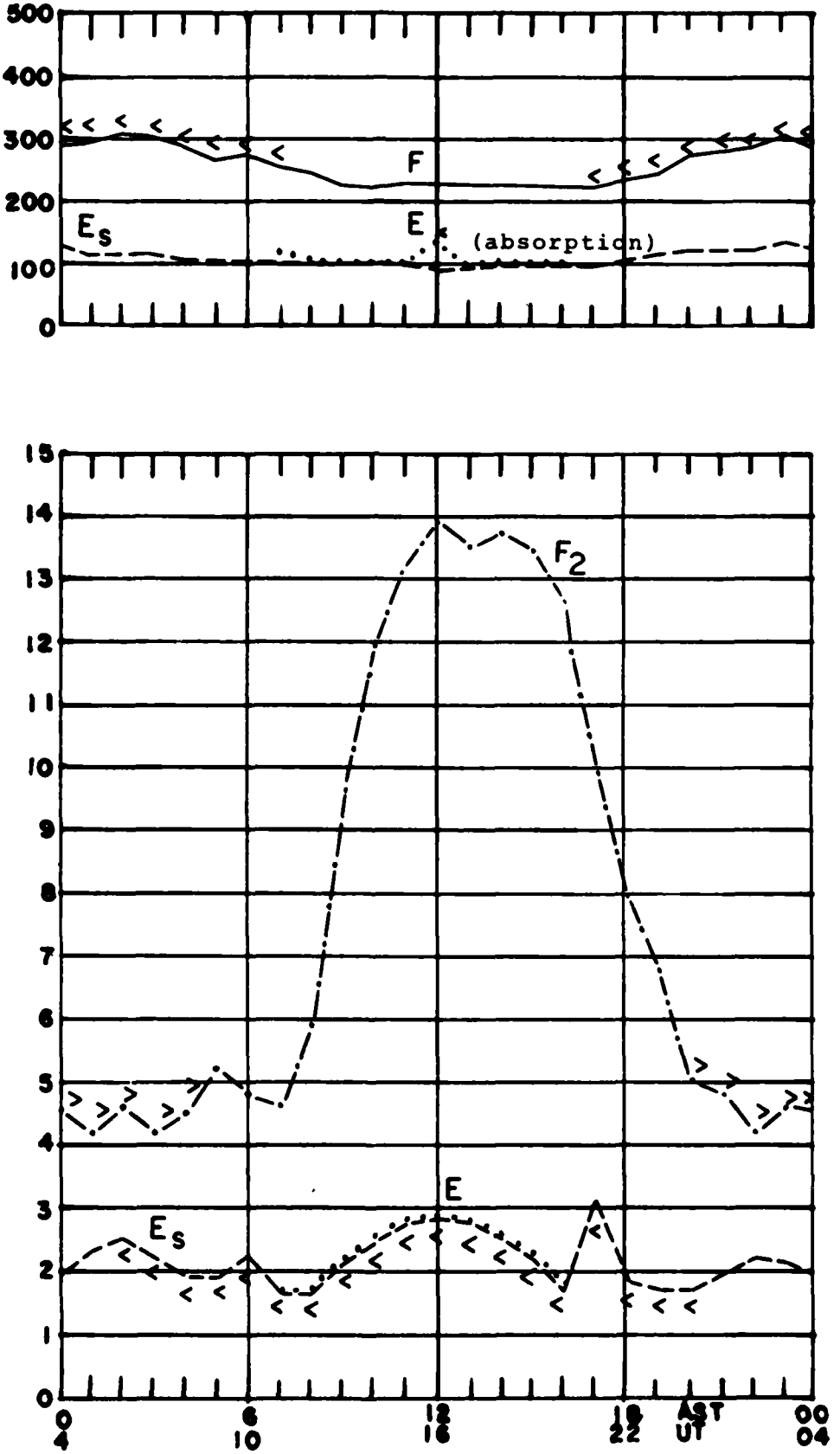

JANUARY 1982

GOOSE BAY, LABRADOR

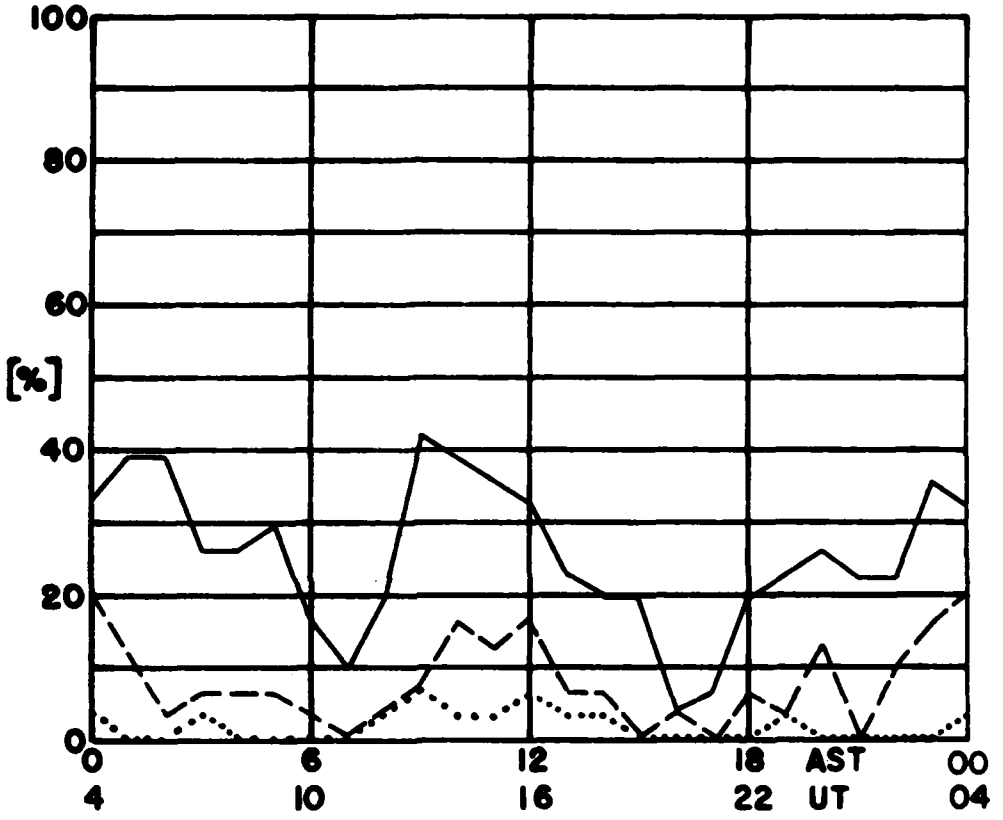

LIMITING FREQUENCY = 3MHz ————————

LIMITING FREQUENCY = 5MHz – – – – – –

LIMITING FREQUENCY = 7MHz .....

PERCENTAGE OF TOTAL TIME DURING WHICH
$f_0 E_s$ IS GREATER THAN THE LIMITING FREQUENCY

MEDIAN VALUES of h' AND fo AT GOOSE BAY, LABRADOR FOR JANUARY 1962

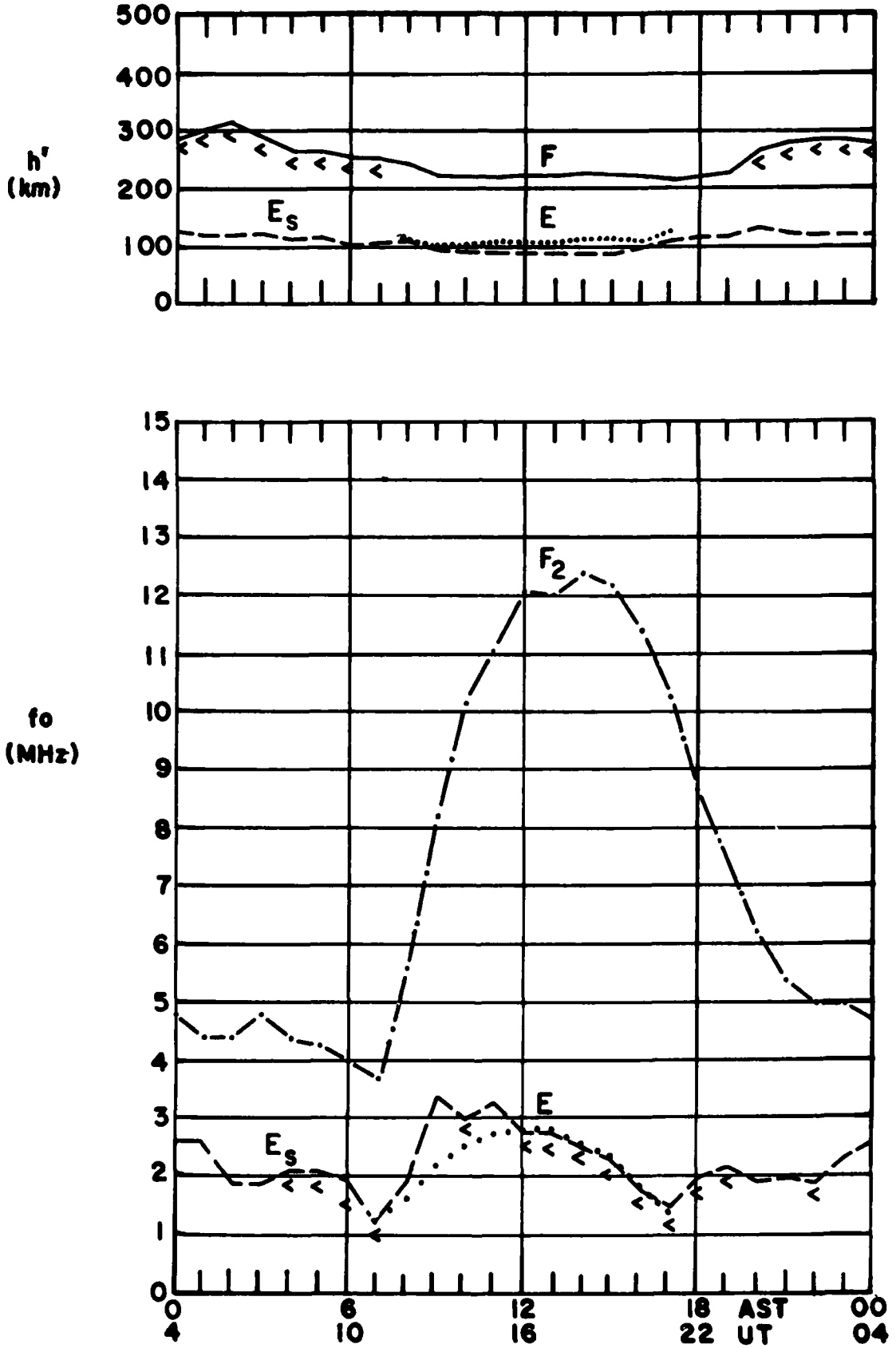

FEBRUARY 1982

GOOSE BAY, LABRADOR

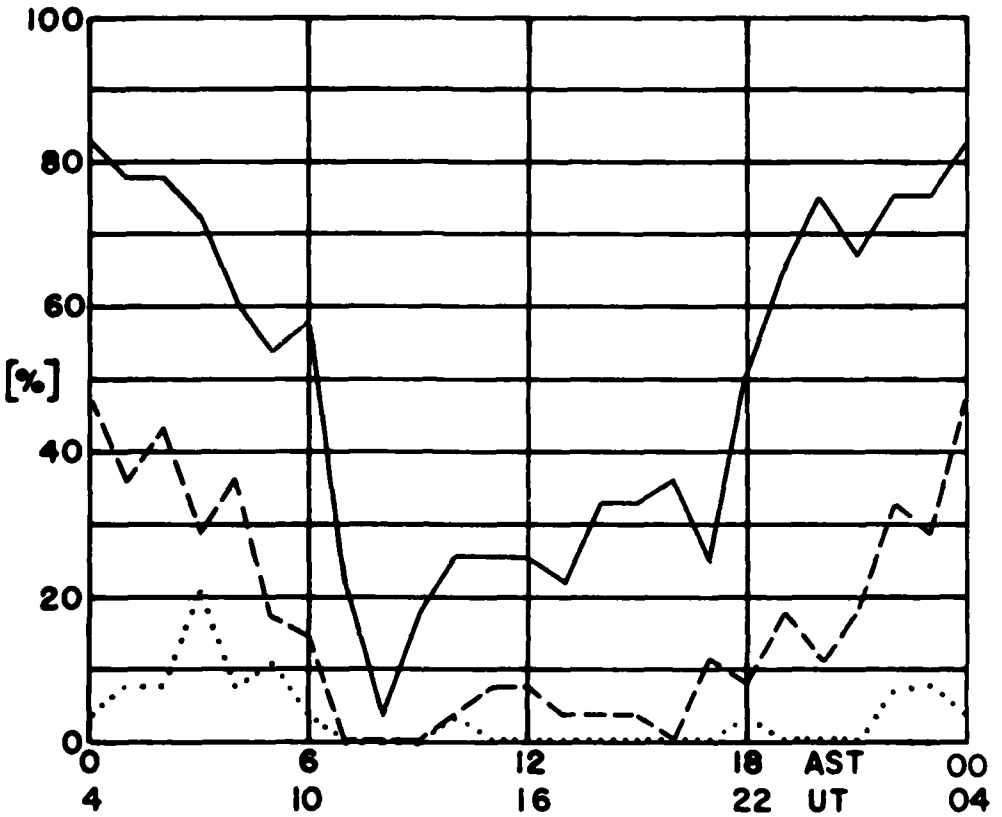

LIMITING FREQUENCY = 3MHz ————————

LIMITING FREQUENCY = 5MHz — — — — —

LIMITING FREQUENCY = 7MHz .....

PERCENTAGE OF TOTAL TIME DURING WHICH
$f_0 E_s$ IS GREATER THAN THE LIMITING FREQUENCY

MEDIAN VALUES of h' AND fo AT GOOSE BAY, LABRADOR FOR FEBRUARY 1982

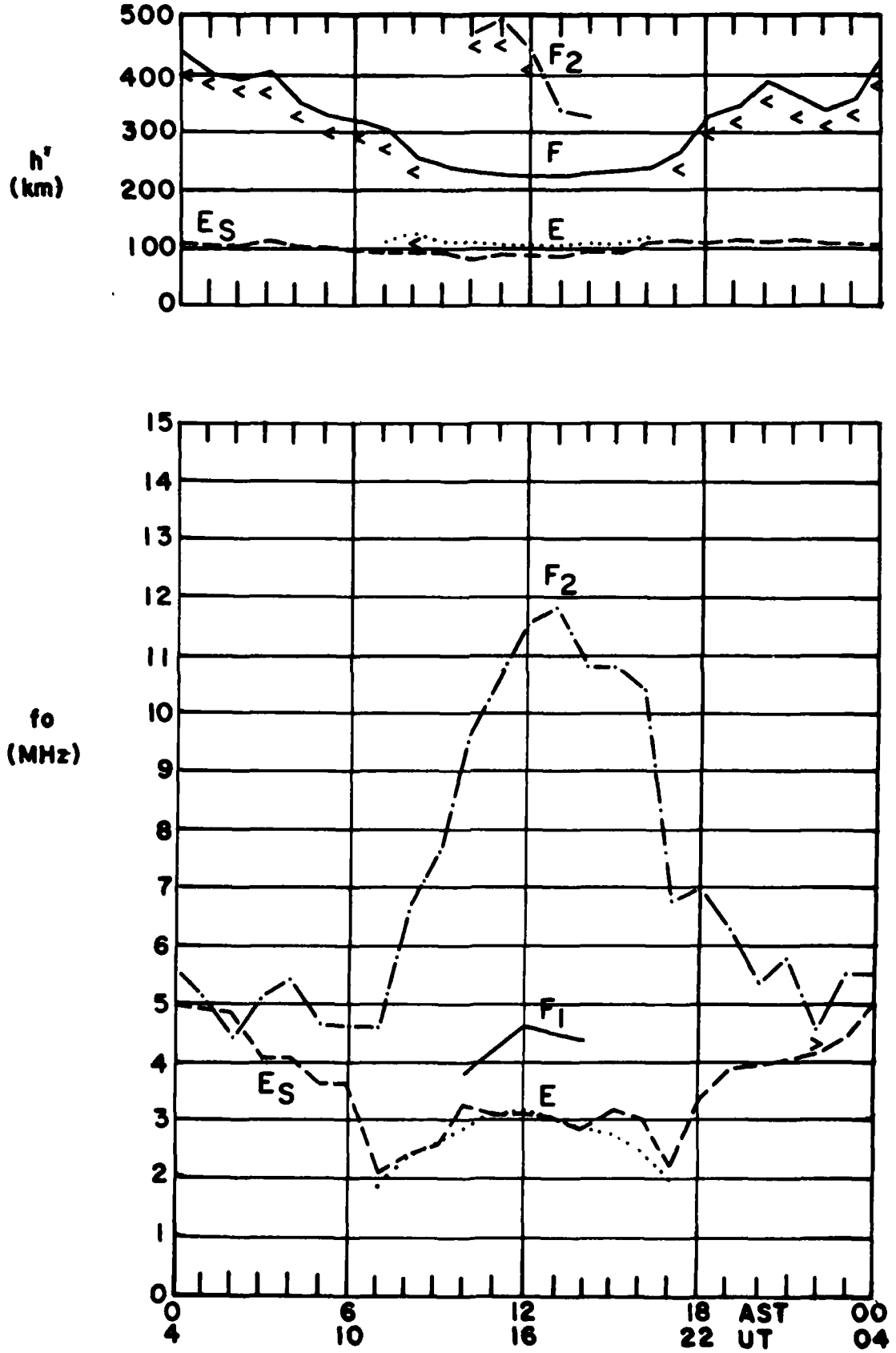

MARCH 1982

GOOSE BAY, LABRADOR

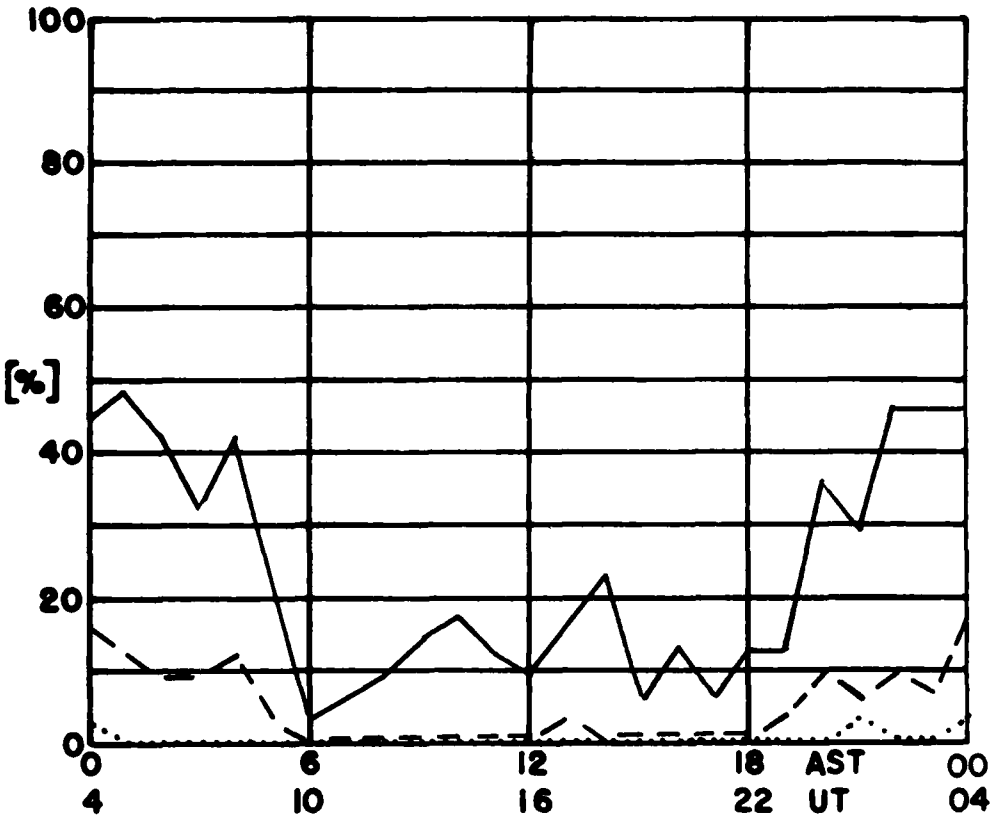

LIMITING FREQUENCY = 3MHz ——————

LIMITING FREQUENCY = 5MHz – – – – – –

LIMITING FREQUENCY = 7MHz .....

PERCENTAGE OF TOTAL TIME DURING WHICH
$f_0 E_s$ IS GREATER THAN THE LIMITING FREQUENCY

MEDIAN VALUES of h' AND fo AT GOOSE BAY, LABRADOR FOR MARCH 1982

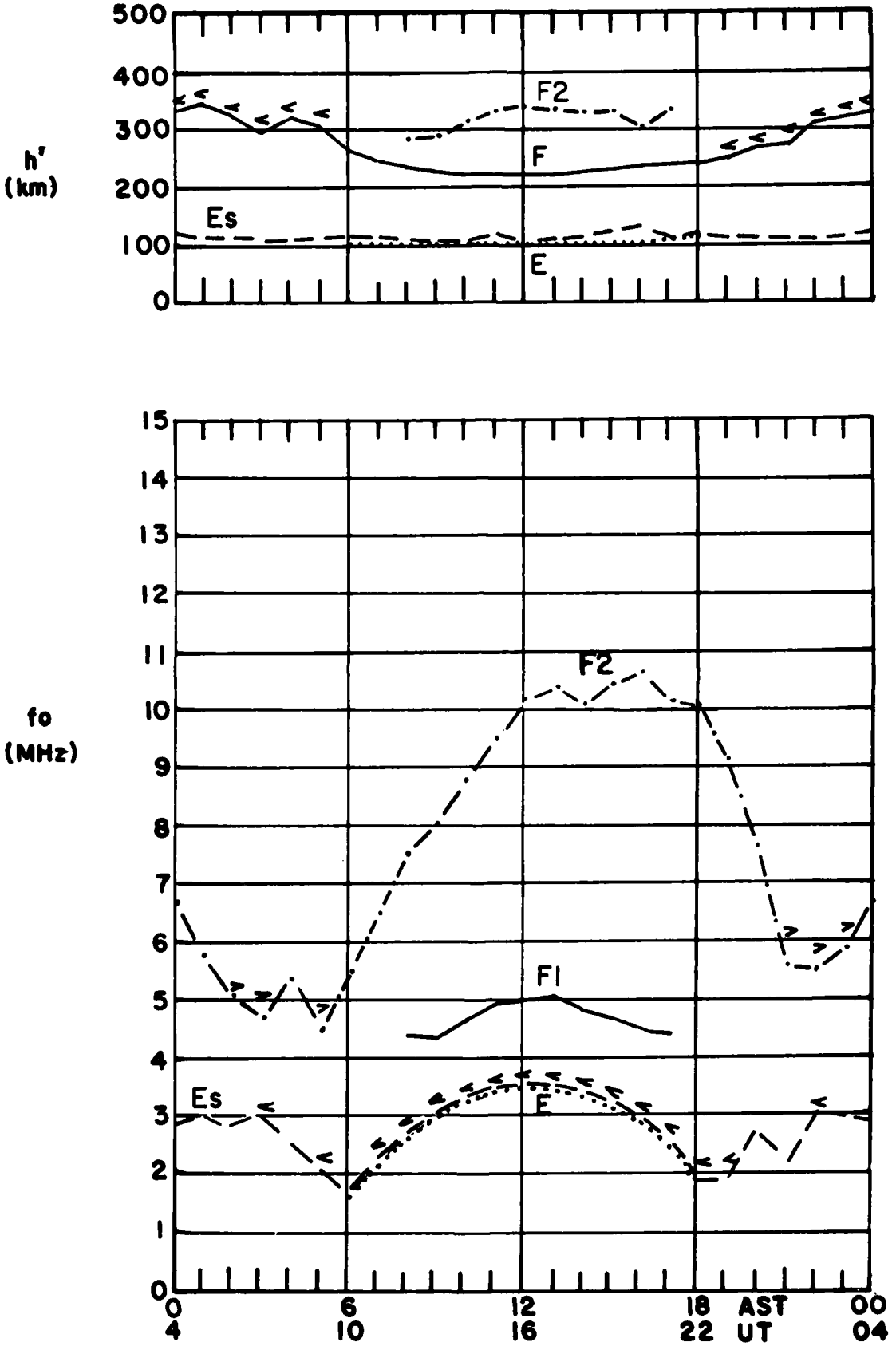

APRIL 1982

GOOSE BAY, LABRADOR

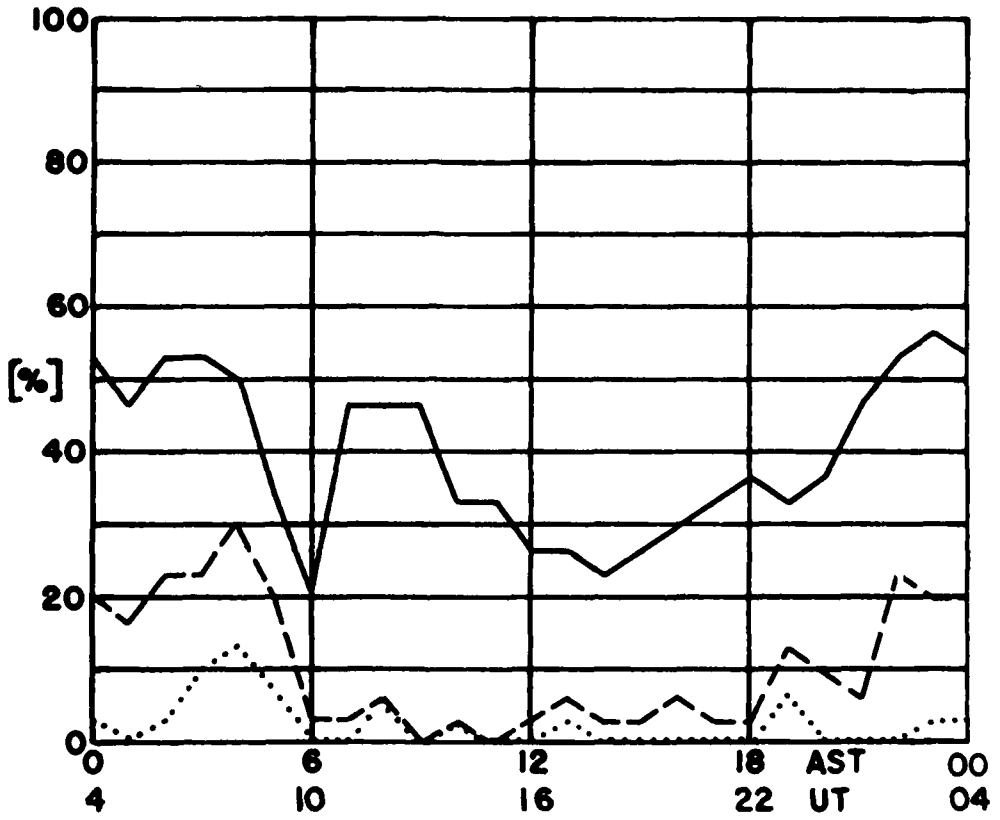

LIMITING FREQUENCY = 3MHz ——————

LIMITING FREQUENCY = 5MHz – – – – – –

LIMITING FREQUENCY = 7MHz .....

PERCENTAGE OF TOTAL TIME DURING WHICH
$f_0 E_s$ IS GREATER THAN THE LIMITING FREQUENCY

MEDIAN VALUES of h' AND fo AT GOOSE BAY, LABRADOR FOR

APRIL 1982

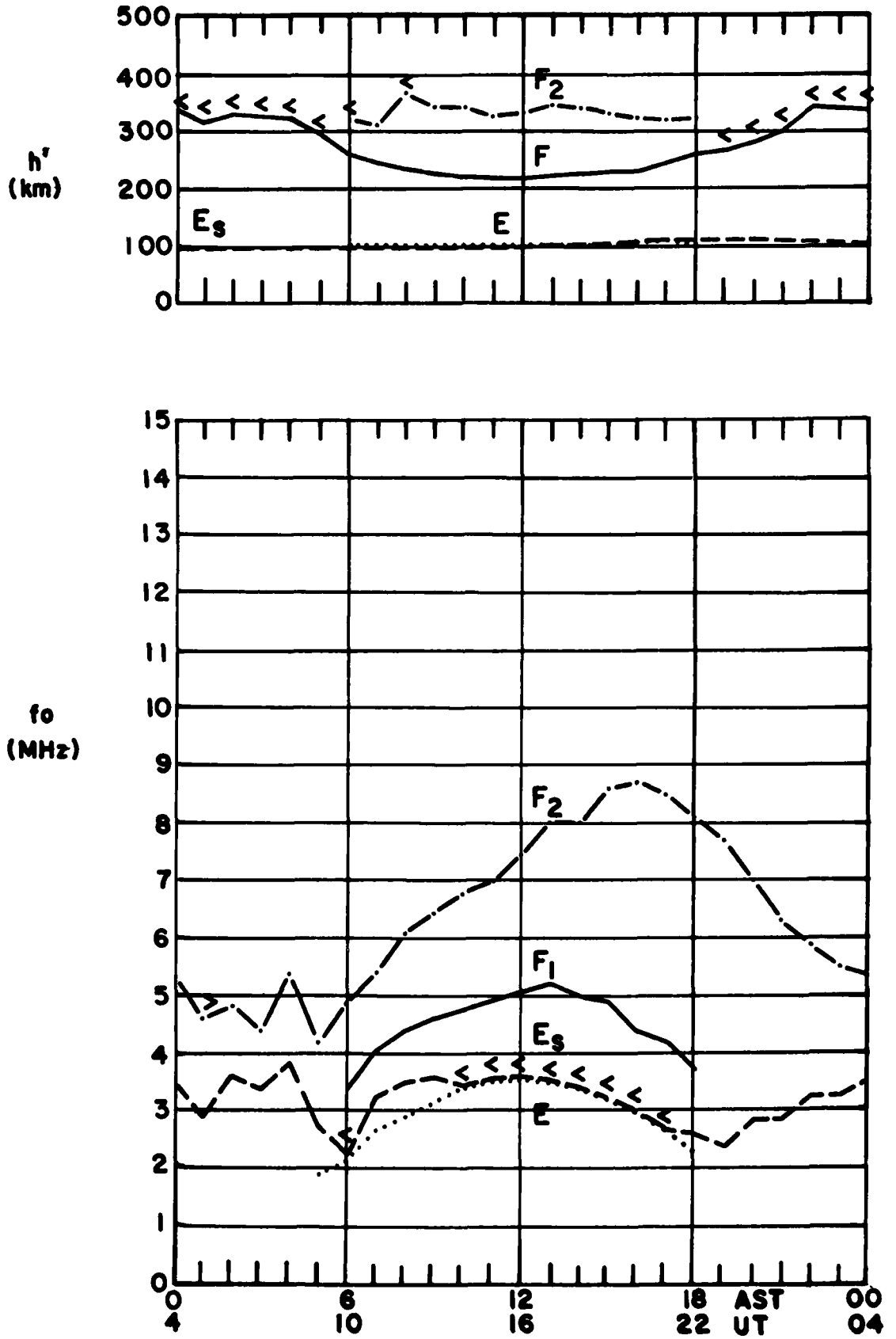

MAY 1982

GOOSE BAY, LABRADOR

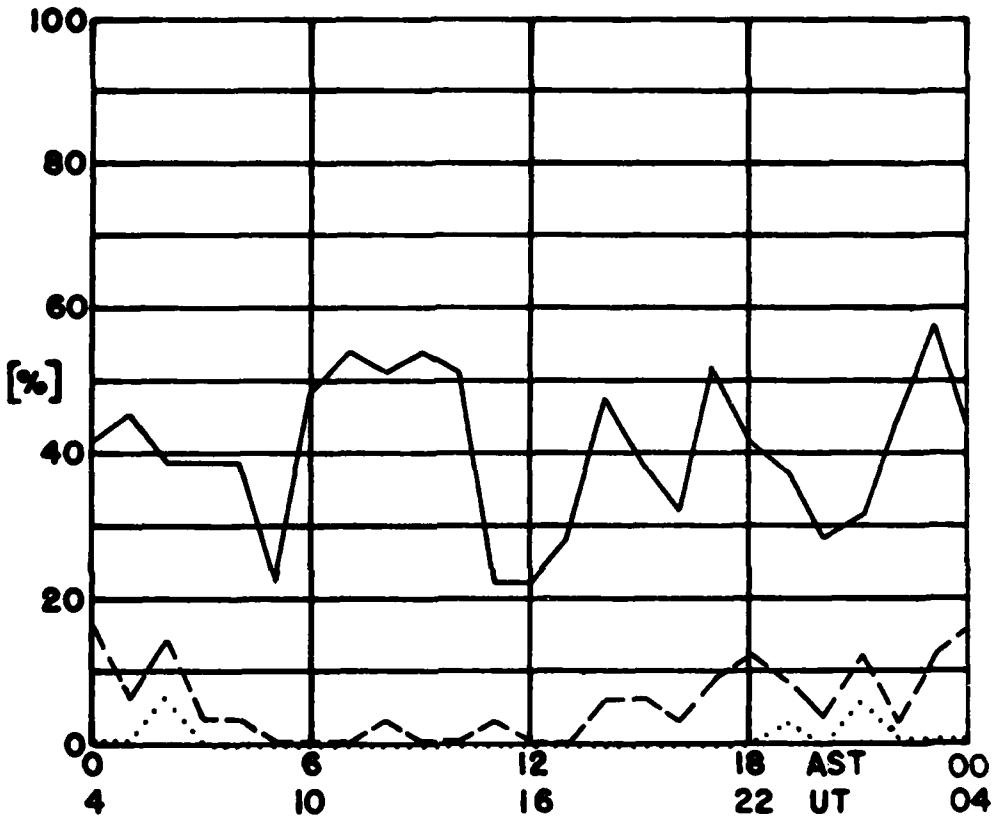

LIMITING FREQUENCY = 3MHz ————————

LIMITING FREQUENCY = 5MHz — — — — —

LIMITING FREQUENCY = 7MHz .....

PERCENTAGE OF TOTAL TIME DURING WHICH
f_0E_s IS GREATER THAN THE LIMITING FREQUENCY

MEDIAN VALUES of h' AND fo AT GOOSE BAY, LABRADOR FOR

MAY 1982

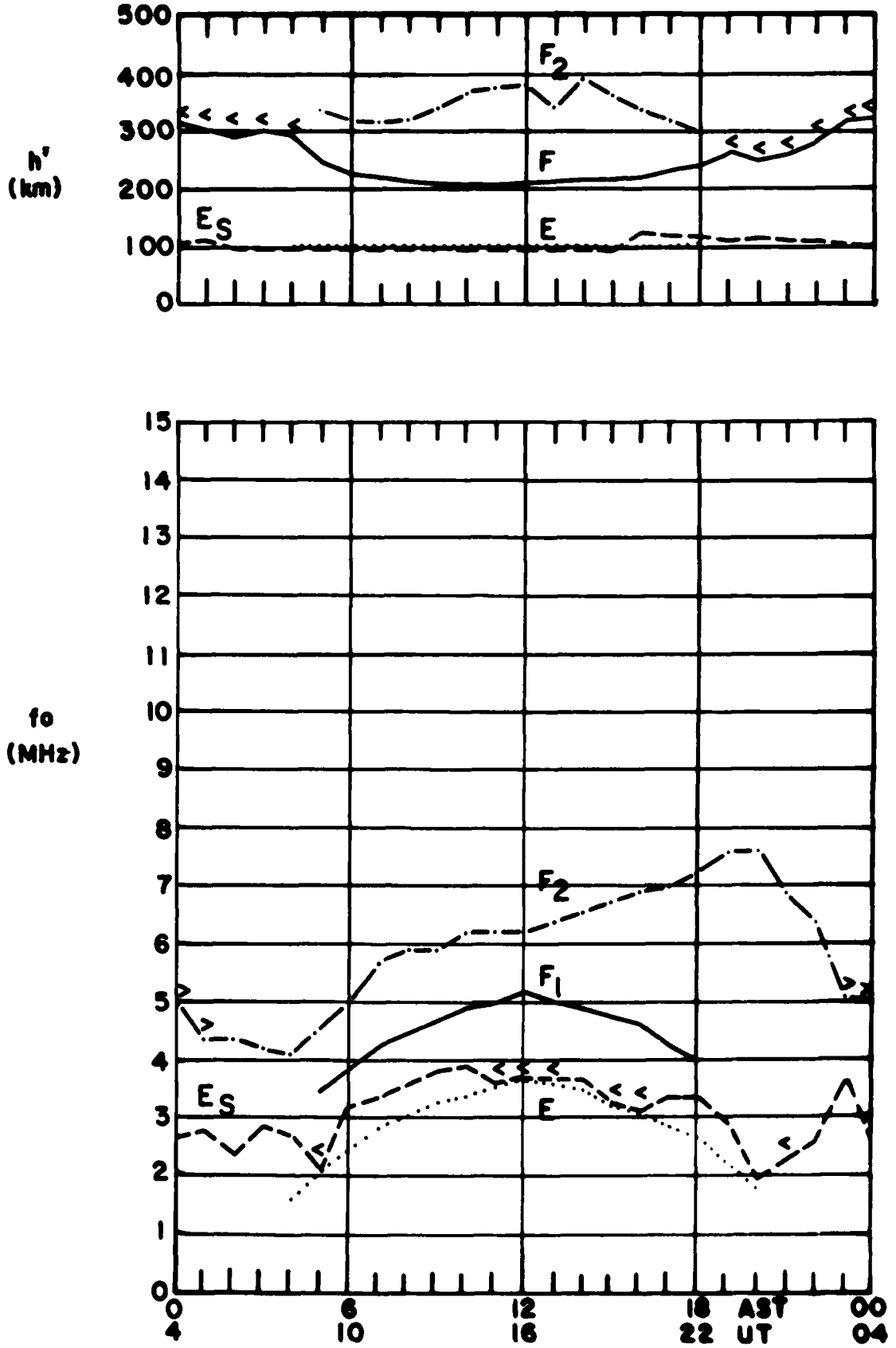

JUNE 1982

GOOSE BAY, LABRADOR

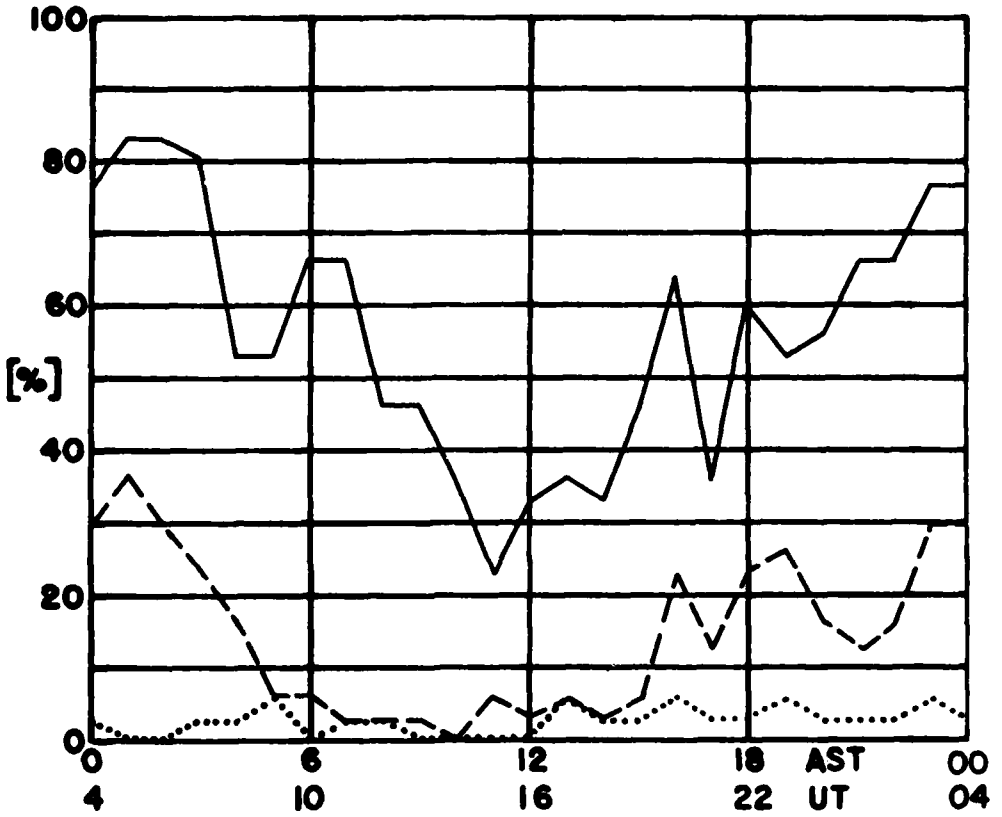

LIMITING FREQUENCY = 3MHz ——————

LIMITING FREQUENCY = 5MHz — — — — —

LIMITING FREQUENCY = 7MHz .....

PERCENTAGE OF TOTAL TIME DURING WHICH
$f_0 E_s$ IS GREATER THAN THE LIMITING FREQUENCY

MEDIAN VALUES of h' AND fo AT GOOSE BAY, LABRADOR FOR

JUNE 1982

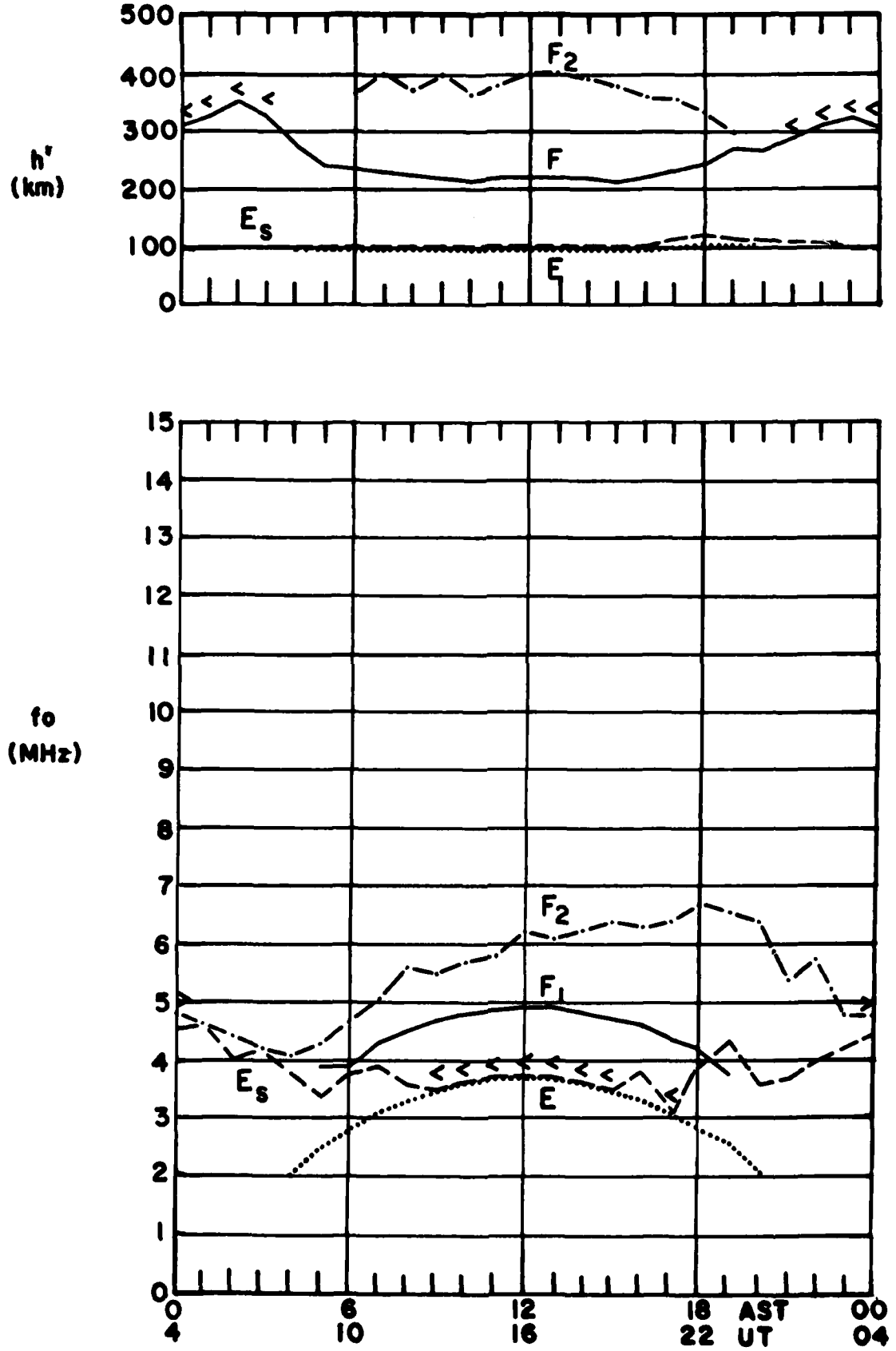

JULY 1982

GOOSE BAY, LABRADOR

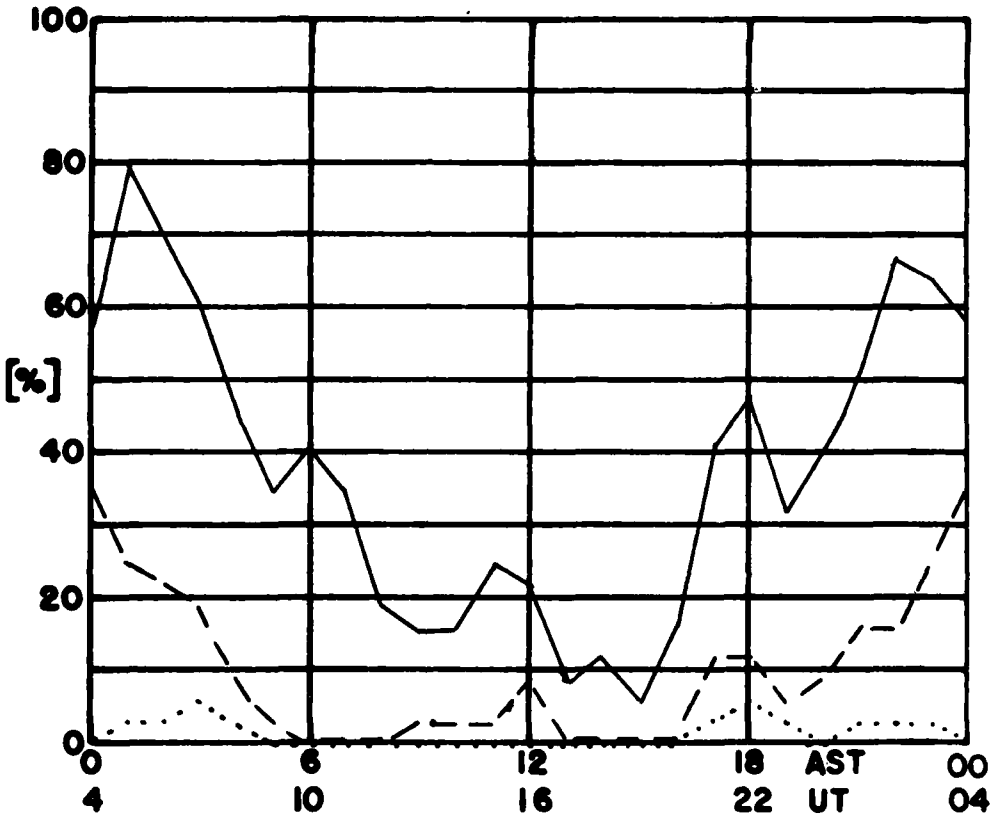

LIMITING FREQUENCY = 3MHz ————————

LIMITING FREQUENCY = 5MHz — — — — — —

LIMITING FREQUENCY = 7MHz .....

PERCENTAGE OF TOTAL TIME DURING WHICH
f_0E_s IS GREATER THAN THE LIMITING FREQUENCY

MEDIAN VALUES of h' AND fo AT GOOSE BAY, LABRADOR FOR JULY 1982

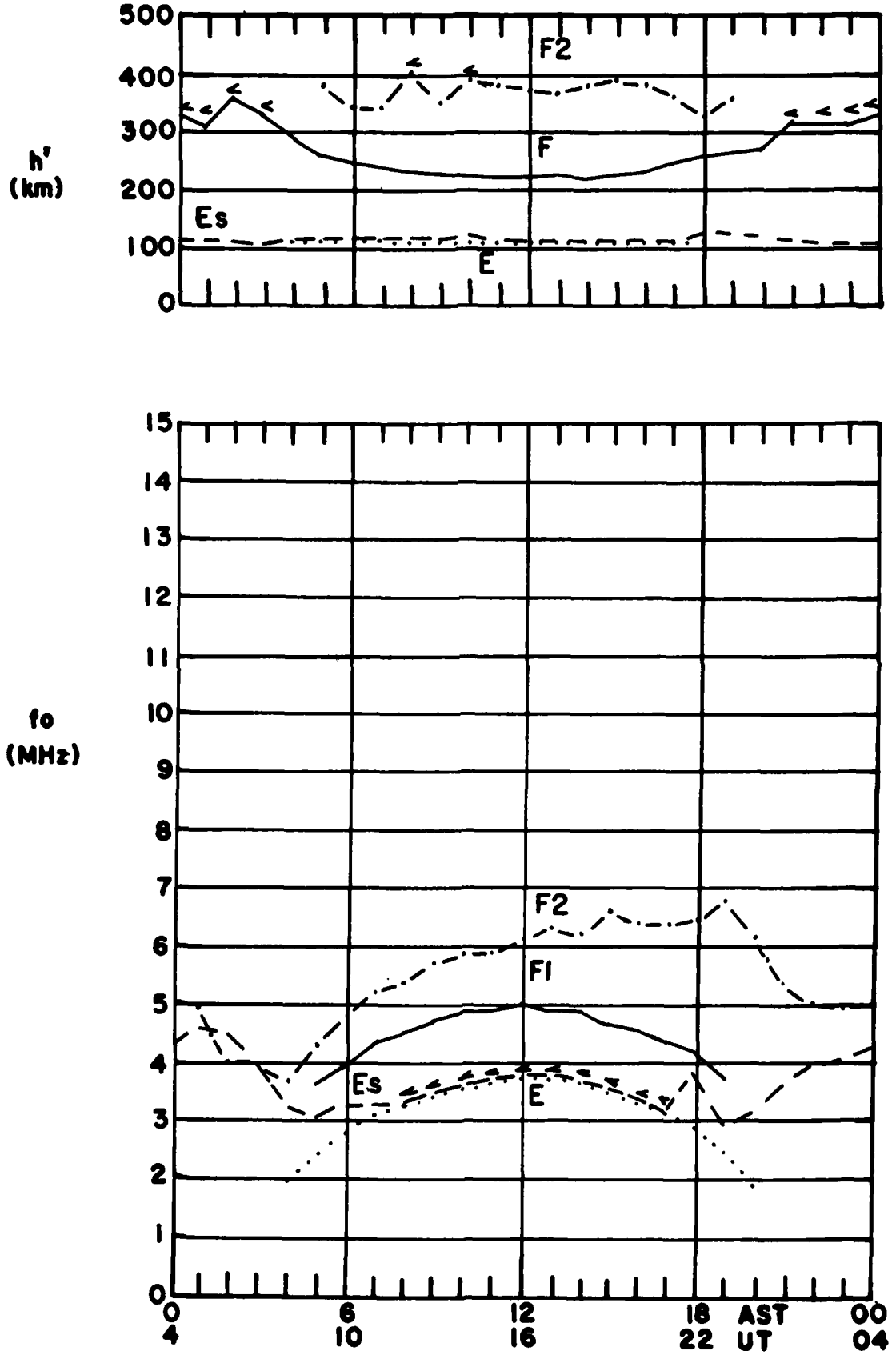

AUGUST 1982

GOOSE BAY, LABRADOR

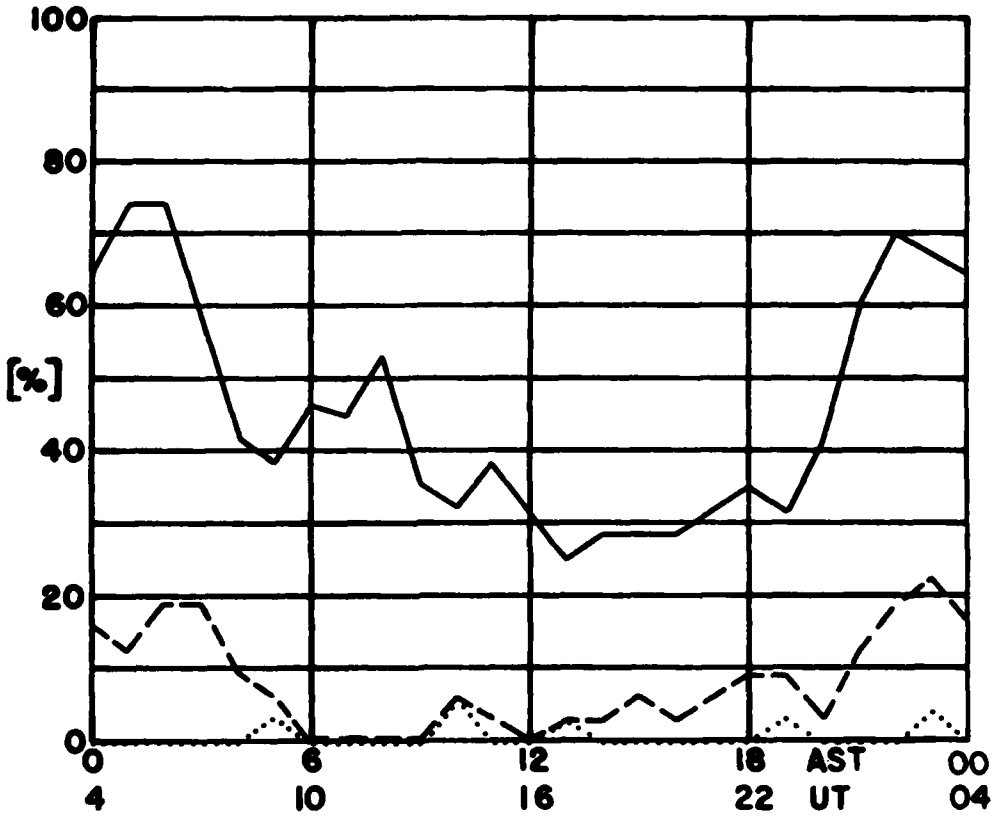

LIMITING FREQUENCY = 3MHz ————————

LIMITING FREQUENCY = 5MHz — — — — —

LIMITING FREQUENCY = 7MHz .....

PERCENTAGE OF TOTAL TIME DURING WHICH
f_0E_s IS GREATER THAN THE LIMITING FREQUENCY

MEDIAN VALUES of h' AND fo AT GOOSE BAY, LABRADOR FOR AUGUST 1982

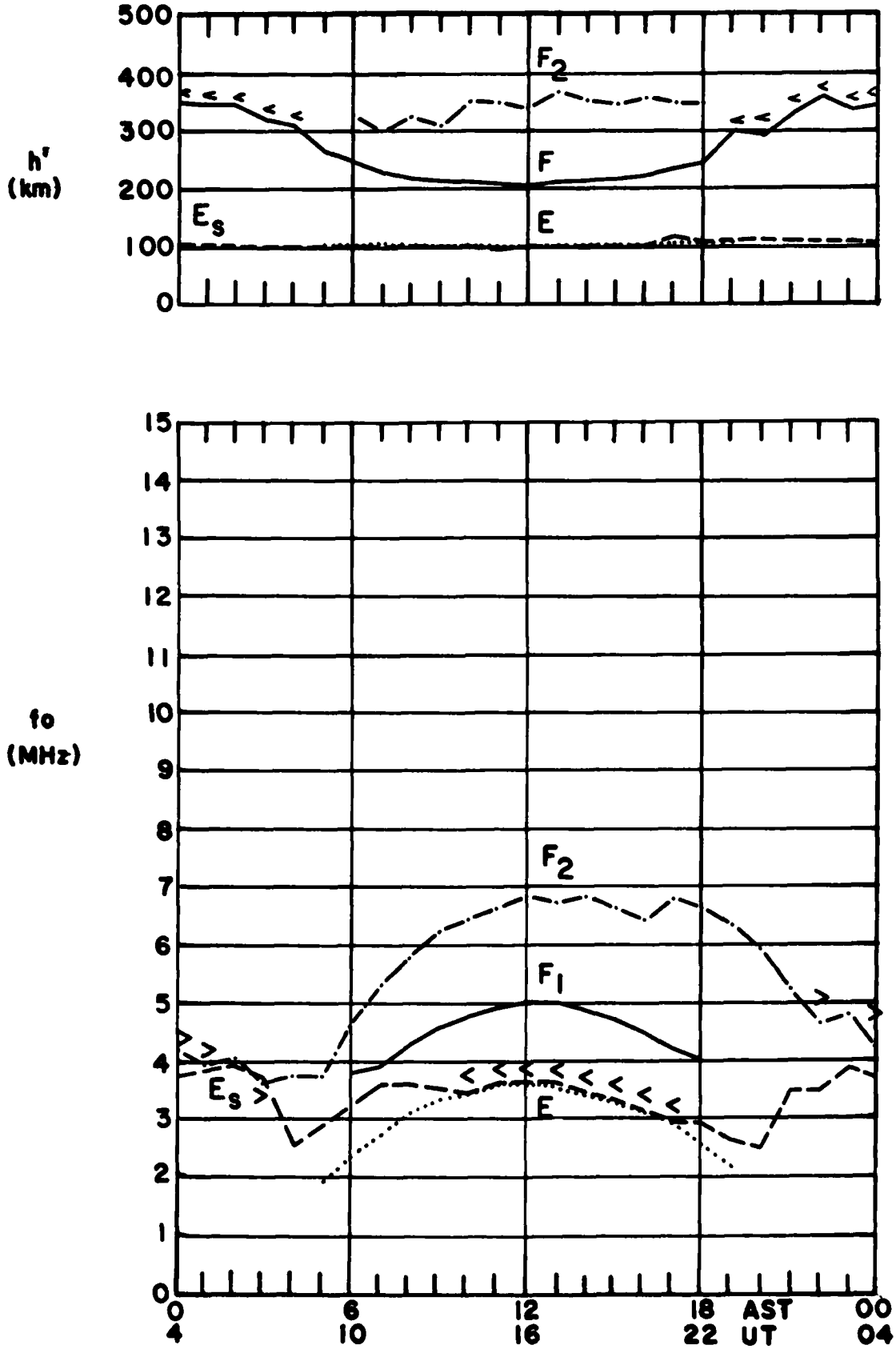

SEPTEMBER 1982

GOOSE BAY, LABRADOR

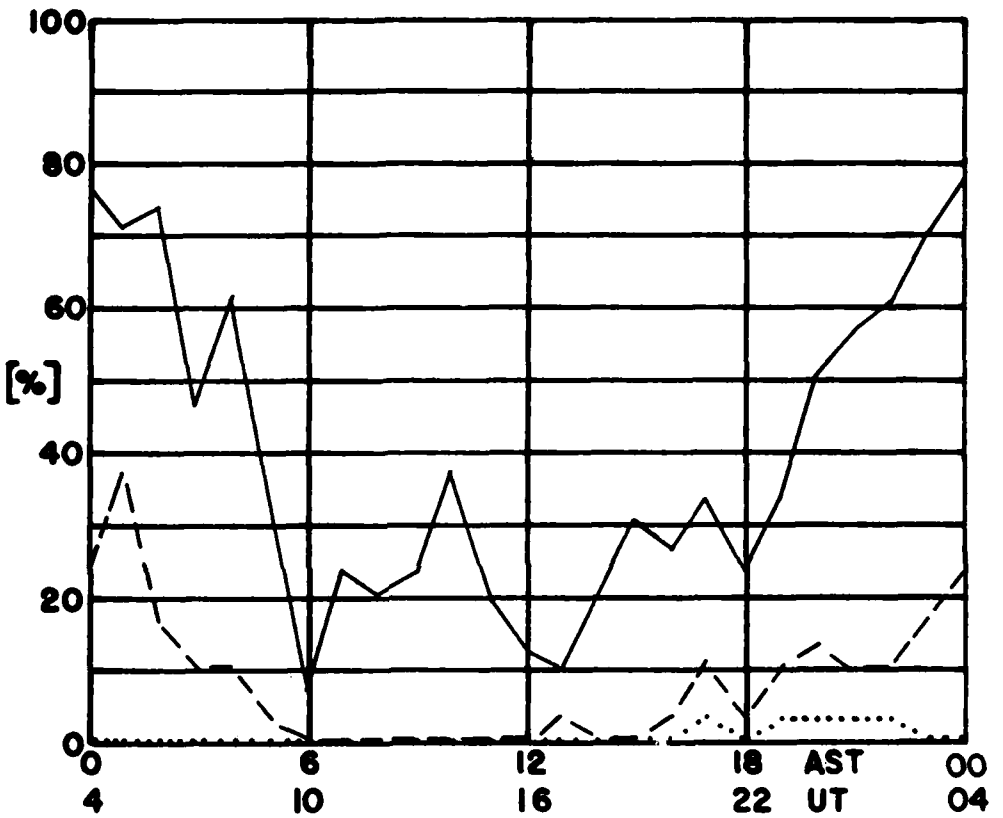

LIMITING FREQUENCY = 3MHz ————————

LIMITING FREQUENCY = 5MHz — — — — — —

LIMITING FREQUENCY = 7MHz .....

PERCENTAGE OF TOTAL TIME DURING WHICH
$f_0 E_s$ IS GREATER THAN THE LIMITING FREQUENCY

MEDIAN VALUES of h' AND fo AT GOOSE BAY, LABRADOR FOR SEPTEMBER 1982

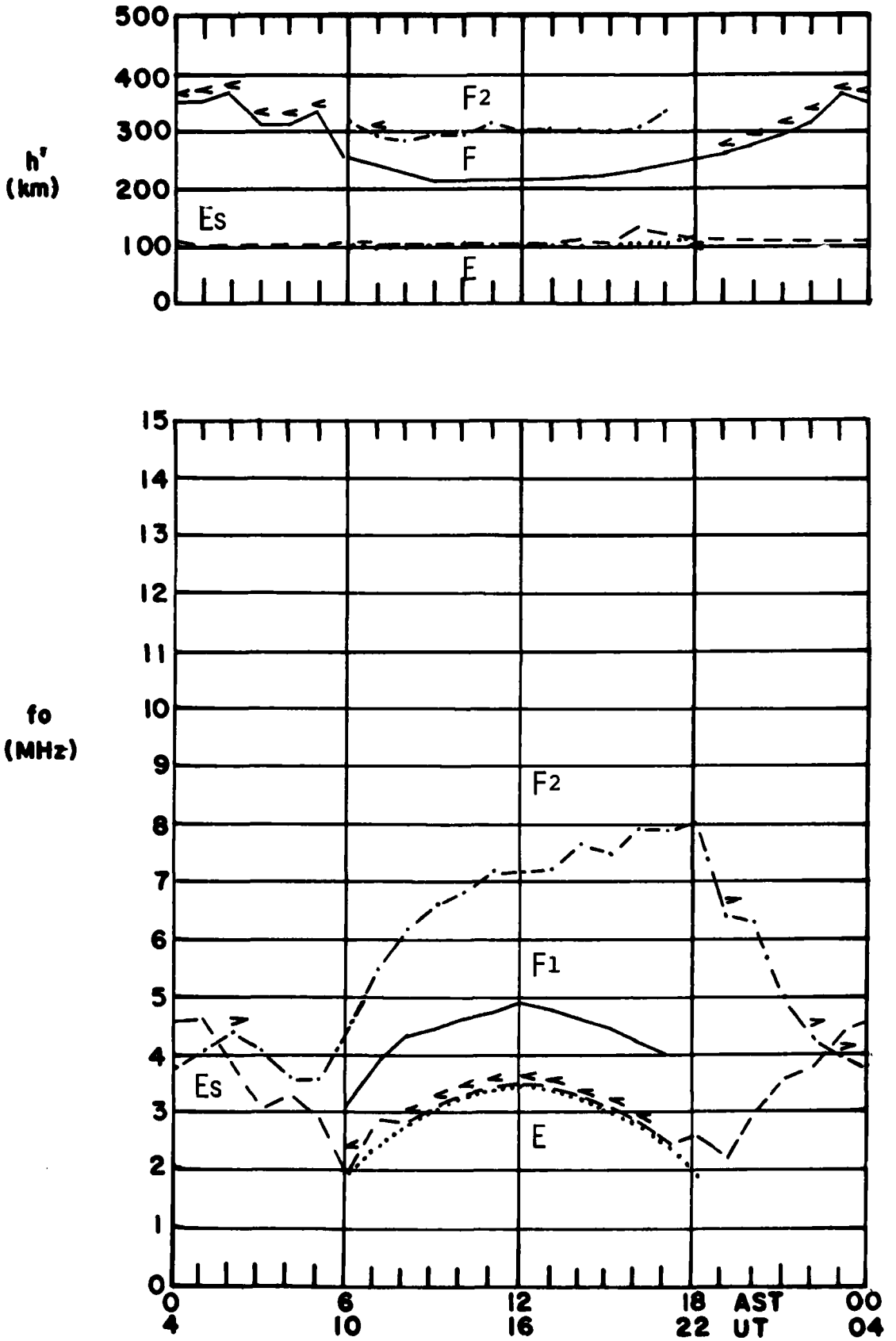

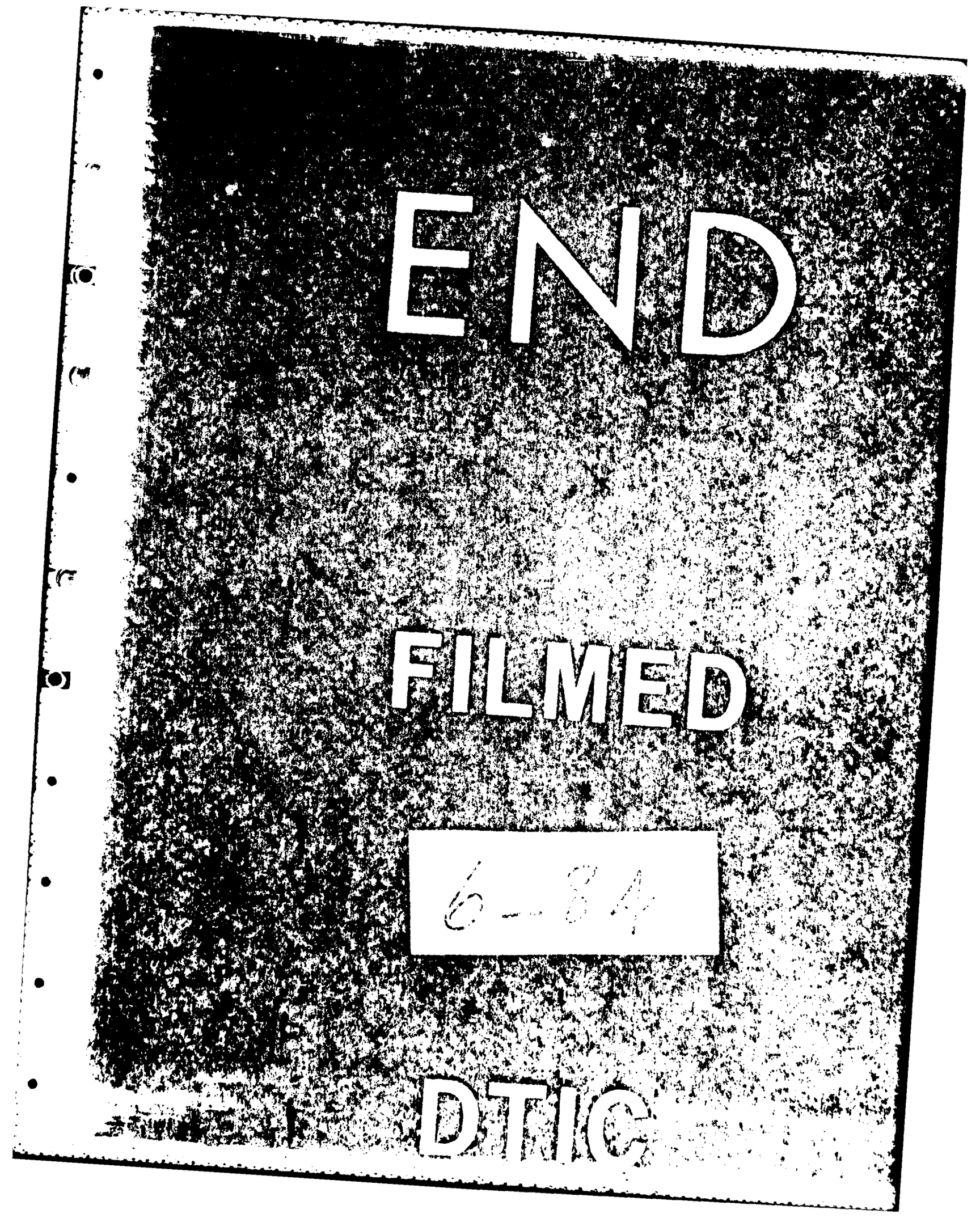
END
FILMED
6-84
DTIC